Investigation of the Effects of Electrolytes on Radical Cation Species and Electrode Materials on Anodic Oxidation of Styrenes

2020.3

Tokyo University of Agriculture and Technology,
Graduate School of Bio-Applications and Systems Engineering,
Department of Food and Energy Systems Science
Yasushi IMADA

Table of contents

1. Introduction

1-1. Electro-organic chemistry

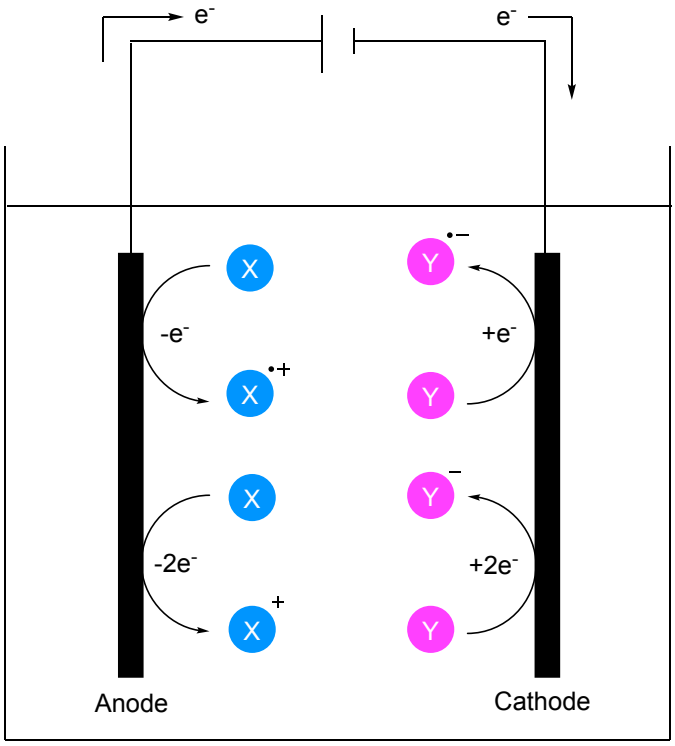

Figure 1. Conceptual figure of electrolysis.

Electro-organic chemistry has received a great attention as a powerful and eco-friendly synthetic methodology.[1] As the conceptual figure shows (Figure 1), electrochemical reactions are taken place heterogeneously, that is, electron transfer occurs between molecule and the surface of electrode: anodic oxidation and cathodic reduction. This feature gives birth to the following merits:

1) The reaction fields of oxidation and reduction are separated

Only oxidation happens on anode, and only reduction occurs on cathode. Therefore, reactive cationic/anionic species generated on electrodes can be accumulated. In addition, divided cell can be useful for more efficient accumulation of reactive intermediates because an anodic chamber and a cathodic chamber are physically separated.[1c,2]

2) Environmentally benign reaction system

Unlike traditional oxidation/reduction require the utilization of the stoichiometric amount of oxidants/reductants which are derived from petroleum and heavy metals, electron transfer

induced by potential energy (electric energy) is driving force in electrolysis. This is why it is called green synthetic toolbox.

3) Facile manipulation and precise reaction control

In electrolysis, we can control electrochemical redox reactions on a switchable manner. Potentiostat and galvanostat allow us to tune current or potential precisely.

4) Scalable

As electron transfer itself is “reagent” in electrochemical reactions, scaling up leads to cost effective. Moreover, the high reproducibility of scaling up has been achieved in a lot of previous reports.[3]

On the other hand, electrolysis has also some issues to be overcome:

1) Electrolyte is prerequisite

In electrolysis, electric double layer has to be made on the surface of electrodes to apply potential energy. Hence, electrolyte is necessary to ensure conductivity. Electrolyte can be waste and has to be separated from products.

2) Many parameters to be optimized

A lot of parameters need to be tuned to accomplish optimization of electrochemical reactions. Not only solvents, concentration of substrates, temperature, but also electrode materials, electrolytes, current density, etc...

In particular, electrolytes and electrode materials have significant impact on reaction efficiency. Although these factors can be issues in electrochemistry, they can also be the keys to control the reactions. However, in the most cases the effects of electrolytes and electrode materials have not been disclosed. Thus, I decided to work on these two topics to illuminate their roles.

1-2. Electro-catalytic cycloadditions with unique electrolyte $LiClO_4/CH_3NO_2$

Our laboratory has been developing electrochemical C-C bond formations via radical cation species.[1] For examples, [4+2] cycloaddition (radical cation Diels-Alder reaction)[1a] and [2+2] cycloaddition[1b] were established (Scheme 1). In both cases, electron transfer itself catalysts them, which means that only catalytic amount of electricity is sufficient to

accomplish the reactions (Figure 2).[1a] This will be quite important technology to exploit "electron-catalytic" reactions more and more, resulting in dramatically decreasing the consumption of reagents. However, there is a critical issue to realize it. $LiClO_4/CH_3NO_2$ electrolyte solution is uniquely efficient for our developed reactions via radical cation intermediates, and the reason has not been clear for the last 20 years. Therefore, the strong motivation of elucidating it made me worked on it.

Scheme 1. Electrochemical [4+2] and [2+2] cycloadditions via radical cation intermediates.

[4+2] cycloaddition

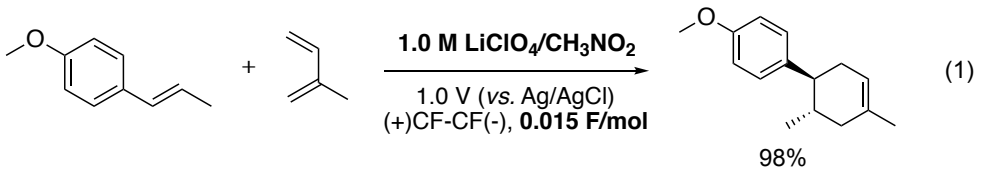

[2+2] cycloaddition

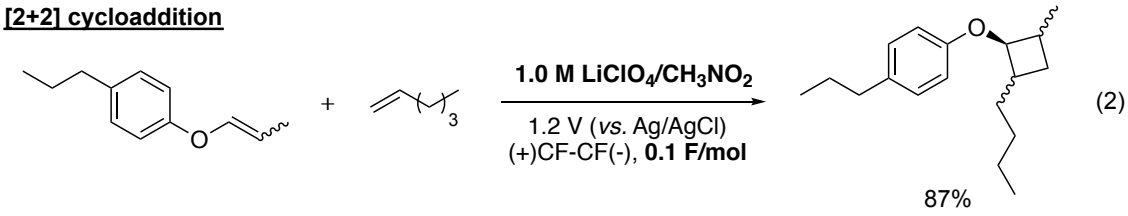

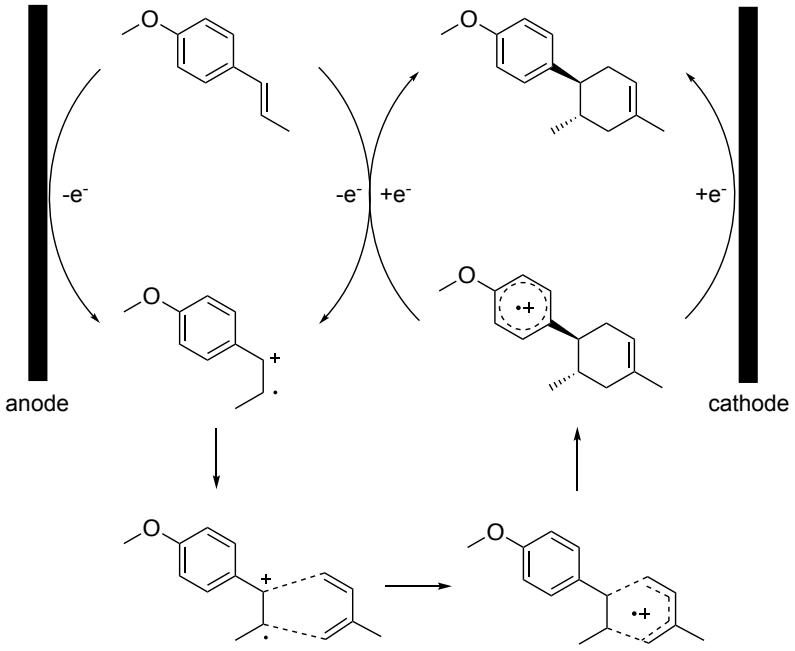

Figure 2. Expected mechanism of radical cation chain cycles for electrochemical [4+2] cycloadditions.

1-3. Styrene derivatives and their utility

Styrene is firstly isolated from a natural resin (called storax) in 1839. After many years later, Staudinger established the formation of polystyrene from styrene monomer in 1922 (published in “Die hochmolekularen organischen Verbindungen -Kautschuk und Cellulose-“). This discovery opened the door for polymer science and industry, and styrene captured scientists’ interests. Subsequently, the industrial production method of styrene was established in 1930s. The popular synthetic way of styrene is dehydrogenation of ethylbenzene using metal catalyst. It is said that global styrene production will reach to 33,425 thousand tons in 2023 (reported in “The Global Styrene Market”). Thanks to this innovation, a huge amount of styrene came to be supplied and became available for chemists.

Then, they started to explore a variety of transformation from styrene into functionalized molecules (Figure 3).[1] Today, styrene and its derivatives are one of the important building blocks in organic synthesis[1] as well as in polymer chemistry.[2] Moreover, many natural compounds have been total synthesized using styrene derivatives by organic chemists (examples are shown in Figure 4).[3]

Since styrene and its derivatives are popular molecules both in academy and in industry, a variety of synthetic methodology has been applied for them. While the functionalization of styrenes by traditional chemical approach has been well established, there is still much room to apply radical ion chemistry for it. Single electron transfer (SET) strategy which can generate radical cation/anion can be sustainable synthetic method because electron itself is a green reagent. As we have a technology of electrochemistry, it occurred to me that further derivatizations of styrenes would be possible with electrolysis.

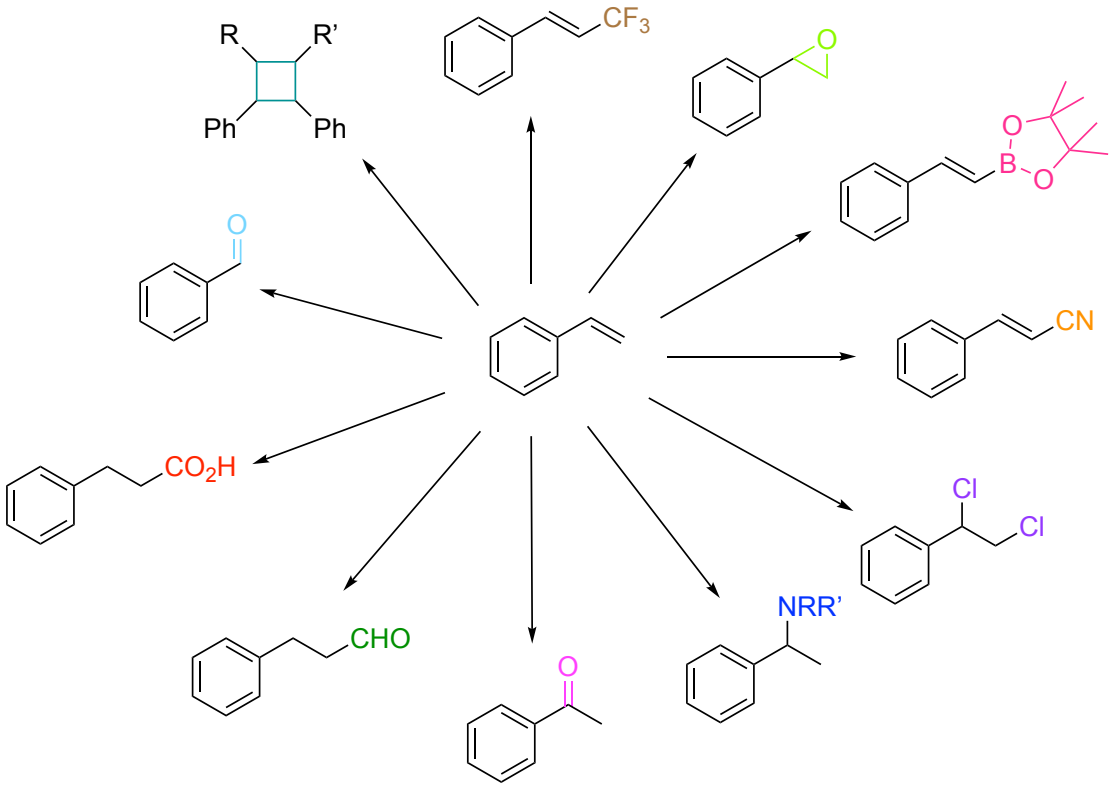

Figure 3. Examples of transformations of styrene.

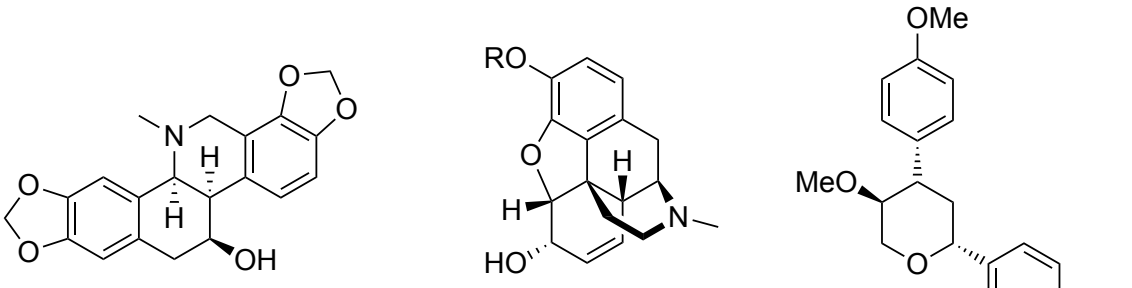

Chelidonine

R = H : **Morphine**
R = Me : **Codein**

(-)-Dimethylsugiresinol

Figure 4. Examples of natural compounds which were total synthesized by organic chemists.

2. Investigation of electrolytes which are effective for C-C bond formation via radical cation species

2-1. Understanding the effect of $LiClO_4$ / NM on radical cation chemistry: leading to the exploration of alternative electrolytes

Introduction

Redox chemistry has raised a great attention in recent years. In particular, safe and green redox process, such as homogeneous photoredox catalysts,[1,2] heterogeneous photocatalysts[3] and electrochemistry,[4–6] has been intensively exploited. These redox toolboxes allow unique chemical conversions which have not been accomplished by traditional organic chemistry.

During our continuous research on redox chemistry, we previously showed that anions have a critical impact on radical cation species which are generated by single electron transfer (SET).[7] In that study, we were firstly interested in the notably lowered reaction efficiency of radical cation Diels-Alder reaction under electrochemical condition compared to photoredox conditions. We attributed this difference to the effect of anions derived from supporting electrolyte. To prove this hypothesis, Ru-catalyzed photoredox Diels-Alder reactions were carried out in the presence of additional salts. The result showed that the more donating anions are, the less efficient the reaction was. We also demonstrated that the addition of fluorinated alcohol such as 1,1,1,3,3,3-hexafluoroisopropanol (HFIP) and 2,2,2-trifluoroethanol (TFE), which are known to bind anions due to their strong hydrogen-bond donation, can cancel the effect of anions and ensure the reactivities of radical cations.

Very recently, Yoon and co-workers reported quite similar discovery on the anions effect on Ru-catalyzed radical cation Diels-Alder reactions.[8] They showed counter-anions have an influence on both radical cation species initiation and the chain propagation. The modulation of ion-interactions was performed to optimize the radical cation reactivities.

Based upon those studies, electrochemically-generated radical cations has to receive the negative effects of anions more crucially since the use of stoichiometric amount of supporting electrolytes is prerequisite. Then, we proposed that using fluorinated alcohol like as HFIP or TFE as a solvent or additive could be helpful to achieve electrochemical radical ion reactions.[7] On the other hand, the use of lithium salt/nitroalkane has been recognized as an effective electrolytes for electrochemical cycloadditions[9-17] and metathesis[18] via radical cations. In spite of its versatility, this electrolyte effect has been unclear for the last 20 years.

In order to confirm the effect of lithium salt and solvent in radical cation chemistry, we firstly explored alternative salts for $LiClO_4$ for radical cation Diels-Alder reaction as a model reaction (Table 1). *Trans*-Anethol (**1**) and isoprene (**2**) were used as model substrates. Also, we utilized TON (turnover number) as comparison criteria to evaluate the efficiency of radical cation reactions. The reaction proceeded smoothly when 1.0 M solution of $LiClO_4$, LiFSI (lithium bis (fluorosulfonyl)imide) and LiTFSI (lithium bis(trifluoromethanesulfonyl)imide) in $MeNO_2$ were used as electrolytes with almost 10 TON of electron-catalysis (Table 1, Entry 1-3). 1.0 M $LiClO_4$ in $EtNO_2$ afforded almost same result (Entry 4). Since $LiClO_4$ was not dissolved in 1-$PrNO_2$, 0.3 M LiTFSI solution (the solubility was still restricted up to 0.3 M) was prepared and showed its feasibility for this reaction with TON of 3.3 (Entry 5). Interestingly, the higher concentration of $LiClO_4$, the higher TON was (Entry 6, 7). On the other hand, diluted supporting electrolyte offered lowere TON (Entry 8). It is important that the use of tetrabutylammonium cation instead of lithium cation or highly donating solvent (MeCN) apparently decreased the reactivity (Entry 9, 10). In addition, the other Li-salts were not effective compared to LiFSI and LiTFSI (Entry 13-15). These results were also observed in electrochemical [2+2] cyclization via radical cation (Table 2).

Table 1. Summary of electrolytes effects on radical cation Diels-Alder reaction.

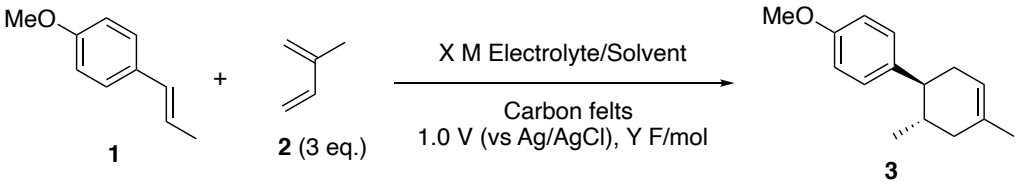

1 **2** (3 eq.) **3**

Entry[a]	Electrolyte	X, (M)	Solvent	Y, (F/mol)	Yield,[b] (%)	TON
1	$LiClO_4$	1.0	$MeNO_2$	0.1	98	10
2	$LiClO_4$	1.0	$EtNO_2$	0.1	98	10
3	$LiClO_4$	1.0	$MeNO_2$	0.03	46	15
4	$LiClO_4$	2.0	$MeNO_2$	0.03	58	19
5	$LiClO_4$	0.1	$MeNO_2$	0.1	81	8.1
6	Bu_4NClO_4	1.0	$MeNO_2$	1.0	11	0.11
7	$LiClO_4$	1.0	MeCN	1.0	6	0.06
8	LiFSI	1.0	$MeNO_2$	0.1	98	10
9	LiFSI	0.1	$MeNO_2$	0.1	72	7.2
10	LiTFSI	1.0	$MeNO_2$	0.1	98	10
11	LiTFSI	0.1	$MeNO_2$	0.1	76	7.6

12[c]	LiTFSI	0.3	1-$PrNO_2$	0.3	98	3.3
13	$LiBF_4$	0.1	$MeNO_2$	0.1	30	0.3
14	$LiPF_6$	1.0	$MeNO_2$	0.1	0	0
15	LiOTf	0.1	$MeNO_2$	0.1	69	6.9

[a] All reactions were performed on a 1.0 mmol scale of **1** and 3 eq. **2** in 10 mL of electrolyte solution at room temperature under constant potential electrolysis (1.0 V vs. Ag/AgCl) otherwise noted. [b] Yields were determined by ^1H NMR analysis using benzaldehyde as an internal standard. [c] 1.2 V (vs Ag/AgCl) was applied.

Table 2. Summary of electrolytes effects on electrocatalytic [2+2] cyclization via radical cation.

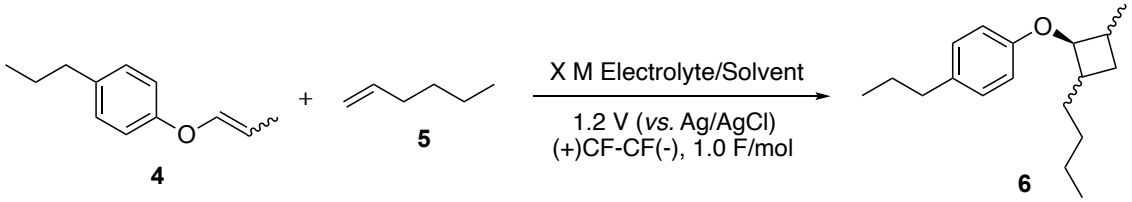

Entry[a]	Electrolyte	X, (M)	Solvent	Yield,[b] (%)	TON
1	$LiClO_4$	1.0	$MeNO_2$	87	0.87
2	LiFSI	1.0	$MeNO_2$	88	0.88
3	LiTFSI	1.0	$MeNO_2$	90	0.90
4	$LiBF_4$	0.1	$MeNO_2$	30	0.30
5	$LiPF_6$	1.0	$MeNO_2$	0	0
6	LiOTf	0.1	$MeNO_2$	17	0.17
7	$LiClO_4$	1.0	$EtNO_2$	85	0.85
8	LiTFSI	0.3	1-$PrNO_2$	79	0.79
9	$LiClO_4$	0.1	$MeNO_2$	77	0.77
10	$LiClO_4$	2.0	$MeNO_2$	91	0.91
11	Bu_4NClO_4	1.0	$MeNO_2$	12	0.12
12	$LiClO_4$	1.0	MeCN	0	0

[a] All reactions were performed on a 0.1 mmol scale of **5** and 20 eq. **6** in 10 mL of electrolyte solution at room temperature under constant potential electrolysis (1.2 V vs. Ag/AgCl). [b] Yields were determined by ^1H NMR analysis using benzaldehyde as an internal standard.

We have confirmed that at least all of lithium cations, perchlorate or sulfonimide anions, and nitroalkane are crucial, and reactivities are suppressed when lacking of these components. In this chapter, mechanistic aspects into their electrolyte's role in electrochemical radical cation reactions are elucidated by analogy with fluorinated alcohols.

What are common properties between lithium salt/nitroalkane and fluorinated alcohol-based electrolytes is described in Figure 1. Nitroalkane is a polar and less-donating

solvent. Hence, lithium cations are weakly coordinated by nitroalkane, showing their strong Lewis acidity.[19,20] Lithium cations could contact with anions to generate contact ion pairs or aggregation especially in highly concentrated conditions. Here, we hypothesized that the coordinated anions demonstrate weaker donating ability, resulting in the efficient reactivities of radical cation intermediates.

Lithium salts/nitroalkane

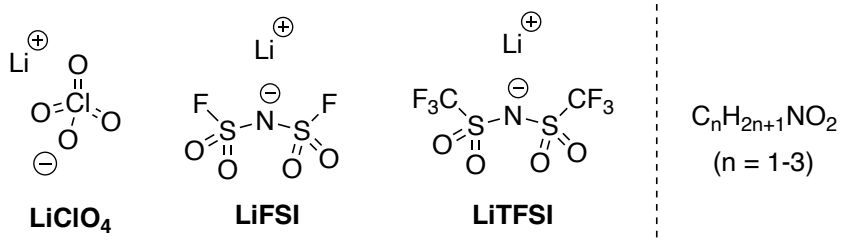

- Lewis acidic Li cation to bind anions
- Nitroalkane is polar and less donating

Fluorinated alcohols

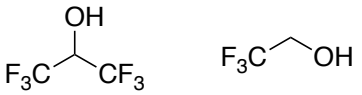

- Strong hydrogen bond donors to bind anions

Figure 1. Properties of lithium salts/nitroalkane and fluorinated alcohols.

Although the features of fluorinated alcohols are explained in the past literatures,[21,22] they are recognized as polar solvents and strong hydrogen-bond donors. Owing to these properties, they can capture anions.

To deeper understand the effect of the concentration of lithium salts in nitroalkane, Raman and NMR measurements were carried out.

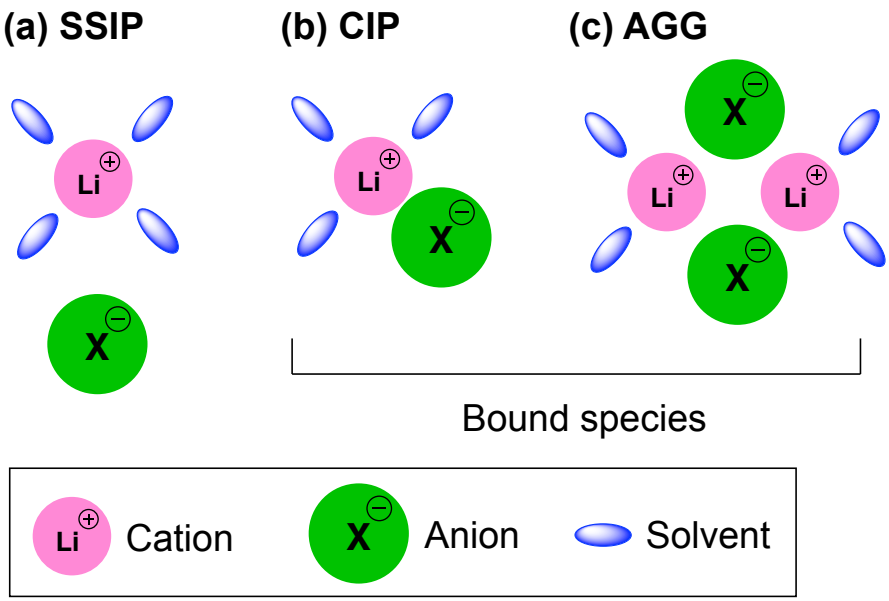

Figure 2. Conceptual figures of (a) solvent separated ion pair (SSIP), (b) contact ion pair (CIP), (c) aggregation (AGG).

In lithium ion battery field, the in-situ structure of electrolytes has been intensively examined. Many previous works demonstrated that the states of lithium salts in solution can change depending on the concentration by Raman spectroscopy. From diluted conditions to higher concentrated conditions, the complex structure changes from a solvent-separated ion pair (SSIP) to a contacted ion pair (CIP) and an aggregate (AGG) species (Figure 2).[25–34] This shift is explained by the change of the corresponding peak fraction of Raman spectra. The titration of different concentration of LiFSI and LiTFSI in $MeNO_2$ was performed by Raman spectroscopy (Figure 3,4). We focused on the peak shifts around 700-800 cm^{-1} which arises from S-N-S vibration mode because this region has been often observed to investigate the structure change of LiFSI[26-28] (Figure 5a) and LiTFSI[29-31] (Figure 5b). In the case of LiFSI, three distinct peaks, SSIP (727 cm^{-1}), CIP (737 cm^{-1}) and AGG (751 cm^{-1}) were observed by peak fitting. Although these numbers are slightly higher than those of previous reports,[26-28] this difference is attributable to the less donating ability of $MeNO_2$. It is confirmed that the higher ration of bound species (CIP and AGG) is, the higher concentrated lithium salt is. The free anions seem not to be in the solution more than 1.5 M concentration. As for LiTFSI in $MeNO_2$, two distinct peaks of SSIP (742 cm^{-1}) and bound species (749 cm^{-1}) were detected by peak fitting. These are in grate agreement with previous literatures.[29-31] This solution also showed that the higher concentration of lithium salts, the more dominant the bound species are. Then, we tried Raman spectroscopy analysis of $LiClO_4/MeNO_2$ solution, but the detailed peak fitting was difficult because the peaks of $LiClO_4$ was mostly overlapped by that of $MeNO_2$ (Figure 5c).

However, the appearance of 942 cm^{-1} peak supports that the existance of bound species of $LiClO_4$ due to the accordance to previously reports (SSIP, CIP and AGG peaks at 933, 939 and 946 cm^{-1} in $LiClO_4$/tetraglyme.[34]). Moreover, $LiClO_4$ is known that it is aggregates on concentrated conditions in $MeNO_2$ by IR spectroscopy study.[35]

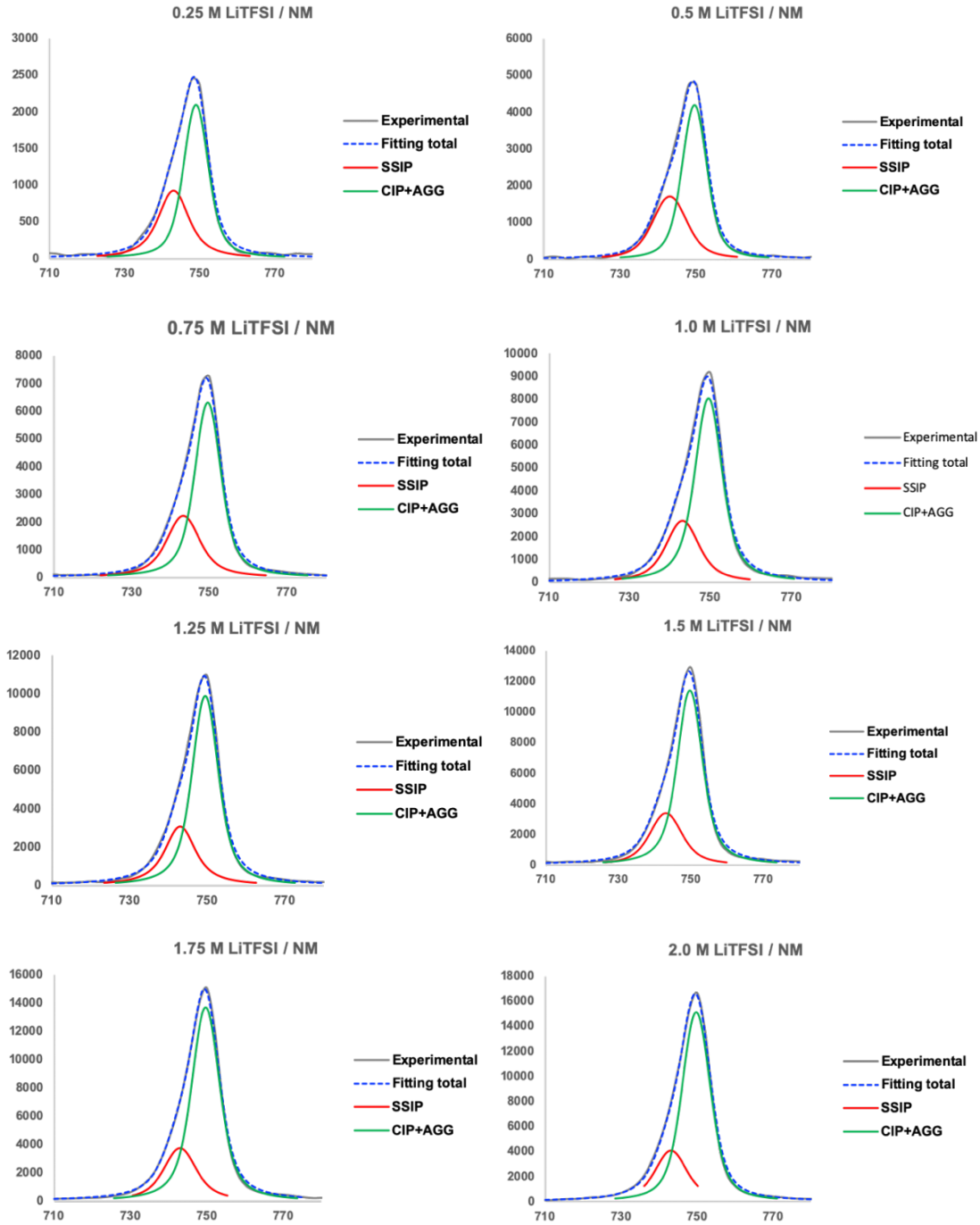

Figure 3. Peaks of Raman spectroscopy in the range of 710-780 cm^{-1} of 0.25-2.0 M LiTFSI/$MeNO_2$.

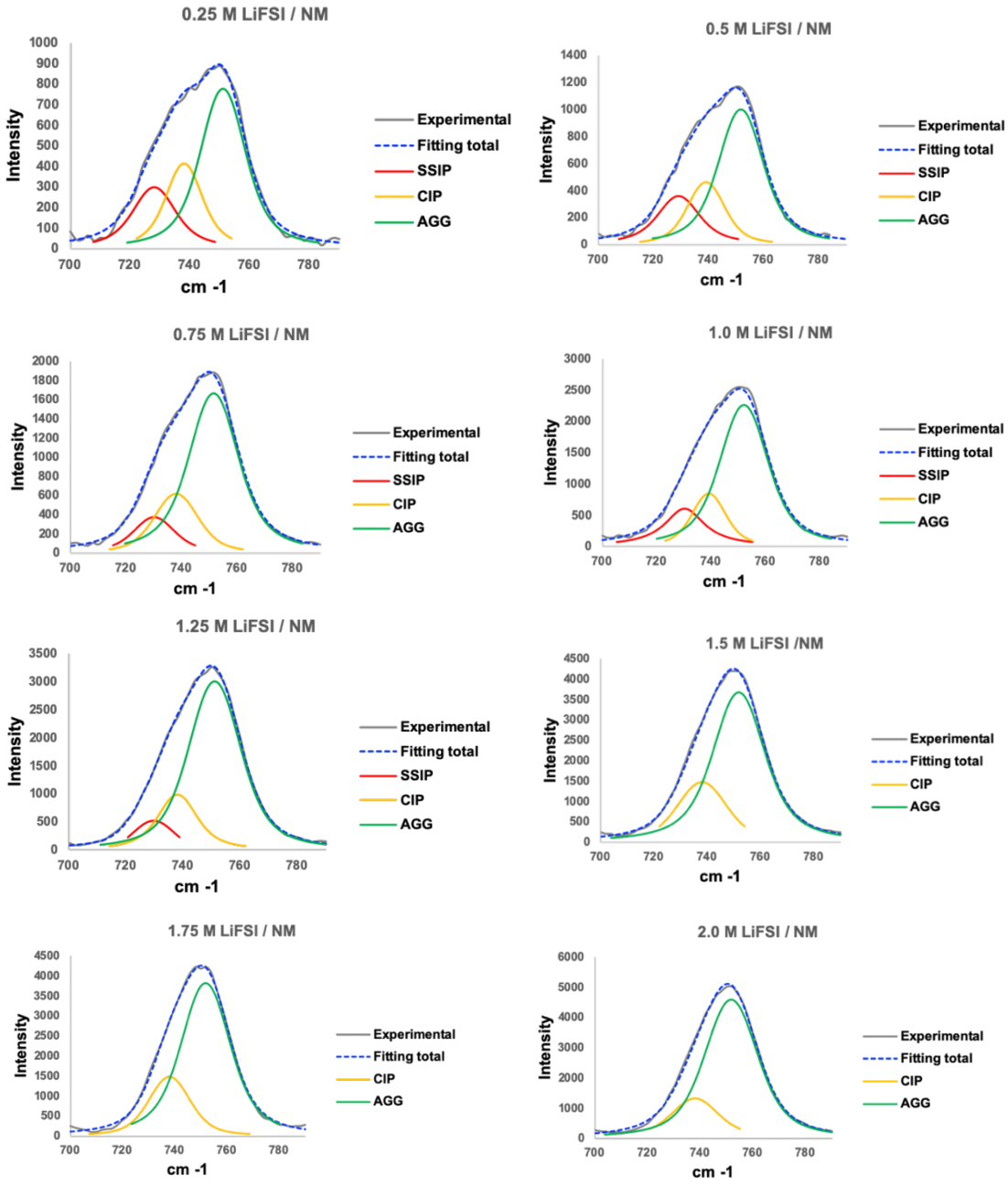

Figure 4. Peaks of Raman spectroscopy in the range of 700-790 cm^{-1} of 0.25-2.0 M LiFSI/$MeNO_2$.

a)

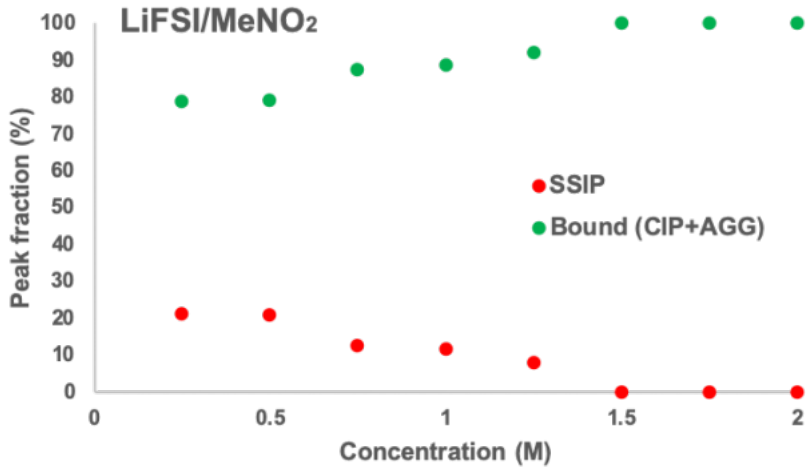
LiFSI/MeNO2
Peak fraction (%)
Concentration (M)
SSIP
Bound (CIP+AGG)

b)

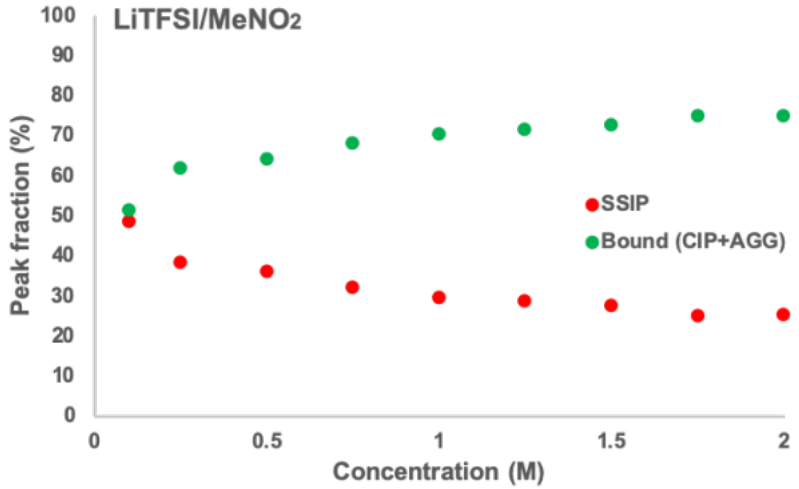
LiTFSI/MeNO2
Peak fraction (%)
Concentration (M)
SSIP
Bound (CIP+AGG)

c)

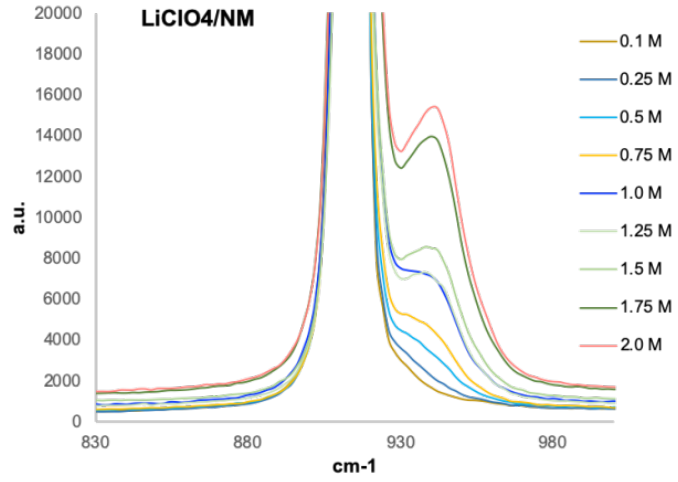
LiClO4/NM
a.u.
cm-1
0.1 M
0.25 M
0.5 M
0.75 M
1.0 M
1.25 M
1.5 M
1.75 M
2.0 M

Figure 5. The shifts of peak fractions of concentration dependence in Raman spectroscopy and chemical shifts in ^{7}Li NMR spectroscopy. (a, b) Peak fraction for Raman spectroscopy of (a) LiFSI, (b) LiTFSI and (c) $LiClO_4$ in $MeNO_2$.

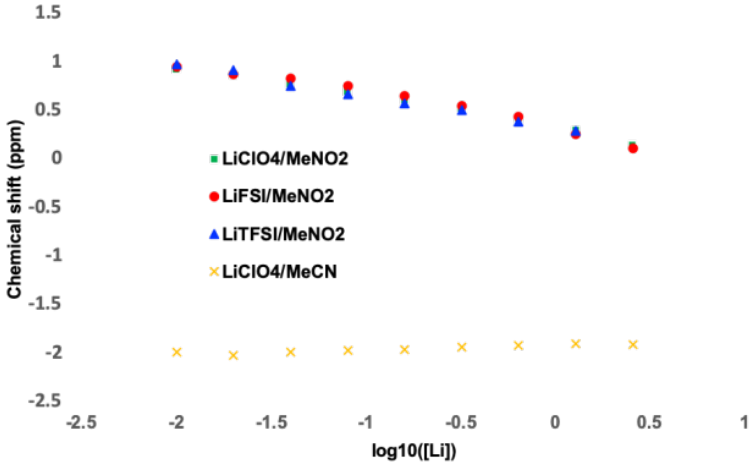

Figure 6. Plots of ^{7}Li NMR chemical shift versus concentration of Li salt in $MeNO_2$ and MeCN. LiCl in D_2O was used as an external standard. NMR data point for LiTFSI at 2.56 M (log10[Li] = 0.408) is not shown due to the insolubility of the salt at this concentration.

Next, we conducted ^{7}Li NMR investigation with different concentration of lithium salts in $MeNO_2$ and MeCN (Figure 6). In $MeNO_2$, the chemical shift of Li^+ of $LiClO_4$, LiFSI and LiTFSI shifted in higher magnetic fields. This suggests that the higher electron density of Li^+ is derived from the more coordinating anions on higher concentrated conditions, which means CIP and/or AGG are formed. Significantly, the chemical shifts of Li^+ of $LiClO_4$ in MeCN were not rarely shifted. This is probably because the strong Lewis basicity of MeCN leads to the dominant coordination of Li^+-MeCN even on concentrated conditions.

Then, we moved on to cyclic voltammetry (CV) studies with different concentration of supporting electrolytes. In $LiClO_4$/LiFSI/LiTFSI in $MeNO_2$ solution, the oxidation potentials of **1** were lowered with higher concentration (Figure 7). The negative shifts of oxidation potentials are recognized as the effect of more stable oxidant species (**1**$^{\bullet+}$).[37] This phenomenon was also observed when using HFIP and TFE as a solvent or additives.[7] On the other hand, when using Bu_4NClO_4/$MeNO_2$, which is known to have free cations and anions in the solution, the oxidation peaks of **1** were rarely shifted up to 2.0 M. Based on these outcomes, the bound anions in higher concentration give less coordination to radical cation intermediates, leading to the stability.

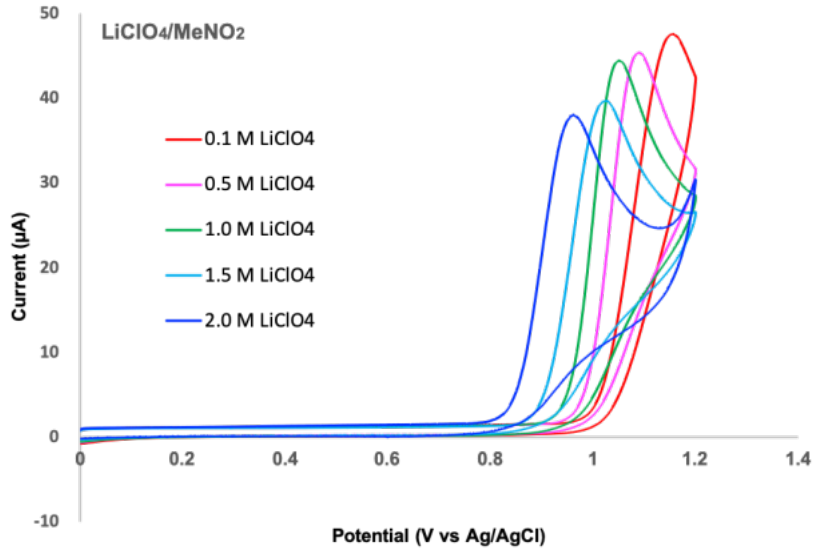
LiClO4/MeNO2
0.1 M LiClO4
0.5 M LiClO4
1.0 M LiClO4
1.5 M LiClO4
2.0 M LiClO4
Current (µA)
Potential (V vs Ag/AgCl)

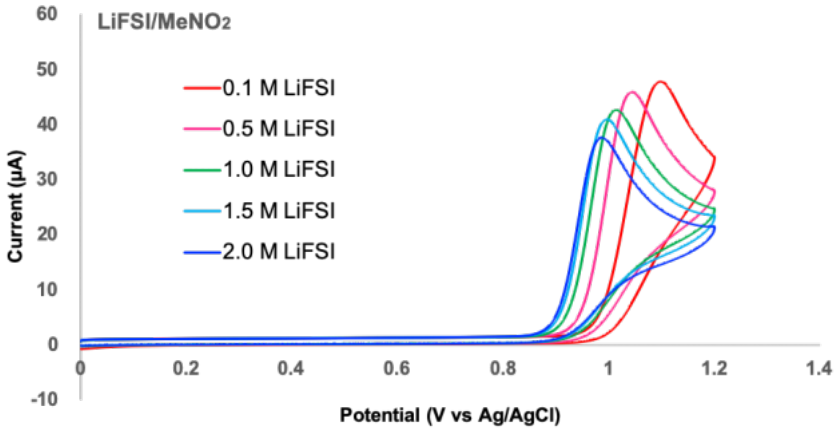
LiFSI/MeNO2
0.1 M LiFSI
0.5 M LiFSI
1.0 M LiFSI
1.5 M LiFSI
2.0 M LiFSI
Current (µA)
Potential (V vs Ag/AgCl)

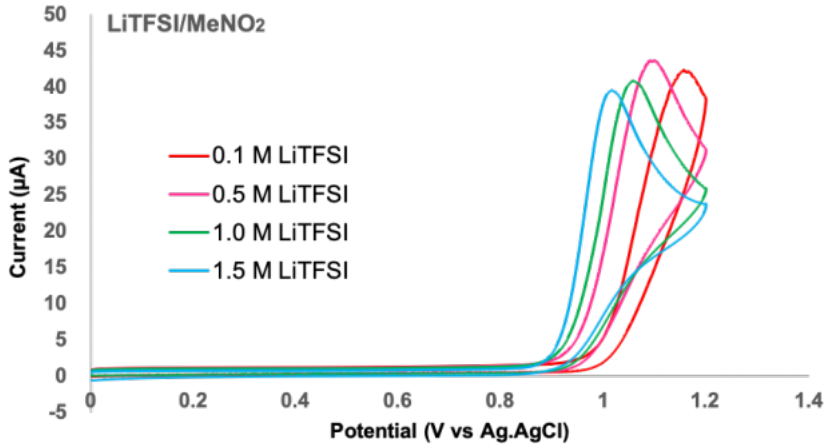
LiTFSI/MeNO2
0.1 M LiTFSI
0.5 M LiTFSI
1.0 M LiTFSI
1.5 M LiTFSI
Current (µA)
Potential (V vs Ag.AgCl)

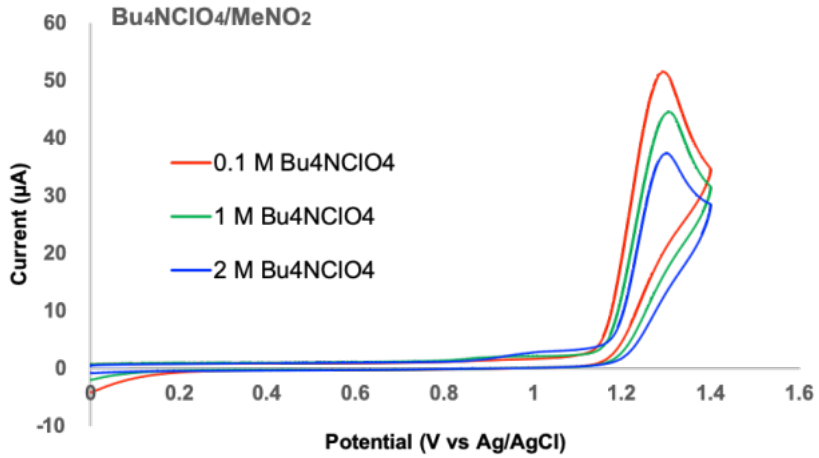

Figure 7. Cyclic voltammograms of **1** (2 mM) measured at a scan rate of 100 mV/s with different lithium salts or Bu_4NClO_4 in $MeNO_2$. 2.0 M of LiTFSI was not completely soluble in $MeNO_2$.

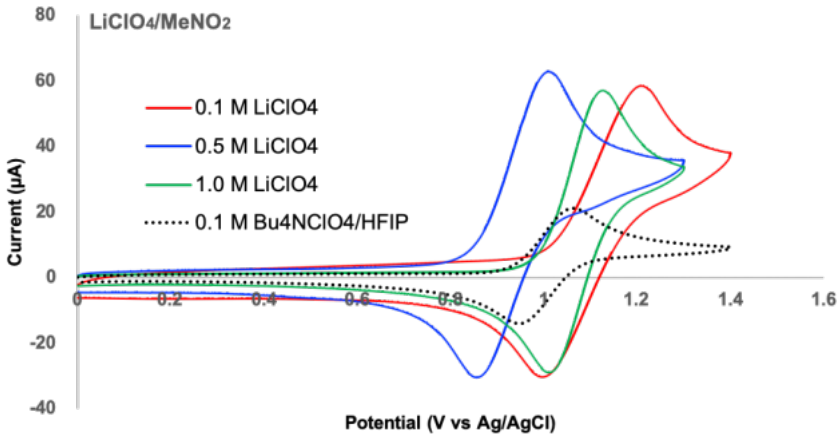

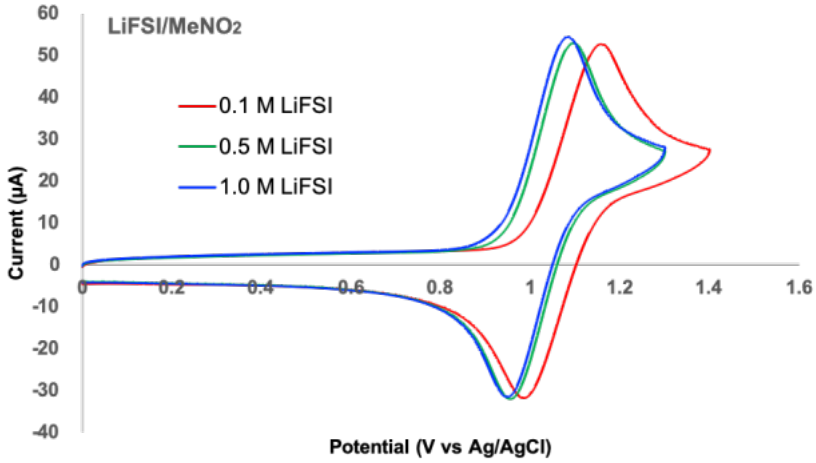

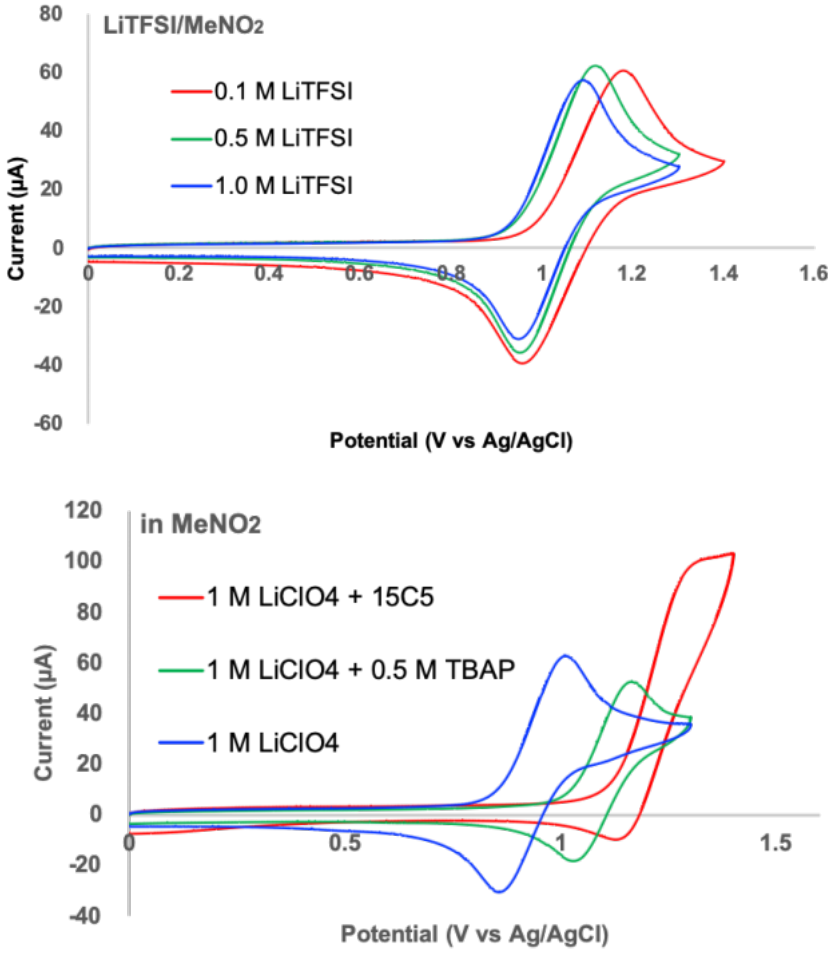

Figure 8. Cyclic voltammograms of **4** (2 mM) measured at a scan rate of 100 mV/s with different lithium salts or additives of Bu_4NClO_4 and 15-crown-5-ether.

Furthermore, we previously reported that 1,4-dimethoxybenzene (**4**) for CV analysis is very instructive as the corresponding radical cation is more stable than $\mathbf{1}^{\bullet+}$ and show the reversibility of its redox events in the presence of less donating anions.[7] We performed CV measurements with different electrolytes using **4** in the same way (Figure 8). As expected, the oxidation potentials of **4** were negatively shifted with increasing Li-salt concentration, agreeing to those of **1**. In particular, the oxidation potential of **4** in 1.0 M $LiClO_4/MeNO_2$ is 0.94 V vs Ag/AgCl, which is lower than 1.01 V vs Ag/AgCl in 0.1 M Bu_4NClO_4/HFIP, suggesting 1.0 M $LiClO_4/MeNO_2$ has great stability effect for radical cation species.

Subsequently, the mixed supporting electrolyte of Bu_4NClO_4 and $LiClO_4$ in $MeNO_2$ to increase free ClO_4 anions showed higher oxidation potential of **4**. Moreover, the addition of 1.0 M 15-crown-5-ether (15C5) in 1.0 M $LiClO_4$/NM was tested because the crown ether is known to bind Li cation.[38] The waves of **4** dramatically changed, and the gained cyclic

voltammogram was more similar to irreversible oxidation wave recorded in 1.0 M $Bu4NClO_4$/NM. All these results agree with the hypothesis that the formation of bound species in Li salts/nitroalkane electrolyte stabilizes the radical cations.

The expected complex structure of lithium salts/nitroalkane are described in Figure 9. In the strong Lewis basic solvents such as MeCN, anions are free due to the coordination of MeCN to Li^+. Also, in diluted condition of Li salt/nitroalkane, the anions are relatively free in the state of SSIP. In both these medias, anions can coordinate to in-situ generated radical cation intermediates, leading to less efficient reactivities. On the other hand, in the highly concentrated (1.0 M~) Li salt/nitroalkane solution, Li^+ and anions form CIP and/or AGG (bound species). This state enables captured anions and ensures the radical cation reactivities. This effect is quite similar to that of fluorinated alcohols.

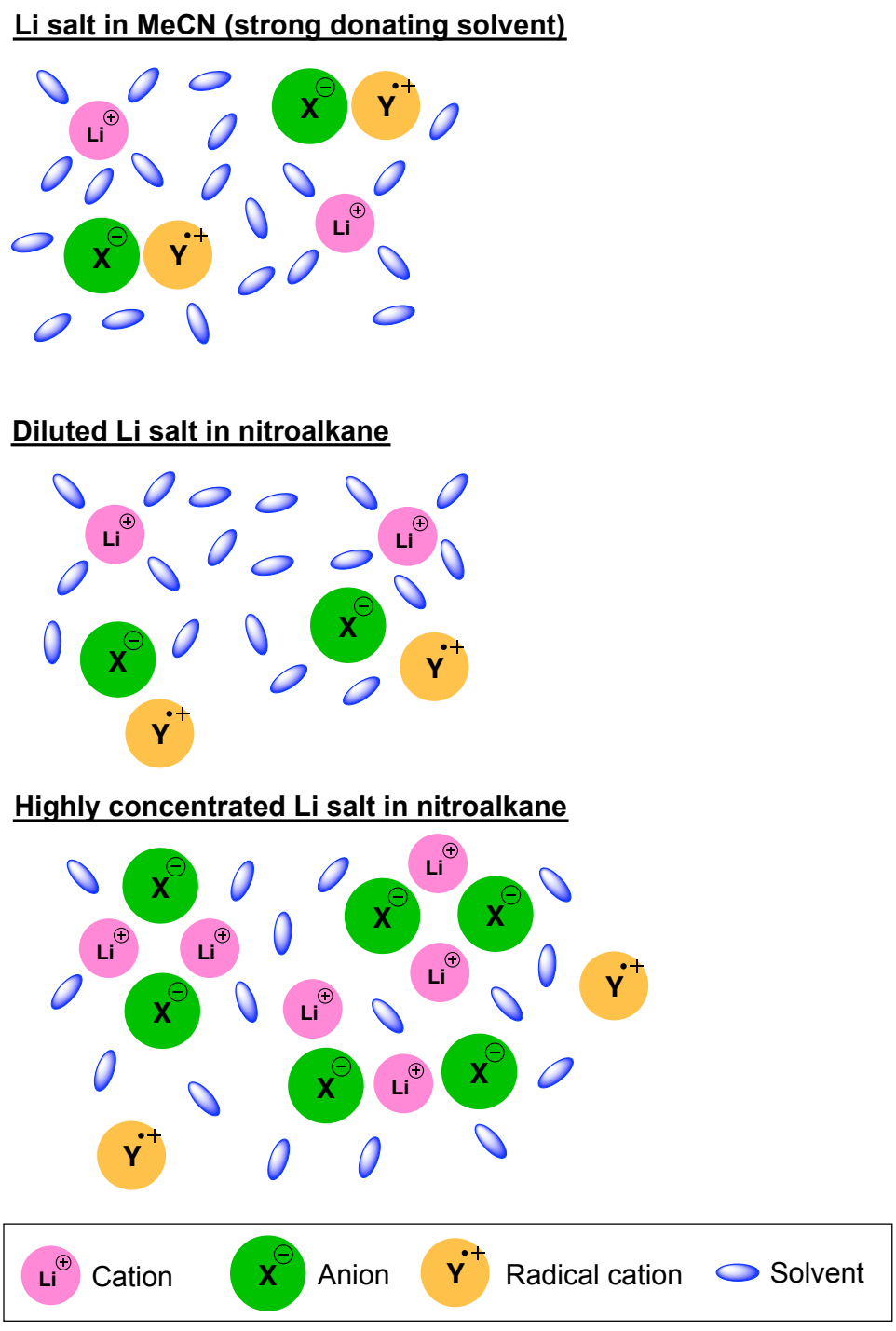

Figure 9. Expected mechanism of electrolyte and radical cation in polar solvent.

In summary, we disclosed the Li salt/nitroalkane effect on radical cation species by Raman, NMR and CV studies. The concept of trapping anions, which is based upon the analogy with fluorinated alcohols, is the key on radical cation chemistry. In both medias, the donating abilities of anions are cancelled, ensuring the inherent reactivities of radical

cations. We believe that this research will be informative for further developments of redox reactions via radical cations.

2-2. Application of LiTFSI / NM electrolytes for electrocatalytic Diels-Alder reactions with lipophilic compounds.

Introduction

Electrochemical methods have proven to be robust redox toolboxes in organic chemistry.[1] Reductive and oxidative single electron transfer (SET) are occurred even under mild conditions by employing electrons as reagents or catalysts.[2] The power of reduction and oxidation can be easily tuned by the potentials applied. The selection of additives/mediators[3] and electrode materials[4] can uniquely have a significant impact on the reactions. The only thing that must be payed attention is that the electrolytic solution must have enough electrical conductivity. This is why polar solvents are usually utilized with a large amount of supporting electrolyte, which would subsequently be a waste. Moreover, substrates have to be soluble in polar electrolytes, which means that the utilization of hydrophobic compounds can be limited. Although some electro-organic chemists developed the reaction systems that allow recycling and/or decreasing supporting electrolyte,[5] the use of hydrophobic compounds remains an significant issue.

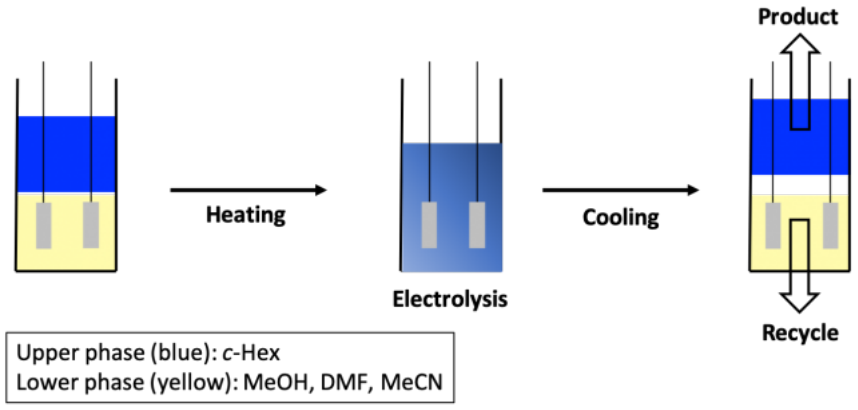

Figure 1. Schematic illustration of electrochemical reactions in thermomorphic systems.

In our previous study, we discovered that cyclohexane (*c*-Hex) can form thermomorphic systems with general polar solvents like as MeOH, MeCN, or DMF, where monophasic and biphasic conditions were reversibly switched by changing temperature (Figure 1).[6] While both hydrophobic and hydrophilic compounds and/or reagents are soluble on the monophasic condition due to its homogeneity, selective separation is enabled on the biphasic condition. This thermomorphic media was tried for some electrochemical

reactions, demonstrating the availability of hydrophobic compounds.[7] Hydrophobic products were selectively collected in the upper phase (*c*-Hex) under biphasic conditions, and the lower electrolytes could be recycled for further reactions.

Our laboratory has been developing reactions which are triggered by anodic oxidation[8] in highly concentrated lithium perchlorate ($LiClO_4$)/nitromethane ($MeNO_2$) electrolytes.[9] As this solution is critical in those reactions, recycling and/or reducing the amount of $LiClO_4$ are highly desired. Although the biphasic medias of *c*-Hex and $LiClO_4$/$MeNO_2$ solution have shown applications,[10] thermomorphic properties were not accomplished, presumably owing to the salting-out effect. Hence, using hydrophobic substrates in $LiClO_4$/$MeNO_2$ solution is still limited. During our continuous research, we recently showed that $EtNO_2$ could work as an alternative to $MeNO_2$ for some reactions,[11] and that lithium bis(trifluoromethane)sulfonamide (LiTFSI) could be taken place of $LiClO_4$ in $MeNO_2$.[9] The question is, LiTFSI/$EtNO_2$ solution can be a less polar electrolyte compared to $LiClO_4$/$MeNO_2$ solution, which can form a thermomorphic system with *c*-Hex? Herein, the discovery of a new thermomorphic system that realizes the reusing of the supporting electrolyte and the use of hydrophobic substrates is reported.

Results and Discussion

Our studies were initiated with the examination of the LiTFSI/$EtNO_2$ solution using an electrocatalytic Diels-Alder reaction of *trans*-anethole (**1**) with isoprene (**2**) as model substrates (Table 1). Previously, we found that the reaction was finished with a catalytic amount of electricity in $LiClO_4$/$MeNO_2$ or LiTFSI/$MeNO_2$ solutions to give the product (**3**) in 98% yields (Entries 1 and 2). The reaction conducted in 0.5 M LiTFSI/$EtNO_2$ solution also afforded **3** in excellent yield (Entry 3). Moreover, *c*-Hex and LiTFSI/$EtNO_2$ solution (vol=1:1) formed a thermomorphic system, becoming a monophasic condition at room temperature and a biphasic condition at -7 °C. In order to check the utility of this media for a hydrophobic substrate, the dienophile (**4**) was synthesized and utilized. However, **4** was rarely soluble in a 1:1 (v/v) mixture of *c*-Hex and 0.5 M LiTFSI/$EtNO_2$ solution. This was confirmed by cyclic voltammetry (CV), showing that no significant oxidation peak was observed (Figure 2).

Table 1. Electrocatalytic Diels-Alder reaction of *trans*-anethole (**1**).

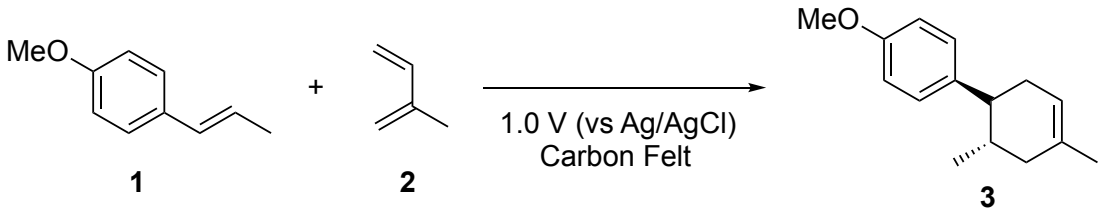

1 **2** **3**

Entry[a]	Conditions	Yield (%)[b]
1	1.0 M $LiClO_4/MeNO_2$, 0.1 F/mol	98
2	1.0 M LiTFSI/$MeNO_2$, 0.1 F/mol	98
3	0.5 M LiTFSI/$EtNO_2$, 0.2 F/mol	97
4	0.3 M LiTFSI/$PrNO_2$, 0.3 F/mol	98

[a] All reactions were carried out on a 0.1 mmol scale of **1** with 3 eq. of **2** in a 10 mL nitroalkane solution at r.t.; [b] Determined by ^1H NMR analysis using benzaldehyde as an internal standard.

Then, our interests turned into the utilization of 1-nitropropane ($PrNO_2$) instead of $EtNO_2$. **1** was reacted with **2** gave product **3** in 98% yield in 0.3 M LiTFSI/$PrNO_2$ solution (Table 1, Entry 4). In addition, *c*-Hex with LiTFSI/$PrNO_2$ did not afford a biphasic media even at the freezing point of *c*-Hex, though the media is mixable at room temperature. We finally discovered that methyl cyclohexane (Me-c-Hex) could form a thermomorphic system with LiTFSI/$PrNO_2$ solution, inducing a monophasic condition at room temperature and a biphasic condition at -50 °C. Remarkably, **4** was dissolved in a 1:1 (v/v) mixture of Me-*c*-Hex and 0.3 M LiTFSI/$PrNO_2$ solution and its oxidation peak was observed at 1.0 V (vs Ag/AgCl) in the CV analysis (Figure 3). Delightedly, when **4** was reacted with **2** was conducted in a 1:1 (v/v) mixture of Me-c-Hex and 0.3 M LiTFSI/$PrNO_2$ solution, the corresponding cycloadduct (**5**) was furnished in 98% yield with a catalytic amount of electricity. The product was selectively collected from the upper phase (Me-c-Hex) under the biphasic condition at -50 °C (Scheme 1 and Figure 4). More importantly, the left LiTFSI/$PrNO_2$ solution was able to be reused 5 times (Figure 5).

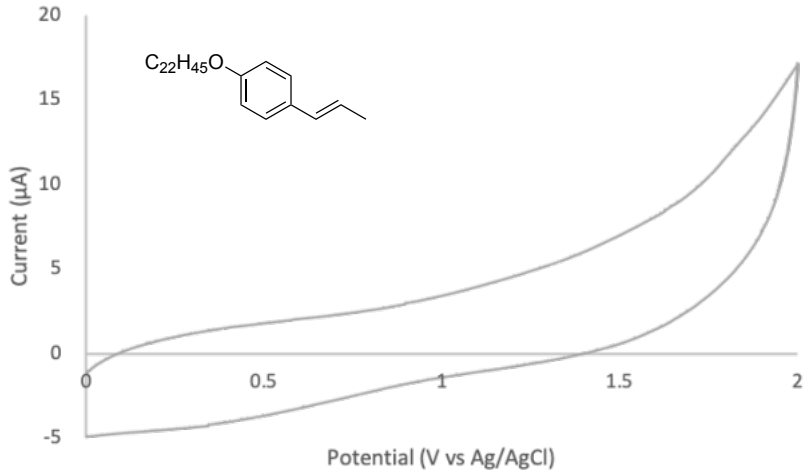

Figure 2. Cyclic voltammograms of the dienophile (**4**) in 0.5 M LiTFSI/$EtNO_2$ solution with *c*-Hex. Scan rate: 0.1 V/sec.

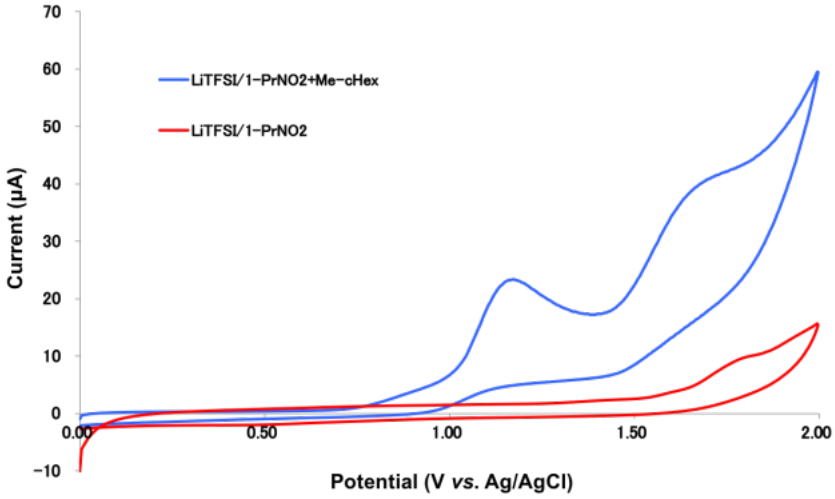

Figure 3. Cyclic voltammograms of the dienophile (**4**) in 0.3 M LiTFSI/$PrNO_2$ solution with (red) or without (blue) Me-*c*-Hex. Scan rate: 0.1 V/s.

Eventually, the scope of dienophiles and dienes was examined to show the potential of the thermomorphic system (Table 2). The Diels-Alder adducts (**6-12**), aside from the cycloadduct (**8**), were yielded in 80-98% yields. In all reactions, catalytic amount of electricity was sufficient to finish the reactions and the hydrophobic products were selectively collected in the upper phase (Me-*c*-Hex) at -50 °C, achieving simple separation processes.

Scheme 1. Electrocatalytic Diels-Alder reaction of **4** and **2**.

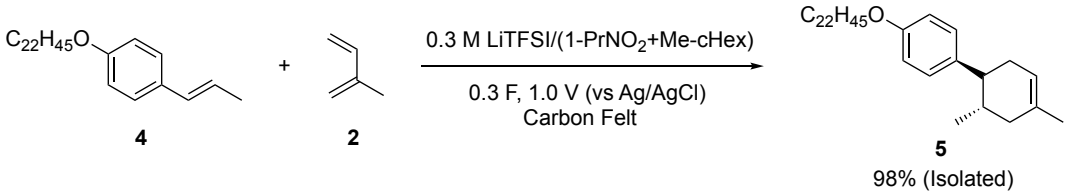

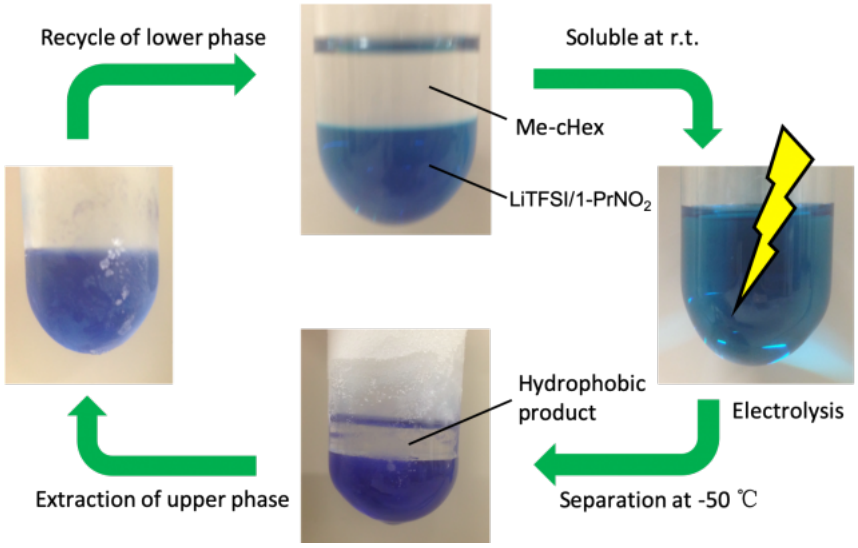

Figure 4. Schematic ilustration of electrochemical reactions in a thermomorphic Me-*c*-Hex-LiTFSI/1-PrNO$_2$ solution. 1-PrNO$_2$ was dyed with methylene blue.

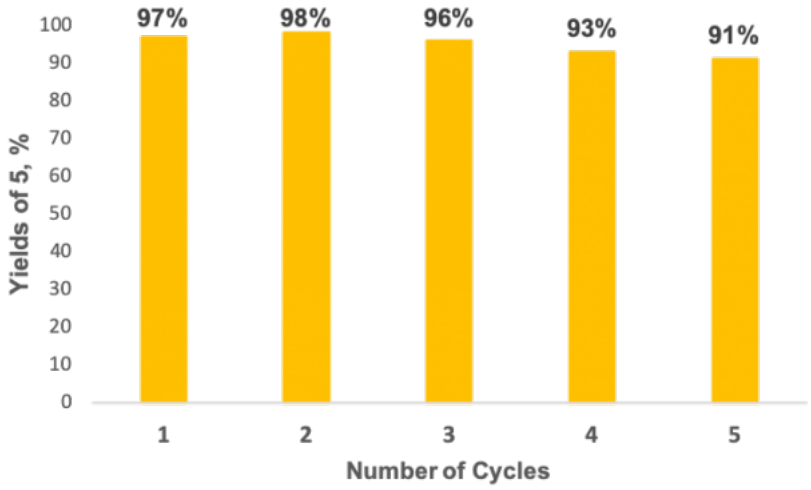

Figure 5. Reusability of LiTFSI/PrNO$_2$ solution.

Table 2. Scope of the dienophiles for electrocatalytic Diels-Alder reactions.[a]

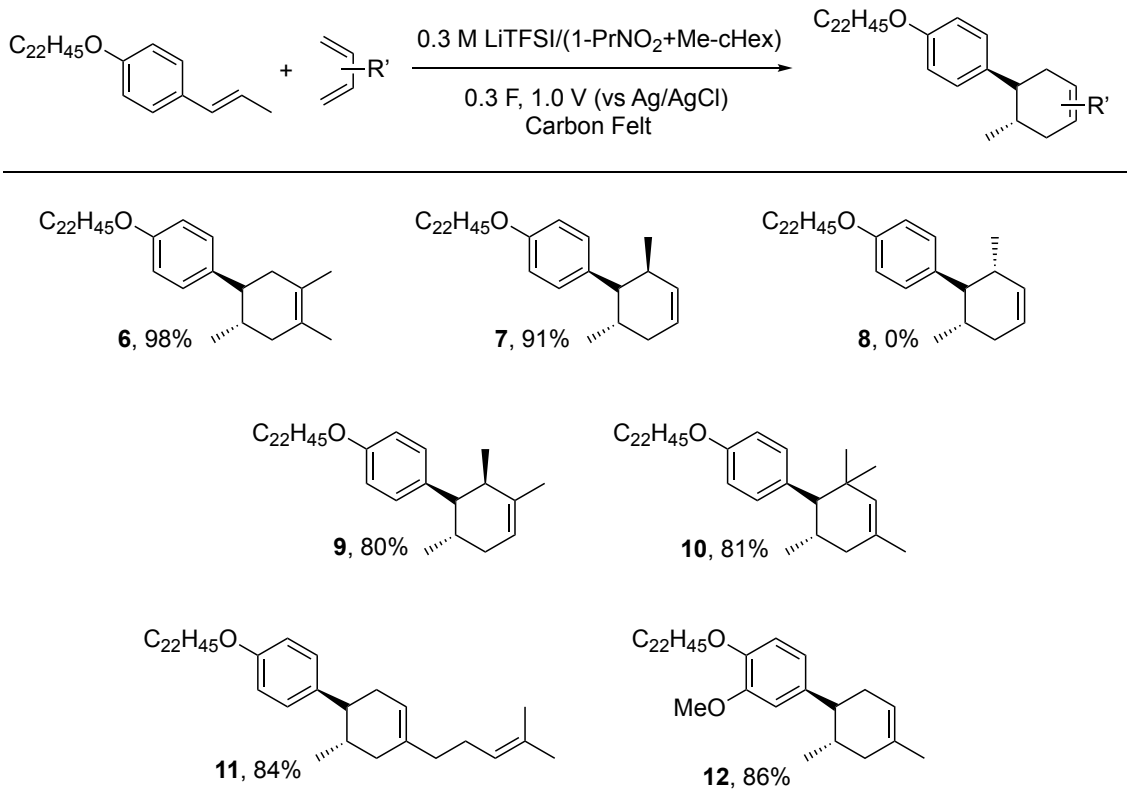

[a] All reactions were carried out on a 0.1 mmol scale of the dienophiles with 3 eq. of dienes at r.t.

Conclusions

In summary, we have showed that the LiTFSI/$PrNO_2$ solution is a less polar alternative to the $LiClO_4$/$MeNO_2$ solution, and it can form a thermomorphic media with Me-*c*-Hex. The monophasic condition at room temperature serves as a less polar electrolyte solution, enabling the use of hydrophobic dienophiles for electrochemical Diels-Alder reactions. The [4+2] cycloadducts could selectively be collected in the upper phase (Me-*c*-Hex) under the biphasic condition at -50 ^{o}C, realizing facile separation process and the recycling of the supporting electrolyte. We believe that our developed thermomorphic media would be utilized for further electrochemical reactions for hydrophobic substrates.

3. Electrode material selective functionalization of styrenes with oxygen: olefin cleavage and tetrahydrofurans formation

Introduction

Electrolysis is a powerful and eco-friendly method for oxidative and reductive conversions.[1] Electrochemical reactions can be tuned by a variety of factors to explore new types of reactivity for a particular compound (such as electrode materials,[2] supporting electrolyte,[3] current density[4]). For instance, our group has disclosed that particular electrolytes could be efficient to achieve some electrocatalytic reactions.[3,5] The effects of electrode materials are also significant. Reticulated vitreous carbon or carbon felt (CF) electrodes have been often used owing to their cost efficiency and versatility. However, unique electrode materials can be effective tools to achieve particular electro-chemical events.[6] The Waldvogel group has intensively developed electrochemical reactions taking advantage of a variety of electrode materials.[6b,c, 7] They showed that different products were gained by utilizing variant electrode materials from the same starting material (Pummerer's ketone with platinum electrode and phenol-coupling product with boron-doped diamond electrode).[6b,8] Recently, Xu has also achieved cathode-material selective derivatization of ketoximes.[9] Moreover, Koper demonstrated that Au electrodes afforded dimethyl carbonate from CO and methanol, but Pt did methyl formate.[10] Those examples prove that electrode materials play a significant role in product selectivity.

Styrenes are important structural motifs in organic chemistry. Hence, a lot of derivatizations of styrenes have been reported, such as hydrocarboxylations,[11] hydroformylations,[12] aminations[13] and so forth.[14] One of the examples that has received a great attention in recent years is the oxidative C=C cleavage.[15] Conversion of olefins into carbonyls in one step is straightforward and cost-effective. To replace traditional ozonolysis[16] because of the toxicity, many scientists have exploited alternative toolboxes using transition-metal catalysts,[15b,c] radical initiators,[15d,e] photocatalysts[15f-h] and organocatalysts.[15i] These methods are superior in that molecular oxygen, which is safer and sustainable, is used as the oxidant and oxygen resource. Nevertheless, there are still negative points, such as expensive cost, toxicity, high temperature, specific wavelength light source, or troublesome manipulation. Hence, simpler and cleaner methods are highly demanded. Another important property of styrene is that they can induce cyclization.[17] A variety of methods, such as chemical oxidation,[17a] photo-redox,[17b,c] energy transfer,[17d] and electrochemistry,[17e] have been developed to obtain cycloadducts. However, cyclizations involving C-O bond formation via radical ions of styrenes have hardly been

developed.[18] Moreover, cycloadditions between electron-deficient styrenes are still difficult, which could be due to its relatively low nucleophilicity.

Here, electrode material (platinum and carbon) selective conversion of styrenes with O_2 into carbonyl compounds and tetrahydrofurans (THF) are described. Furthermore, electrochemical analysis spotlighted why Pt and carbon electrodes offer different reactions.

Results and Discussion

Our research was initiated with the optimization of the electrochemical C=C cleavage (Table 1). We selected 1,1-Diphenylethylene as a model compound. It was delighted that the olefin cleavage was accomplished in 78% yield with Pt electrodes (entry 1). CH_3NO_2 as a solvent also yielded the product in a similar reactivity (entry 2). The use of Pt for both anode and cathode was more efficient than CF electrodes (entries 3-4). Unexpectedly, THF product **1c** was gained predominantly when anode was CF. We found that 6 F/mol and 1.3 mA/cm^2 were the optimal electrolytic conditions (entries 5 and 8). The screening of supporting electrolytes showed Bu_4NClO_4 is the most efficient (entries 6,7). O_2 and electrolysis were necessary in this reaction (entries 9,10).

Table 1. Optimization of the electrochemical olefin cleavage.[a]

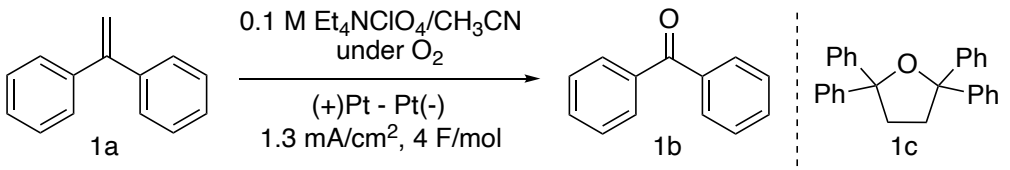

Entry	Deviation from standard conditions	**1b**, Yield[b] (%)
1	None	78
2	CH_3NO_2 instead of CH_3CN	72
3	(+)CF - CF(-) instead of (+)Pt - Pt(-)	11
4	(+)Pt - CF(-) instead of (+)Pt - Pt(-)	68
5	5 mA/cm^2 instead of 1.3 mA/cm^2	63
6	Et_4NBF_4 instead of Et_4NClO_4	72
7	Bu_4NClO_4 instead of Et_4NClO_4	88
8	**6 F/mol and Bu_4NClO_4 instead of 4 F/mol and Et_4NClO_4**	**96**
9	Under Ar	trace
10	Without electrolysis	trace

[a] All reactions were carried out on a 0.5 mmol scale of 1,1-diphenylethylene in a 10 mL solution saturated with O_2 in an undivided cell at room temperature. [b] Isolated yields. CF = Carbon Felt, Pt = Platinum.

As we could optimize the conditions, we examined the scope of the oxidative C=C cleavage (Scheme 1). A variety of styrenes were reacted in 50-96% yields. *α*-Methylstyrene derivatives (**2a**–**5a**) afforded the corresponding ketones in good yields (**2b**-**5b**). Styrene (**6a**) and *β-cis/trans*-methylstyrene resulted in moderate yields (**7a**-**8a**). A bulky substituent (**9a**) could be transformed. Electron-poor styrenes and halogen substituents (**10a**-**14a**) yielded the carbonyls in good to high yields. Notably, Bexarotene (Targretin), which is an anti-cancer agent for cutaneous T-cell lymphoma, was functionalized in 52% yield (**15b**).

Scheme 1. Scope of oxidative cleavage of olefins. Electrolysis was carried out in a 10 mL solution saturated with O_2 on a 0.5 mmol scale of substrate in an undivided cell at RT. [a] Yields were determined by GC/MS integration. [b] CH_3NO_2 was used as solvent. [c] 7 F was applied. [d] 3 F was applied. [e] 4 F was applied. [f] 5 F was applied. [g] 0.1 mmol substrate was used due to solubility issue.

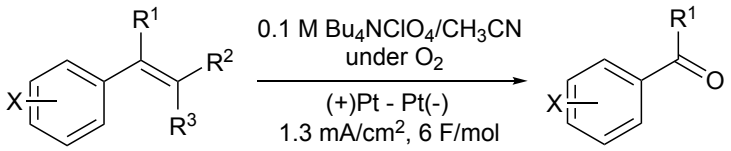

Substrate	Product and Yield[a]	Substrate	Product and Yield[a]
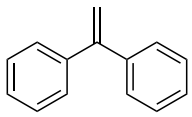 1a	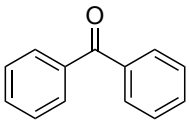 1b, 96%	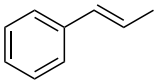 8a	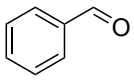 8b, 68%
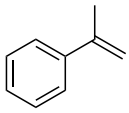 2a	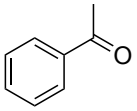 2b, 87%	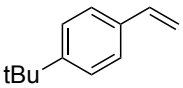 9a[e]	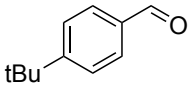 9b, 77%
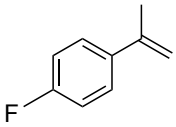 3a	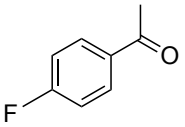 3b, 79%	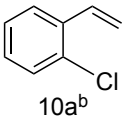 10a[b]	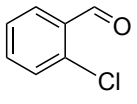 10b, 85%
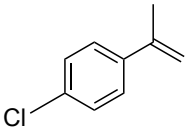 4a[c]	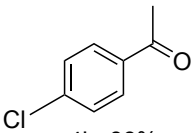 4b, 88%	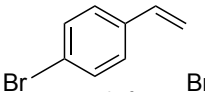 11a[b, f]	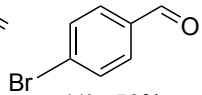 11b, 50%
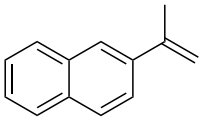 5a[d]	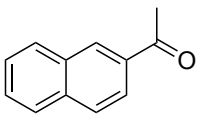 5b, 68%	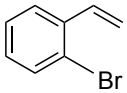 12a[e]	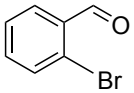 12b, 85%
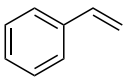 6a[b]	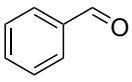 6b, 55%	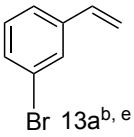 13a[b, e]	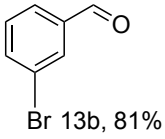 13b, 81%
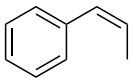 7a[e]	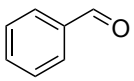 7b, 74%	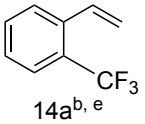 14a[b, e]	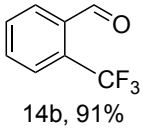 14b, 91%
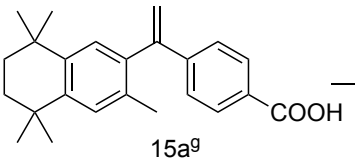 15a[g] Bexarotene	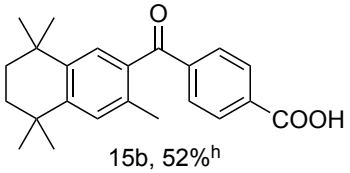 15b, 52%[h]		

Then, our interests were turned into the exploration of the THF formation using carbon electrodes (Scheme 2). Natural compounds like lignans often contain the structure of 2,5-diaryltetrahydrofuran.[19] Although good stereoselectivity was not achieved, selective THF formation over olefin cleavage was accomplished with a variety of styrene derivatives in 36-98% yields. Remarkably, the stereoisomers of the products (except **8c** and **10c**) could be separated by normal column chromatography. *α*-Substituted styrenes were converted into the desired THF products in excellent yields (**1c**-**5c**). As starting materials could not be consumed completely and overoxidation was taken place, **6c** and **7c** were produced in low to moderate yields even though the olefin cleavage was still minor. Halogen-substituted styrenes were smoothly functionalized with good chemoselectivity (**8c**-**11c**). X-ray analysis allowed us to obtain the crystal structures of *trans*-**3c** and *cis*-**9c**.[20] It is interesting that **7a**, **8a** and **14a** did not react. In some cases, an excess amount of charge was required, presumably owing to the competitive oxidation of the superoxide radical anion ($E_{ox\_O_2^{\bullet-}/O2}$ = -0.56 V vs. Ag wire.[21]

Scheme 2. Scope of THF derivative synthesis. Electrolysis was carried out in a 10 mL solution saturated with O_2 on a 0.5 mmol scale of substrate in an undivided cell at RT. [a] Yields of isolated product. [b] Ratios of stereoisomers (*cis*/*trans*) were determined by GC analysis. [c] Yields were determined by GC/MS integration. [d] CH_3NO_2 was used as solvent. N.R.=no reaction.

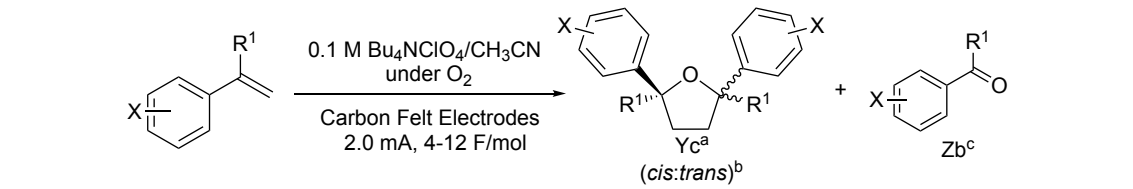

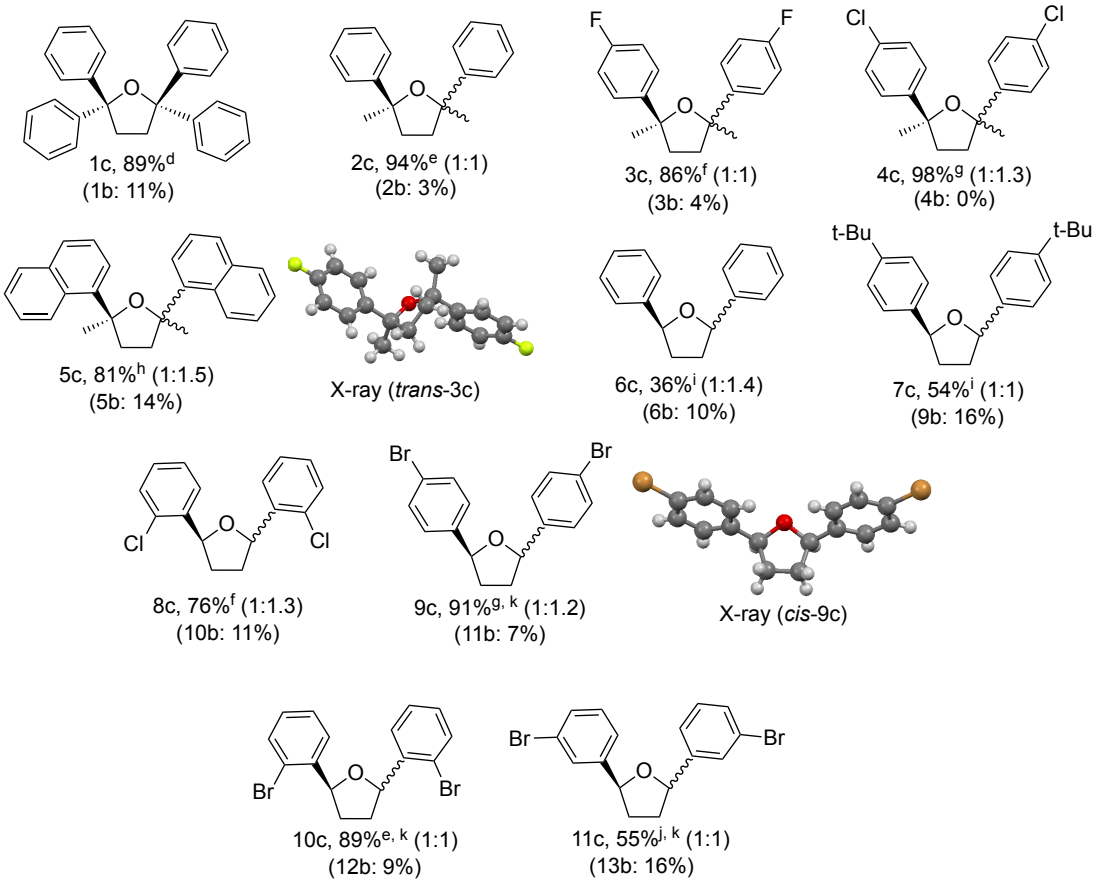

Unsuccessful Substrates

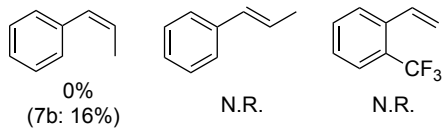

As we confirmed the substrate scope, we started mechanistic studies. Given that the electrolytic conditions were the same except for the electrode materials, the difference in reactions should derive from the chemical events on the surface of the electrodes. We performed electrochemical studies to investigate the electrode material effects. First, we conducted cyclic voltammetry (CV) measurements. It is noted that we utilized glassy

carbon (GC) electrode instead of CF since GC gave similar result to that of CF (Scheme 3). CV examinations (Table 2) demonstrated that the oxidation potentials of styrenes (**4a**, **11a**, and **12a**) on the GC electrode were 0.23-0.38 V (vs. Fc/Fc+) lower than on a Pt electrode.[22] It is reasoned that the HOMO energy of styrenes is higher by 0.23-0.38 eV on the GC electrode than on the Pt electrode.[23] This shift could be explained by π-π stacking or π-H interaction[24] between styrenes and the sp^2-structure of the carbon electrode, that is, styrenes could be adsorbed on the carbon electrodes, not on Pt electrodes.

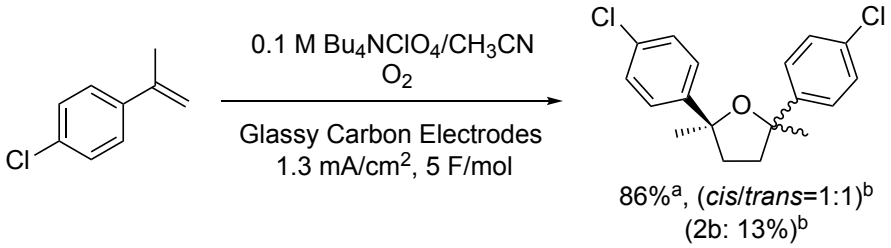

Scheme 3. Mechanistic experiments. [a] Isolated yield. [b] Determined by ^{1}H NMR analysis.

Table 2. Oxidation potentials of styrenes on different working electrodes.[a]

Styrenes	**E_{ox} (GC)**	**E_{ox} (Pt)**	**$\Delta(E_{ox\_GC} - E_{ox\_Pt})$**	**$\Delta(E_{HOMO\_GC} - E_{HOMO\_Pt})$**[b][26]
6a[23]	1.54 (V *vs* SCE)	1.90 (V *vs* SCE)	-0.36 (V *vs* SCE)	-
2a[23]	1.48 (V *vs* SCE)	1.76 (V *vs* SCE)	-0.26 (V *vs* SCE)	-
4a	1.11 (V *vs* Fc/Fc^+)	1.34 (V *vs* Fc/Fc^+)	-0.23 (V *vs* Fc/Fc^+)	+0.23 eV
11a	1.14 (V *vs* Fc/Fc^+)	1.38 (V *vs* Fc/Fc^+)	-0.24 (V *vs* Fc/Fc^+)	+0.24 eV
12a	1.16 (V *vs* Fc/Fc^+)	1.54 (V *vs* Fc/Fc^+)	-0.38 (V *vs* Fc/Fc^+)	+0.38 eV

[a] Oxidation potentials of **2a** and **6a** are from ref. [25]. Oxidation potentials (onset potentials) of **4a**, **7a**, **8a**, **11a**, **12a** and **14a** were obtained by CV (Figure S2). [b] E_{HOMO} values are calculated based on E_{onset_ox} (*vs* Fc/Fc^+) (see reference [26]).

Next, successive scans were carried out with **4a** (Figure 1a,b). Interestingly, the peak top current for the oxidation of **4a** with GC gradually diminished and the oxidation potential correspondingly increased (Figure 1a). This change is ascribable to oligomer/polymer

deposited on the surface of the GC,[25] suppressing further oxidation of **4a** and decreasing the rate of electron transfer. On the other hand, the adsorptions did not seem to be occurred because the oxidation waves on Pt were identical after the second cycle.

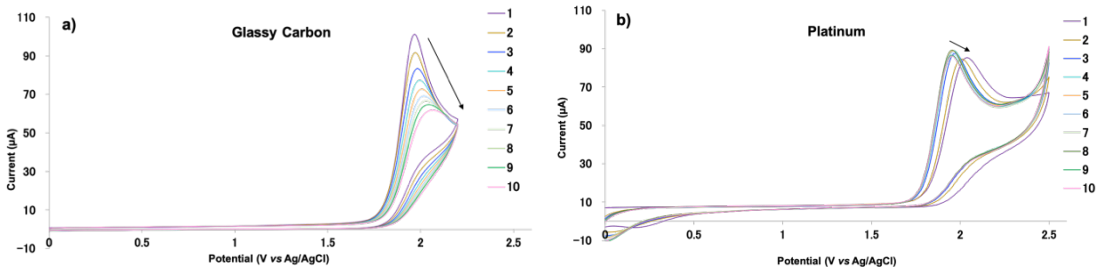

Figure 1. a) Cyclic voltammograms of **4a** on GC electrode with successive scans (10 cycles). 2 mM **4a** in 0.1m Bu_4NBF_4 in CH_3CN; scan rate: 0.1 V/s; b) Cyclic voltammograms of **4a** on Pt electrode with successive scans (10 cycles). 2 mM **4a** in 0.1m Bu_4NBF_4 in CH_3CN; scan rate: 0.1 V/s. electrode area of GC and Pt: 7.1 mm^2.

Subsequently, it occurred to us that giving the inverse properties to the surface of each electrode by modifications respectively would yield the correspondingly inverse products. GC electrode was modified with sulfamic acid[26] to make the surface hydrophilic, preventing styrenes from adsorbed (Figure 2a). XPS analysis observed the modification (Figure 2c,d) On the other hand, Pt electrode was covered with graphene, rendering the surface close to carbon electrode (Figure 2b). This modification was confirmed by K-NEXAFS analysis (Figure 2e). To our delight, **4a** was converted into the carbonyl product (**4b**) on sulfamic-modified GC anode (Scheme 4, eq1), and **4a** was transformed into tetrahydrofuran **4c** in 61% on graphene-modified Pt anode (Scheme 4, eq2).

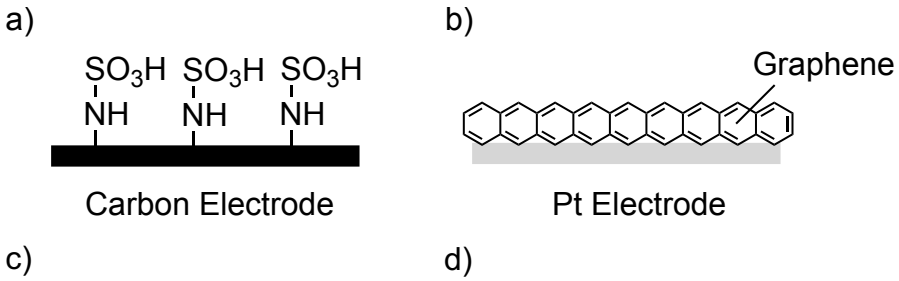

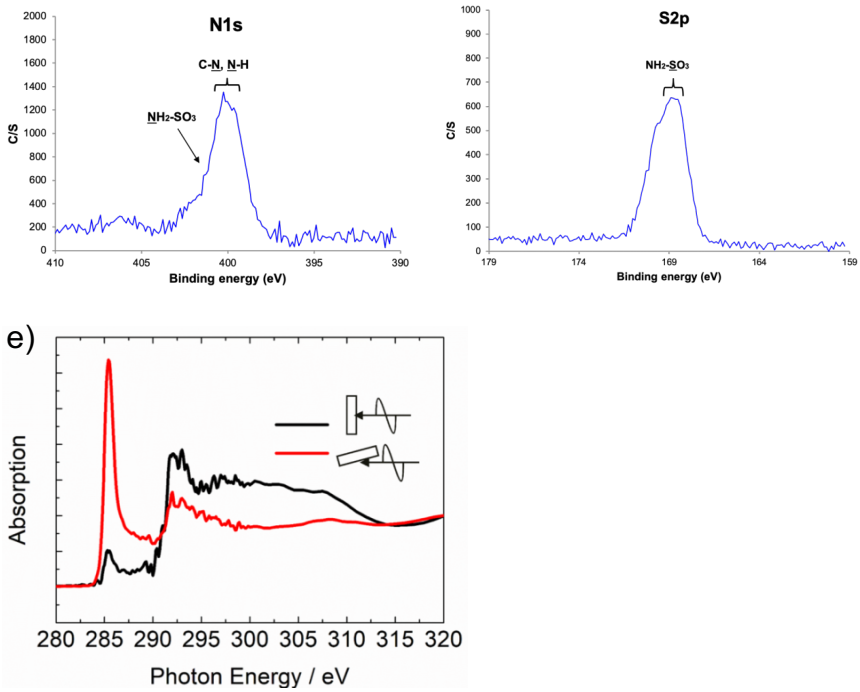

Figure 2. a) Conceptual figure of sulfamic acid-modified glassy carbon electrode.; b) Conceptual figure of graphene-modified platinum electrode.; c) XPS analysis of N1s with narrow scan-69.00 eV to confirm sulfamic acid-modification on glassy carbon electrode.; d) XPS analysis of S2p with narrow scan-69.00 eV to confirm sulfamic acid-modification on glassy carbon electrode.; e) K-NEXAFS (Near the Carbon K-edge X-ray Absorption Fine Structure) analysis of graphene-modified platinum electrode.

Scheme 4. Electrolysis was carried out in a 10 mL solution saturated with O_2 on a 0.5 mmol scale of substrate in an undivided cell at RT. Eq(1): equipped with sulfamic acid-modified anode (glassy carbon electrode) was utilized. Eq(2): equipped with graphene-modified anode (platinum electrode) was utilized.

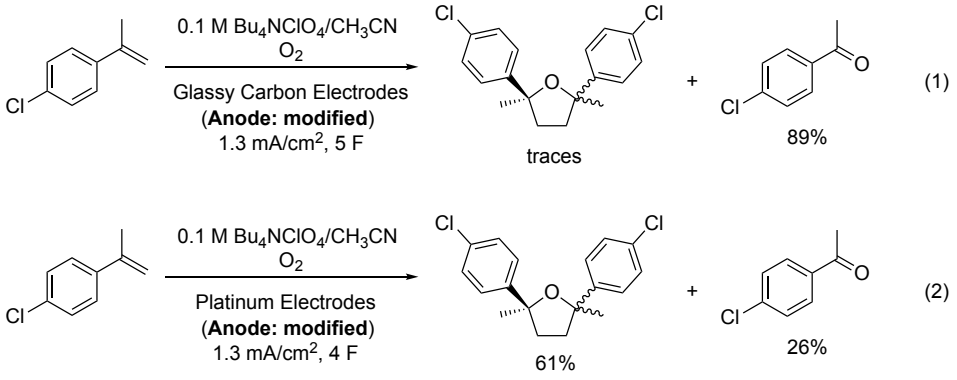

Overall, these investigations indicate that oxidized styrenes are more likely to be captured by the neutral species on carbon electrode than on Pt electrode (Figure 3). It is considered that dimerization can be more easily caused because of the absorbed styrene/its radical cation on carbon electrode. Yet we cannot exclude the possibility that

this variation could be owing to the ability of Pt to absorb $O_2/O_2^{\bullet-}$,[27] which induces the capture of radical cations by $O_2/O_2^{\bullet-}$.

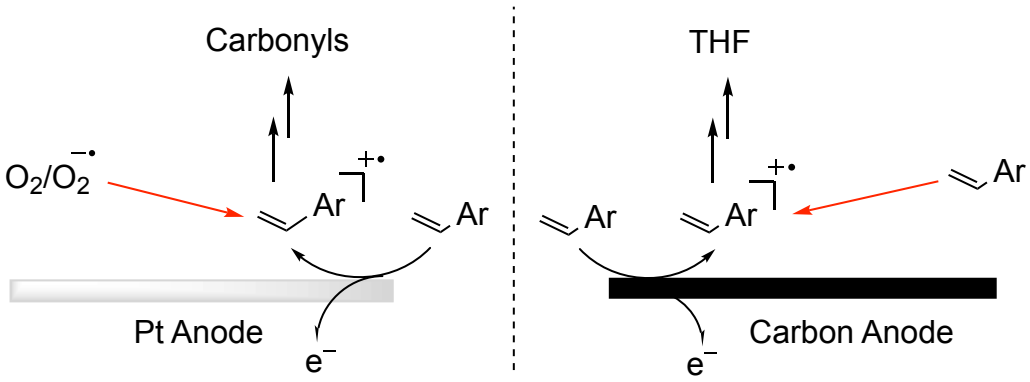

Figure 3. a) Conceptual figure of expected chemical events on different electrodes.

To obtain deeper insight into the reaction pathways, we conducted DFT calculations (B3LYP/6-31G + (d,p)) and mechanistic experiments. According to the DFT calculations, it was shown that the highest spin density of radical cation styrenes is positioned at the *β*-position (Figure 4), agreeing to a previous report.[15h] Mechanistic experiments demonstrated that epoxide **2e** is one of the intermediates that can be converted into carbonyls, but this should be a minor pathway because **2e** could not be completely consumed even at 6 F/mol [Scheme 5, Eqs. (1), (2)]. Moreover, isotopic experiments proved that O_2 is the oxygen source for both reactions [Scheme 5, Eqs. (3), (4)] and the reduction of O_2 is critical in both reactions [Scheme 5, Eqs. (5), (6)].

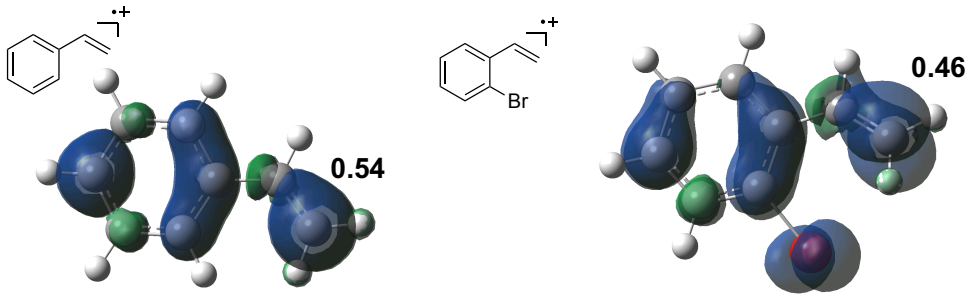

Figure 4. The spin distribution and spin densities of radical cations of 1,1-Diphenylethylene, Styrene, 2-Bromostyrene obtained by DFT calculations (B3LYP/6-31G+(d,p)) (isoval = 0.0016).

Scheme 5. Mechanistic experiments.

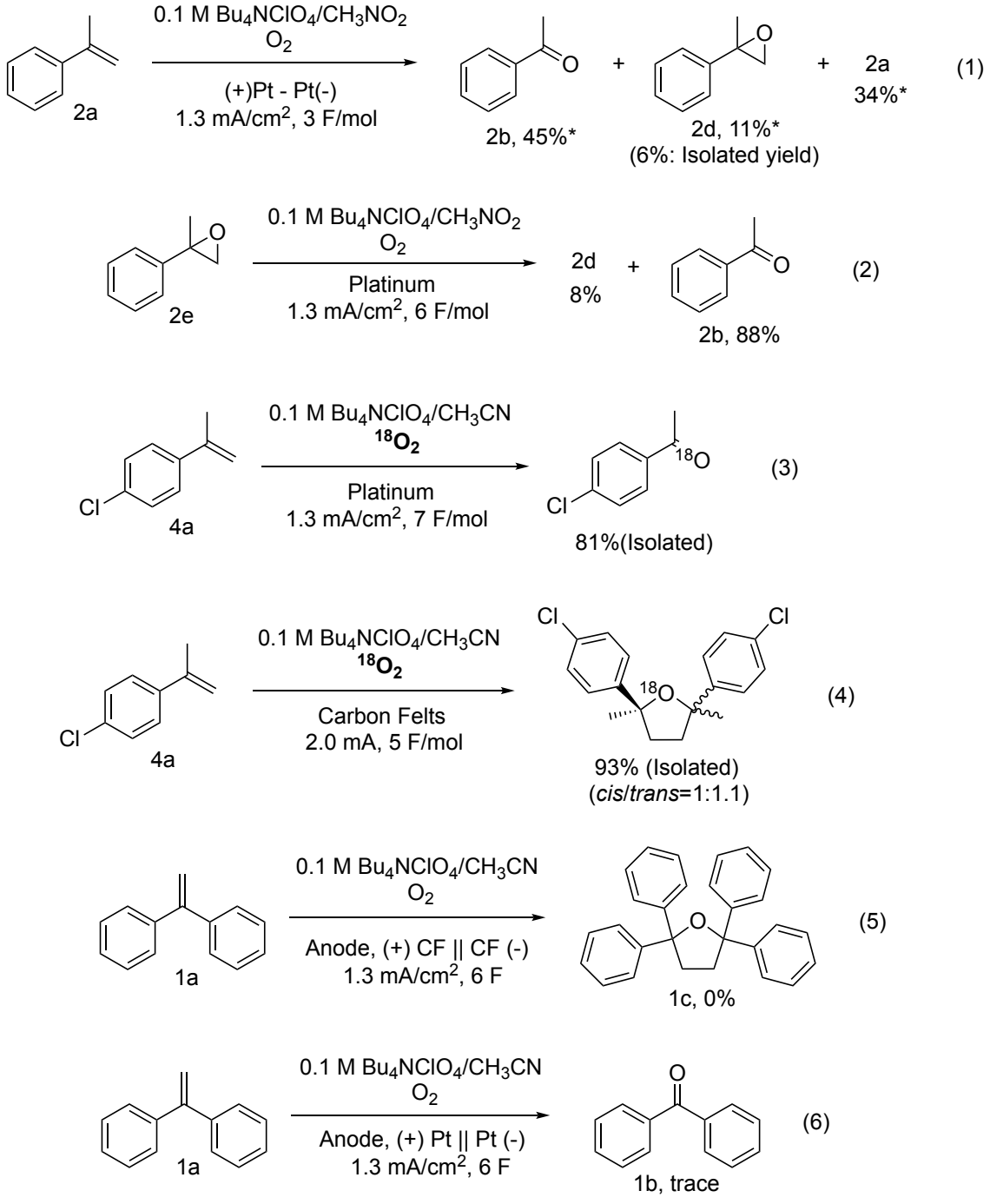

Expected mechanisms are depicted in Figure 5. For the C=C cleavage (Figure 5a), there are two routes to produce carbonyl products. Taking consideration that $O_2^{\bullet-}$ can be generated by the reduction of O_2 ($E_{O_2/O_2^{\bullet-}}$ = -1.48 V vs. Ag wire)[21, 28] (Figure 6) and it has a fairly long lifetime in aprotic solvents,[29] $O_2^{\bullet-}$ could capture the radical cation **2a**$^{\bullet+}$. Dioxetane intermediate **2d** (major path) and epoxide intermediate **2e** (minor path) are

formed. The dioxetane is immediately decomposed[30] into the aimed carbonyls (formaldehyde was detected by GC/MS, Figure 7). In the THF formation (Figure 5b), after anodic oxidation of **2a** on the carbon electrode, **2a**$^{\bullet+}$ is trapped by **2a** at the β-position. Subsequently, $O_2^{\bullet-}$ bonds to **2aa**$^{\bullet+}$, leading to **2c**.

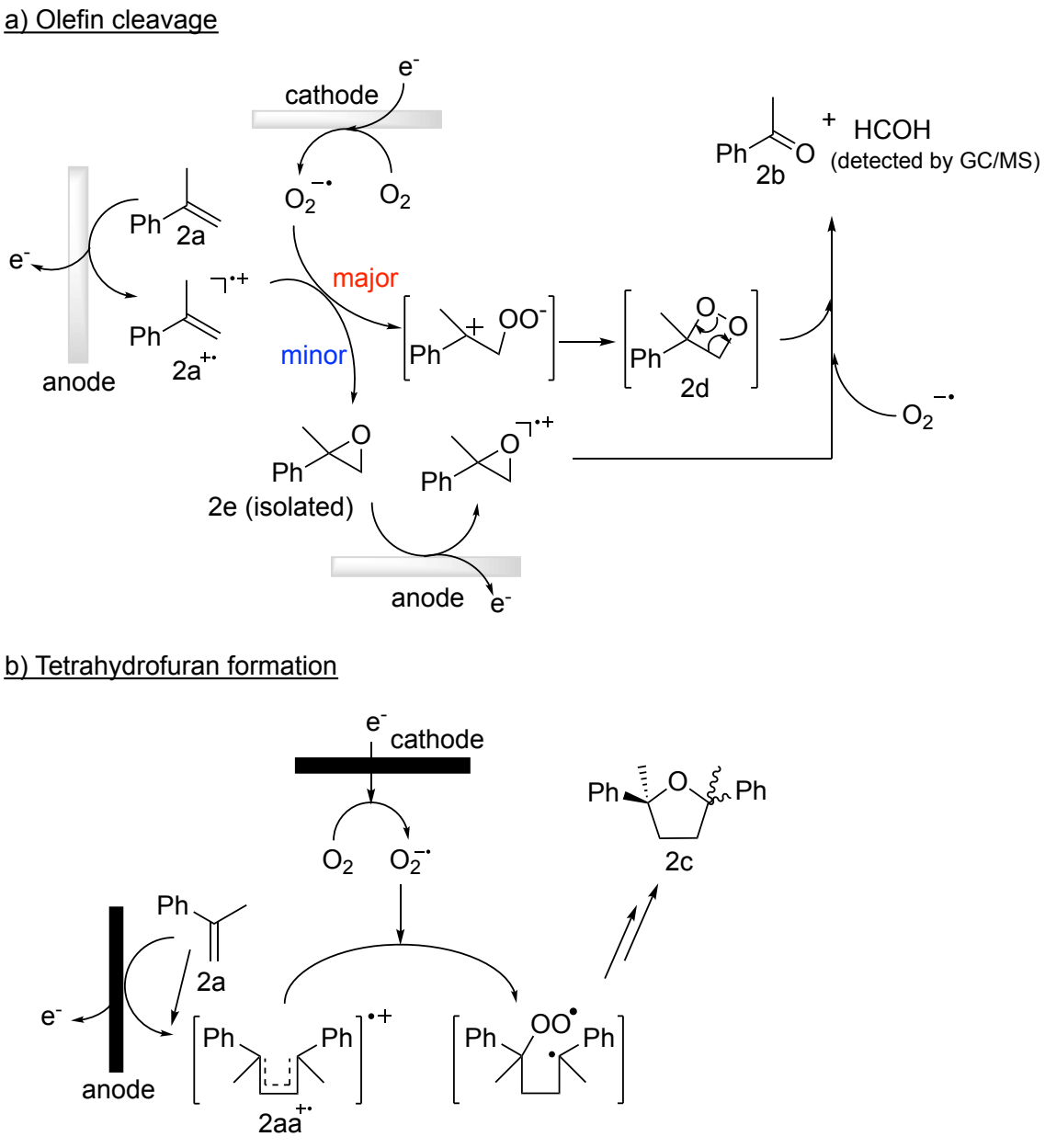

Figure 5. Plausible mechanisms of (a) olefin cleavage and (b) THF formation.

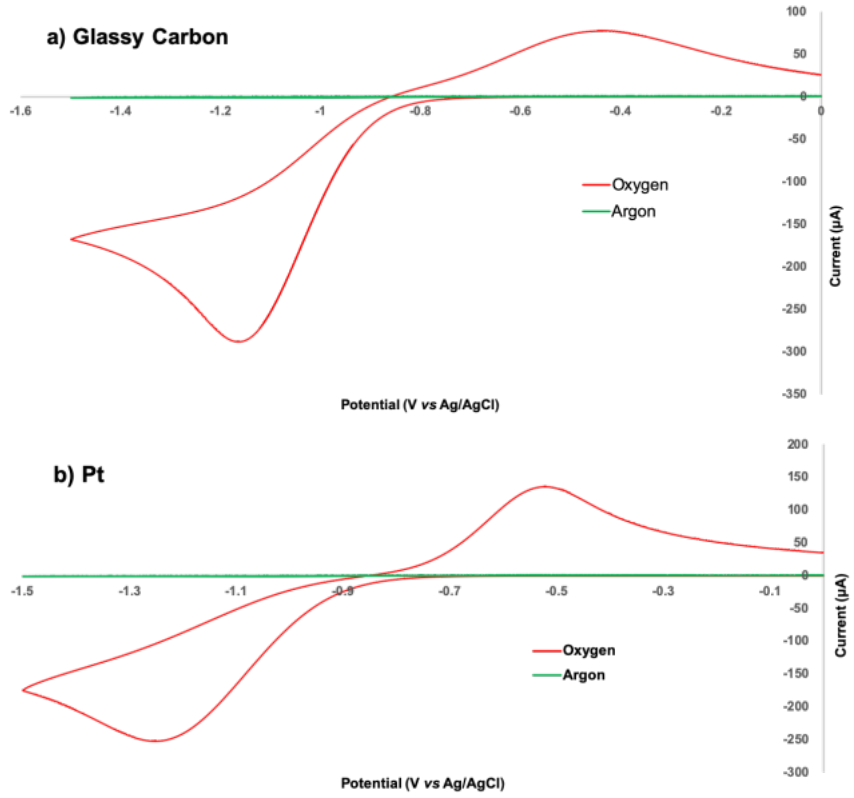

$$O_2 + e^- \rightleftharpoons O_2^{-\bullet} \qquad (1)$$

Figure 6. a) Cyclic voltammogram of 0.1 M Bu_4NBF_4/CH_3CN with glassy carbon working electrode (7.1 mm^2). Scan rate: 0.1 V/s. Red line: Oxygen dissolved in CH_3CN. Blue line: Argon bubbled in CH_3CN. b) Cyclic voltammogram of 0.1 M Bu_4NBF_4/CH_3CN with platinum working electrode (7.1 mm^2). Scan rate: 0.1 V/s. Red line: Oxygen dissolved in CH_3CN. Blue line: Argon bubbled in CH_3CN. Both reduction waves are in accord with eq (1).

a) b)

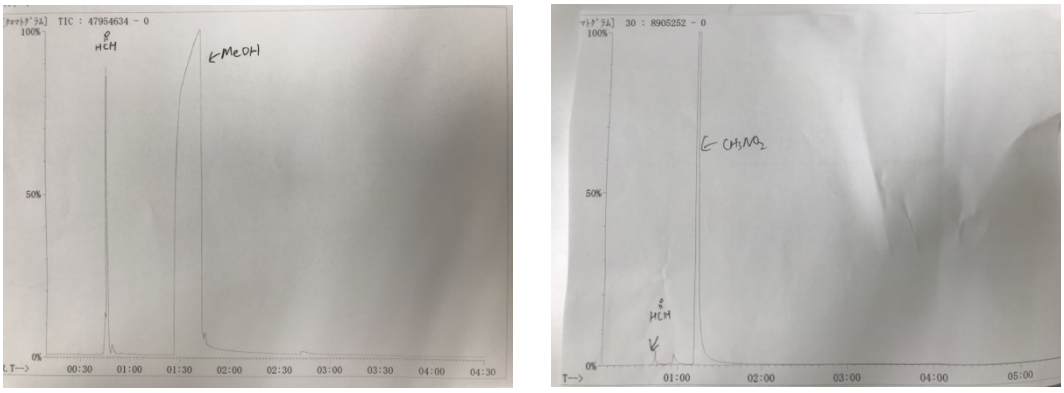

Figure 7. a) Standard material: 10% formaldehyde solution dissolved in methanol. b) Reaction solution: Electrolysis were carried out in 10 mL nitromethane saturated with O_2 on 0.5 mmol scale of α-Methylstyrene in an undivided cell at

r.t. and stopped at 3 F/mol. Method: Initial temperature 30 ℃, hold 2.0 min, increment 10 ℃/min, final temperature 150 ℃, hold 5 min.

Conclusions

In conclusion, we discovered an electrode material selective derivatization of styrenes. Pt and carbon electrodes offered different products (carbonyls and THF) selectively. O_2 was utilized as a safe and reasonable oxygen source. A broad substrate scope was confirmed in both reactions. Electrochemical analysis has shed light on that the styrene radical cation intermediate is more likely to be captured by styrene first on the carbon electrode. On the other hand, the Pt electrode should allow the intermediate to be trapped by $O_2^{\bullet-}$. This discovery is informative for further research on electrolysis.

4. Summary

In summary, it was turned out that $LiClO_4$, LiTFSI and LiFSI in nitroalkane have the effect of ensuring the inherent reactivity of radical cation species respectively. ^{7}Li NMR studies and raman spectroscopy showed that those Li salts form the contact ion pair and/or aggregation in CH_3NO_2 solution, that is, Li cations trap the corresponding anions. It is reasoned that radical cation species could be free in those solutions like in fluorinated alcohol solutions, leading to their higher reactivities. This discovery is crucial for C-C bond formation via radical cation in electrochemical reactions. Surprisingly, this electrolyte effect had been unclear for the last 20 years.

Furthermore, the effect of electrode materials on anodic oxidation of styrenes was also elucidated. Cyclic voltammetry studies and experiments with modified electrodes exhibited that styrenes tend to be adsorbed on the surface of carbon electrodes, leading to the better chance for dimerization. The feature enabled different functionalization of styrenes with oxygen by different electrode materials (tetrahydrofuran formation on carbon electrode and C=C cleavage on platinum electrode).

I believe that these findings will be quite useful for further development of electrochemical reactions.

5. Acknowledgement

I would like to give my thank to Prof. Kazuhiro Chiba, Prof. Siegfried R. Waldvogel, Prof. Yoshikazu Kitano, Dr. Yohei Okada, Dr. Naoki Shida, Dr. Yusuke Yamaguchi, Dr. Anton

Wiebe and Dr. Tile Gieshoff for educating me. Thanks to a lot of discussion with them, I have been able to achieve many publications. In addition, I could master thinking way of science as well as knowledge of chemistry through collaborating work with them. Furthermore, I appreciate financial supports. This work was partially supported by JSPS KAKENHI (Grant-in- Aid for Scientific Research (B), 15H04494 to K. C., Grant-in-Aid for Young Scientists (A), 16H06193 to Y. O. and Grant-in-Aid for JSPS Fellows, K218J22018 to Y. I.). Also, we thank the DFG (GSC 266, WA 1276/17-1, WA 1276/14-1) for financial support. Support of the Advanced Lab of Electrochemistry and Electrosynthesis—ELYSION (Carl Zeiss Stiftung) is gratefully acknowledged. Y.I. gratefully acknowledges support from the Program for Leading Graduate School of TUAT, granted by the Ministry of Education, Culture, Science and Technology (MEXT), Japan. Y.I. thanks the Material Science in Mainz (MAINZ) graduate school for financial support.

6. Equipment

NMR

^{1}H, ^{7}Li, ^{13}C and ^{19}F NMR spectra were recorded in $CDCl_3$ with either JEOL ECA-600 spectrometer (1H 600 MHz, 13C 150 MHz) or JEOL ECA-400 spectrometer (^{1}H 400 MHz, ^{13}C 100 MHz).

ESI-MS

Mass spectra were obtained on JEOL JMS T-100LP mass spectrometer.

GC-MS

GC-MS spectra were recorded on an Agilent Technologies 6890N GC-system with an JEOL JMS-Q1000GC and a HP-5 colomn (0.25 mm×30 m, film: 0.25 μm). Standard method: Initial temperature 40 ℃, hold 1.5 min, increment 20 ℃/min, final temperature 280 ℃, hold 5 min.

Column chromatography

Silica gel (particle size 40−50 μm) was used for column chromatography.

TLC

TCI precoated silica gel F254 plates (thickness 0.25 mm) was used for thin-layer chromatography (TLC) analysis.

Melting points

Measurement of melting point was conducted with MEL-TEMP® capillary melting point apparatus (AC/DC input 210-230 V AC) (Barnstead/Thermolyne Corp.).

Cyclic voltammetry and Chronoamperometry

Cyclic voltammetry (CV) and Chronoamperometry were carried out ALS electrochemical analyzer 611DN using grassy carbon/platinum (7.1 mm^2) as working electrode, platinum wire as counter electrode and Ag/AgCl as reference electrode.

X-ray analysis

All data were collected on Rigaku R-AXIS RAPID and Rigaku XtaLAB mini.

XPS analysis

All data were collected on Quantera SXM (PHI, Inc)

Raman spectroscopy

Laser Raman spectroscopy was conducted at room temperature using an EZRaman-N-785-B1S instrument (TOKYO INSTRUMENTS, Inc.) with a laser wavelength of 785 nm at 300 mW.

K-NEXAFS

The analysis was carried out at the soft X-ray beamline BL-7A at the Photon Factory (Institute of Materials Structure Science, High Energy Accelerator Research Organization, Japan).

Reagents

All materials were obtained from TCI fine chemicals, Wako Pure Chemical Industries, Kanto Chemical, and Sigma Aldrich and used without further purification.

7. Experiments

7-1. Understanding the effect of $LiClO_4$ / NM on radical cation chemistry: Leading to the exploration of alternative electrolytes

7-1-1. ^{7}Li NMR

The samples of different concentration (0.1~2.56 M) of Li salts ($LiClO_4$, LiFSI and LiTFSI) dissolved in $MeNO_2$ or MeCN were prepared. The shifts of chemical shft of ^{7}Li of each sample were measured using 0.1 M LiCl in D_2O as an external standard.

7-1-2. Raman spectroscopy

The samples of different concentration (0.1~2.56 M) Li salts ($LiClO_4$, LiFSI and LiTFSI) dissolved in $MeNO_2$ were prepared. Laser Raman spectroscopy was conducted at room temperature using an EZRaman-N-785-B1S instrument (TOKYO INSTRUMENTS, Inc.) with a laser wavelength of 785 nm at 300 mW. The peaks were fitted in the wavenumber range of 800

to 700 cm^{-1} for LiFSI/$MeNO_2$ and 770 to 720 cm^{-1} for LiTFSI/$MeNO_2$ by Gaussian-Lorentzian function with IGOR PRO 8.03.

7-1-3. Cyclic voltammetry

2 mM substrate in 0.1 M supporting electrolyte/solvent was measured by cyclic voltammetry. Scan rate: 0.1 V/s. Working electrode: glassy carbon (7.1 mm^2). Counter electrode: Pt wire. Reference electrode: Ag/AgCl.

7-1-4. Radical cation Diels-Alder reaction

All reactions were carried out on a 1.0 mmol scale of *trans*-anethole and 3 eq. isoprane in 10 mL of electrolyte solution at room temperature under constant potential electrolysis (1.0 V vs. Ag/AgCl). The electrolysis was conducted in an undivided cell. The electrolytic cell was equipped with carbon felt electrodes for anode and cathode. After electrolysis, the crude products were extracted with dichloromethane and the organic phase was washed with water. After the organic phase was dried over $MgSO_4$, the crude products were purified by column chromatography (EtOAc:Hex = 1:20).

7-1-5. Electrochemical [2+2] cycloaddition

All reactions were carried out on a 0.1 mmol scale of enyloxybenzene and 20 eq. 1-hexene in 10 mL of electrolyte solution at room temperature under constant potential electrolysis (1.2 V vs. Ag/AgCl). The electrolysis was conducted in an undivided cell. The electrolytic cell was equipped with carbon felt electrodes for anode and cathode. After electrolysis, the crude products were extracted with dichloromethane and the organic phase was washed with water. After the organic phase was dried over $MgSO_4$, the crude products were purified by column chromatography (EtOAc:Hex = 1:20).

7-2. Application of LiTFSI / NM electrolyte for electrochemical radical cation Diels-Alder reaction with lipophilic compounds.

7-2-1. Preparation of Dienophile

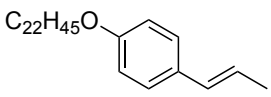

(4-Hydroxyphenyl)-1-propene (0.5 g, 3.73 mmol) and 1-Bromodocosane (2.179 g, 5.6 mmol) were transferred into round bottom flask. 30 mL dry DMF and K_2CO_3 (4 g, 29 mmol) were

added. The reaction solution was stirred at 90 ℃ for 21 h. After the reaction, the products were extracted by *n*-Hex and washed organic phase with water. The organic phase was dried over $MgSO_4$. After the solution was evaporated, the crude products was washed with acetonitrile (heating at 40 ℃), yielding the pure product as a white solid (91%, 1.5 g, 3.39 mmol).

^{1}H NMR (600 MHz, Chloroform-*d*) δ 7.24 (d, *J* = 8.7 Hz, 2H), 6.82 (d, *J* = 8.7 Hz, 2H), 6.33 (d, *J* = 15.7 Hz, 1H), 6.12–6.05 (m, 1H), 3.93 (t, *J* = 6.6 Hz, 2H), 1.85 (dd, *J* = 6.6, 1.7 Hz, 2H), 1.80–1.73 (m, 2H), 1.47–1.22 (m, 38H), 0.88 (t, *J* = 7.0 Hz, 3H).
^{13}C NMR (101 MHz, Chloroform-*d*) δ 130.52, 126.96, 123.45, 114.63, 68.17, 32.08, 29.85, 29.81, 29.52, 26.19, 22.85, 18.58, 14.28.
HRMS $[M+Na]^+$ for $C_{31}H_{54}NaO$ calc: 465.4072 found: 465.4101

7-2-2. General protocol for electrocatalytic Diels-Alder reactions (GP)

A solution of Lithium Bis(trifluorosulfonylmethane)imide (LiTFSI) (861 mg, 3 mmol) in 5 mL 1-Nitropropane ($PrNO_2$) was transferred into an undivided cell. 5 mL Methylcyclohexane (Me-*c*-Hex) was added in to the solution and stirred at room temperature to make the solution a mono-phase. Dienophile (0.1 mmol) and diene (3 eq, 0.3 mmol) were added into the solution. The electrolysis cell was equipped with a carbon felt anode and a carbon felt cathode. A constant potential electrolysis with a potential of 1.0 V (*vs* Ag/AgCl) was carried out at room temperature. 2.89 C (0.3 F per dienophile) was applied. After the electrolysis, the solution was cooled down at -50 ℃ to make the solution bi-phasic. Extraction of only upper phase (Me-*c*-Hex) and evaporation afforded the [4+2] cycloadduct products. If necessary, after the extraction of upper phase, the crude products were purified by column chromatography.

7-2-3. Products of Diels-Alder reactions

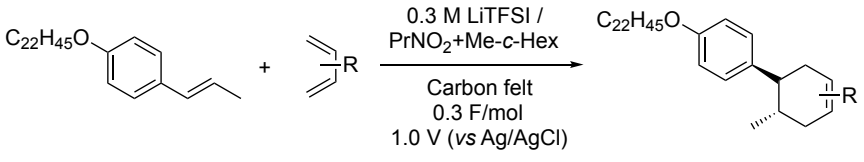

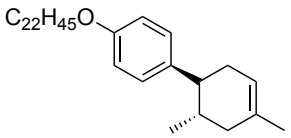

According to **GP,** 44.2 mg (0.1 mmol) dienophile and isoprene (30 µl, 0.3 mmol) were added into the $PrNO_2$+Me-*c*-Hex (=1:1) solution (0.3 M LiTFSI). Electrolysis was performed at room temperature with a potential of 1.0 (*vs* Ag/AgCl). After electrolysis (0.3 F per dienophile), the

solution was cooled down at -50 °C to make the solution bi-phasic. Extraction of only upper phase (Me-*c*-Hex) and evaporation afforded the [4+2] cycloadduct product as a white solid (yield: 98 %, 50 mg, 0.098 mmol).

^{1}H NMR (600 MHz, Chloroform-*d*) δ 7.06 (d, *J* = 8.6 Hz, 2H), 6.83 (d, *J* = 8.6 Hz, 2H), 5.49–5.41 (m, 1H), 3.93 (t, *J* = 6.6 Hz, 2H), 2.32–2.05 (m, 3H), 1.92–1.64 (m, 6H), 1.49 – 1.20 (m, 40H), 0.88 (t, *J* = 7.0 Hz, 3H), 0.71 (d, *J* = 6.4 Hz, 3H).
^{13}C NMR (151 MHz, CHLOROFORM-*D*) δ 157.49, 138.09, 133.96, 128.59, 121.08, 114.41, 68.10, 47.09, 40.00, 35.41, 34.10, 32.08, 29.85, 29.81, 29.75, 29.58, 29.52, 26.24, 23.53, 22.85, 20.39, 14.27.
HRMS $[M+H]^+$ for $C_{36}H_{63}O$ calc: 511.4800 found: 511.4796

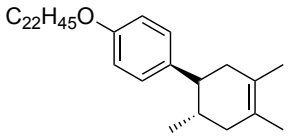

According to **GP,** 44.2 mg (0.1 mmol) dienophile and 2,3-dimethyl-1,3-butadiene (30 µl, 0.3 mmol) were added into the $PrNO_2$+Me-*c*-Hex (=1:1) solution (0.3 M LiTFSI). Electrolysis was performed at room temperature with a potential of 1.0 (*vs* Ag/AgCl). After electrolysis (0.3 F per dienophile), the solution was cooled down at -50 °C to make the solution bi-phasic. Extraction of only upper phase (Me-*c*-Hex) and evaporation afforded the [4+2] cycloadduct product as a white solid (yield: 98 %, 51 mg, 0.098 mmol).
^{1}H NMR (600 MHz, Chloroform-*d*) δ 7.06 (d, *J* = 8.4 Hz, 2H), 6.82 (d, *J* = 8.4 Hz, 2H), 3.93 (t, *J* = 6.6 Hz, 2H), 2.32 (td, *J* = 10.7, 5.6 Hz, 1H), 2.20 – 2.03 (m, 3H), 1.88 – 1.72 (m, 4H), 1.62 (d, *J* = 16.8 Hz, 6H), 1.48 – 1.26 (m, 36H), 0.88 (t, *J* = 6.7 Hz, 3H), 0.69 (d, *J* = 5.8 Hz, 3H).
^{13}C NMR (151 MHz, CHLOROFORM-*D*) δ 157.47, 138.10, 128.55, 125.65, 125.45, 114.41, 68.10, 47.96, 41.98, 41.79, 34.39, 32.08, 29.85, 29.82, 29.76, 29.74, 29.58, 29.52, 26.24, 22.85, 20.15, 18.86, 18.79, 14.28.
HRMS $[M+H]^+$ for $C_{37}H_{65}O$ calc: 525.4957 found: 525.4927

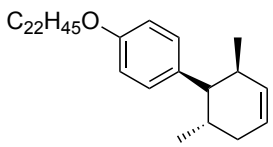

According to **GP,** 44.2 mg (0.1 mmol) dienophile and *trans*-1,3-pentadiene (30 µl, 0.3 mmol) were added into the $PrNO_2$+Me-*c*-Hex (=1:1) solution (0.3 M LiTFSI). Electrolysis was

performed at room temperature with a potential of 1.0 (*vs* Ag/AgCl). After electrolysis (0.3 F per dienophile), the solution was cooled down at -50 ℃ to make the solution bi-phasic. After the extraction of only upper phase (Me-*c*-Hex) and evaporation, the crude products were purified by column chromatography (*n*-hexane:ethyl acetate = 40:1; column 28 mm x 100 mm), yielding the product as a colorless liquid (yield: 91 %, 46 mg, 0.091 mmol).

^{1}H NMR (600 MHz, Chloroform-*d*) δ 7.04 (d, *J* = 8.6 Hz, 2H), 6.83 (d, *J* = 8.6 Hz, 2H), 5.76 – 5.70 (m, 1H), 5.67 – 5.60 (m, 1H), 3.93 (t, *J* = 6.6 Hz, 2H), 2.65 (dd, *J* = 10.9, 5.4 Hz, 1H), 2.32 – 2.08 (m, 3H), 1.85 – 1.74 (m, 3H), 1.49 – 1.41 (m, 2H), 1.38 – 1.20 (m, 36H), 0.88 (t, *J* = 7.0 Hz, 3H), 0.83 (d, *J* = 6.5 Hz, 3H), 0.74 (d, *J* = 7.2 Hz, 3H).
^{13}C NMR (151 MHz, CHLOROFORM-*D*) δ 157.33, 135.32, 133.65, 130.21, 125.26, 113.91, 68.04, 50.62, 35.71, 34.94, 32.08, 29.85, 29.82, 29.77, 29.75, 29.59, 29.55, 29.52, 26.58, 26.26, 22.85, 20.70, 16.94, 14.28.
HRMS $[M+H]^+$ for $C_{36}H_{63}O$ calc: 511.4801 found: 511.4790

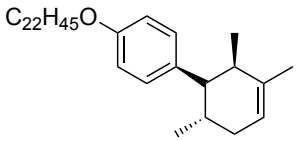

According to **GP,** 44.2 mg (0.1 mmol) dienophile and 3-methyl-1,3-pentadiene (*cis/trans* mixture) (34 µl, 0.3 mmol) were added into the $PrNO_2$+Me-*c*-Hex (=1:1) solution (0.3 M LiTFSI). Electrolysis was performed at room temperature with a potential of 1.0 (*vs* Ag/AgCl). After electrolysis (0.3 F per dienophile), the solution was cooled down at -50 ℃ to make the solution bi-phasic. After the extraction of only upper phase (Me-*c*-Hex) and evaporation, the crude products were purified by column chromatography (*n*-hexane:ethyl acetate = 40:1; column 28 mm x 100 mm), yielding the product as a white solid (yield: 80 %, 42 mg, 0.08 mmol).

^{1}H NMR (600 MHz, Chloroform-*d*) δ 7.04 (d, *J* = 8.6 Hz, 2H), 6.83 (d, *J* = 8.6 Hz, 2H), 5.38 – 5.30 (m, 1H), 3.93 (t, *J* = 6.6 Hz, 2H), 2.60 (dd, *J* = 11.6, 4.9 Hz, 1H), 2.29 – 1.97 (m, 3H), 1.81 – 1.74 (m, 3H), 1.70 (s, 3H), 1.48 – 1.41 (m, 2H), 1.38 – 1.21 (m, 36H), 0.88 (t, *J* = 7.0 Hz, 3H), 0.79 (dd, *J* = 12.2, 6.8 Hz, 6H).
^{13}C NMR (151 MHz, CHLOROFORM-*D*) δ 157.30, 139.20, 135.30, 130.34, 120.41, 113.88, 68.05, 51.29, 40.82, 35.54, 32.08, 29.85, 29.82, 29.77, 29.75, 29.59, 29.55, 29.52, 26.26, 25.22, 22.85, 22.45, 20.69, 14.67, 14.28.
HRMS $[M+Na]^+$ for $C_{37}H_{64}ONa$ calc: 547.4957 found: 547.4969

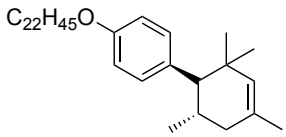

According to **GP,** 44.2 mg (0.1 mmol) dienophile and 2,4-dimethyl-1,3-pentadiene (39 µl, 0.3 mmol) were added into the $PrNO_2$+Me-*c*-Hex (=1:1) solution (0.3 M LiTFSI). Electrolysis was performed at room temperature with a potential of 1.0 (*vs* Ag/AgCl). After electrolysis (0.3 F per dienophile), the solution was cooled down at -50 ℃ to make the solution bi-phasic. After the extraction of only upper phase (Me-*c*-Hex) and evaporation, the crude products were purified by column chromatography (*n*-hexane:ethyl acetate = 40:1; column 28 mm x 100 mm), yielding the product as a white solid (yield: 81 %, 44 mg, 0.081 mmol).

^{1}H NMR (600 MHz, Chloroform-*d*) δ 7.01 (dd, *J* = 44.8, 8.5 Hz, 2H), 6.80 (dd, *J* = 41.8, 8.2 Hz, 2H), 5.19 (s, 1H), 3.93 (t, *J* = 6.6 Hz, 2H), 2.20 – 2.06 (m, 3H), 1.80 – 1.72 (m, 3H), 1.66 (s, 3H), 1.49 – 1.42 (m, 2H), 1.37 – 1.24 (m, 36H), 0.88 (t, *J* = 7.1 Hz, 3H), 0.82 (s, 3H), 0.77 (s, 3H), 0.70 (d, *J* = 7.1 Hz, 3H).
^{13}C NMR (151 MHz, CHLOROFORM-*D*) δ 157.41, 133.51, 133.18, 130.44, 129.45, 113.83, 112.86, 67.99, 57.58, 40.66, 36.38, 32.08, 30.13, 29.85, 29.82, 29.77, 29.75, 29.60, 29.58, 29.52, 28.89, 26.28, 24.89, 23.48, 22.85, 20.94, 14.28.
HRMS $[M+H]^+$ for $C_{38}H_{67}O$ calc: 539.5114 found: 539.5085

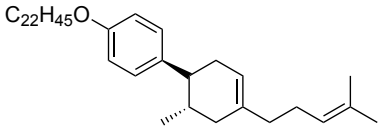

According to **GP,** 44.2 mg (0.1 mmol) dienophile and myrcene (51 µl, 0.3 mmol) were added into the $PrNO_2$+Me-*c*-Hex (=1:1) solution (0.3 M LiTFSI). Electrolysis was performed at room temperature with a potential of 1.0 (*vs* Ag/AgCl). After electrolysis (0.3 F per dienophile), the solution was cooled down at -50 ℃ to make the solution bi-phasic. After the extraction of only upper phase (Me-*c*-Hex) and evaporation, the crude products were purified by column chromatography (*n*-hexane:ethyl acetate = 40:1; column 28 mm x 100 mm), yielding the product as a colorless liquid (yield: 84 %, 49 mg, 0.084 mmol).

^{1}H NMR (600 MHz, Chloroform-*d*) δ 7.06 (d, *J* = 8.5 Hz, 2H), 6.82 (d, *J* = 8.5 Hz, 2H), 5.47 – 5.41 (m, 1H), 5.13 (t, *J* = 6.6 Hz, 1H), 3.92 (t, *J* = 6.6 Hz, 2H), 2.34 – 1.95 (m, 8H), 1.90 – 1.73

(m, 4H), 1.70 (s, 3H), 1.62 (s, 3H), 1.48 – 1.40 (m, 2H), 1.37 – 1.23 (m, 36H), 0.88 (t, *J* = 7.0 Hz, 3H), 0.71 (d, *J* = 6.4 Hz, 3H).

^{13}C NMR (151 MHz, CHLOROFORM-*D*) δ 157.47, 138.15, 137.62, 131.57, 128.59, 124.54, 120.62, 114.39, 68.08, 47.21, 38.26, 37.69, 35.33, 34.11, 32.08, 29.85, 29.83, 29.76, 29.74, 29.58, 29.52, 26.62, 26.24, 25.88, 22.85, 20.43, 17.87, 14.28.

HRMS $[M+H]^+$ for $C_{41}H_{71}O$ calc: 579.5427 found: 579.5454

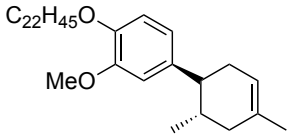

According to **GP**, 44.2 mg (0.1 mmol) dienophile and isoprane (30 µl, 0.3 mmol) were added into the $PrNO_2$+Me-c-Hex (=1:1) solution (0.3 M LiTFSI). Electrolysis was performed at room temperature with a potential of 1.0 (vs Ag/AgCl). After electrolysis (0.3 F per dienophile), the solution was cooled down at -50 °C to make the solution biphasic. After the extraction of only upper phase (Me-c-Hex) and evaporation, the crude products were purified by column chromatography (n-hexane:ethyl acetate = 40:1; column 28 mm x 100 mm), yielding the product as a white solid (yield: 86%, 46 mg, 0.086 mmol).

1H NMR (600 MHz, Chloroform-d) δ 6.80 (d, J = 8.6 Hz, 1H), 6.68 (d, J = 7.0 Hz, 3H), 5.46 – 5.40 (m, 1H), 3.98 (t, J = 6.9 Hz, 3H), 3.84 (s, 4H), 2.30 – 2.04 (m, 5H), 1.92 – 1.76 (m, 4H), 1.69 (s, 3H), 1.48 – 1.41 (m, 3H), 1.25 (s, 39H), 0.88 (t, J = 7.0 Hz, 4H), 0.72 (d, J = 6.4 Hz, 4H).

13C NMR (151 MHz, CHLOROFORM-D) δ 149.40, 146.91, 138.89, 133.96, 120.97, 119.83, 113.02, 111.46, 69.23, 56.15, 47.56, 39.97, 35.32, 34.15, 32.08, 29.85, 29.82, 29.76, 29.73, 29.58, 29.51, 29.44, 26.16, 23.52, 22.84, 20.37, 14.27.

HRMS [M + H]+ for $C_{37}H_{65}O_2$ calc: 541.4984, found: 541.4954.

7-2-4. NMR spectra

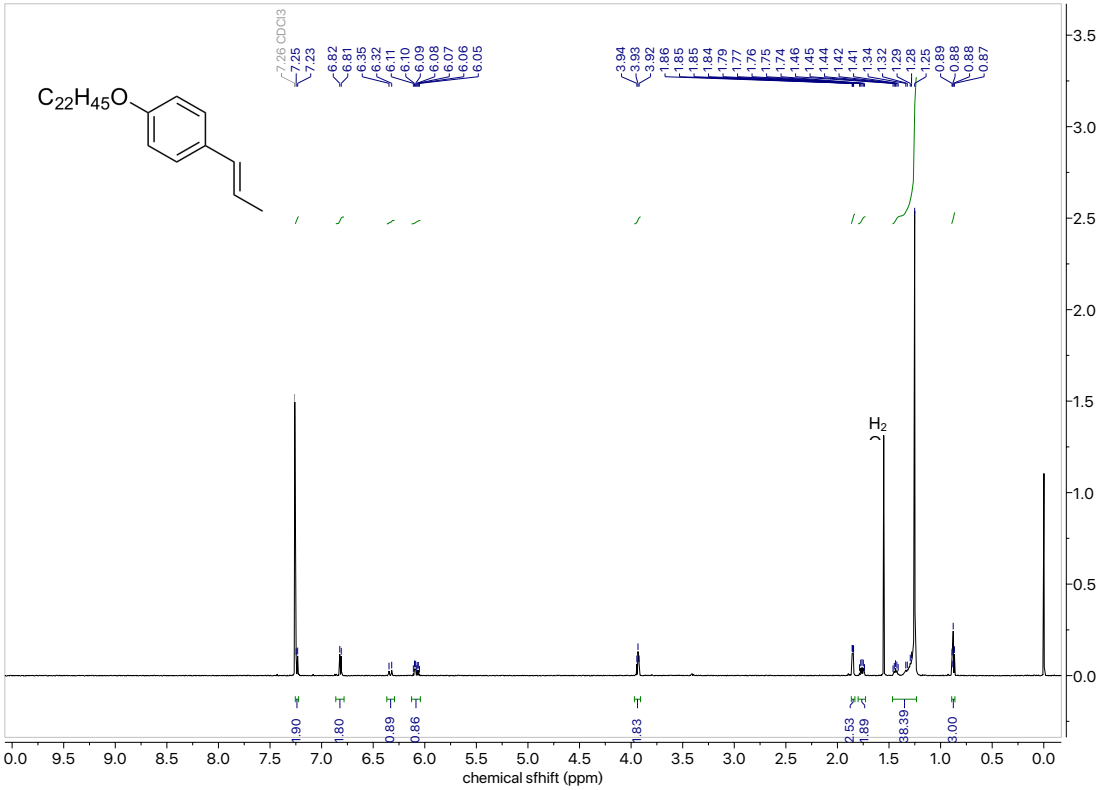

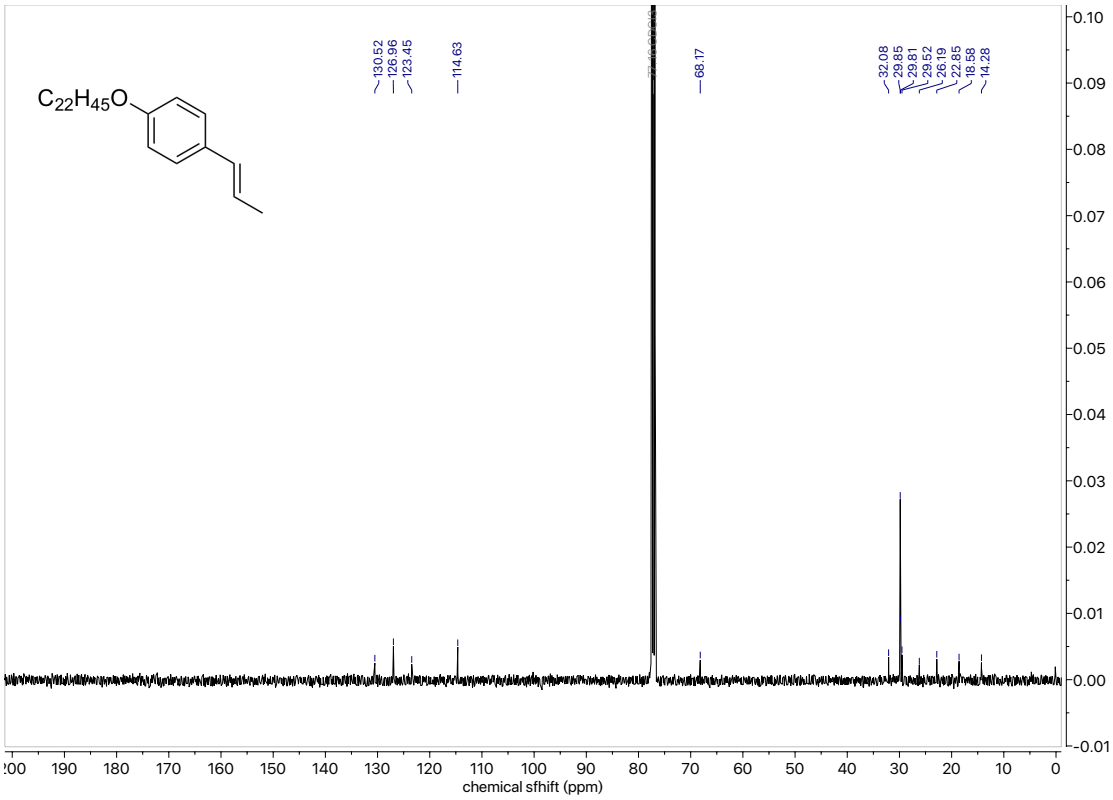

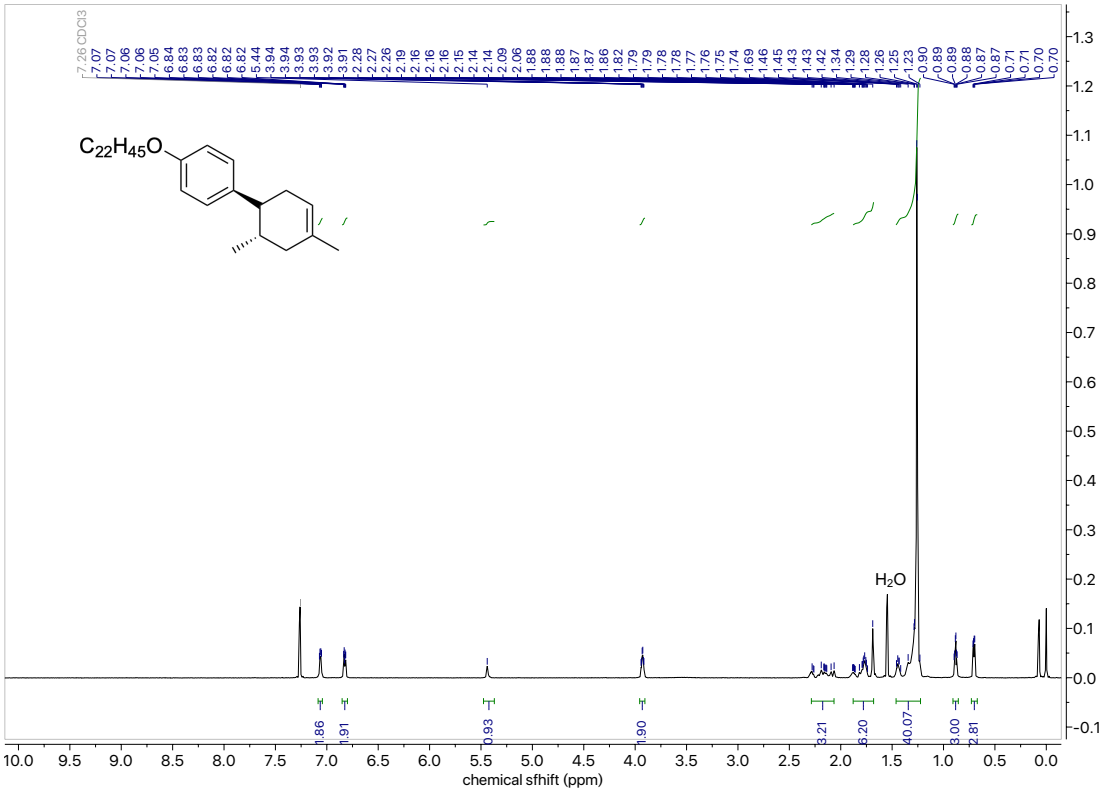
C22H45O
H2O
chemical sfhift (ppm)

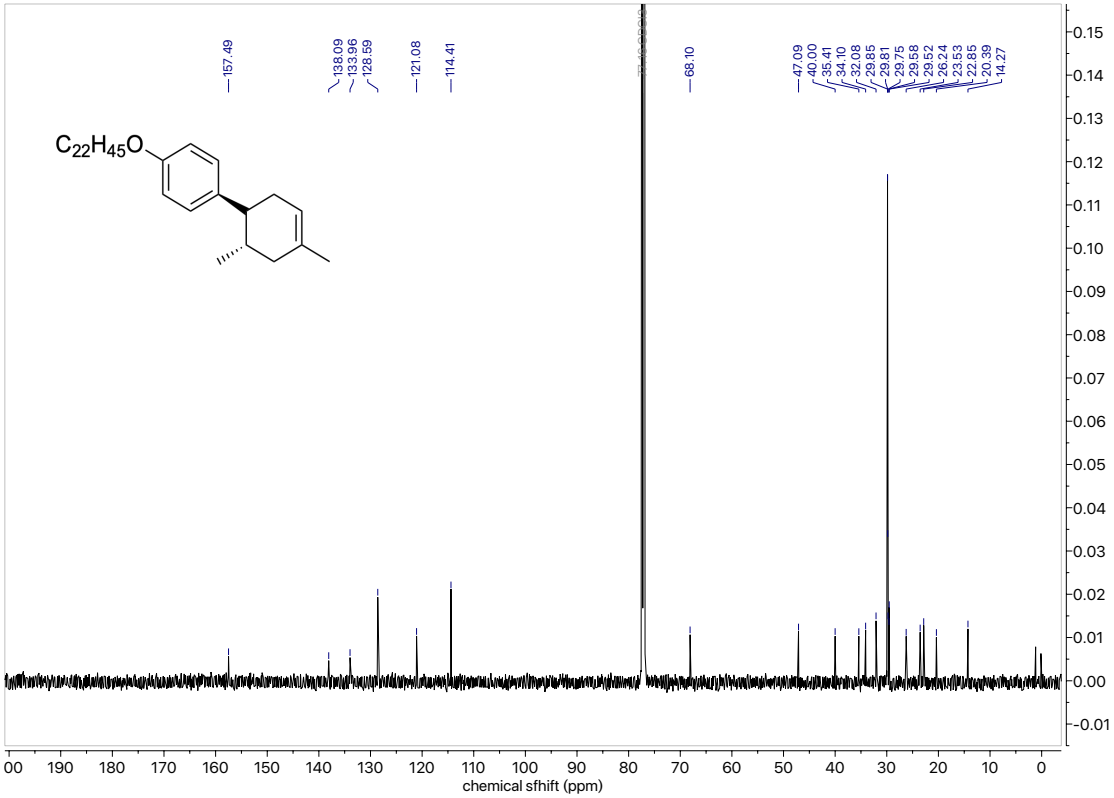
C22H45O
chemical sfhift (ppm)

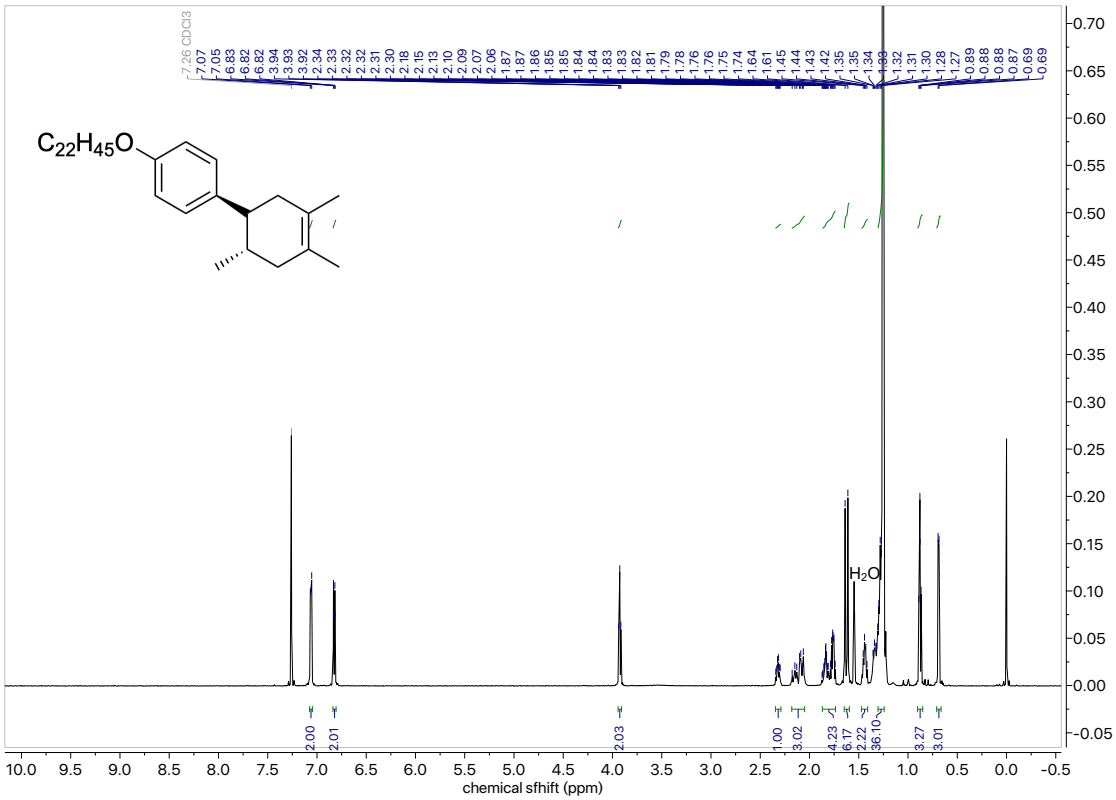
C22H45O
H2O
chemical sfhift (ppm)

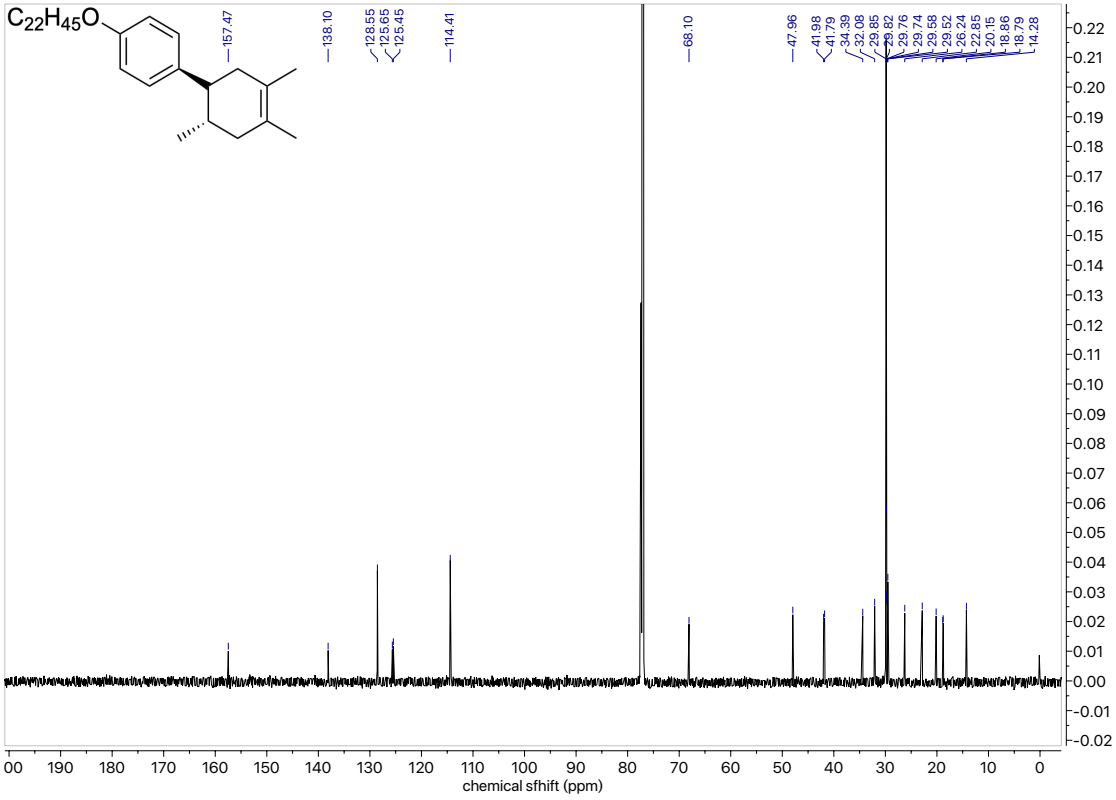
C22H45O
chemical sfhift (ppm)

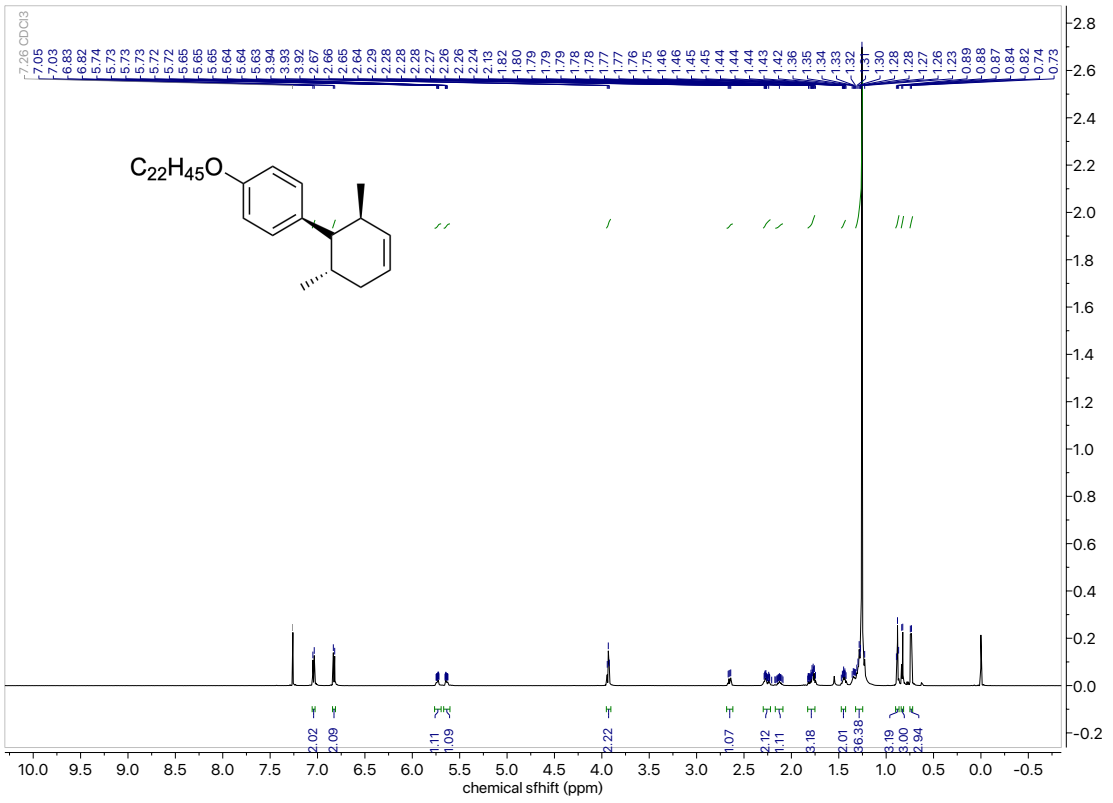
C22H45O
chemical sfhift (ppm)

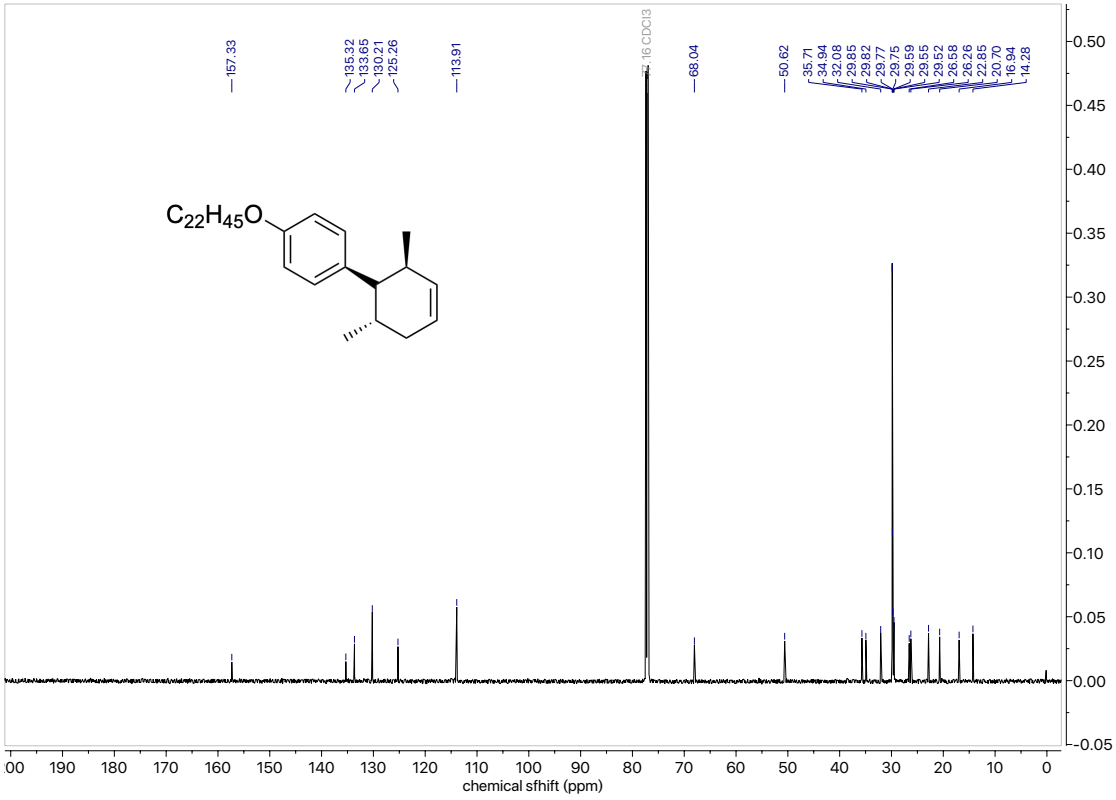
C22H45O
chemical sfhift (ppm)

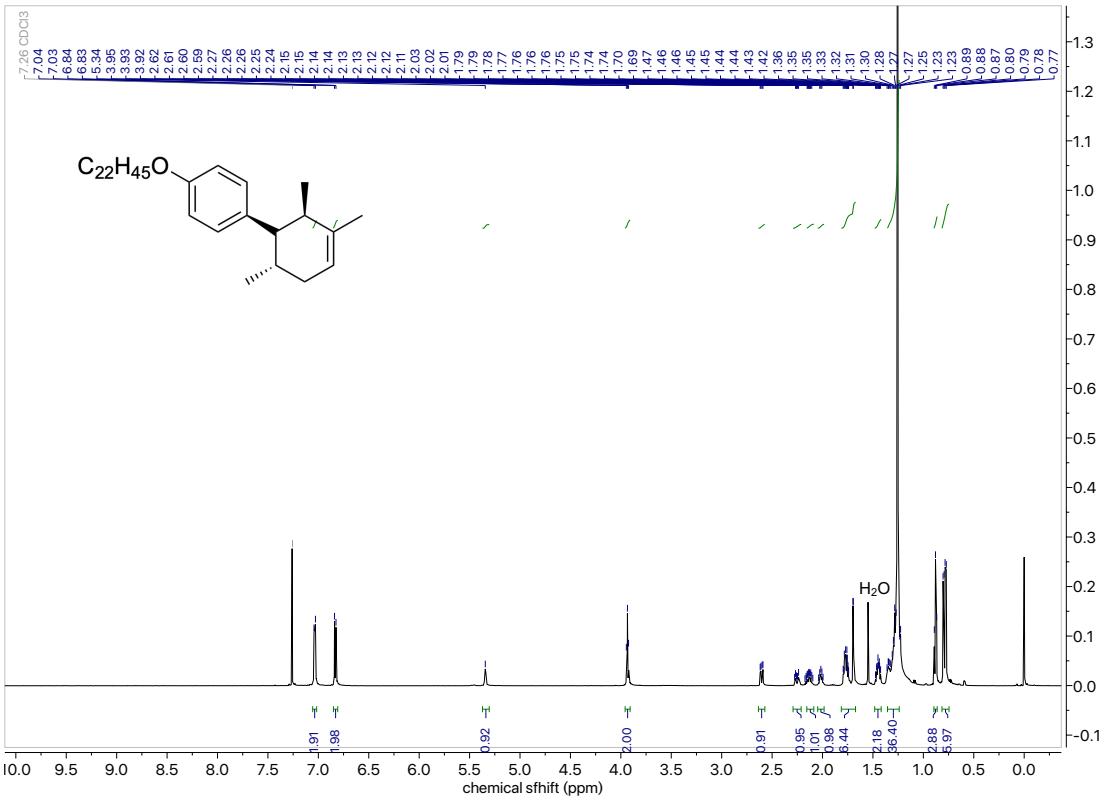
C22H45O
H2O
chemical sfhift (ppm)

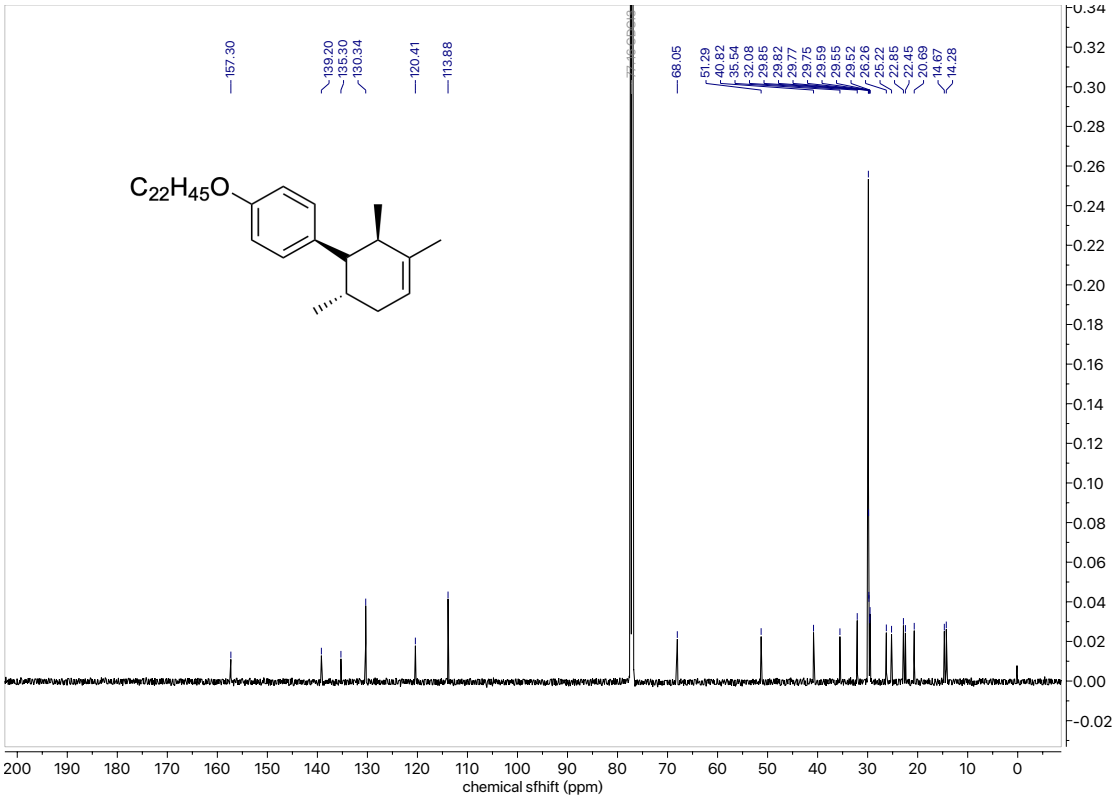
C22H45O
chemical sfhift (ppm)

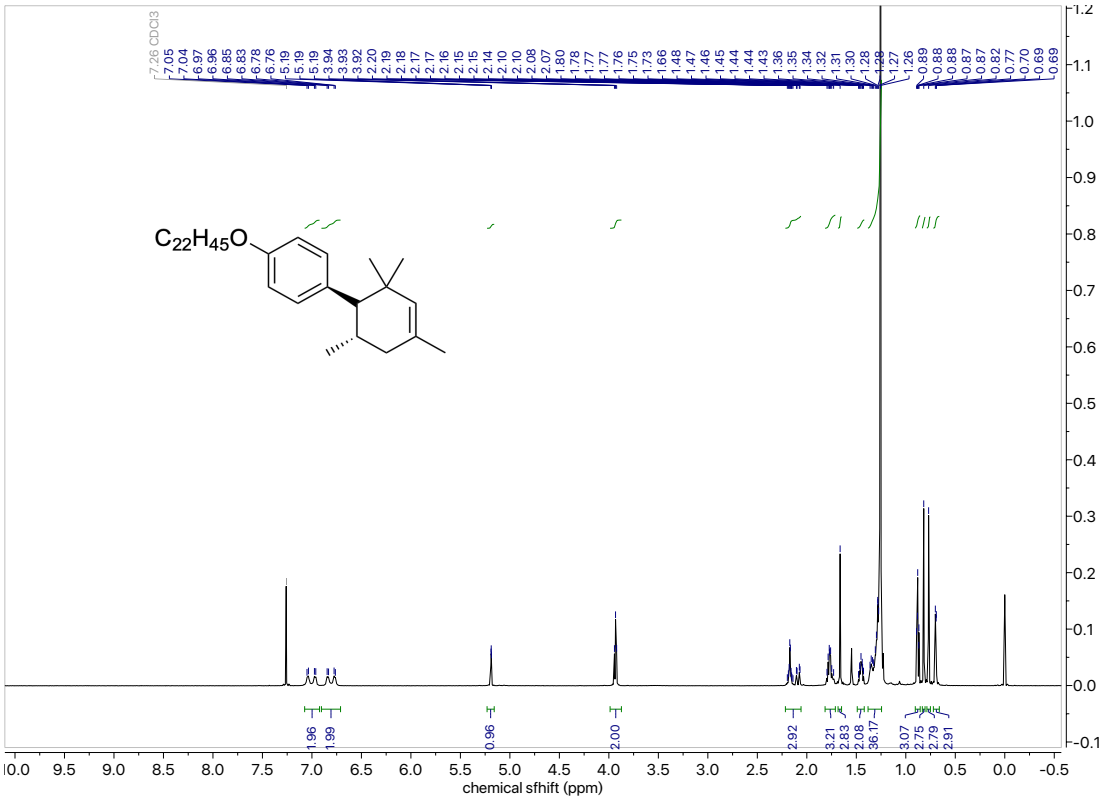
C22H45O
chemical sfhift (ppm)

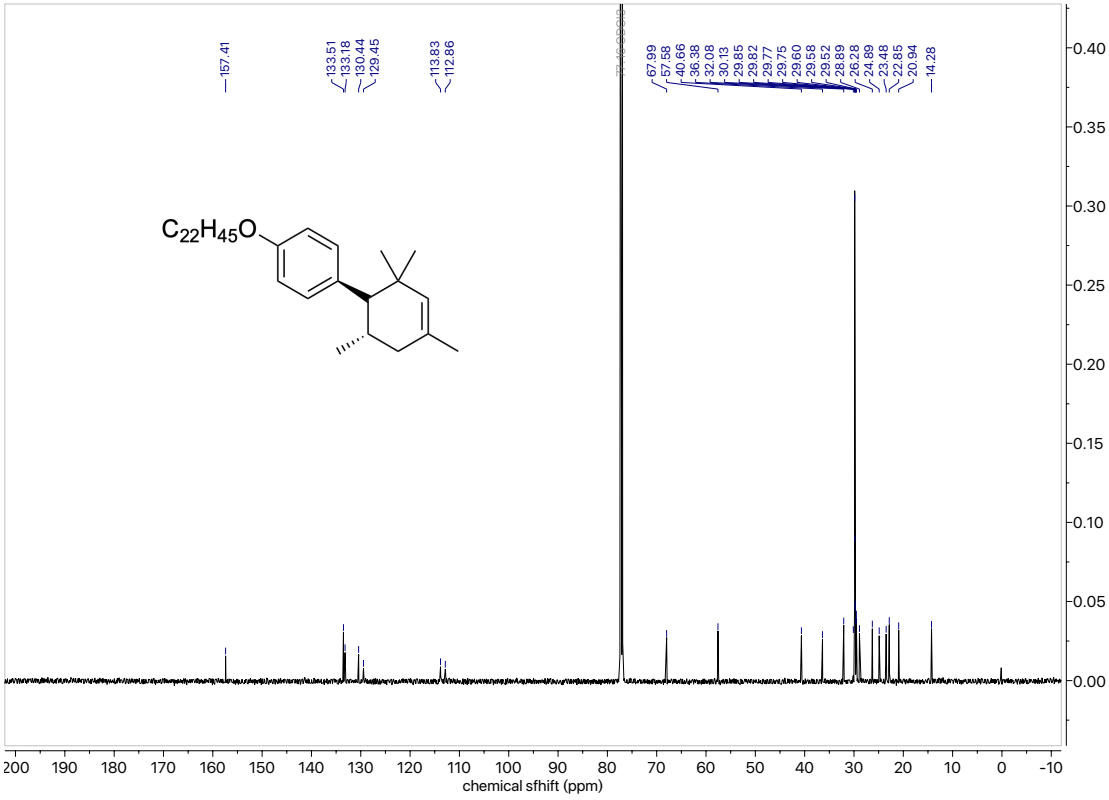
C22H45O
chemical sfhift (ppm)

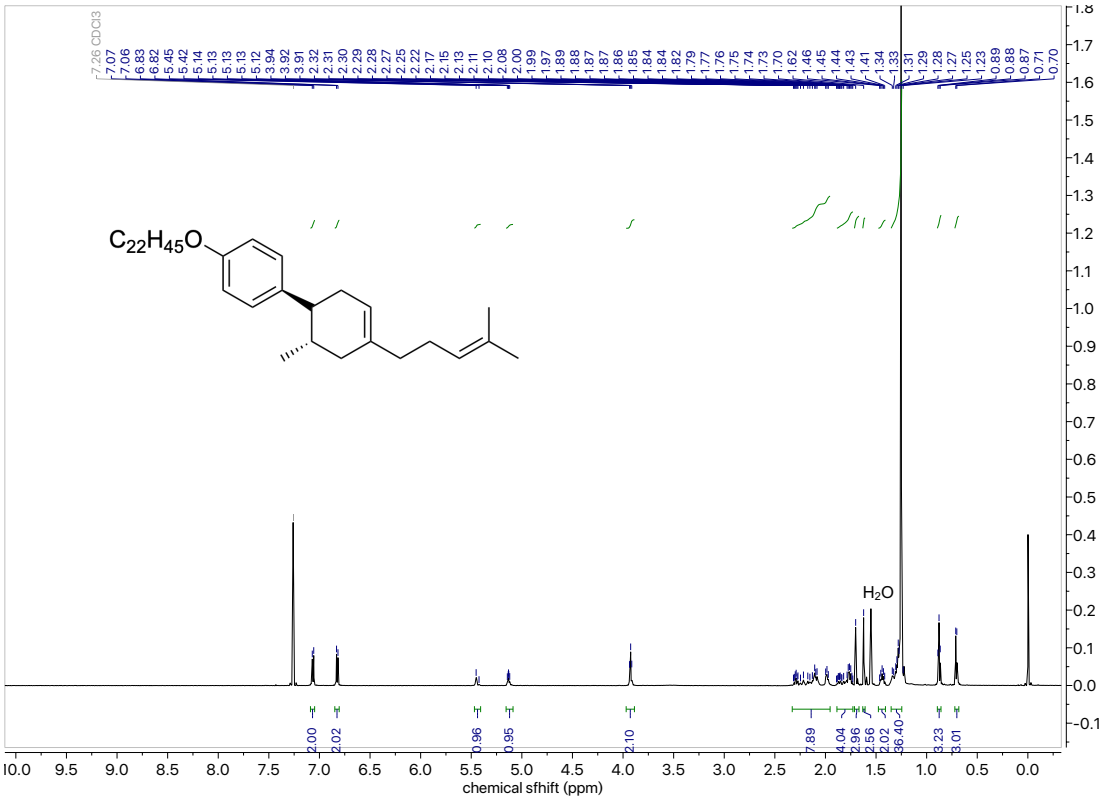
$C_{22}H_{45}O$
H_2O
chemical sfhift (ppm)

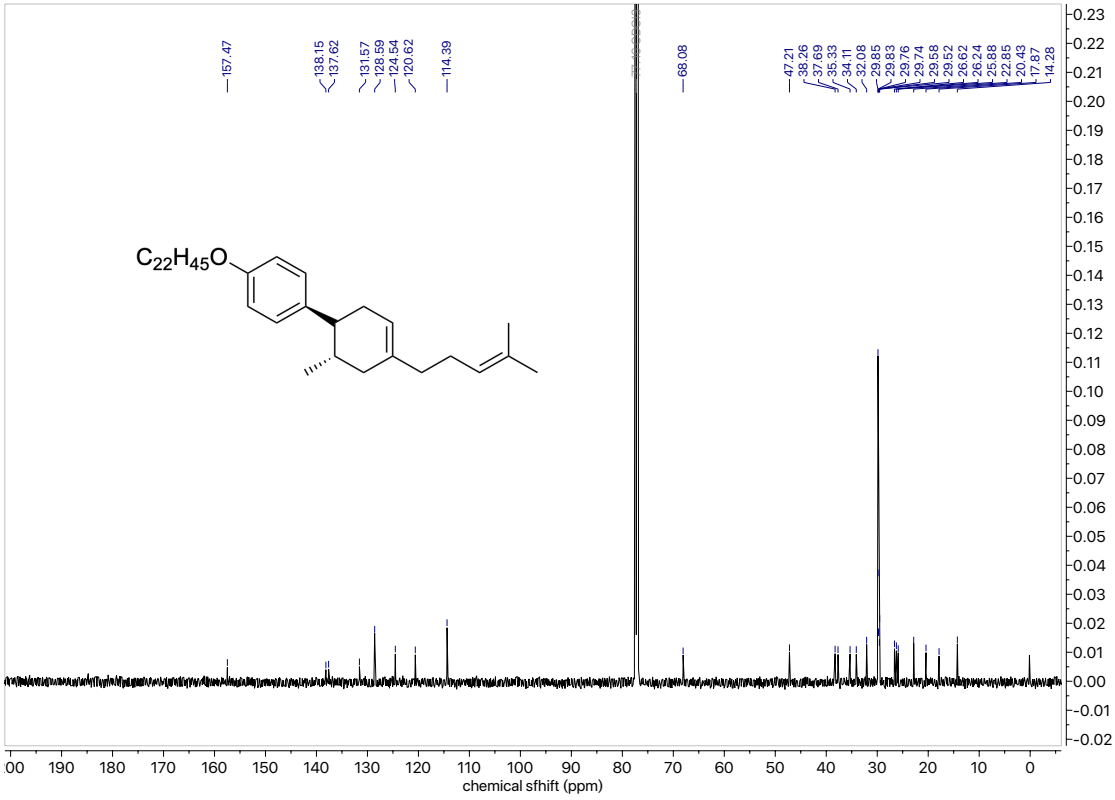
$C_{22}H_{45}O$
chemical sfhift (ppm)

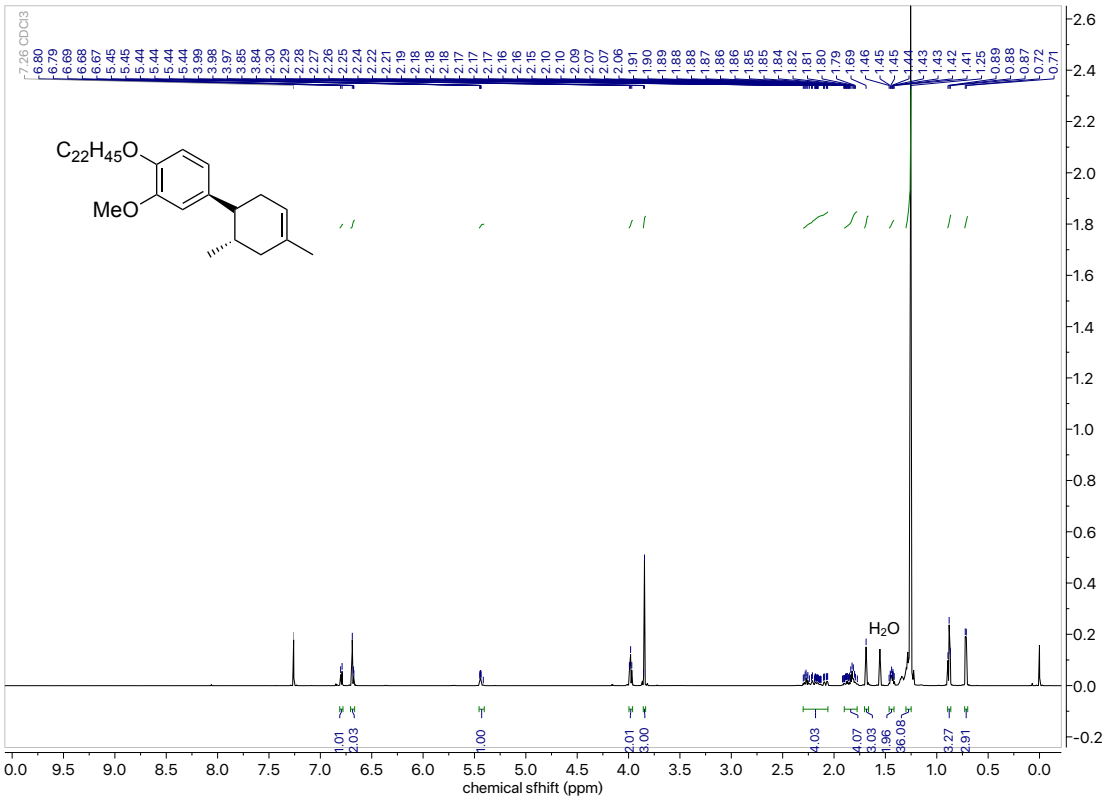
7.26 CDCl3
$C_{22}H_{45}O$
MeO
H_2O
chemical sfhift (ppm)

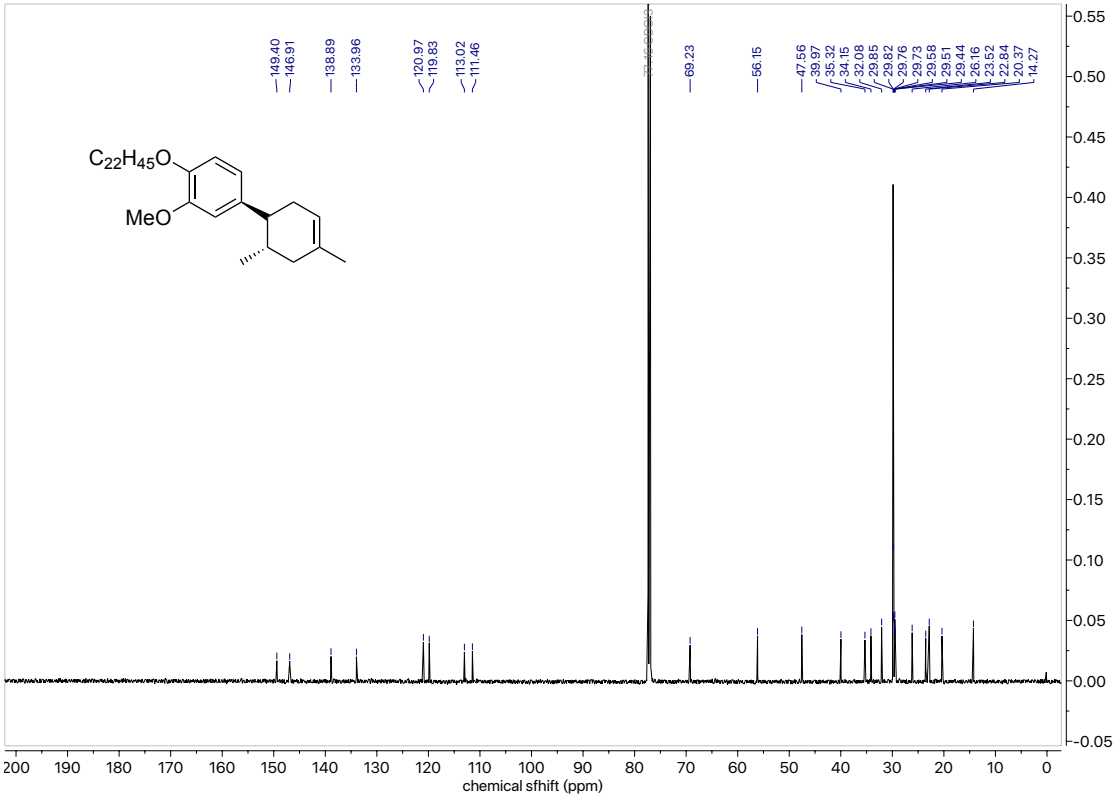
$C_{22}H_{45}O$
MeO
chemical sfhift (ppm)

7-3. Electrode material selective functionalization of styrenes with oxygen: olefin cleavage and tetrahydrofurans formation

Cyclic Voltammetry (CV) Studies

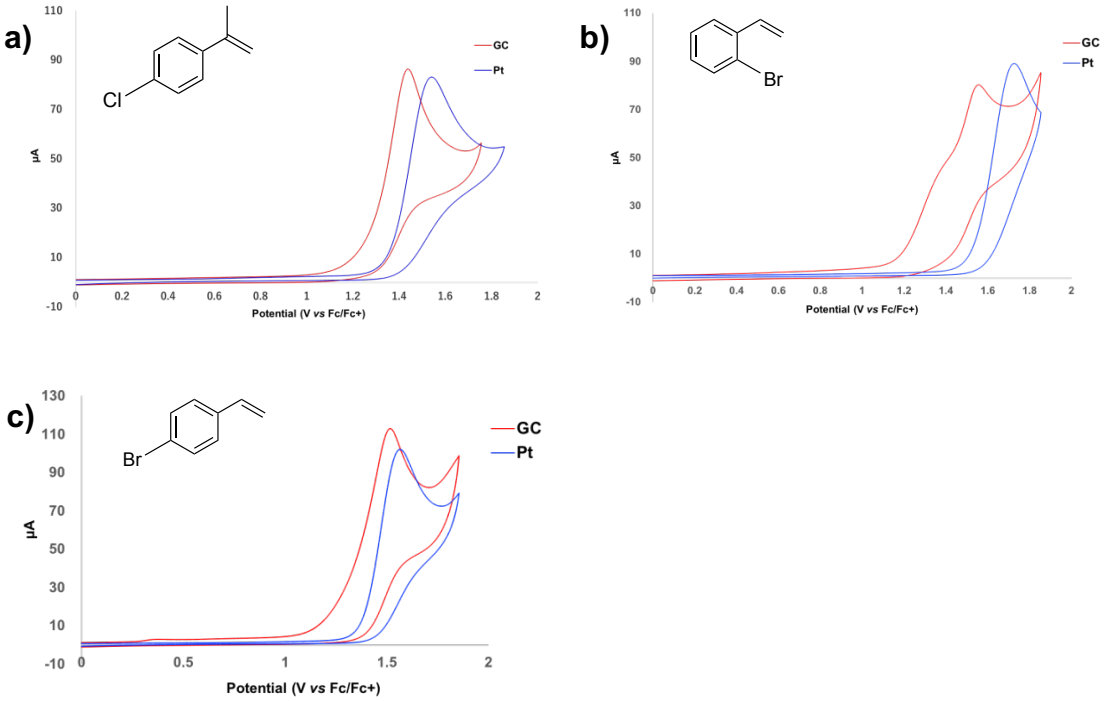

Figure S1. a) Cyclic voltammogram of 2 mM 4-Chloro-α-methylstyrene in 0.1 M Bu_4NBF_4/CH_3CN. b) Cyclic voltammogram of 2 mM 2-Bromostyrene in 0.1 M Bu_4NBF_4/CH_3CN. c) Cyclic voltammogram of 2 mM 4-Bromostyrene in 0.1 M Bu_4NBF_4/CH_3CN. Scan rate: 0.1 V/s. red line: glassy car bon working electrode (7.1 mm^2). blue line: Pt working electrode (7.1 mm^2)

Density Functional Theory (DFT) calculations

Table S1. Cartesian Coordination of the Optimized Structure for the Styrene radical cation calculated at the B3LYP/6-31G+(d,p) level of theory.

Atom	X	Y	Z
C	0.000001038	-0.000002534	-0.000000577
C	0.000002357	0.000000069	0.000000184
C	-0.000000903	0.000000221	-0.000000497
C	-0.000001070	-0.000000189	0.000000136
C	-0.000002633	-0.000002717	-0.000000489
C	0.000000447	-0.000003070	-0.000000911
H	0.000002968	-0.000003113	-0.000001003
H	0.000002904	0.000000227	-0.000000181

H	-0.000003403	0.000000380	0.000000125
H	-0.000003173	-0.000003102	-0.000000741
H	-0.000000103	-0.000004877	-0.000001146
C	-0.000001425	0.000002913	0.000001284
H	-0.000001601	0.000003135	0.000000845
C	0.000001073	0.000004445	0.000000640
H	0.000000746	0.000005088	0.000001428
H	0.000002780	0.000003125	0.000000903

Table S2. Cartesian Coordination of the Optimized Structure for the 2-Bromostyrene radical cation calculated at the B3LYP/6-31G+(d,p) level of theory.

Atom	X	Y	Z
C	-0.000001269	0.000000056	0.000000910
C	-0.000000555	0.000000489	0.000000480
C	-0.000000420	0.000000970	-0.000000149
C	0.000000356	-0.000001057	-0.000000968
C	0.000001204	0.000000590	-0.000000753
C	-0.000000076	-0.000001619	0.000000759
H	0.000000079	-0.000000032	0.000001688
H	-0.000000005	0.000000008	-0.000001302
H	0.000000027	-0.000000115	-0.000000821
H	0.000000107	0.000000679	0.000000384
C	0.000001651	-0.000000126	0.000000064
H	0.000000398	-0.000000529	-0.000001173
C	-0.000002240	0.000000876	-0.000001128
H	0.000000547	-0.000000218	-0.000000364
H	0.000001011	0.000000424	0.000000703
Br	-0.000000815	-0.000000396	0.000001671

Crystal structures of *trans*-3c and *cis*-9c

Crystal structure determination of *trans*-**3c**: $C_{18}H_{18}F_2O$, *Mr* = 288.32; colorless block-like crystals (0.30 x 0.25 x 0.15 mm^3), *T* = 178 K, λ(CuKα) = 1.54187 Å, orthorhombic space group $P2_12_12$, *a* = 8.23236(15) Å, *b* = 16.1327(3) Å, *c* = 5.51150(10) Å, α = 90˚, β = 90˚, γ = 90˚, *V* = 731.98(2) $Å^3$, *Z* = 2, ρ_{calcd} = 1.308 g/cm^3 , θ_{max} = 68.19˚, μ = 0.801 mm^{-1} , *F*(000) = 304, 13385 reflections, 1349 unique reflections (R_{int} = 0.0307),

w=1/[$\sigma^2(F_o^2)$+(0.0623P)^2+0.0114P] where P=(F_o^2+2F_c^2)/3, R_1 = 0.0295 [I > 2σ(I)], R_1 = 0.0319 [all data], wR_2 = 0.0819

Crystal structure determination of *cis*-**9c**: $C_{16}H_{14}Br_2O$, Mr = 382.09; colorless block-like crystals (0.60 x 0.15 x 0.05 mm^3), T = 183 K, λ(MoKα) = 0.71073 Å, monoclinic space group $I2/a$, a = 24.500(2) Å, b = 6.3585(7) Å, c = 18.5072(13) Å, α = 90˚, β = 93.634(6)˚, γ = 90˚, V = 2877.4(4) Å^3, Z = 8, ρ_{calcd} = 1.764 g/cm^3 , θ_{max} = 32.31˚, μ = 5.623 mm^{-1}, F(000) = 1504, 13071 reflections, 5127 unique reflections (R_{int} = 0.0464), w=1/[$\sigma^2(F_o^2)$+(0.0391P)^2] where P=(F_o^2+2F_c^2)/3, R_1 = 0.0463 [I > 2σ(I)], R_1 = 0.0947 [all data], wR_2 = 0.1237

XPS analysis of sulfamic acid modified glassy carbon electrode

After polishing the surface of glassy carbon electrode with alumina, the sulfamic acid film was formed on the electrode by applying the potential scan between -1.5 V to +2.5 V (vs Ag/AgCl) in 0.1 M phosphate buffer solution (pH 7.5). The modification was confirmed by XPS analysis.

X-ray source / X-ray output / range: Single crystal spectroscopy AlKαray / 50.0 W / φ200 μm

Pass energy: narrow scan-69.00 eV (0.125 eV/Step)

Geometry: θ =45 deg.

K-NEXAFS analysis

The polished single crystal of Pt(111) was cleaned under an ultrahigh vacuum by annealing with H_2 gas at 1100 K. After treating with 10 mL benzene at a pressure of 1×10^{-7} Torr at room temperature, the Pt(111) plate was heated at 1000 K for 1 h to gain graphene monolayer on Pt(111) plate.

The analysis was carried out at the soft X-ray beamline BL-7A at the Photon Factory (Institute of Materials Structure Science, High Energy Accelerator Research Organization, Japan). The spectra was measured at 120-300 K by the partial electron yield method, using a microchannel plate at a retarding voltage of 200 V. The incidence angle was set to 0^o and 75^o to observe the orbitals directed in and out of plane.

Unsuccessful olefins for oxidative cleavage

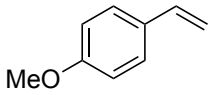

1ab, 0%

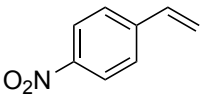

1ac, trace

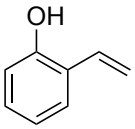

1ad, 0%

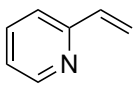

1ae, trace

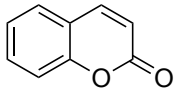

1af, no reaction

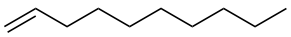

1ag, no reaction

1ah, no reaction

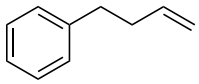

1ai, no reaction

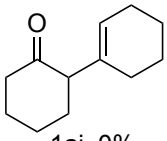

1aj, 0%

1ab and **1ad** led to oligomerization and polymerization. The polymer was observed on the surface of platinum electrode and the solution turned to black color. Nitro group of **1ac** seemed to be reduced to amine and subsequent oligomerization or polymerization. The solution color became black and black polymer was obtained on electrode. **1ae** seemed to afford trace amount of the corresponding aldehyde (by GC-MS analysis) though almost all starting material **1ae** was recovered. No reaction happened to **1af-i**. **1aj** did not afford C=C cleavage.

8- General protocol for oxidative cleavage of olefin (GP I)

A solution of Tetrabutylammonium Perchlorate (**TBAP**) (0.34 g, 1 mmol) in 10 mL Acetonitrile was transferred into an undivided cell. The solution was saturated with oxygen by bubbling with dry oxygen for 5 min. Styrene derivative (0.5 mmol) was added into the solution. The electrolysis cell was equipped with a Platinum anode and a Platinum cathode. A constant current electrolysis with a current density of 1.3 mA/cm^2 was carried out at room temperature. 145 C – 289 C (3.0 F – 6.0 F per styrene) was applied. After the electrolysis, the solution was dissolved in dichloromethane. The organic phase was washed with water. After the organic phase was transferred, dichloromethane was added into the left water phase again and extracted. The solution was dried over $MgSO_4$ and filtered. The crude products were purified by column chromatography.

8-2- Products of oxidative cleavage of olefins

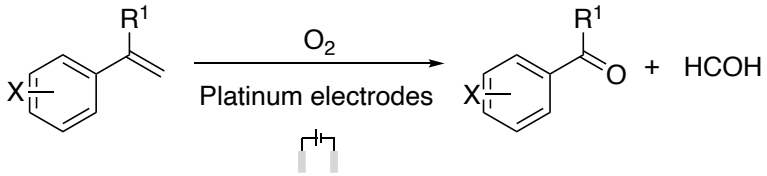

Benzophenone[3]

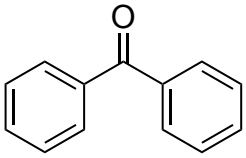

According to **GP I,** 89 µL (0.5 mmol) 1,1-Diphenylethylene was added into the oxygen saturated acetonitrile solution (0.1 M **TBAP**). Electrolysis was performed at room temperature with a current density of 1.3 mA/cm^2. After electrolysis (6.0 F per styrene), the organic phase was extracted with dichloromethane two times and washed with water. The organic phase was dried over $MgSO_4$ and filtered. The crude products were purified by column chromatography (*n*-hexane:ethyl acetate = 10:1; column 38 mm x 120 mm), yielding the product as a while solid (yield: 96 %, 87 mg, 0.48 mmol).

^{1}H NMR (600 MHz, Chloroform-*d*) δ 7.83 – 7.79 (m, 4H), 7.62 – 7.56 (m, 2H), 7.52 – 7.46 (m, 4H).

^{13}C NMR (151 MHz, Chloroform-*d*) δ 196.92, 137.72, 132.56, 130.20, 128.41.

Styrene → Benzaldehyde[3]

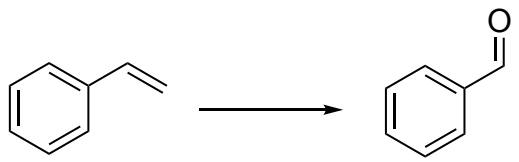

According to **GP I,** 57 µL (0.5 mmol) Styrene was added into the oxygen saturated nitromethane solution (0.1 M **TBAP**). Electrolysis was performed at room temperature with a current density of 1.3 mA/cm^2. After electrolysis (6.0 F per styrene), the organic phase was extracted with dichloromethane two times and washed with water. The organic phase was dried over $MgSO_4$ and filtered. The crude products were purified by column chromatography (*n*-pentane:diethyl ether = 30:1; column 38 mm x 120 mm), yielding the product as a colorless oil (yield: 51 %, 28 mg, 0.26 mmol).

^{1}H NMR (400 MHz, Chloroform-*d*) δ 9.99 (s, 1H), 7.89 – 7.83 (m, 2H), 7.63 – 7.58 (m, 1H), 7.52 – 7.47 (m, 2H).

^{13}C NMR (101 MHz, Chloroform-*d*) δ 192.47, 136.39, 134.51, 129.76, 129.02.

***trans*-β-Methylstyrene → Benzaldehyde**[3]

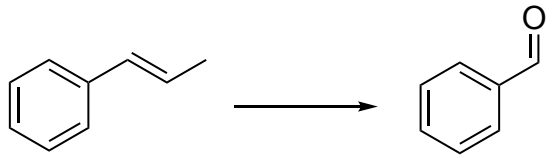

According to **GP I,** 65 µL (0.5 mmol) *trans*-β-Methylstyrene was added into the oxygen saturated acetonitrile solution (0.1 M **TBAP**). Electrolysis was performed at room temperature with a current density of 1.3 mA/cm^2. After electrolysis (6.0 F per styrene), the organic phase was extracted with dichloromethane two times and washed with water. The organic phase was dried over $MgSO_4$ and filtered. The crude products were purified by column chromatography (*n*-pentane:diethyl ether = 30:1; column 38 mm x 120 mm), yielding the product as a colorless oil (yield: 65 %, 35 mg, 0.33 mmol).

^{1}H NMR (600 MHz, Chloroform-*d*) δ 9.96 (s, 1H), 7.84–7.81 (m, 2H), 7.58–7.55 (m, 1H), 7.49–7.45 (m, 2H).

^{13}C NMR (151 MHz, Chloroform-*d*) δ 192.34, 136.30, 134.41, 129.65, 128.93.

***cis*-β-Methylstyrene → Benzaldehyde**[3]

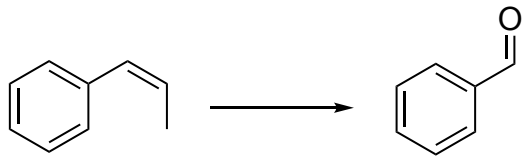

According to **GP I,** 65 µL (0.5 mmol) *cis*-β-Methylstyrene was added into the oxygen saturated acetonitrile solution (0.1 M **TBAP**). Electrolysis was performed at room temperature with a current density of 1.3 mA/cm^2. After electrolysis (4.0 F per styrene), the organic phase was extracted with dichloromethane two times and washed with water. The organic phase was dried over $MgSO_4$ and filtered. The crude products were purified by column chromatography (*n*-pentane:diethyl ether = 30:1; column 38 mm x 120 mm), yielding the product as a colorless oil (yield: 72 %, 38 mg, 0.36 mmol).

^{1}H NMR (600 MHz, Chloroform-*d*) δ 9.96 (s, 1H), 7.84–7.81 (m, 2H), 7.59–7.55 (m, 1H), 7.47 (t, *J* = 7.8 Hz, 2H).

^{13}C NMR (151 MHz, Chloroform-*d*) δ 192.36, 136.29, 134.41, 129.65, 128.93.

4-*tert*-Butylbenzaldehyde[4]

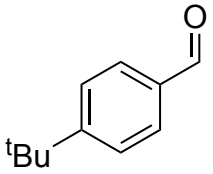

According to **GP I,** 91 µL (0.5 mmol) 4-*tert*-Butylstyrene was added into the oxygen saturated acetonitrile solution (0.1 M **TBAP**). Electrolysis was performed at room temperature with a current density of 1.3 mA/cm^2. After electrolysis (4.0 F per styrene), the organic phase was extracted with dichloromethane two times and washed with water. The organic phase was dried over $MgSO_4$ and filtered. The crude products were purified by column chromatography (*n*-pentane:diethyl ether = 30:1; column 38 mm x 120 mm), yielding the product as a colorless oil (yield: 76 %, 62 mg, 0.38 mmol).

^{1}H NMR (600 MHz, Chloroform-*d*) δ 9.98 (s, 1H), 7.82 (d, *J* = 8.4 Hz, 2H), 7.55 (d, *J* = 8.4 Hz, 2H), 1.35 (s, 14H).

^{13}C NMR (151 MHz, Chloroform-*d*) δ 192.22, 158.56, 134.14, 129.81, 126.10, 35.46, 31.16.

2-Chlorobenzaldehyde[3]

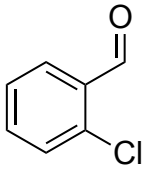

According to **GP I,** 63 µL (0.5 mmol) 2-Chlorostyrene was added into the oxygen saturated nitromethane solution (0.1 M **TBAP**). Electrolysis was performed at room temperature with a current density of 1.3 mA/cm^2. After electrolysis (6.0 F per styrene), the organic phase was extracted with dichloromethane two times and washed with water. The organic phase was dried over $MgSO_4$ and filtered. The crude products were purified by column chromatography (*n*-pentane:diethyl ether = 30:1; column 38 mm x 120 mm), yielding the product as a colorless oil (yield: 79 %, 55 mg, 0.40 mmol).

^{1}H NMR (400 MHz, Chloroform-*d*) δ 10.48 (s, 1H), 7.92 (ddd, *J* = 7.8, 1.8, 0.6 Hz, 1H), 7.56–7.50 (m, 1H), 7.45 (dd, *J* = 8.1, 1.3 Hz, 1H), 7.41–7.36 (m, 1H).

^{13}C NMR (101 MHz, Chloroform-*d*) δ 189.96, 138.06, 135.25, 132.53, 130.71, 129.46, 127.40.

2-Bromobenzaldehyde[6]

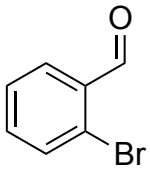

According to **GP I,** 65 µL (0.5 mmol) 2-Bromostyrene was added into the oxygen saturated acetonitrile solution (0.1 M **TBAP**). Electrolysis was performed at room temperature with a current density of 1.3 mA/cm^2. After electrolysis (4.0 F per styrene), the organic phase was extracted with dichloromethane two times and washed with water. The organic phase was dried over $MgSO_4$ and filtered. The crude products were purified by column chromatography (*n*-hexane:ethyl acetate = 10:1; column 38 mm x 120 mm), yielding the product as a colorless oil (yield: 84 %, 77 mg, 0.42 mmol).

^{1}H NMR (400 MHz, Chloroform-*d*) δ 10.34 (s, 1H), 7.91–7.87 (m, 1H), 7.64–7.61 (m, 1H), 7.45–7.38 (m, 2H).

^{13}C NMR (101 MHz, Chloroform-*d*) δ 191.96, 135.46, 133.98, 133.54, 129.93, 128.01, 127.23.

3-Bromobenzaldehyde[7]

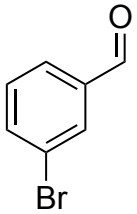

According to **GP I,** 65 µL (0.5 mmol) 3-Bromostyrene was added into the oxygen saturated nitromethane solution (0.1 M **TBAP**). Electrolysis was performed at room temperature with a current density of 1.3 mA/cm^2. After electrolysis (4.0 F per styrene), the organic phase was extracted with dichloromethane two times and washed with water. The organic phase was dried over $MgSO_4$ and filtered. The crude products were purified by column chromatography (*n*-hexane:ethyl acetate = 10:1; column 38 mm x 120 mm), yielding the product as a colorless oil (yield: 77 %, 70 mg, 0.39 mmol).

^{1}H NMR (400 MHz, Chloroform-*d*) δ 9.96 (s, 1H), 8.02 (t, *J* = 1.8 Hz, 1H), 7.81 (d, *J* = 7.7 Hz, 1H), 7.76 (d, *J* = 8.0 Hz, 1H), 7.43 (t, *J* = 7.8 Hz, 1H).

^{13}C NMR (101 MHz, Chloroform-*d*) δ 190.90, 138.06, 137.43, 132.47, 130.74, 128.50, 123.47.

4-Bromobenzaldehyde[4]

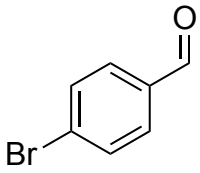

According to **GP I,** 65 µL (0.5 mmol) 4-Bromostyrene was added into the oxygen saturated nitromethane solution (0.1 M **TBAP**). Electrolysis was performed at room temperature with a current density of 1.3 mA/cm^2. After electrolysis (5.0 F per styrene), the organic phase was extracted with dichloromethane two times and washed with water. The organic phase was dried over $MgSO_4$ and filtered. The crude products were purified by column chromatography (*n*-hexane:ethyl acetate = 10:1; column 38 mm x 120 mm), yielding the product as a while solid (yield: 47 %, 43 mg, 0.24 mmol).

^{1}H NMR (400 MHz, Chloroform-*d*) δ 9.98 (s, 1H), 7.77 – 7.73 (m, 2H), 7.71 – 7.66 (m, 2H).

^{13}C NMR (101 MHz, Chloroform-*d*) δ 191.27, 135.18, 132.59, 131.13, 129.95.

2-(Trifluoromethyl)benzaldehyde[8]

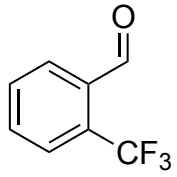

According to **GP I,** 74 µL (0.5 mmol) 2-(Trifluoromethyl)styrene was added into the oxygen saturated nitromethane solution (0.1 M **TBAP**). Electrolysis was performed at room temperature with a current density of 1.3 mA/cm^2. After electrolysis (4.0 F per styrene), the organic phase was extracted with dichloromethane two times and washed with water. The organic phase was dried over $MgSO_4$ and filtered. The crude products were purified by column chromatography (*n*-hexane:ethyl acetate = 10:1; column 38 mm x 120 mm), yielding the product as a colorless oil (yield: 87 %, 76 mg, 0.44 mmol).

^{1}H NMR (400 MHz, Chloroform-*d*) δ 10.39 (s, 1H), 8.15–8.10 (m, 1H), 7.81–7.74 (m, 1H), 7.74–7.67 (m, 2H).

^{13}C NMR (101 MHz, Chloroform-*d*) δ 189.18, 133.78, 132.48, 129.21, 126.26, 126.21, 125.21, 122.48.

^{19}F NMR (376 MHz, Chloroform-*d D*) δ -55.42.

Acetophenone[3]

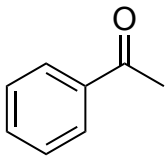

According to **GP I,** 65 µL (0.5 mmol) α-Methylstyrene was added into the oxygen saturated nitromethane solution (0.1 M **TBAP**). Electrolysis was performed at room temperature with a current density of 1.3 mA/cm^2. After electrolysis (6.0 F per styrene), the organic phase was extracted with dichloromethane two times and washed with water. The organic phase was dried over $MgSO_4$ and filtered. The crude products were purified by column chromatography (*n*-pentane:diethyl ether = 30:1; column 38 mm x 120 mm), yielding the product as a white solid (yield: 83 %, 50 mg, 0.42 mmol).

^{1}H NMR (400 MHz, Chloroform-*d*) δ 7.96 (d, *J* = 8.3, 2H), 7.59 – 7.53 (m, 1H), 7.46 (ddd, *J* = 8.7, 6.9, 1.5 Hz, 2H), 2.61 (s, 3H).

^{13}C NMR (101 MHz, Chloroform-*d*) δ 198.34, 137.19, 133.24, 128.69, 128.43, 26.76.

2'-Acetonaphthone[5]

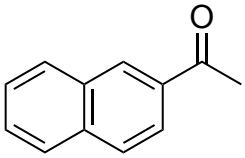

According to **GP I,** 84 mg (0.5 mmol) 2-Isopropenylnaphthalene was added into the oxygen saturated acetonitrile solution (0.1 M **TBAP**). Electrolysis was performed at room temperature with a current density of 1.3 mA/cm^2. After electrolysis (3.0 F per styrene), the organic phase was extracted with dichloromethane two times and washed with water. The organic phase was dried over $MgSO_4$ and filtered. The crude products were purified by column chromatography (*n*-hexane:ethyl acetate = 10:1; column 38 mm x 120 mm), yielding the product as a white solid (yield: 68 %, 58 mg, 0.34 mmol).

^{1}H NMR (600 MHz, Chloroform-*d*) δ 8.48 (s, 1H), 8.04 (dd, *J* = 8.6, 1.8 Hz, 1H), 7.97 (dd, *J* = 8.2, 1.3 Hz, 1H), 7.89 (t, *J* = 9.8 Hz, 2H), 7.61 (td, *J* = 8.2, 1.3 Hz, 1H), 7.56 (td, *J* = 8.1, 1.3 Hz, 1H), 2.74 (s, 3H).

^{13}C NMR (151 MHz, Chloroform-*d*) δ 198.32, 135.72, 134.60, 132.64, 130.37, 129.70, 128.63, 128.57, 127.93, 126.93, 124.03, 26.87.

4'-Fluoroacetophenone[3]

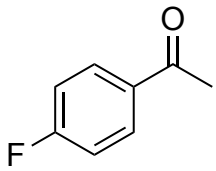

According to **GP I,** 67 µL (0.5 mmol) 4-Fluoro-α-methylstyrene was added into the oxygen saturated acetonitrile solution (0.1 M **TBAP**). Electrolysis was performed at room temperature with a current density of 1.3 mA/cm^2. After electrolysis (6.0 F per styrene), the organic phase was extracted with dichloromethane two times and washed with water. The organic phase was dried over $MgSO_4$ and filtered. The crude products were purified by column chromatography (*n*-pentane:diethyl ether = 10:1; column 38 mm x 120 mm), yielding the product as a colorless oil (yield: 78 %, 54 mg, 0.39 mmol).

^{1}H NMR (400 MHz, Chloroform-*d*) δ 8.05 – 7.93 (m, 2H), 7.17 – 7.08 (m, 2H), 2.59 (s, 3H).
^{13}C NMR (101 MHz, CHLOROFORM-*D*) δ 196.67, 167.16, 164.63, 133.70, 131.13, 115.90, 115.68, 26.70.
^{19}F NMR (376 MHz, Chloroform-*d*) δ -105.18.

4'-Chloroacetophenone[3]

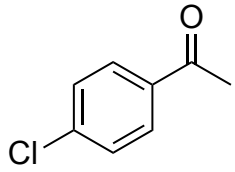

According to **GP I,** 71 µL (0.5 mmol) 4-Chloro-α-methylstyrene was added into the oxygen saturated acetonitrile solution (0.1 M **TBAP**). Electrolysis was performed at room temperature with a current density of 1.3 mA/cm^2. After electrolysis (7.0 F per styrene), the organic phase was extracted with dichloromethane two times and washed with water. The organic phase was dried over $MgSO_4$ and filtered. The crude products were purified by column chromatography (*n*-hexane:ethyl acetate = 20:1; column 38 mm x 120 mm), yielding the product as a white solid (yield: 84 %, 65 mg, 0.42 mmol).

^{1}H NMR (400 MHz, Chloroform-*d*) δ 7.91 – 7.88 (m, 2H), 7.46 – 7.42 (m, 2H), 2.59 (s, 3H).
^{13}C NMR (101 MHz, Chloroform-*d*) δ 197.02, 139.71, 135.53, 129.87, 129.03, 26.73.

1-(4-chlorophenyl)ethan-1-one-^{18}O

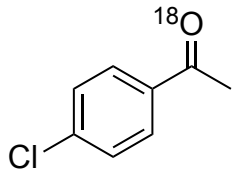

According to **GP I,** 71 µL (0.5 mmol) 4-Chloro-α-methylstyrene was added into the oxygen ($^{18}O_2$) saturated acetonitrile solution (0.1 M **TBAP**). Electrolysis was performed at room temperature with a current density of 1.3 mA/cm^2. After electrolysis (7.0 F per styrene), the organic phase was extracted with dichloromethane two times and washed with water. The organic phase was dried over $MgSO_4$ and filtered. The crude products were purified by column chromatography (*n*-hexane:ethyl acetate = 20:1; column 38 mm x 120 mm), yielding the product as a white solid (yield: 81 %, 63 mg, 0.41 mmol).

^{1}H NMR (600 MHz, Chloroform-*d*) δ 7.92–7.87 (m, 2H), 7.45–7.42 (m, 2H), 2.59 (s, 3H).
^{13}C NMR (151 MHz, CHLOROFORM-*D*) δ 197.00, 139.73, 135.58, 129.87, 129.04, 26.70.
HRMS for C8H7Cl^{18}ONa calc: 179.008313 found: 179.0078268

4-(3,5,5,8,8-pentamethyl-5,6,7,8-tetrahydronaphthalene-2-carbonyl)benzoic acid

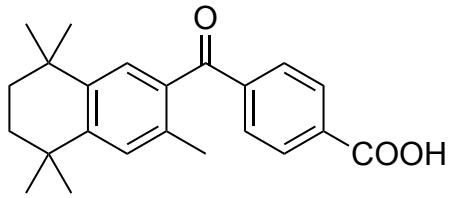

According to **GP I,** 35 mg (0.1 mmol) Bexarotene was added into the oxygen saturated acetonitrile solution (0.1 M **TBAP**). Electrolysis was performed at room temperature with a current density of 1.3 mA/cm^2. After electrolysis (6.0 F per styrene), the organic phase was extracted with dichloromethane two times and washed with NH_4Cl aq. The organic phase was dried over $MgSO_4$ and filtered. The crude products were purified by column chromatography (toluene:diethyl ether = 1:1; column 38 mm x 150 mm), yielding the product as a white solid (yield: 52 %, 18 mg, 0.05 mmol).

Rf (toluene : diethyl ether = 1:1) = 0.08

^{1}H NMR (600 MHz, Chloroform-*d*) δ 8.20 (d, *J* = 8.4 Hz, 2H), 7.89 (d, *J* = 8.3 Hz, 2H), 7.27 (s, 1H), 7.22 (s, 1H), 2.36 (s, 3H), 1.70 (s, 4H), 1.32 (s, 6H), 1.21 (s, 6H).

^{13}C NMR (151 MHz, Chloroform-*d*) δ 197.86, 170.64, 148.67, 142.85, 142.12, 134.83, 134.72, 132.61, 130.28, 130.23, 129.66, 128.73, 35.02, 34.97, 34.53, 34.05, 31.84, 31.76, 30.44, 20.26.

HRMS C23H26O3Na calc: 373.177965 found: 373.1779265

2-Phenylpropylene Oxide[9]

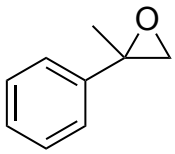

According to **GP I,** 65 µL (0.5 mmol) α-Methylstyrene was added into the oxygen saturated nitromethane solution (0.1 M **TBAP**). Electrolysis was performed at room temperature with a current density of 1.3 mA/cm^2. After electrolysis (3.0 F per styrene), the organic phase was extracted with dichloromethane and washed with water. The organic phase was dried over $MgSO_4$ and filtered. The crude products were purified by column chromatography (*n*-pentane:diethyl ether = 30:1; column 38 mm x 150 mm), yielding the product as a colorless oil (yield: 6 %, 4 mg, 0.03 mmol).

Rf (*n*-hexane : ethyl acetate = 10:1) = 0.50

^{1}H NMR (600 MHz, Chloroform-*d*) δ 7.41–7.30 (m, 4H), 7.32–7.24 (m, 1H), 2.98 (d, *J* = 5.4 Hz, 1H), 2.81 (d, *J* = 5.4 Hz, 1H), 1.73 (s, 3H).

^{13}C NMR (151 MHz, Chloroform-*d*) δ 141.31, 128.48, 127.61, 125.45, 57.20, 56.88, 21.95.

9- General protocol for tetrahydrofuran derivatives formation (GP II)

A solution of Tetrabutylammonium Perchlorate (**TBAP**) (0.34 g, 1 mmol) in 10 mL Acetonitrile was transferred into an undivided cell. The solution was saturated with oxygen by bubbling with dry oxygen for 5 min. Styrene derivative (0.5 mmol) was added into the solution. The electrolysis cell was equipped with a Carbon felt anode and a Carbon felt cathode. A constant current electrolysis with a current 2.0 mA was carried out at room temperature.

193 C – 289 C (4.0 F – 6.0 F per styrene) was applied. After the electrolysis, the solution was dissolved in dichloromethane. The organic phase was washed with water. After the organic

phase was transferred, dichloromethane was added into the left water phase again and extracted. The solution was dried over $MgSO_4$ and filtered. The crude products were purified by column chromatography.

4.1. Products of tetrahydrofurans formation

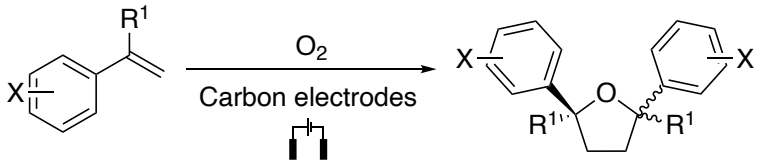

2,2,5,5-tetraphenyltetrahydrofuran

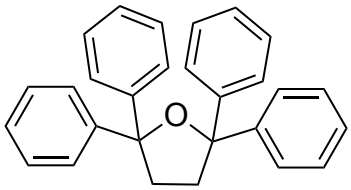

According to **GP II,** 89 µL (0.5 mmol) 1,1-Diphenylethylene was added into the oxygen saturated acetonitrile solution (0.1 M **TBAP**). Electrolysis was performed at room temperature with a current of 2.0 mA. After electrolysis (6.0 F per styrene), the organic phase was extracted with dichloromethane and washed with water. The organic phase was dried over $MgSO_4$ and filtered. The crude products were purified by column chromatography (*n*-hexane:ethyl acetate = 10:1; column 38 mm x 120 mm), yielding the product as a while solid (yield: 89 %, 83 mg, 0.22 mmol).

Rf (*n*-hexane : ethyl acetate = 10:1) = 0.50
melting point: 157.2 ℃-158.1 ℃
^{1}H NMR (600 MHz, Chloroform-*d*) δ 7.45–7.41 (m, 8H), 7.24–7.20 (m, 8H), 7.17–7.13 (m, 4H), 2.65 (s, 3H).
^{13}C NMR (151 MHz, CHLOROFORM-*D*) δ 147.42, 128.03, 126.52, 126.08, 89.57, 37.55.
HRMS for C28H25O calc: 377.1905 found: 377.1895

(2*S*,5*S*)-2,5-diphenyltetrahydrofuran (left) and (2*R*,5*S*)-2,5-diphenyltetrahydrofuran (right)

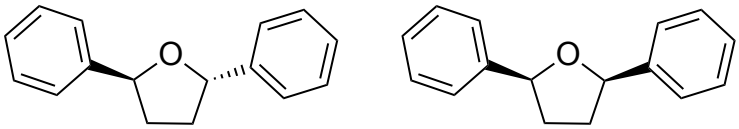

According to **GP II,** 57 µL (0.5 mmol) Styrene was added into the oxygen saturated acetonitrile solution (0.1 M **TBAP**). Electrolysis was performed at room temperature with a current of 2.0 mA. After electrolysis (12.0 F per styrene), the organic phase was extracted with dichloromethane and washed with water. The organic phase was dried over $MgSO_4$ and filtered. The crude products were purified by column chromatography (*n*-hexane:ethyl acetate = 10:1; column 38 mm x 120 mm), yielding the product as a while solid (total yield: 36 %, 20 mg, 0.09 mmol).

(2*S*,5*S*)-2,5-diphenyltetrahydrofuran

Rf (*n*-hexane : ethyl acetate = 10:1) = 0.59

Colorless liquid

^{1}H NMR (600 MHz, Chloroform-*d*) δ 7.41 (d, *J* = 6.0 Hz, 4H), 7.36 (t, *J* = 8.5 Hz, 4H), 7.29–7.25 (m, 2H), 5.27 (t, *J* = 6.7 Hz, 2H), 2.54–2.45 (m, 2H), 2.05–1.97 (m, 2H).

^{13}C NMR (151 MHz, Chloroform-*d*) δ 143.77, 128.51, 127.34, 125.72, 81.49, 35.75.

HRMS for C16H17O calc: 225.1279 found: 225.1250

(2*R*,5*S*)-2,5-diphenyltetrahydrofuran

Rf (*n*-hexane : ethyl acetate = 10:1) = 0.50

Colorless liquid

^{1}H NMR (600 MHz, Chloroform-*d*) δ 7.45 (d, *J* = 12.0 Hz, 4H), 7.36 (t, *J* = 8.5 Hz, 4H), 7.30–7.27 (m, 2H), 5.06 (t, *J* = 6.0 Hz, 2H), 2.47-2.41 (m, 2H), 2.02–1.94 (m, 2H).

^{13}C NMR (151 MHz, Chloroform-*d*) δ 143.05, 128.49, 127.44, 126.14, 81.37, 34.53.

HRMS for C16H17O calc: 225.1279 found: 225.1303

(2*S*,5*S*)-2,5-bis(4-(*tert*-butyl)phenyl)tetrahydrofuran (left) and (2*R*,5*S*)-2,5-bis(4-(*tert*-butyl)phenyl)tetrahydrofuran

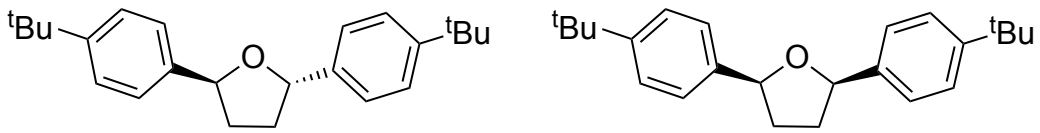

According to **GP II,** 91 µL (0.5 mmol) 4-*tert*-Butylstyrene was added into the oxygen saturated acetonitrile solution (0.1 M **TBAP**). Electrolysis was performed at room temperature with a

current of 2.0 mA. After electrolysis (12.0 F per styrene), the organic phase was extracted with dichloromethane and washed with water. The organic phase was dried over $MgSO_4$ and filtered. The crude products were purified by column chromatography (*n*-hexane:ethyl acetate = 10:1; column 38 mm x 120 mm), yielding the product as a while solid (total yield: 54 %, 45.3 mg, 0.14 mmol).

(2*S*,5*S*)-2,5-bis(4-(*tert*-butyl)phenyl)tetrahydrofuran

Rf (*n*-hexane : ethyl acetate = 10:1) = 0.39

melting point: 111.1 ℃ - 111.9 ℃

^{1}H NMR (600 MHz, Chloroform-*d*) δ 7.39–7.33 (m, 8H), 5.22 (td, *J* = 7.8, 5.5 Hz, 2H), 2.50–2.43 (m, 2H), 2.06–1.98 (m, 2H), 1.32 (s, 18H).

^{13}C NMR (151 MHz, Chloroform-*d*) δ 150.19, 140.72, 125.56, 125.38, 81.07, 35.43, 34.62, 31.53.

HRMS for C24H32ONa calc: 359.2350 found: 359.2367

(2*R*,5*S*)-2,5-bis(4-(*tert*-butyl)phenyl)tetrahydrofuran

Rf (*n*-hexane : ethyl acetate = 10:1) = 0.33

melting point: 88.7 ℃ - 89.1 ℃

^{1}H NMR (600 MHz, Chloroform-*d*) δ 7.38 (d, *J* = 0.8 Hz, 8H), 5.02 (td, *J* = 5.0, 2.5 Hz, 2H), 2.45–2.34 (m, 2H), 2.05–1.94 (m, 2H), 1.32 (s, 18H).

^{13}C NMR (151 MHz, CHLOROFORM-*D*) δ 150.27, 140.10, 125.96, 125.35, 81.17, 34.64, 34.41, 31.53.

HRMS for C24H32ONa calc: 359.2350 found: 359.2369

(*S*)-2,5-bis(2-bromophenyl)tetrahydrofuran

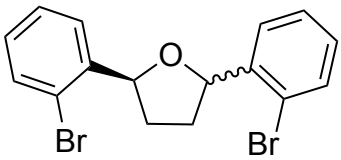

According to **GP II,** 65 µL (0.5 mmol) 2-Bromostyrene was added into the oxygen saturated nitromethane solution (0.1 M **TBAP**). Electrolysis was performed at room temperature with a current of 2.0 mA. After electrolysis (9.0 F per styrene), the organic phase was extracted with dichloromethane and washed with water. The organic phase was dried over $MgSO_4$ and filtered. The crude products were purified by column chromatography (*n*-hexane:ethyl acetate = 10:1; column 38 mm x 120 mm), yielding the product as a colorless oil (yield: 89 %, 85 mg, 0.22 mmol).

colorless liquid

Rf (*n*-hexane : ethyl acetate = 10:1) = 0.68

^{1}H NMR (600 MHz, Chloroform-*d*) δ 7.80 (dd, *J* = 7.8, 1.7 Hz, 1H), 7.63 (dd, *J* = 7.8, 1.1 Hz, 1H), 7.55 (ddd, *J* = 12.5, 8.0, 1.2 Hz, 2H), 7.37 (dtd, *J* = 20.0, 7.5, 1.2 Hz, 2H), 7.16 (dtd, *J* = 12.6, 7.6, 1.8 Hz, 2H), 5.61 (t, *J* = 3.0 Hz, 1H), 5.29 (t, *J* = 3.0 Hz, 1H), 2.74–2.60 (m, 2H), 1.93–1.71 (m, 2H).

^{13}C NMR (151 MHz, CHLOROFORM-*D*) δ 142.96, 142.14, 132.81, 132.77, 128.80, 128.74, 127.73, 127.70, 126.98, 126.82, 121.84, 121.30, 81.44, 80.16, 33.54, 33.11.

HRMS for C16H15Br2O calc: 380.9489 found: 380.9467

(2*S*,5*S*)-2,5-bis(3-bromophenyl)tetrahydrofuran (left) and (2*R*,5*S*)-2,5-bis(3-bromophenyl)tetrahydrofuran (right)

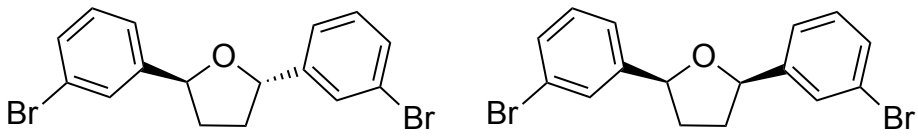

According to **GP II,** 65 µL (0.5 mmol) 3-Bromostyrene was added into the oxygen saturated nitromethane solution (0.1 M **TBAP**). Electrolysis was performed at room temperature with a current of 2.0 mA. After electrolysis (10.0 F per styrene), the organic phase was extracted with dichloromethane and washed with water. The organic phase was dried over $MgSO_4$ and filtered. The crude products were purified by column chromatography (*n*-hexane:ethyl acetate = 10:1; column 38 mm x 120 mm), yielding the product as a while solid (total yield: 55 %, 52 mg, 0.14 mmol).

(2*S*,5*S*)-2,5-bis(3-bromophenyl)tetrahydrofuran

colorless liquid

Rf (*n*-hexane : ethyl acetate = 10:1) = 0.41

^{1}H NMR (400 MHz, Chloroform-*d*) δ 7.56 (t, *J* = 1.9 Hz, 2H), 7.40 (dt, *J* = 7.8, 1.2 Hz, 2H), 7.32–7.29 (m, 2H), 7.22 (t, *J* = 7.8 Hz, 2H), 5.22 (td, *J* = 7.7, 5.5 Hz, 2H), 2.53–2.43 (m, 2H), 2.01–1.91 (m, 2H).

^{13}C NMR (101 MHz, Chloroform-*d*) δ 145.90, 130.49, 130.15, 128.68, 124.26, 122.78, 80.81, 35.56.

HRMS for C16H15Br2O calc: 380.9489 found: 380.9467

(2*R*,5*S*)-2,5-bis(3-bromophenyl)tetrahydrofuran

colorless liquid

Rf (*n*-hexane : ethyl acetate = 10:1) = 0.34

^{1}H NMR (400 MHz, Chloroform-*d*) δ 7.56 (t, *J* = 1.9 Hz, 2H), 7.42 (dt, *J* = 7.9, 1.1 Hz, 2H), 7.35 (d, *J* = 8.0 Hz, 2H), 7.24 (t, *J* = 8.0 Hz, 2H), 5.00 (td, *J* = 6.0, 1.9 Hz, 2H), 2.48–2.39 (m, 2H), 1.99–1.89 (m, 2H).

^{13}C NMR (101 MHz, Chloroform-*d*) δ 145.03, 130.63, 130.18, 129.20, 124.66, 122.68, 80.67, 34.20.

HRMS for C16H15Br2O calc: 380.9489 found: 380.9478

(2*S*,5*S*)-2,5-bis(4-bromophenyl)tetrahydrofuran (left) and (2*R*,5*S*)-2,5-bis(4-bromophenyl)tetrahydrofuran (right)

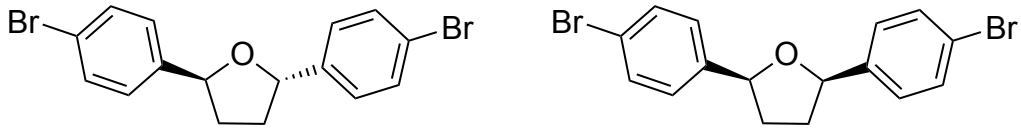

According to **GP II,** 65 µL (0.5 mmol) 4-Bromostyrene was added into the oxygen saturated nitromethane solution (0.1 M **TBAP**). Electrolysis was performed at room temperature with a current of 2.0 mA. After electrolysis (5.0 F per styrene), the organic phase was extracted with dichloromethane and washed with water. The organic phase was dried over $MgSO_4$ and filtered. The crude products were purified by column chromatography (*n*-hexane:ethyl acetate = 10:1; column 38 mm x 120 mm), yielding the product as a while solid (total yield: 91 %, 87 mg, 0.23 mmol).

(2*S*,5*S*)-2,5-bis(4-bromophenyl)tetrahydrofuran

Rf (*n*-hexane : ethyl acetate = 10:1) = 0.44

melting point: 71.0 ℃ - 71.8 ℃

^{1}H NMR (600 MHz, Chloroform-*d*) δ 7.49–7.46 (m, 4H), 7.28–7.26 (m, 4H), 5.20 (td, *J* = 7.8, 3.0 Hz, 2H), 2.49–2.43 (m, 2H), 1.97–1.89 (m, 2H).

^{13}C NMR (151 MHz, Chloroform-*d*) δ 142.57, 131.61, 127.38, 121.14, 80.93, 35.65.

HRMS for C16H14Br2ONa calc: 402.9309 found: 402.9326

(2*R*,5*S*)-2,5-bis(4-bromophenyl)tetrahydrofuran

Rf (*n*-hexane : ethyl acetate = 10:1) = 0.31

melting point: 104.1 ℃ - 104.6 ℃

Crystallization was carried out by adding CH_2Cl_2 to a solution of *cis*-9c in methanol. Crystals occurred after storage at r.t. for 1 week.

^{1}H NMR (400 MHz, Chloroform-*d*) δ 7.50–7.46 (m, 4H), 7.31–7.27 (m, 4H), 5.00 (td, *J* = 5.2, 2.6 Hz, 2H), 2.48–2.38 (m, 2H), 1.97–1.86 (m, 2H).
^{13}C NMR (101 MHz, Chloroform-*d*) δ 141.86, 131.63, 127.78, 121.30, 80.76, 34.28.
HRMS for C16H15Br2O calc: 380.9489 found: 380.9477

(*S*)-2,5-bis(2-chlorophenyl)tetrahydrofuran

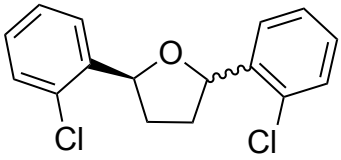

According to **GP II,** 63 µL (0.5 mmol) 2-Chlorostyrene was added into the oxygen saturated acetonitrile solution (0.1 M **TBAP**). Electrolysis was performed at room temperature with a current of 2.0 mA. After electrolysis (8.0 F per styrene), the organic phase was extracted with dichloromethane and washed with water. The organic phase was dried over $MgSO_4$ and filtered. The crude products were purified by column chromatography (*n*-hexane:ethyl acetate = 10:1; column 38 mm x 120 mm), yielding the product as a colorless oil (yield: 76 %, 55 mg, 0.19 mmol).

Rf (*n*-hexane : ethyl acetate = 10:1) = 0.55
Colorless oil
^{1}H NMR (600 MHz, Chloroform-*d*) δ 7.80 (dd, *J* = 7.8, 1.2 Hz, 1H), 7.63 (dd, *J* = 7.8, 1.1 Hz, 1H), 7.39–7.28 (m, 4H), 7.25–7.19 (m, 2H), 5.64 (t, *J* = 6.0 Hz, 1H), 5.33 (t, *J* = 6.5, 4.3 Hz, 1H), 2.71–2.59 (m, 2H), 1.93–1.75 (m, 2H).
^{13}C NMR (151 MHz, CHLOROFORM-*D*) δ 141.44, 140.59, 131.96, 131.53, 129.53, 129.51, 128.43, 128.38, 127.11, 127.08, 126.74, 126.55, 79.20, 78.09, 33.53, 33.03.
HRMS for C16H15Cl2O calc: 293.0499 found: 293.0473

(2*S*,5*S*)-2,5-dimethyl-2,5-diphenyltetrahydrofuran (left) and (2*R*,5*S*)-2,5-dimethyl-2,5-diphenyltetrahydrofuran (right)

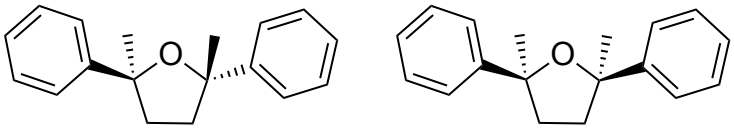

According to **GP II,** 65 µL (0.5 mmol) α-Methylstyrene was added into the oxygen saturated acetonitrile solution (0.1 M **TBAP**). Electrolysis was performed at room temperature with a current of 2.0 mA. After electrolysis (9.0 F per styrene), the organic phase was extracted with

dichloromethane and washed with water. The organic phase was dried over $MgSO_4$ and filtered. The crude products were purified by column chromatography (*n*-hexane:ethyl acetate = 10:1; column 38 mm x 120 mm), yielding the product as a while solid (total yield: 94 %, 59 mg, 0.24 mmol).

(2*S*,5*S*)-2,5-dimethyl-2,5-diphenyltetrahydrofuran

Rf (*n*-hexane : ethyl acetate = 10:1) = 0.58

Colorless liquid

^{1}H NMR (400 MHz, Chloroform-*d*) δ 7.56–7.52 (m, 4H), 7.38–7.32 (m, 4H), 7.26–7.21 (m, 2H), 2.34–2.24 (m, 2H), 2.11–1.99 (m, 2H), 1.57 (s, 6H).

^{13}C NMR (101 MHz, Chloroform-*d*) δ 149.51, 128.06, 126.35, 124.99, 85.41, 39.65, 30.79.

HRMS for C18H20ONa calc: 275.1411 found: 275.1415

(2*R*,5*S*)-2,5-dimethyl-2,5-diphenyltetrahydrofuran

Rf (*n*-hexane : ethyl acetate = 10:1) = 0.48

Colorless liquid

^{1}H NMR (400 MHz, Chloroform-*d*) δ 7.44–7.40 (m, 4H), 7.28–7.23 (m, 4H), 7.19–7.14 (m, 2H), 2.33–2.19 (m, 4H), 1.63 (s, 6H).

^{13}C NMR (101 MHz, CHLOROFORM-*D*) δ 148.90, 128.02, 126.30, 125.20, 85.55, 38.74, 32.20.

HRMS for C18H20ONa calc: 275.1411 found: 275.1405

(2*S*,5*S*)-2,5-dimethyl-2,5-di(naphthalen-2-yl)tetrahydrofuran (left) and (2*R*,5*S*)-2,5-dimethyl-2,5-di(naphthalen-2-yl)tetrahydrofuran (right)

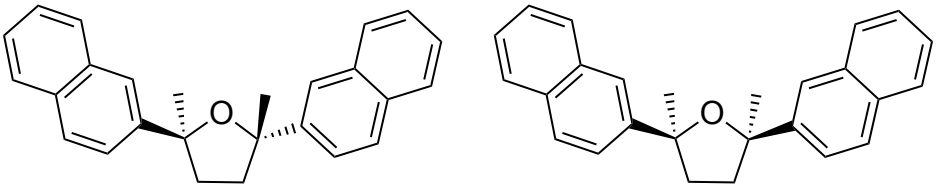

According to **GP II,** 84 mg (0.5 mmol) 2-Isopropenylnaphthalene was added into the oxygen saturated acetonitrile solution (0.1 M **TBAP**). Electrolysis was performed at room temperature with a current of 2.0 mA. After electrolysis (4.0 F per styrene), the organic phase was extracted with dichloromethane and washed with water. The organic phase was dried over $MgSO_4$ and filtered. The crude products were purified by column chromatography (*n*-hexane:ethyl acetate = 10:1; column 38 mm x 120 mm), yielding the product as a while solid (total yield: 81 %, 72 mg, 0.20 mmol).

(2*S*,5*S*)-2,5-dimethyl-2,5-di(naphthalen-2-yl)tetrahydrofuran

Rf (*n*-hexane : ethyl acetate = 10:1) = 0.58

melting point: 129.7 °C - 130.4 °C

^{1}H NMR (400 MHz, Chloroform-*d*) δ 8.09 (d, *J* = 1.8 Hz, 2H), 7.90–7.83 (m, 6H), 7.63 (dd, *J* = 8.6, 1.9 Hz, 2H), 7.53–7.43 (m, 4H), 2.50–2.39 (m, 2H), 2.21–2.10 (m, 2H), 1.71 (s, 6H).

^{13}C NMR (101 MHz, Chloroform-*d*) δ 146.78, 133.34, 132.40, 128.30, 127.88, 127.67, 126.15, 125.67, 124.15, 123.31, 85.81, 39.56, 30.84.

HRMS for C26H24ONa calc: 375.1724 found: 375.1701

(2*R*,5*S*)-2,5-dimethyl-2,5-di(naphthalen-2-yl)tetrahydrofuran

Rf (*n*-hexane : ethyl acetate = 10:1) = 0.52

melting point: 113.1 °C - 113.9 °C

^{1}H NMR (400 MHz, Chloroform-*d*) δ 7.92 (d, *J* = 1.6 Hz, 2H), 7.80–7.75 (m, 4H), 7.69–7.65 (m, 2H), 7.58 (dd, *J* = 8.6, 1.9 Hz, 2H), 7.42–7.37 (m, 4H), 2.46–2.34 (m, 4H), 1.75 (s, 6H).

^{13}C NMR (101 MHz, Chloroform-*d*) δ 146.11, 133.19, 132.27, 128.21, 127.74, 127.56, 125.99, 125.55, 124.34, 123.51, 85.88, 38.70, 32.06.

HRMS for C26H25O calc: 353.1905 found: 353.1922

(2*S*,5*S*)-2,5-bis(4-fluorophenyl)-2,5-dimethyltetrahydrofuran (left) and (2*R*,5*S*)-2,5-bis(4-fluorophenyl)-2,5-dimethyltetrahydrofuran (right)

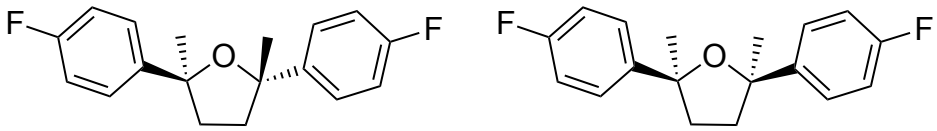

According to **GP II,** 67 µL (0.5 mmol) 4-Fluoro-α-methylstyrene was added into the oxygen saturated acetonitrile solution (0.1 M **TBAP**). Electrolysis was performed at room temperature with a current of 2.0 mA. After electrolysis (8.0 F per styrene), the organic phase was extracted with dichloromethane and washed with water. The organic phase was dried over $MgSO_4$ and filtered. The crude products were purified by column chromatography (*n*-hexane:ethyl acetate = 10:1; column 38 mm x 120 mm), yielding the product as a while solid (total yield: 86 %, 62 mg, 0.22 mmol).

(2*S*,5*S*)-2,5-bis(4-fluorophenyl)-2,5-dimethyltetrahydrofuran

Rf (*n*-hexane : ethyl acetate = 10:1) = 0.58

melting point: 105.8 °C - 106.7 °C

Crystallization was carried out by adding CH_2Cl_2 to a solution of *trans*-3c in methanol. Crystals were obtained after storage at r.t. for 24 h.

^{1}H NMR (400 MHz, Chloroform-*d*) δ 7.51–7.44 (m, 4H), 7.05–6.99 (m, 4H), 2.29–2.20 (m, 2H), 2.09–1.99 (m, 2H), 1.52 (s, 6H).
^{13}C NMR (101 MHz, Chloroform-*d*) δ 162.80, 160.37, 145.06, 145.03, 126.57, 126.49, 114.87, 114.66, 85.17, 39.69, 30.87.
^{19}F NMR (376 MHz, Chloroform-) δ -117.30.
HRMS for C18H19F2O calc: 289.1403 found: 289.1389

(2*R*,5*S*)-2,5-bis(4-fluorophenyl)-2,5-dimethyltetrahydrofuran

Rf (*n*-hexane : ethyl acetate = 10:1) = 0.52
Colorless liquid
^{1}H NMR (600 MHz, Chloroform-*d*) δ 7.35–7.31 (m, 4H), 6.96–6.91 (m, 4H), 2.31–2.25 (m, 2H), 2.21–2.15 (m, 2H), 1.59 (s, 6H).
^{13}C NMR (151 MHz, Chloroform-*d*) δ 162.31, 160.69, 144.50, 144.48, 126.74, 126.69, 85.29, 38.72, 32.20.
^{19}F NMR (376 MHz, Chloroform-*d*) δ -117.20.
HRMS for C18H19F2O calc: 289.1403 found: 289.1415

(2*S*,5*S*)-2,5-bis(4-chlorophenyl)-2,5-dimethyltetrahydrofuran (left) and (2*R*,5*S*)-2,5-bis(4-chlorophenyl)-2,5-dimethyltetrahydrofuran (right)

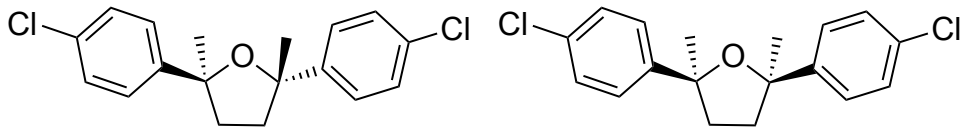

According to **GP II,** 67 µL (0.5 mmol) 4-Chloro-α-methylstyrene was added into the oxygen saturated acetonitrile solution (0.1 M **TBAP**). Electrolysis was performed at room temperature with a current of 2.0 mA. After electrolysis (5.0 F per styrene), the organic phase was extracted with dichloromethane and washed with water. The organic phase was dried over $MgSO_4$ and filtered. The crude products were purified by column chromatography (*n*-hexane:ethyl acetate = 10:1; column 38 mm x 120 mm), yielding the product as a while solid (total yield: 98 %, 78 mg, 0.25 mmol).

(2*S*,5*S*)-2,5-bis(4-chlorophenyl)-2,5-dimethyltetrahydrofuran

Rf (*n*-hexane : ethyl acetate = 10:1) = 0.60
melting point: 131.1 ℃ - 131.4 ℃

^{1}H NMR (400 MHz, Chloroform-*d*) δ 7.47–7.43 (m, 4H), 7.33–7.29 (m, 4H), 2.29–2.19 (m, 2H), 2.08–1.98 (m, 2H), 1.51 (s, 6H).

^{13}C NMR (101 MHz, Chloroform-*d*) δ 147.84, 132.24, 128.25, 126.48, 85.24, 39.57, 30.75.

HRMS for C18H19Cl2O calc: 321.0812 found: 321.0839

(2*R*,5*S*)-2,5-bis(4-chlorophenyl)-2,5-dimethyltetrahydrofuran

Rf (*n*-hexane : ethyl acetate = 10:1) = 0.52

Colorless liquid

^{1}H NMR (600 MHz, Chloroform-*d*) δ 7.32–7.29 (m, 4H), 7.24–7.21 (m, 4H), 2.31–2.25 (m, 2H), 2.19–2.13 (m, 2H), 1.58 (s, 3H).

^{13}C NMR (151 MHz, Chloroform-*d*) δ 147.18, 132.17, 128.21, 126.59, 85.31, 38.55, 32.04.

HRMS for C18H19Cl2O calc: 321.0812 found: 321.0798

(2*S*,5*S*)-2,5-bis(4-chlorophenyl)-2,5-dimethyltetrahydrofuran-1-^{18}O (left) and (2*R*,5*S*)-2,5-bis(4-chlorophenyl)-2,5-dimethyltetrahydrofuran-1-^{18}O (right)

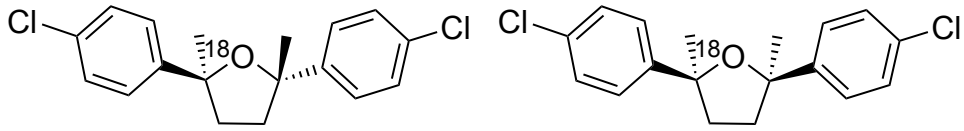

According to **GP II,** 67 µL (0.5 mmol) 4-Chloro-α-methylstyrene was added into the oxygen ($^{18}O_2$) saturated acetonitrile solution (0.1 M **TBAP**). Electrolysis was performed at room temperature with a current of 2.0 mA. After electrolysis (5.0 F per styrene), the organic phase was extracted with dichloromethane and washed with water. The organic phase was dried over $MgSO_4$ and filtered. The crude products were purified by column chromatography (*n*-hexane:ethyl acetate = 10:1; column 38 mm x 120 mm), yielding the product as a while solid (total yield: 93 %, 75 mg, 0.23 mmol).

(2*S*,5*S*)-2,5-bis(4-chlorophenyl)-2,5-dimethyltetrahydrofuran-1-^{18}O

^{1}H NMR (600 MHz, Chloroform-*d*) δ 7.46–7.43 (m, 4H), 7.32–7.29 (m, 4H), 2.28–2.23 (m, 2H), 2.06–1.99 (m, 2H), 1.51 (s, 6H).

^{13}C NMR (151 MHz, CHLOROFORM-*D*) δ 147.87, 132.26, 128.26, 126.49, 85.24, 85.22, 39.57, 30.76.

HRMS for C18H18Cl2^{18}ONa calc: 345.0632 found: 345.0614

(2*R*,5*S*)-2,5-bis(4-chlorophenyl)-2,5-dimethyltetrahydrofuran-1-^{18}O

^{1}H NMR (600 MHz, Chloroform-*d*) δ 7.32–7.29 (m, 4H), 7.24–7.21 (m, 4H), 2.31–2.25 (m, 2H), 2.19–2.14 (m, 2H), 1.58 (s, 6H).

^{13}C NMR (151 MHz, CHLOROFORM-*D*) δ 147.21, 132.20, 128.22, 126.61, 85.32, 85.29, 38.57, 32.04.

HRMS for C18H18Cl2^{18}ONa calc: 345.0632 found: 345.0647

7-3-X. Reference

[1] M. Katz, P. Riemenschneider, H. Wendt, *Electrochim. Acta,* **1972**, *17*, 1595–1607.

[2] R. L. McCreery, *Chem. Rev.* **2008**, *108*, 2646–2687.

[3] Y. Deng, X. J. Wei, H. Wang, Y. Sun, T. Noèl, X. Wang, *Angew. Chem. Int. Ed.* **2017**, *56*, 832-836.

[4] G. Z. Wang, X. L. Li, J. J. Dai, H. J. Xu, *J. Org. Chem.* **2014**, *79*, 7220-7225.

[5] B. Skillinghaug, C. Sköld, J. Rydfjord, F. Svensson, M. Behrends, J. Sävmarker, P. J. R. Sjöberg, M. Larhed, *J. Org. Chem.* **2014**, *79*, 12018-12032.

[6] W. Li, J. Li, Y. Wu, N. Fuller, M. A. Markus, *J. Org. Chem.* **2010**, *75*, 1077-1086.

[7] B. R. Kim, H. G. Lee, E. J. Kim, S. G. Lee, Y. J. Yoon, *J. Org. Chem.* **2010**, *75*, 484-486.

[8] B. T. Gregg, K. C. Golden, J. F. Quinn, *J. Org. Chem.* **2007**, *72*, 5890-5893.

[9] M. W. C. Robinson, A. M. Davies, R. Buckle, I. Mabbett, S. H. Taylor, A. E. Graham, *Org. Biomol. Chem.* **2009**, *7*, 2559-2564.

7-3-X. NMR spectra

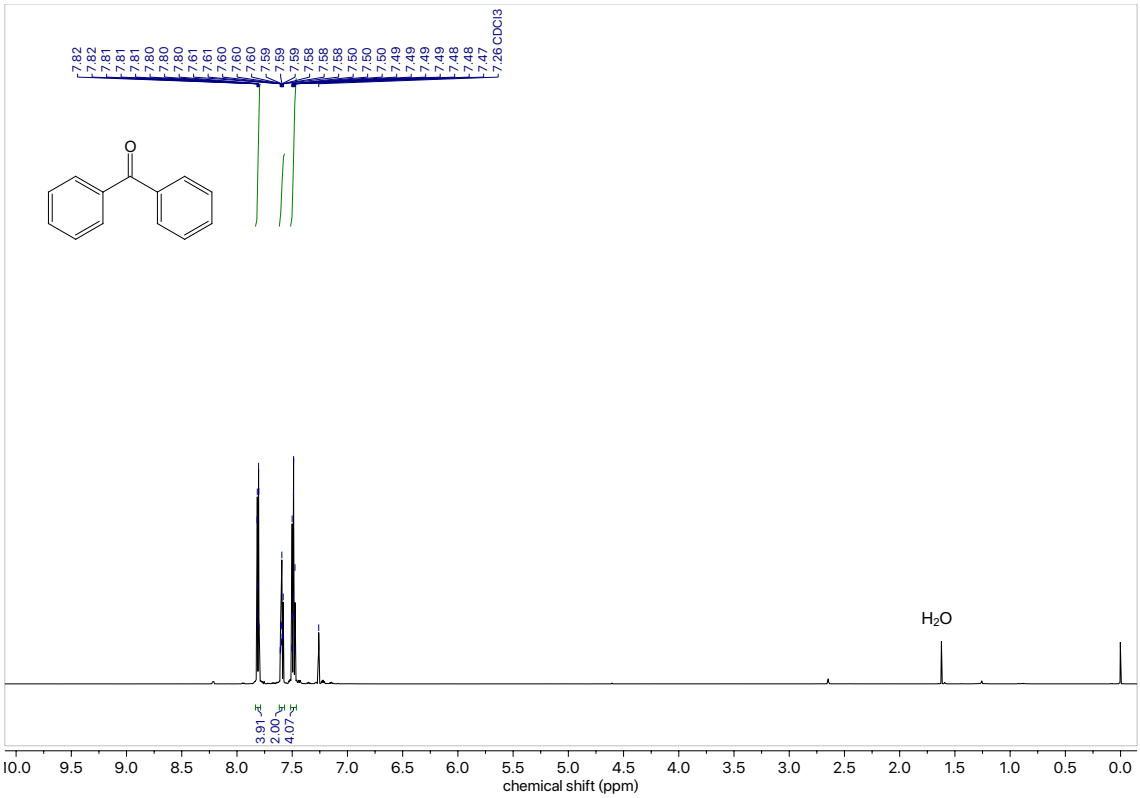

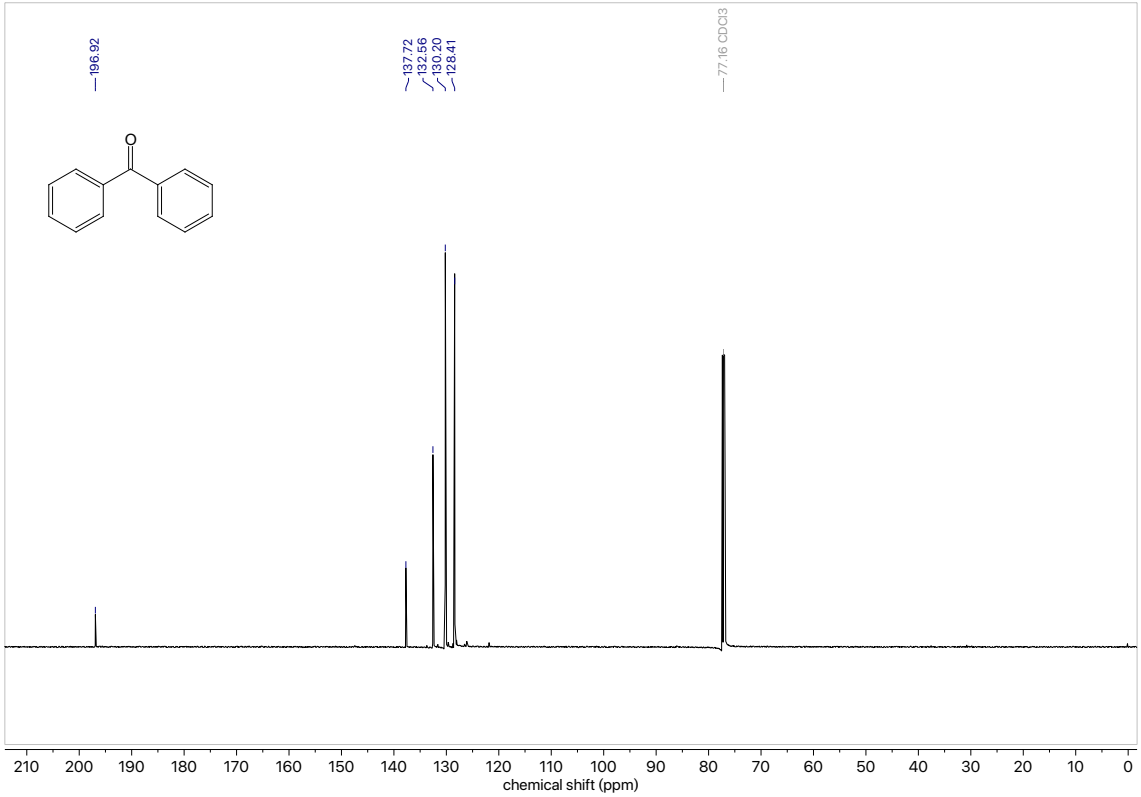
196.92
137.72
132.56
130.20
128.41
77.16 CDCl3
O
210 200 190 180 170 160 150 140 130 120 110 100 90 80 70 60 50 40 30 20 10 0
chemical shift (ppm)

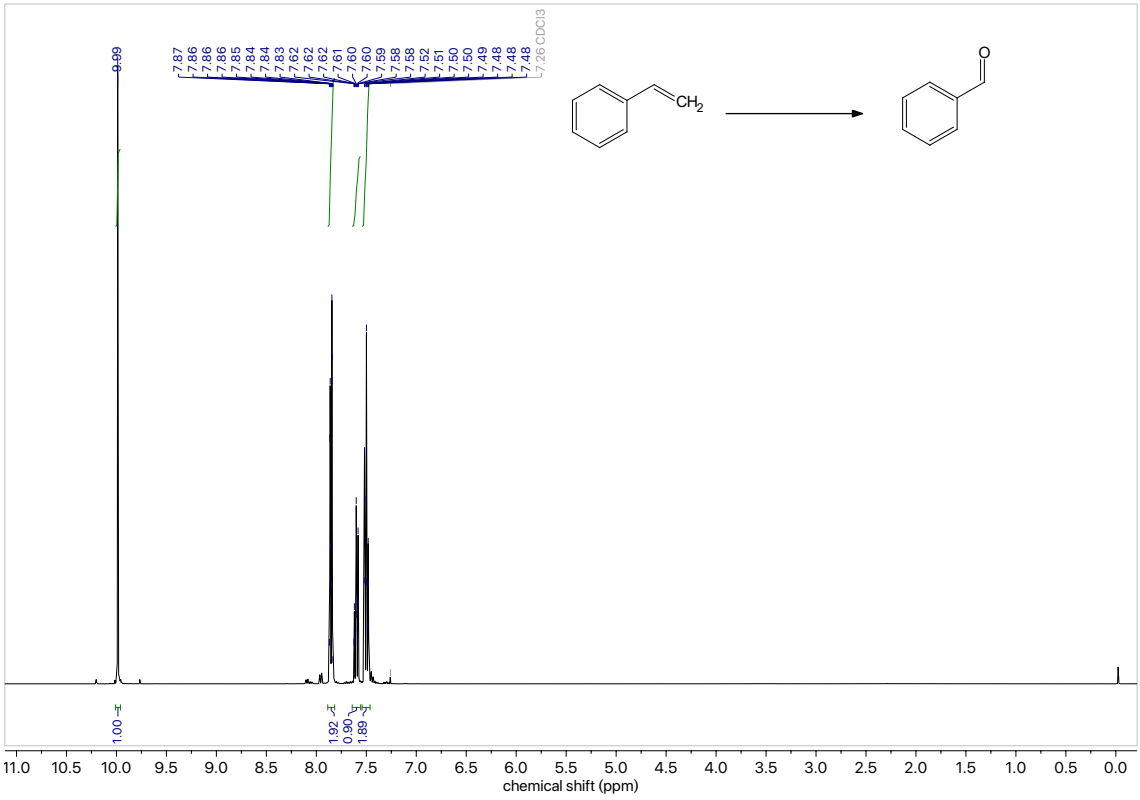
9.99
7.87
7.86
7.86
7.86
7.85
7.84
7.84
7.83
7.62
7.62
7.62
7.61
7.60
7.60
7.59
7.58
7.58
7.52
7.51
7.50
7.50
7.49
7.48
7.48
7.48
7.26 CDCl3
CH2
O
1.00
1.92
0.90
1.89
11.0 10.5 10.0 9.5 9.0 8.5 8.0 7.5 7.0 6.5 6.0 5.5 5.0 4.5 4.0 3.5 3.0 2.5 2.0 1.5 1.0 0.5 0.0
chemical shift (ppm)

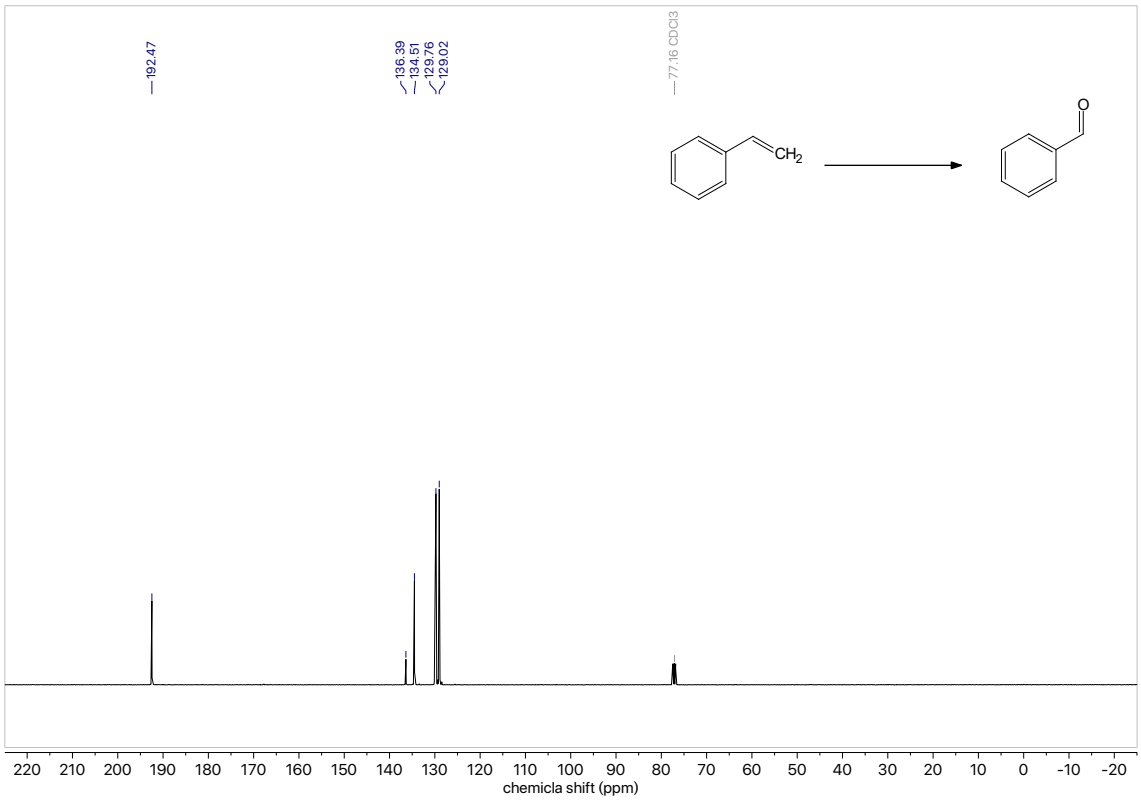
192.47
136.39
134.51
129.76
129.02
77.16 CDCl3
CH2
O
220 210 200 190 180 170 160 150 140 130 120 110 100 90 80 70 60 50 40 30 20 10 0 -10 -20
chemicla shift (ppm)

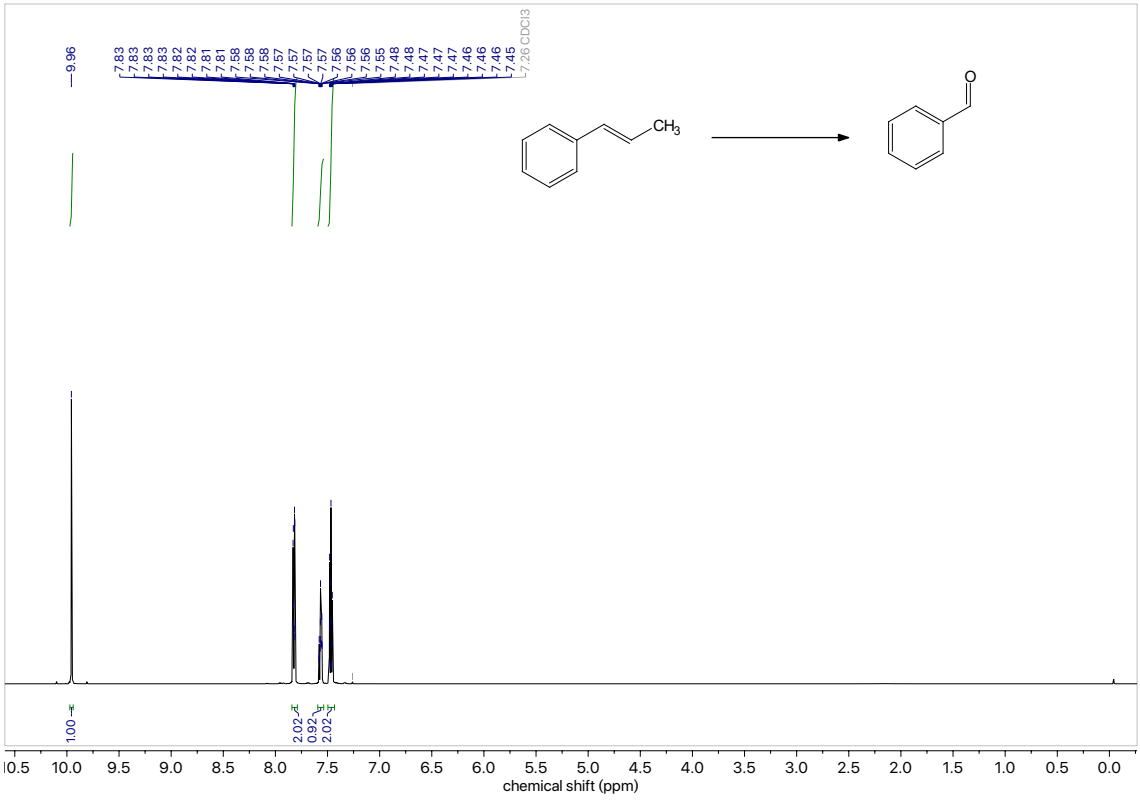
9.96
7.83
7.83
7.83
7.83
7.82
7.82
7.81
7.81
7.58
7.58
7.58
7.57
7.57
7.57
7.57
7.56
7.56
7.56
7.55
7.48
7.48
7.47
7.47
7.47
7.46
7.46
7.46
7.45
7.26 CDCl3
CH3
O
1.00
2.02
0.92
2.02
10.5 10.0 9.5 9.0 8.5 8.0 7.5 7.0 6.5 6.0 5.5 5.0 4.5 4.0 3.5 3.0 2.5 2.0 1.5 1.0 0.5 0.0
chemical shift (ppm)

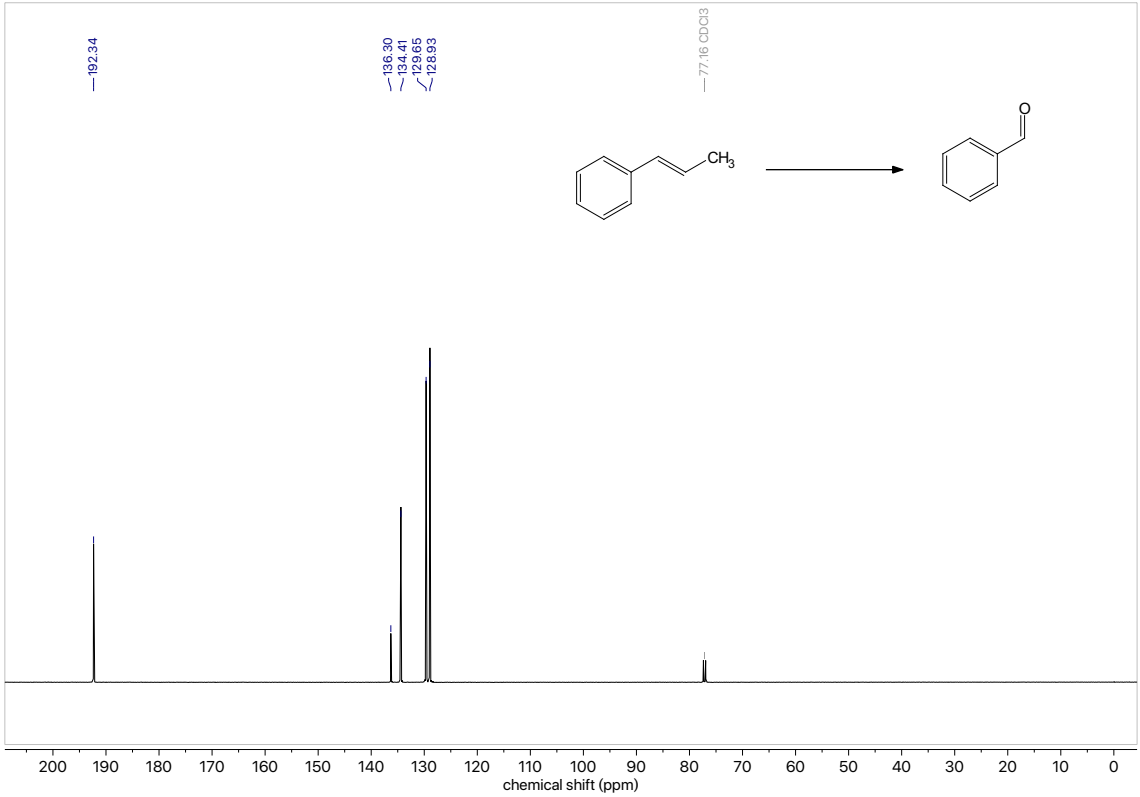
192.34
136.30
134.41
129.65
128.93
77.16 CDCl3
CH3
O
200 190 180 170 160 150 140 130 120 110 100 90 80 70 60 50 40 30 20 10 0
chemical shift (ppm)

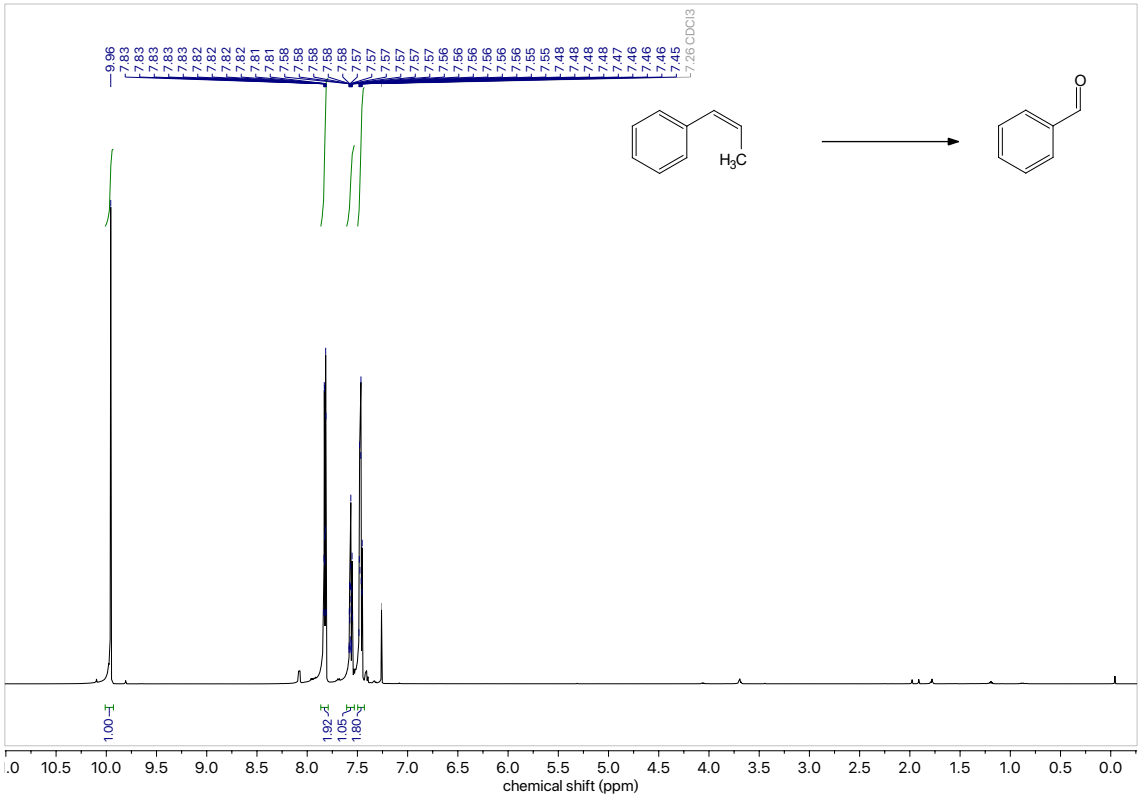
9.96
7.83
7.82
7.81
7.58
7.57
7.56
7.55
7.48
7.47
7.46
7.45
7.26 CDCl3
H3C
O
1.00
1.92
1.05
1.80
10.5 10.0 9.5 9.0 8.5 8.0 7.5 7.0 6.5 6.0 5.5 5.0 4.5 4.0 3.5 3.0 2.5 2.0 1.5 1.0 0.5 0.0
chemical shift (ppm)

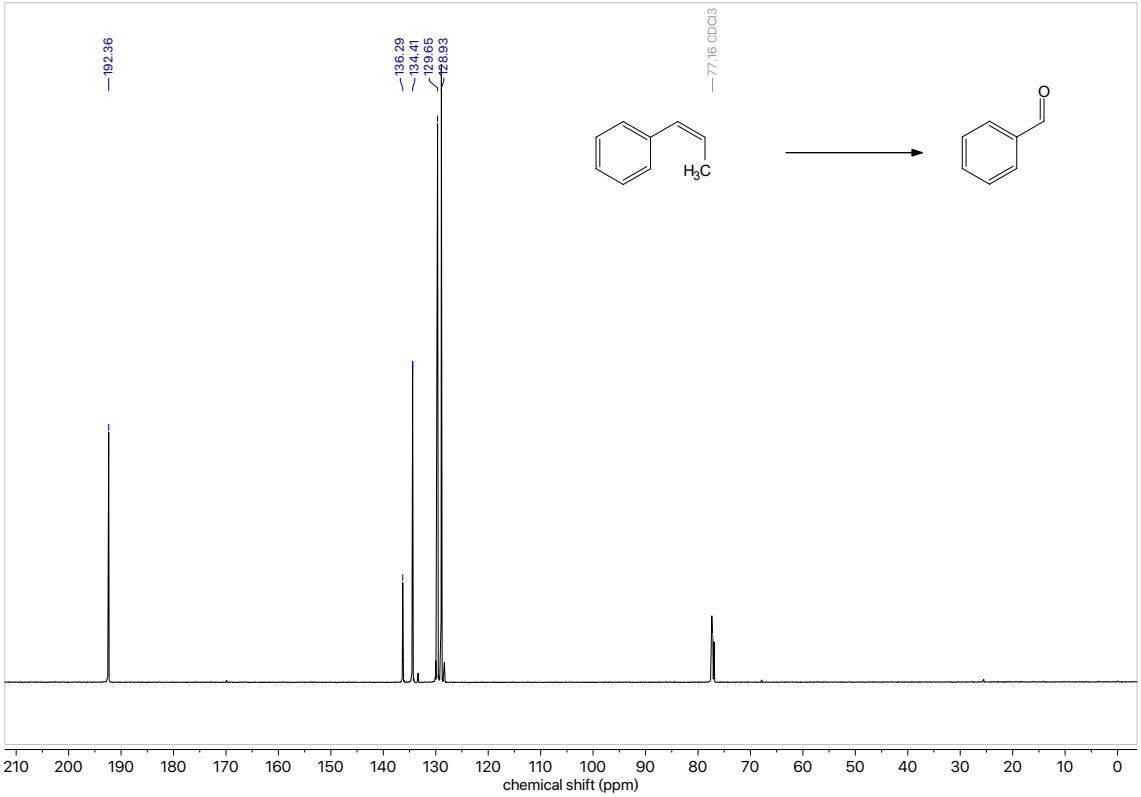
192.36
136.29
134.41
129.65
128.93
77.16 CDCl3
O
H3C
210 200 190 180 170 160 150 140 130 120 110 100 90 80 70 60 50 40 30 20 10 0
chemical shift (ppm)

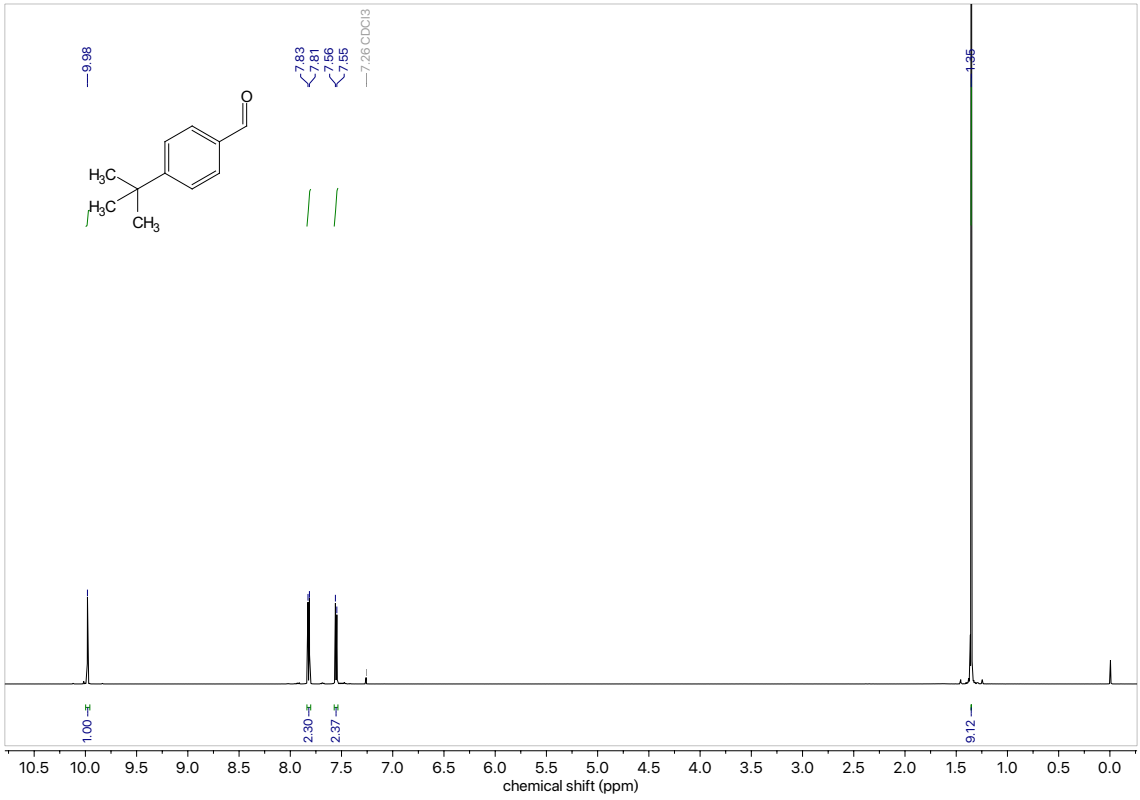
9.98
7.83
7.81
7.56
7.55
7.26 CDCl3
1.35
O
H3C
H3C
CH3
1.00
2.30
2.37
9.12
10.5 10.0 9.5 9.0 8.5 8.0 7.5 7.0 6.5 6.0 5.5 5.0 4.5 4.0 3.5 3.0 2.5 2.0 1.5 1.0 0.5 0.0
chemical shift (ppm)

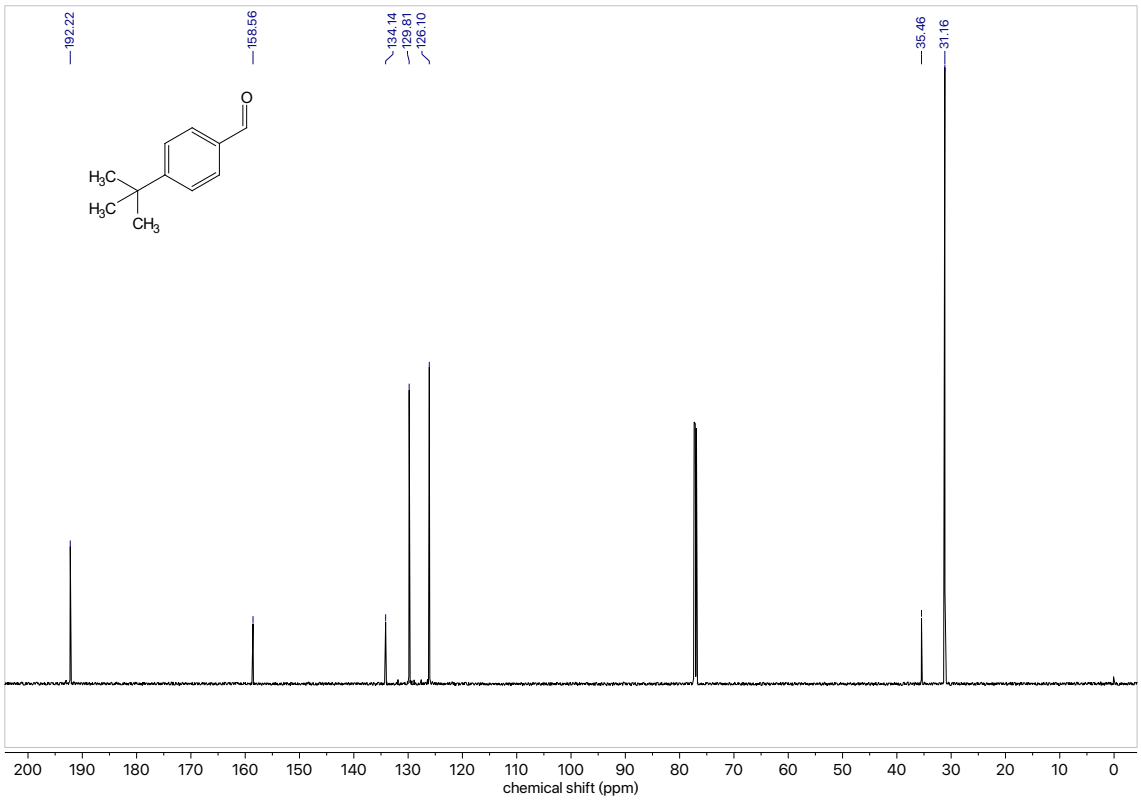
192.22
158.56
134.14
129.81
126.10
35.46
31.16
O
H3C
H3C
CH3
200 190 180 170 160 150 140 130 120 110 100 90 80 70 60 50 40 30 20 10 0
chemical shift (ppm)

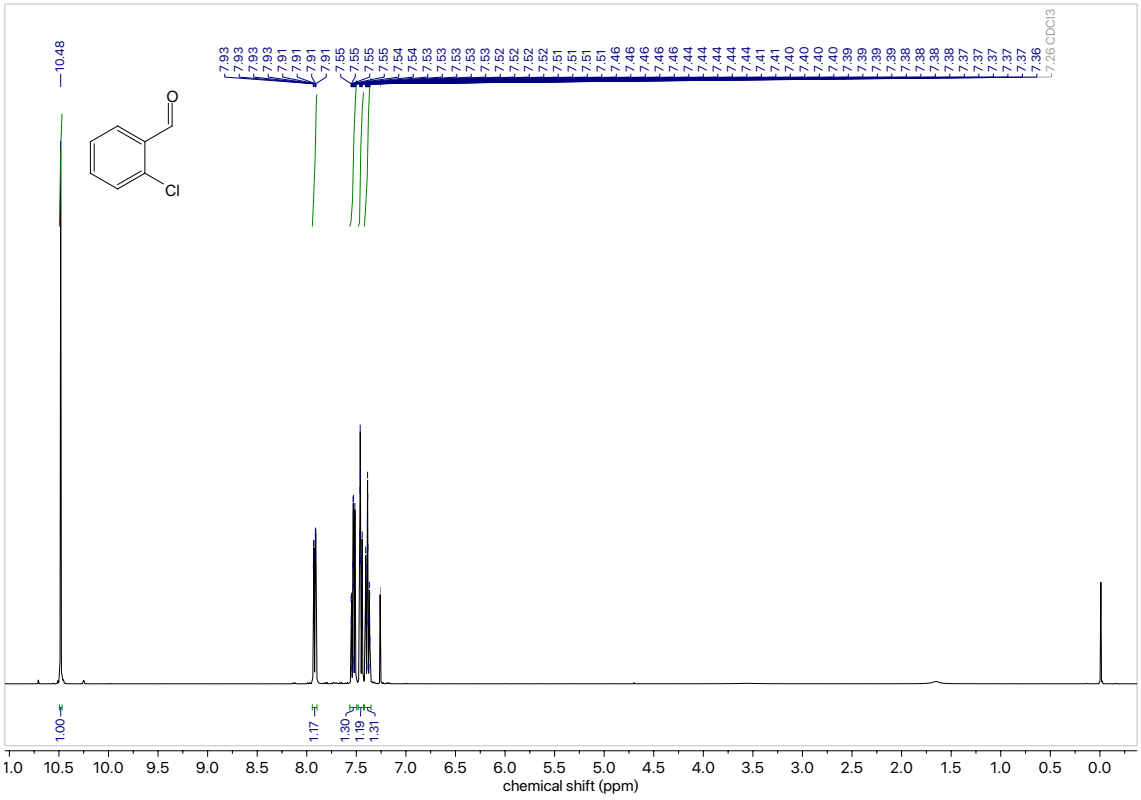
10.48
7.93 7.91 7.55 7.54 7.53 7.52 7.51 7.46 7.44 7.41 7.40 7.39 7.38 7.37 7.36
7.26 CDCl3
O
Cl
1.00
1.17
1.30
1.19
1.31
1.0 10.5 10.0 9.5 9.0 8.5 8.0 7.5 7.0 6.5 6.0 5.5 5.0 4.5 4.0 3.5 3.0 2.5 2.0 1.5 1.0 0.5 0.0
chemical shift (ppm)

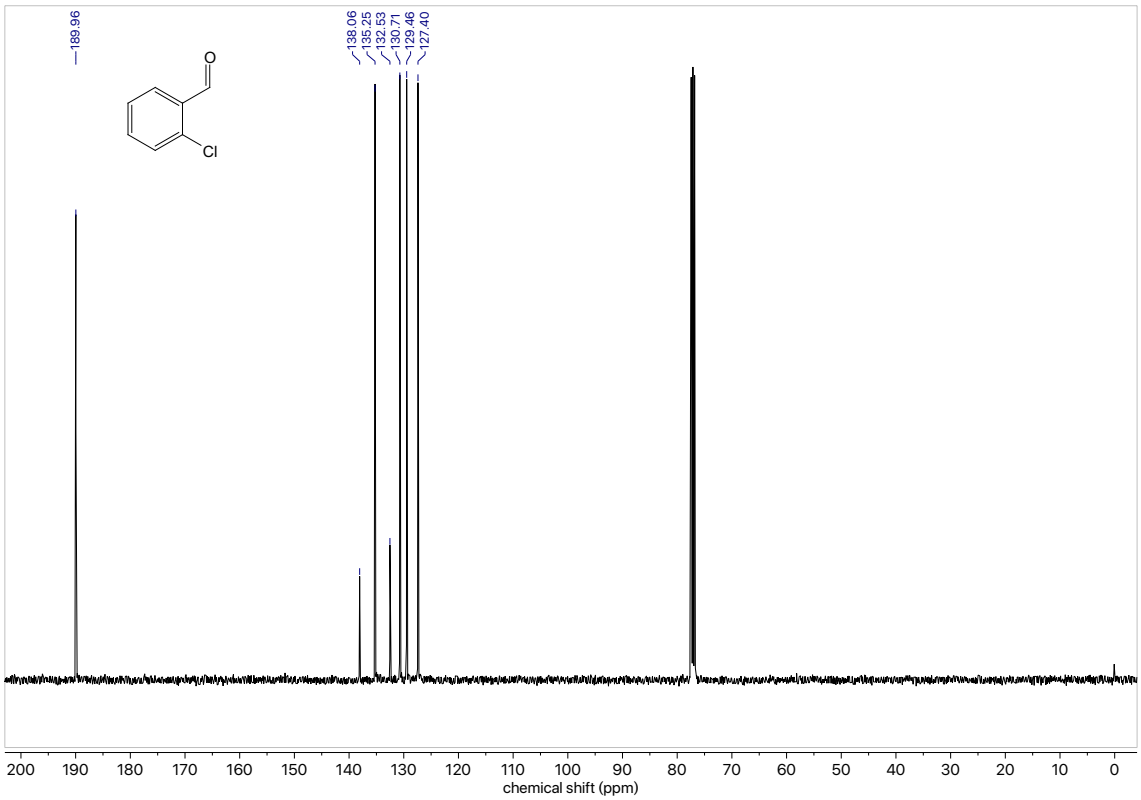
189.96
138.06
135.25
132.53
130.71
129.46
127.40
O
Cl
200 190 180 170 160 150 140 130 120 110 100 90 80 70 60 50 40 30 20 10 0
chemical shift (ppm)

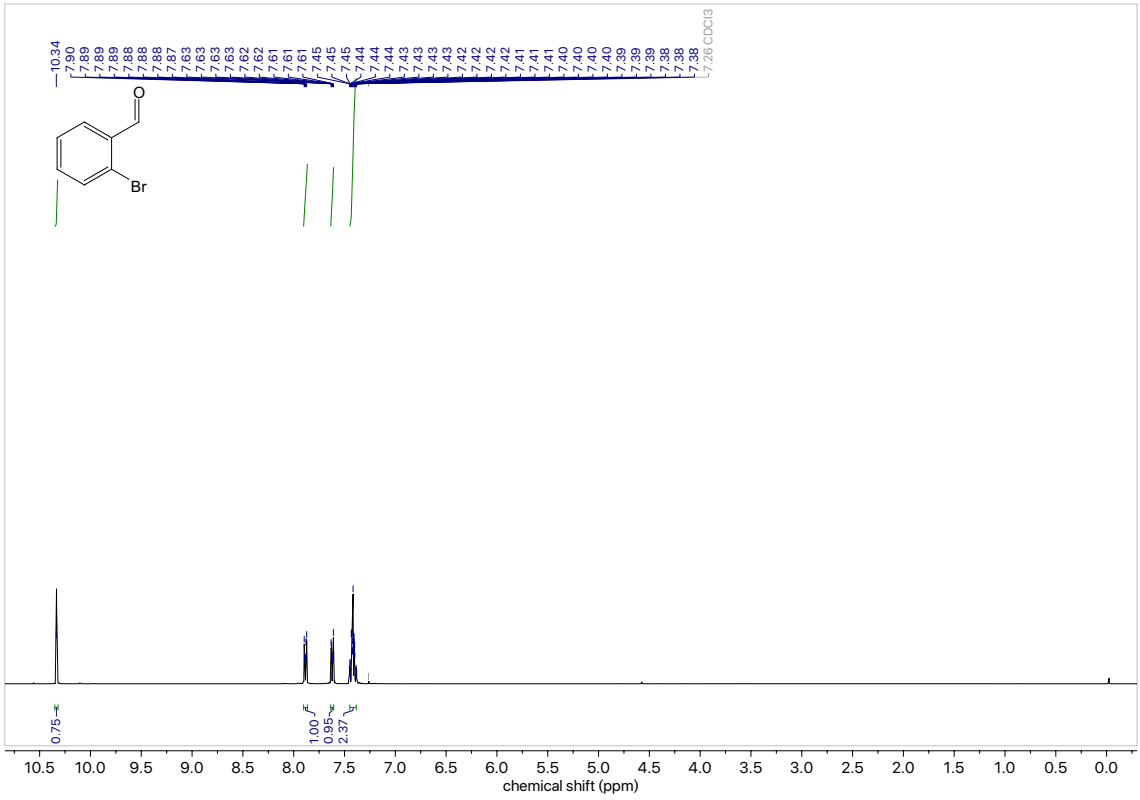
10.34
7.90
7.89
7.89
7.89
7.88
7.88
7.88
7.87
7.63
7.63
7.63
7.62
7.62
7.61
7.61
7.61
7.45
7.45
7.45
7.44
7.44
7.44
7.43
7.43
7.43
7.42
7.42
7.42
7.42
7.41
7.41
7.41
7.40
7.40
7.40
7.40
7.39
7.39
7.39
7.38
7.38
7.38
7.26 CDCl3
O
Br
0.75
1.00
0.95
2.37
10.5 10.0 9.5 9.0 8.5 8.0 7.5 7.0 6.5 6.0 5.5 5.0 4.5 4.0 3.5 3.0 2.5 2.0 1.5 1.0 0.5 0.0
chemical shift (ppm)

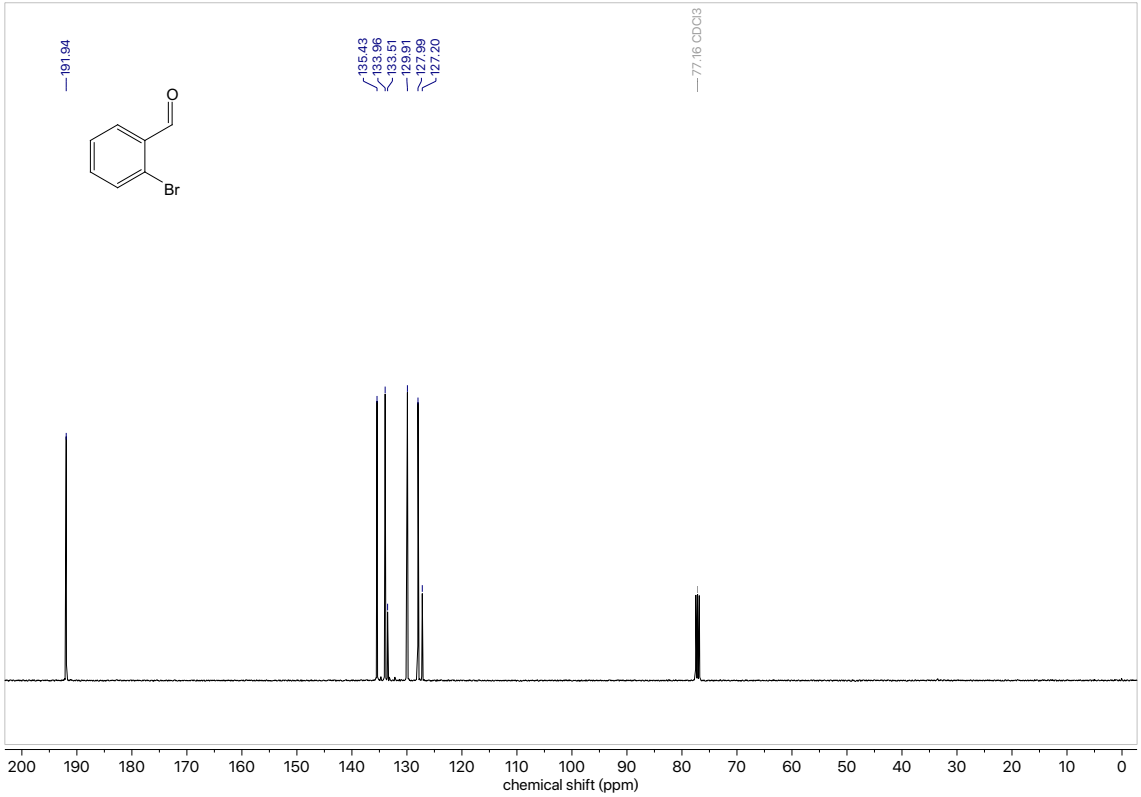
191.94
135.43
133.96
133.51
129.91
127.99
127.20
77.16 CDCl3
O
Br
200 190 180 170 160 150 140 130 120 110 100 90 80 70 60 50 40 30 20 10 0
chemical shift (ppm)

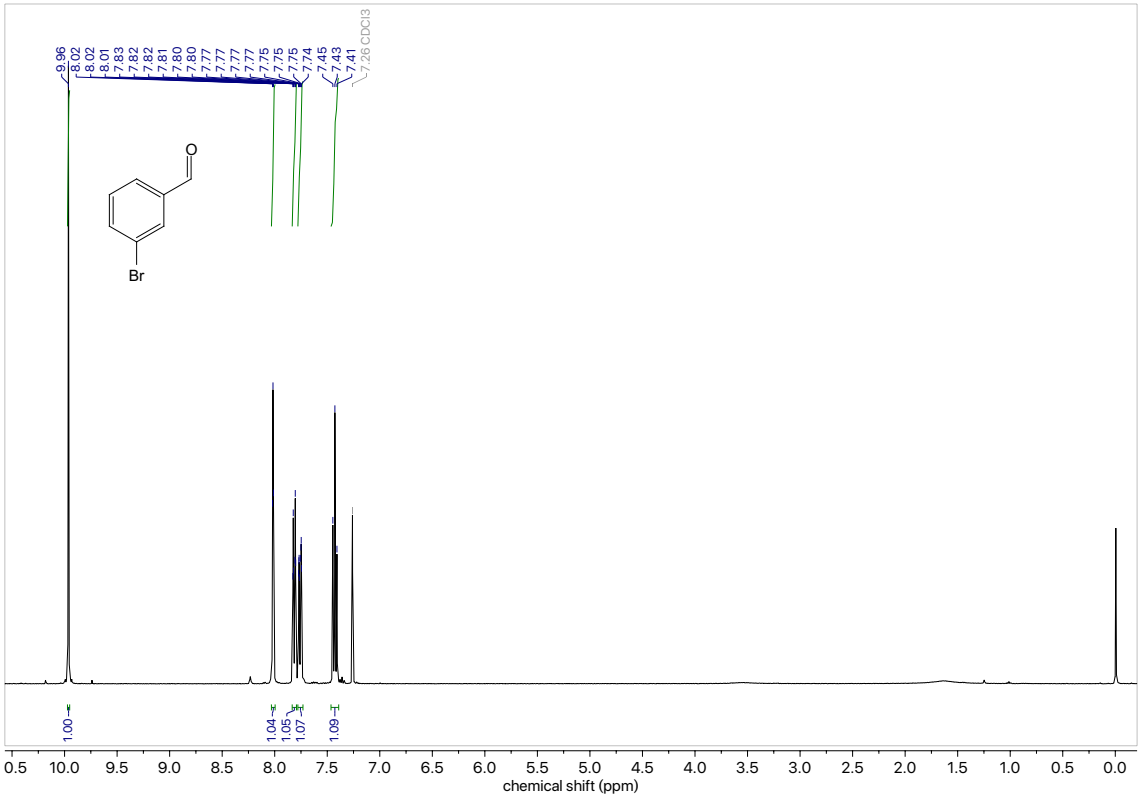
9.96
8.02
8.02
8.01
7.83
7.82
7.82
7.81
7.80
7.80
7.77
7.77
7.77
7.77
7.75
7.75
7.75
7.74
7.45
7.43
7.41
7.26 CDCl3
O
Br
1.00
1.04
1.05
1.07
1.09
0.5 10.0 9.5 9.0 8.5 8.0 7.5 7.0 6.5 6.0 5.5 5.0 4.5 4.0 3.5 3.0 2.5 2.0 1.5 1.0 0.5 0.0
chemical shift (ppm)

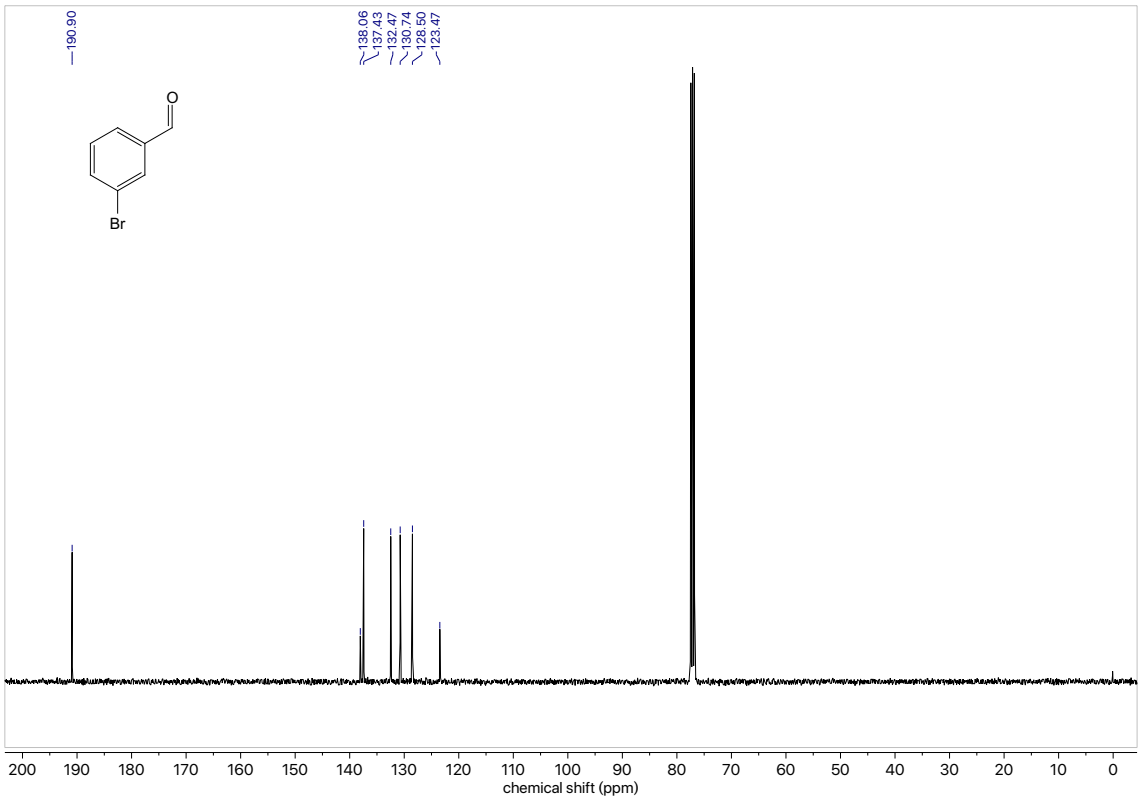
190.90
138.06
137.43
132.47
130.74
128.50
123.47
O
Br
200 190 180 170 160 150 140 130 120 110 100 90 80 70 60 50 40 30 20 10 0
chemical shift (ppm)

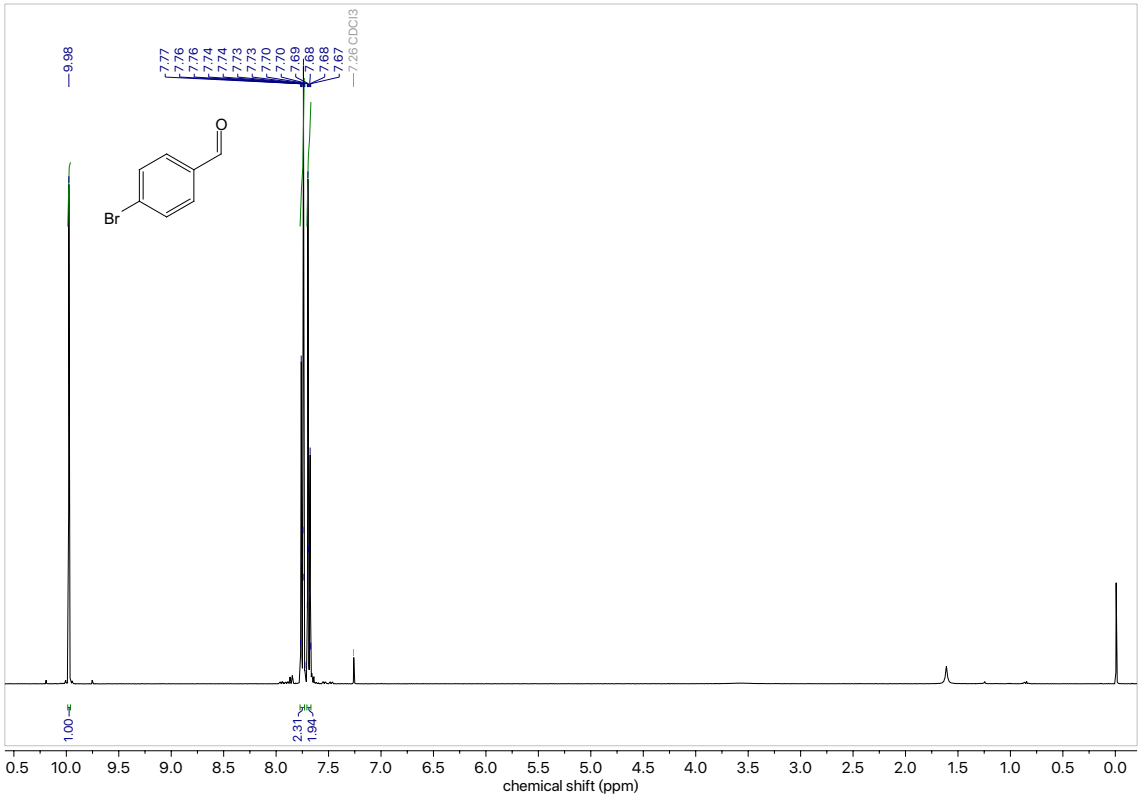
9.98
7.77
7.76
7.76
7.74
7.74
7.73
7.73
7.70
7.70
7.69
7.68
7.68
7.67
7.26 CDCl3
O
Br
1.00
2.31
1.94
0.5 10.0 9.5 9.0 8.5 8.0 7.5 7.0 6.5 6.0 5.5 5.0 4.5 4.0 3.5 3.0 2.5 2.0 1.5 1.0 0.5 0.0
chemical shift (ppm)

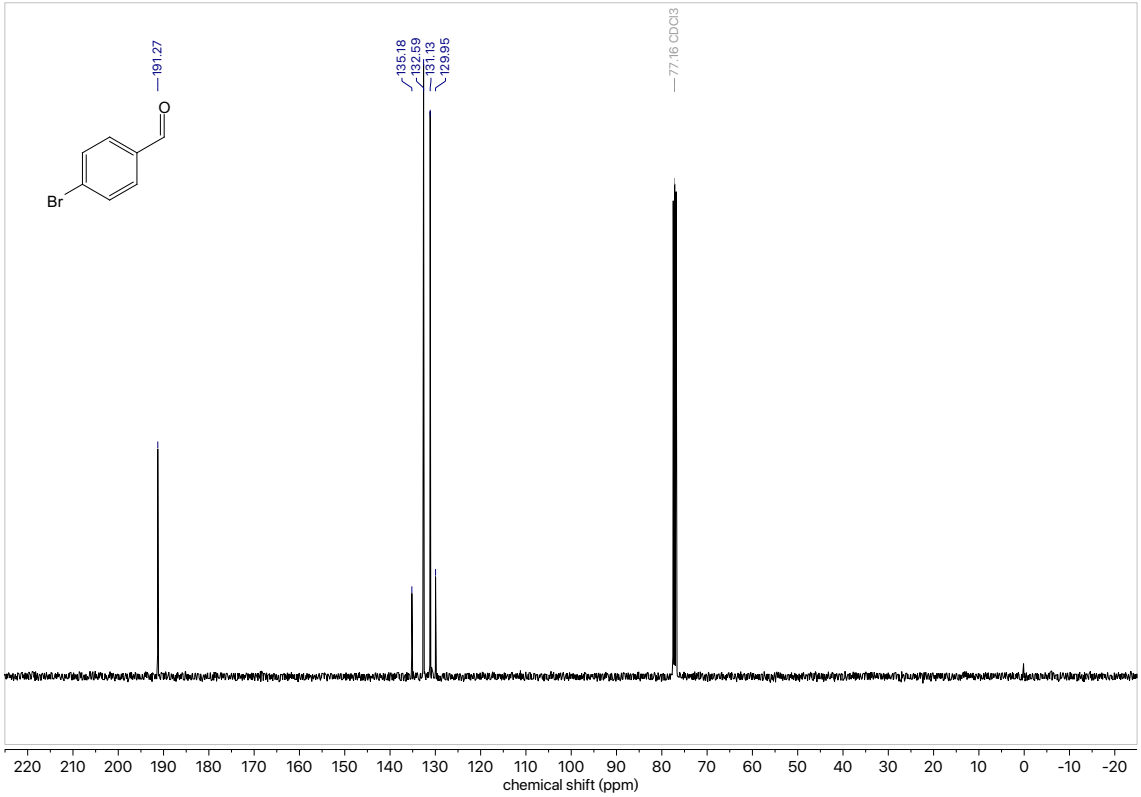
191.27
135.18
132.59
131.13
129.95
77.16 CDCl3
O
Br
220 210 200 190 180 170 160 150 140 130 120 110 100 90 80 70 60 50 40 30 20 10 0 -10 -20
chemical shift (ppm)

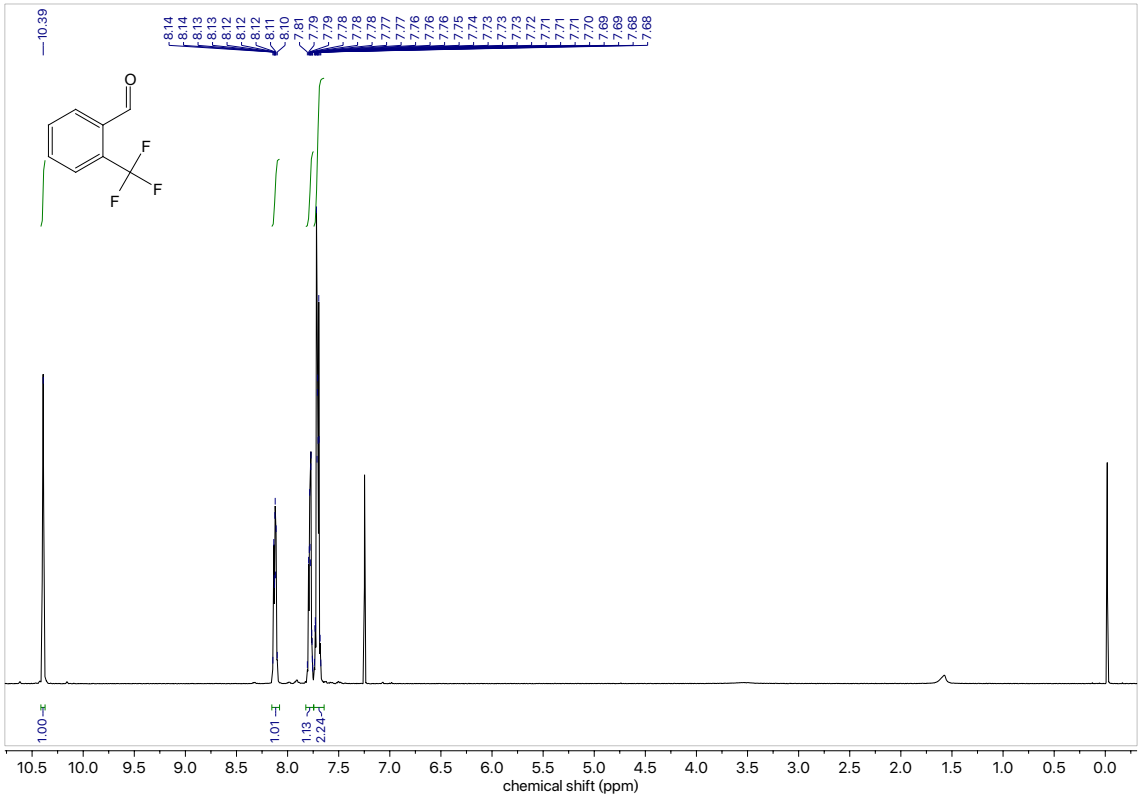
10.39
8.14 8.14 8.13 8.13 8.12 8.12 8.12 8.11 8.10
7.81 7.79 7.79 7.78 7.78 7.78 7.77 7.77 7.76 7.76 7.76 7.75 7.74 7.73 7.73 7.73 7.72 7.71 7.71 7.71 7.70 7.69 7.69 7.68 7.68
O
F
F
F
1.00
1.01
1.13
2.24
10.5 10.0 9.5 9.0 8.5 8.0 7.5 7.0 6.5 6.0 5.5 5.0 4.5 4.0 3.5 3.0 2.5 2.0 1.5 1.0 0.5 0.0
chemical shift (ppm)

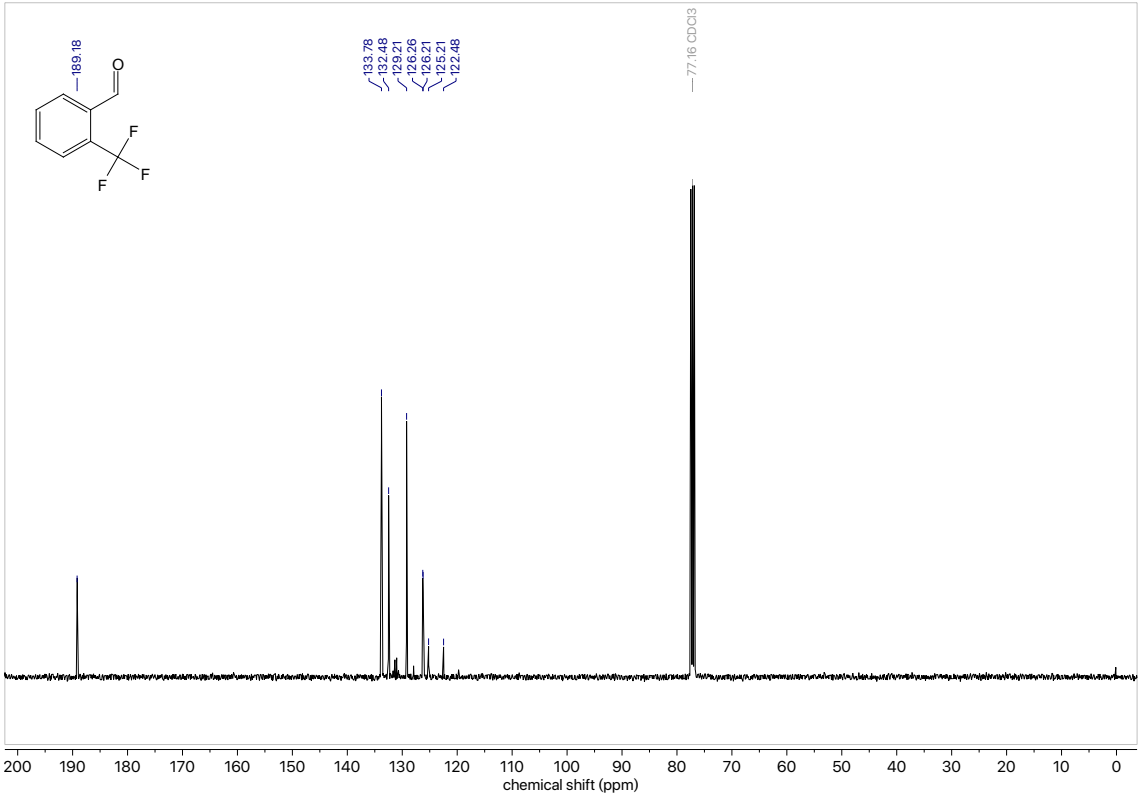
189.18
133.78
132.48
129.21
126.26
126.21
125.21
122.48
77.16 CDCl3
O
F
F
F
200 190 180 170 160 150 140 130 120 110 100 90 80 70 60 50 40 30 20 10 0
chemical shift (ppm)

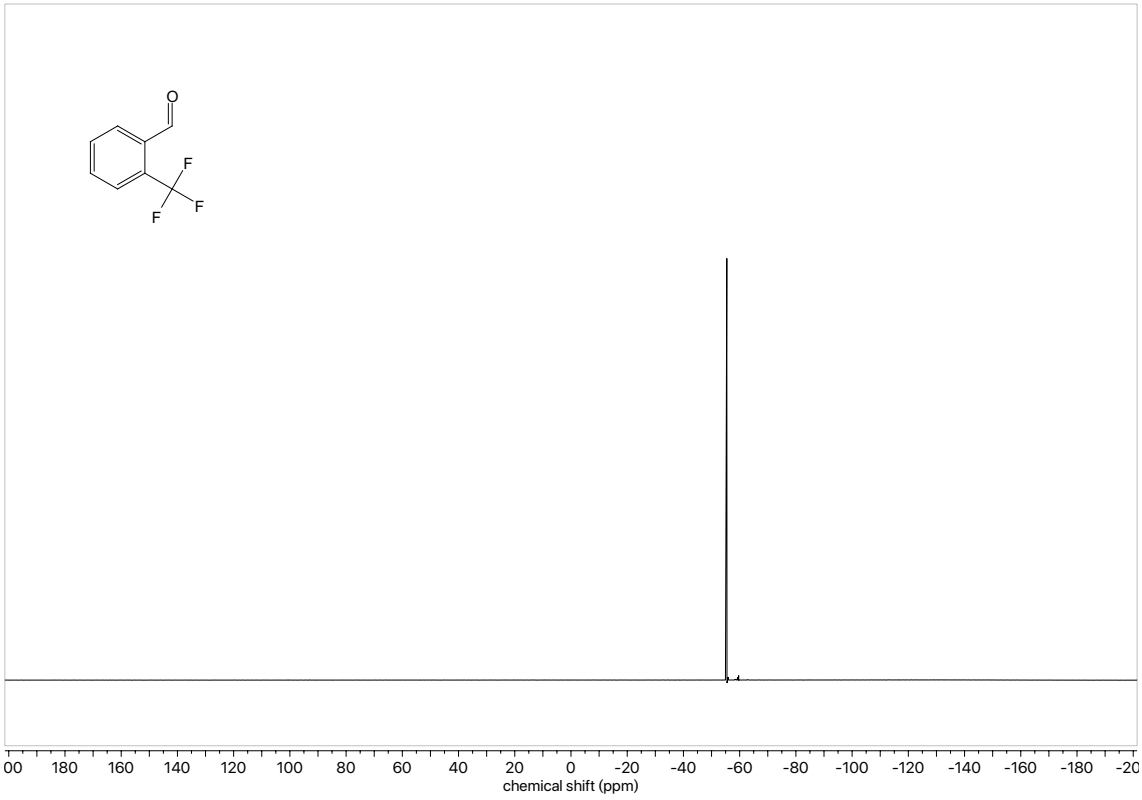
O
F
F
F
00 180 160 140 120 100 80 60 40 20 0 -20 -40 -60 -80 -100 -120 -140 -160 -180 -20
chemical shift (ppm)

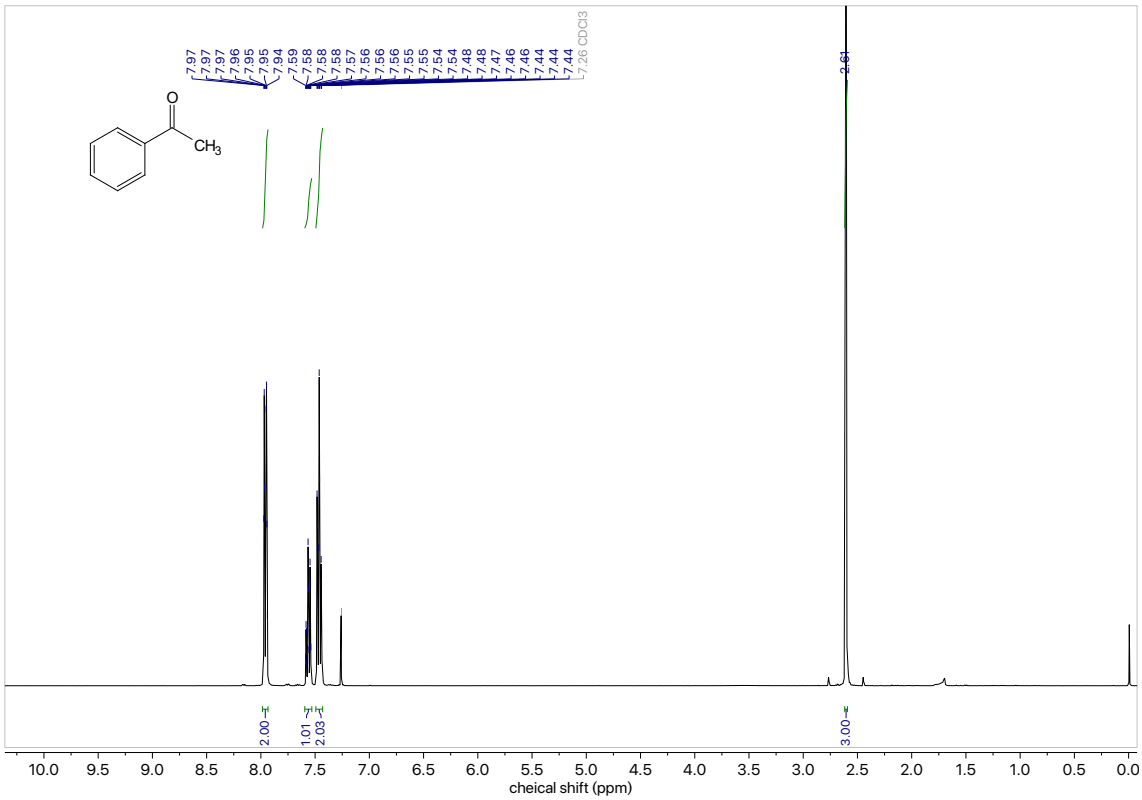
7.97
7.97
7.97
7.96
7.95
7.95
7.94
7.59
7.58
7.58
7.58
7.57
7.56
7.56
7.56
7.55
7.55
7.54
7.54
7.48
7.48
7.47
7.46
7.46
7.44
7.44
7.44
7.26 CDCl3
2.61
O
CH3
2.00
1.01
2.03
3.00
10.0 9.5 9.0 8.5 8.0 7.5 7.0 6.5 6.0 5.5 5.0 4.5 4.0 3.5 3.0 2.5 2.0 1.5 1.0 0.5 0.0
cheical shift (ppm)

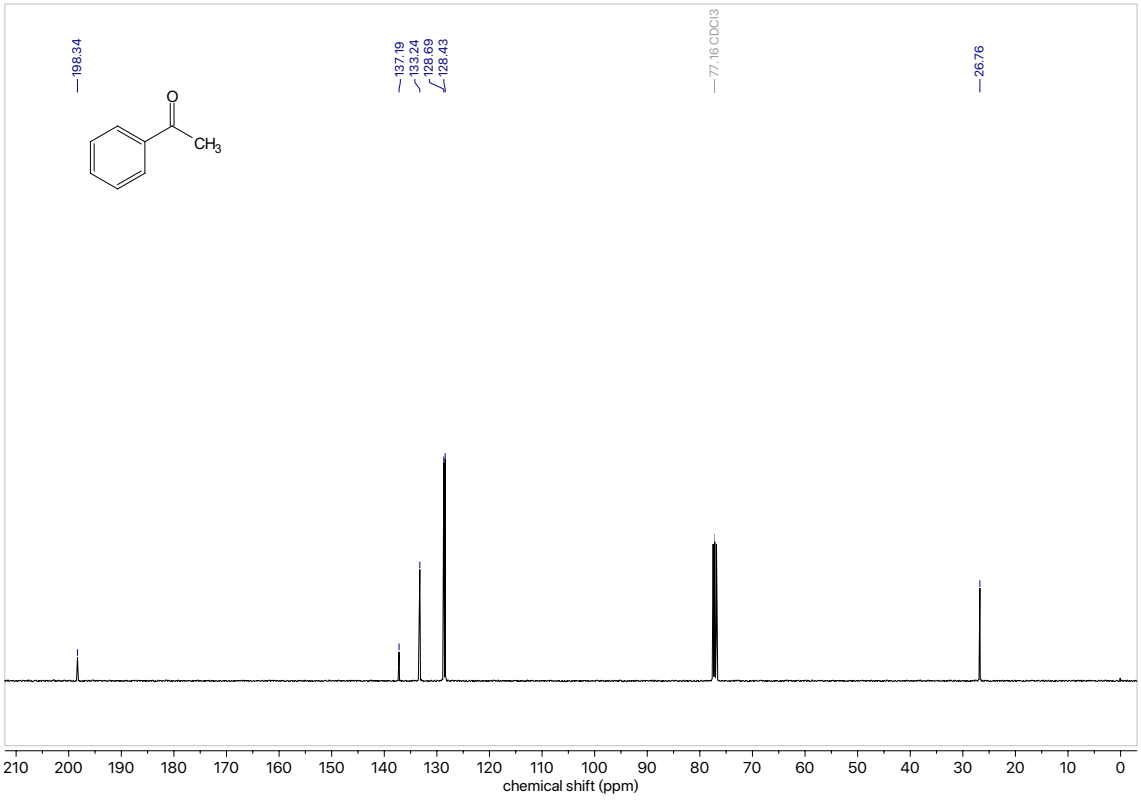
198.34
137.19
133.24
128.69
128.43
77.16 CDCl3
26.76
O
CH3
210 200 190 180 170 160 150 140 130 120 110 100 90 80 70 60 50 40 30 20 10 0
chemical shift (ppm)

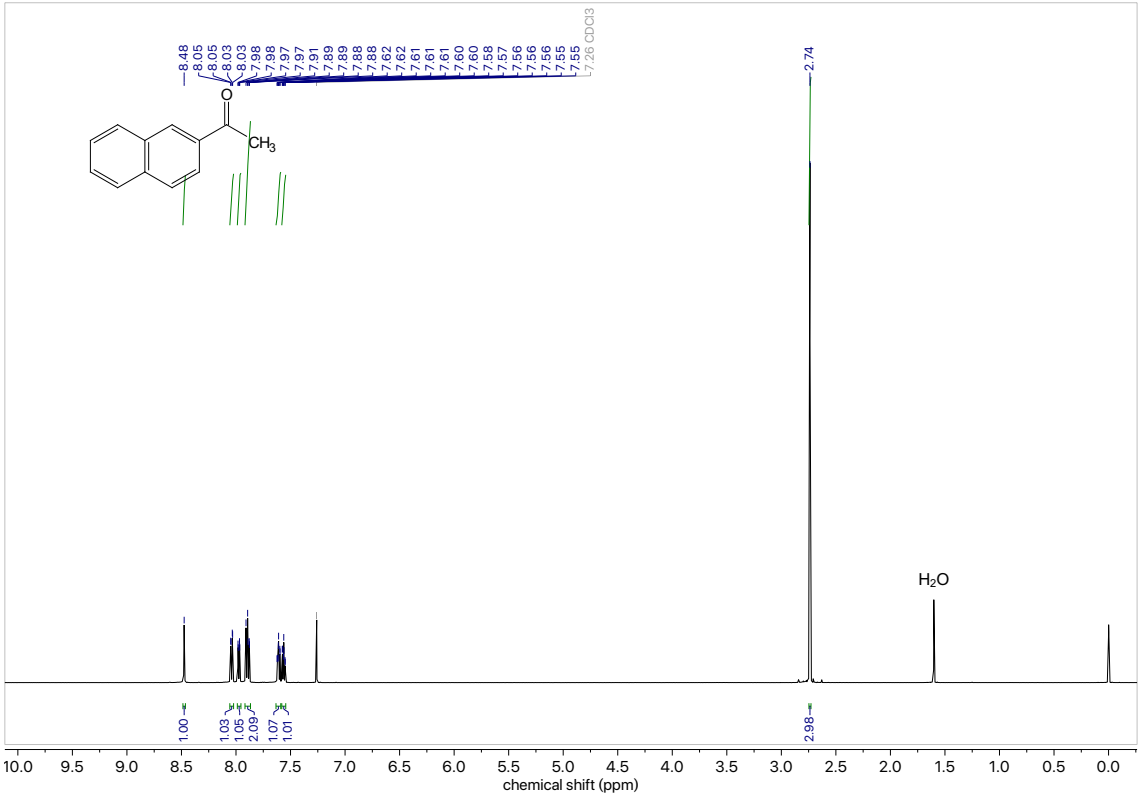
8.48
8.05
8.05
8.03
8.03
7.98
7.98
7.97
7.97
7.91
7.89
7.89
7.88
7.88
7.62
7.62
7.61
7.61
7.61
7.60
7.60
7.58
7.57
7.56
7.56
7.56
7.55
7.55
7.26 CDCl3
2.74
O
CH3
H2O
1.00
1.03
1.05
2.09
1.07
1.01
2.98
10.0 9.5 9.0 8.5 8.0 7.5 7.0 6.5 6.0 5.5 5.0 4.5 4.0 3.5 3.0 2.5 2.0 1.5 1.0 0.5 0.0
chemical shift (ppm)

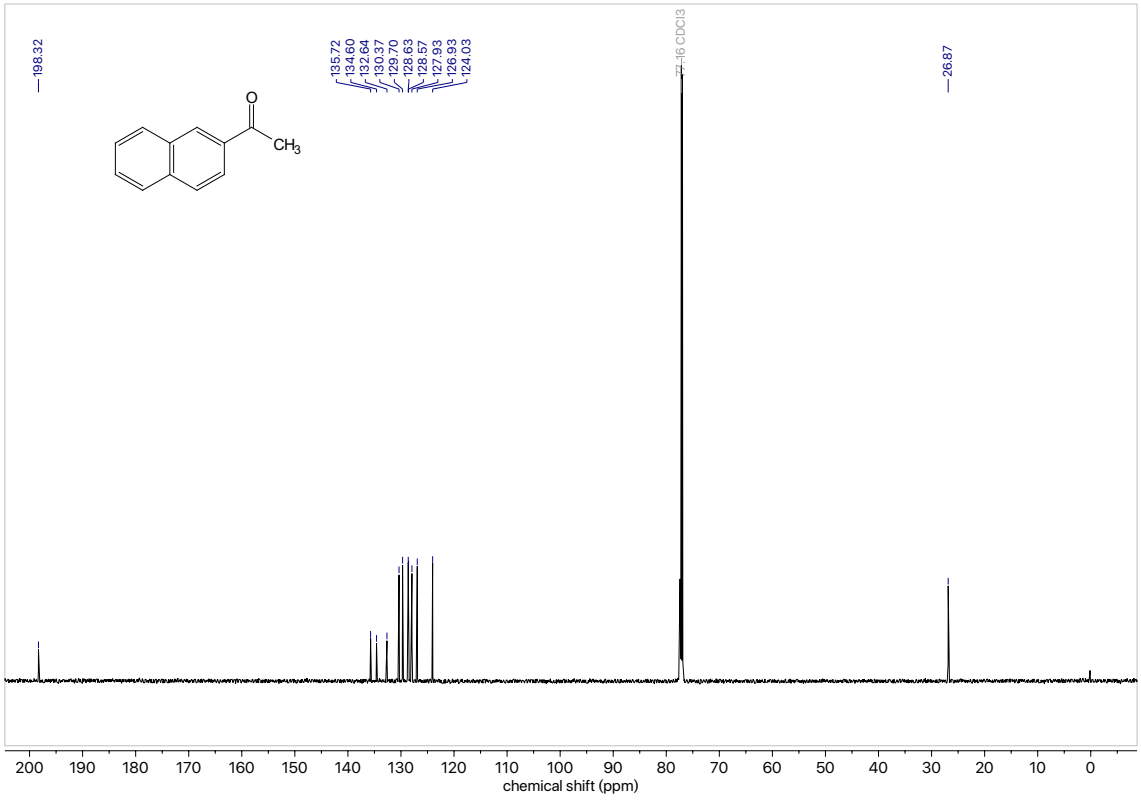
198.32
135.72
134.60
132.64
130.37
129.70
128.63
128.57
127.93
126.93
124.03
77.16 CDCl3
26.87
O
CH3
200 190 180 170 160 150 140 130 120 110 100 90 80 70 60 50 40 30 20 10 0
chemical shift (ppm)

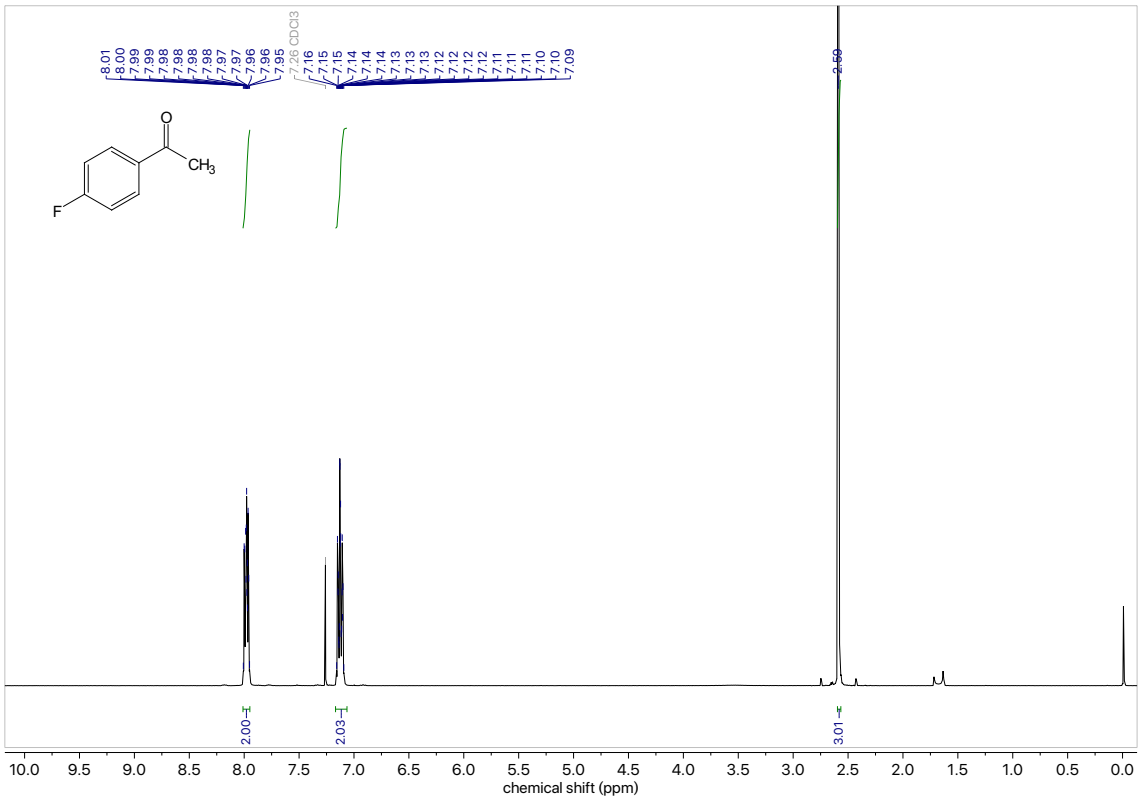
8.01
8.00
7.99
7.98
7.98
7.98
7.98
7.97
7.97
7.96
7.96
7.95
7.26 CDCl3
7.16
7.15
7.15
7.14
7.14
7.13
7.13
7.12
7.12
7.12
7.11
7.11
7.10
7.10
7.09
2.59
O
CH3
F
2.00
2.03
3.01
10.0 9.5 9.0 8.5 8.0 7.5 7.0 6.5 6.0 5.5 5.0 4.5 4.0 3.5 3.0 2.5 2.0 1.5 1.0 0.5 0.0
chemical shift (ppm)

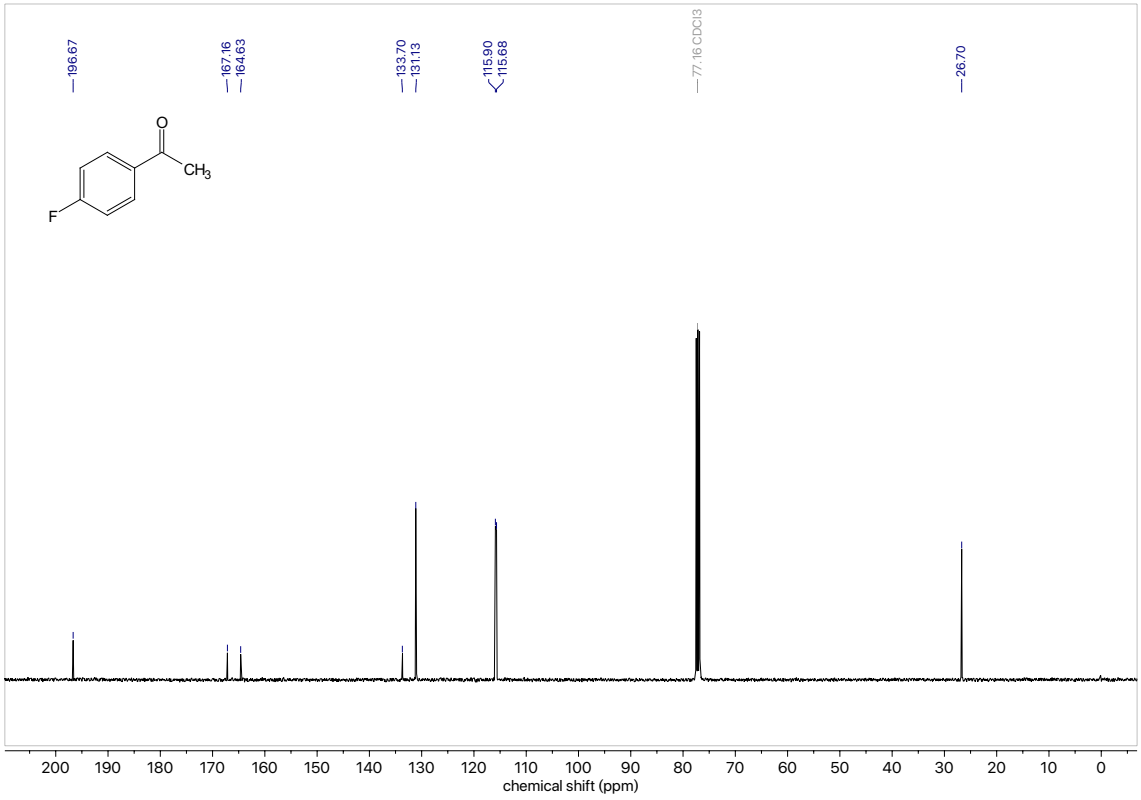
196.67
167.16
164.63
133.70
131.13
115.90
115.68
77.16 CDCl3
26.70
O
CH3
F
200 190 180 170 160 150 140 130 120 110 100 90 80 70 60 50 40 30 20 10 0
chemical shift (ppm)

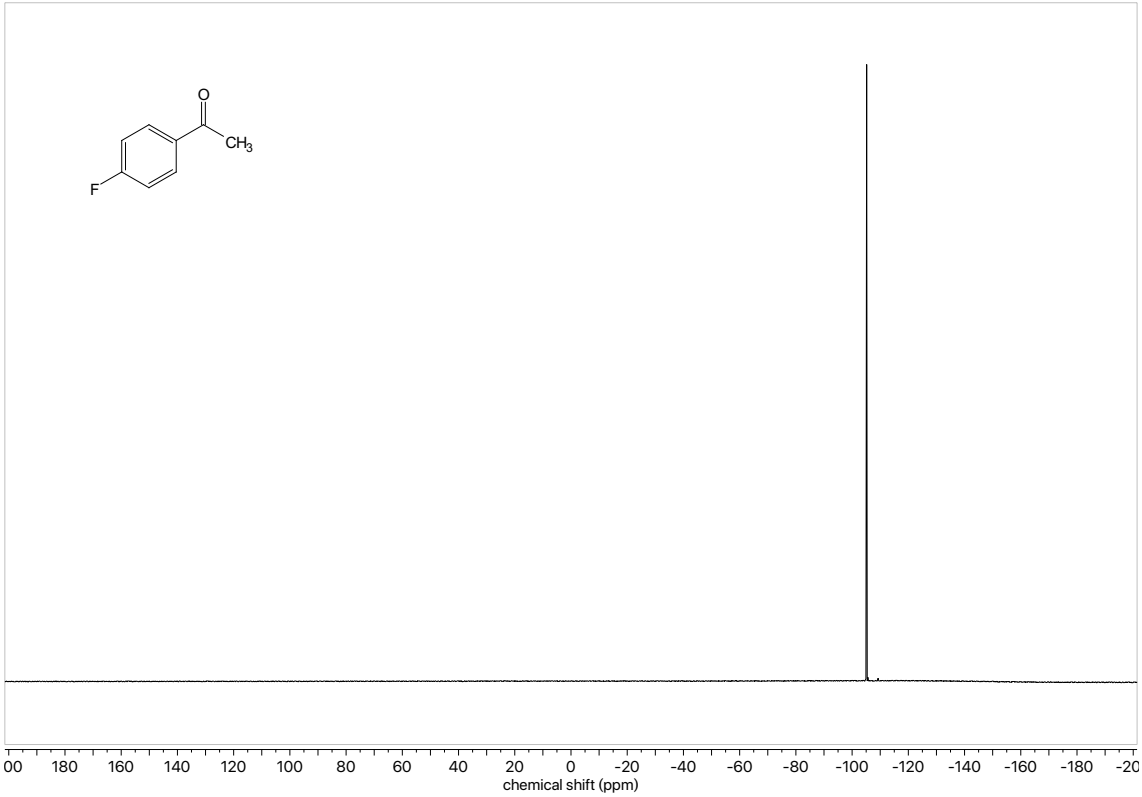
O
CH3
F
00 180 160 140 120 100 80 60 40 20 0 -20 -40 -60 -80 -100 -120 -140 -160 -180 -20
chemical shift (ppm)

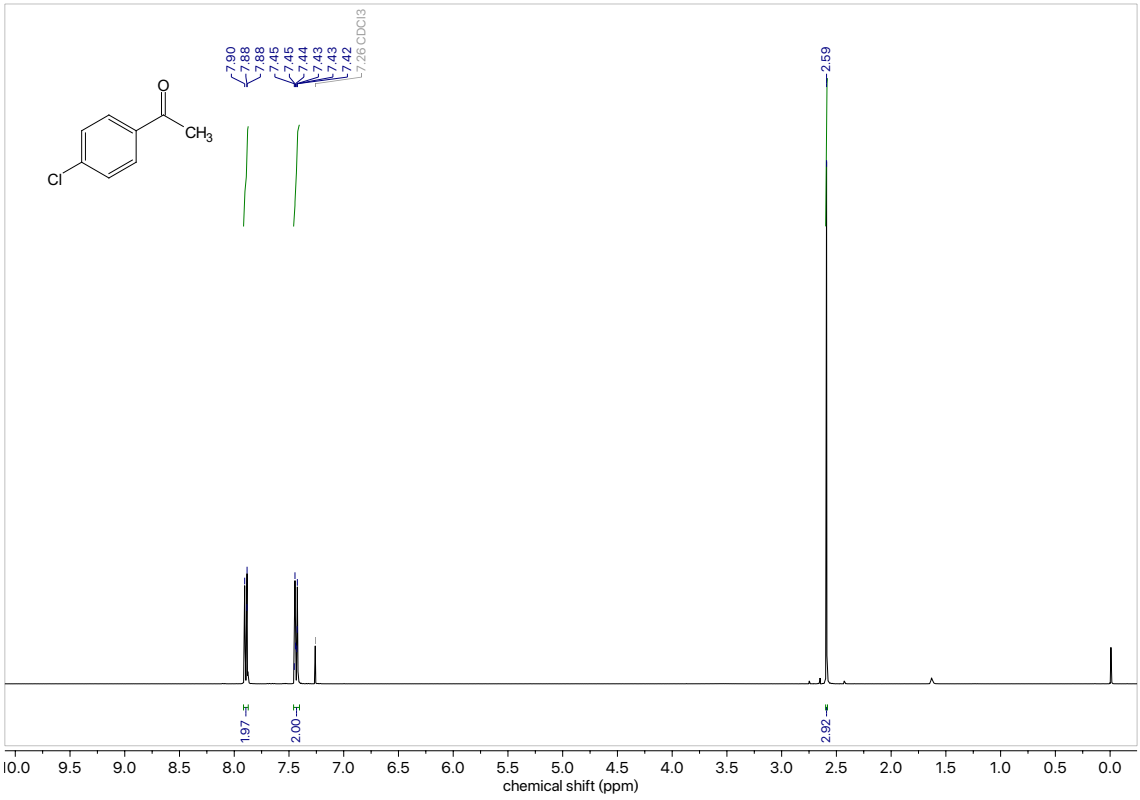
7.90
7.88
7.88
7.45
7.45
7.44
7.43
7.43
7.42
7.26 CDCl3
2.59
O
CH3
Cl
1.97
2.00
2.92
10.0 9.5 9.0 8.5 8.0 7.5 7.0 6.5 6.0 5.5 5.0 4.5 4.0 3.5 3.0 2.5 2.0 1.5 1.0 0.5 0.0
chemical shift (ppm)

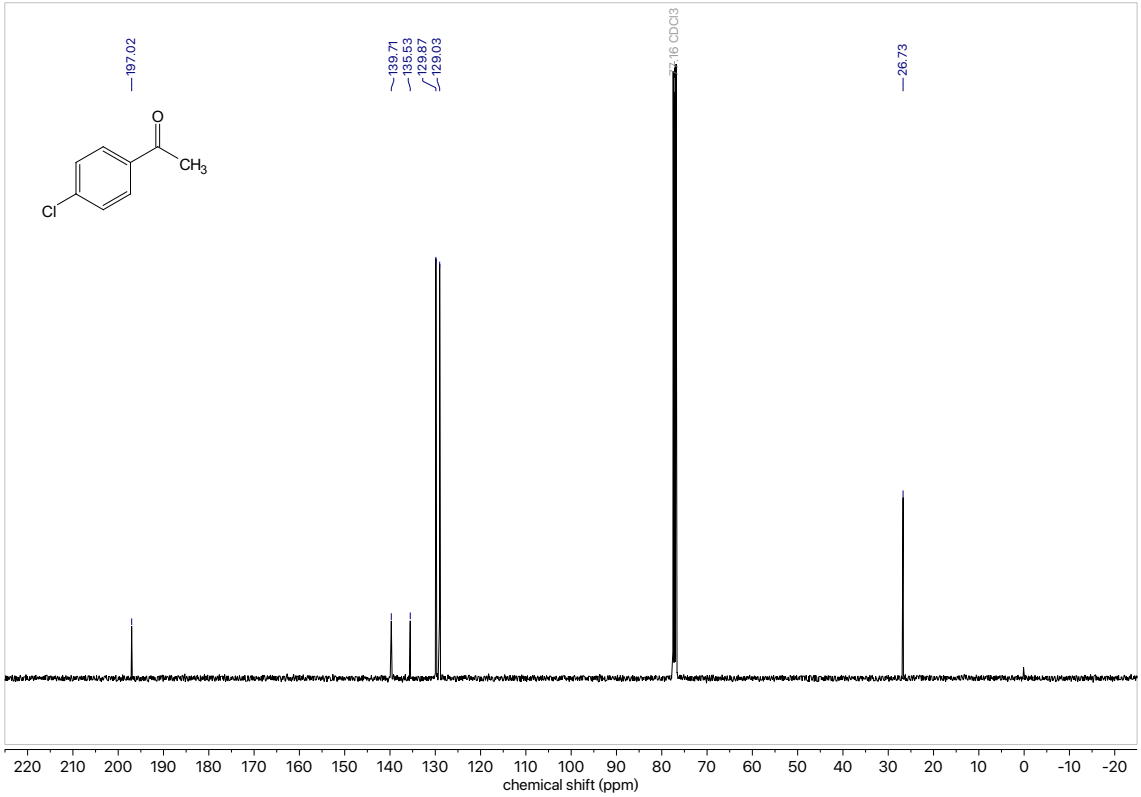
197.02
139.71
135.53
129.87
129.03
77.16 CDCl3
26.73
O
CH3
Cl
220 210 200 190 180 170 160 150 140 130 120 110 100 90 80 70 60 50 40 30 20 10 0 -10 -20
chemical shift (ppm)

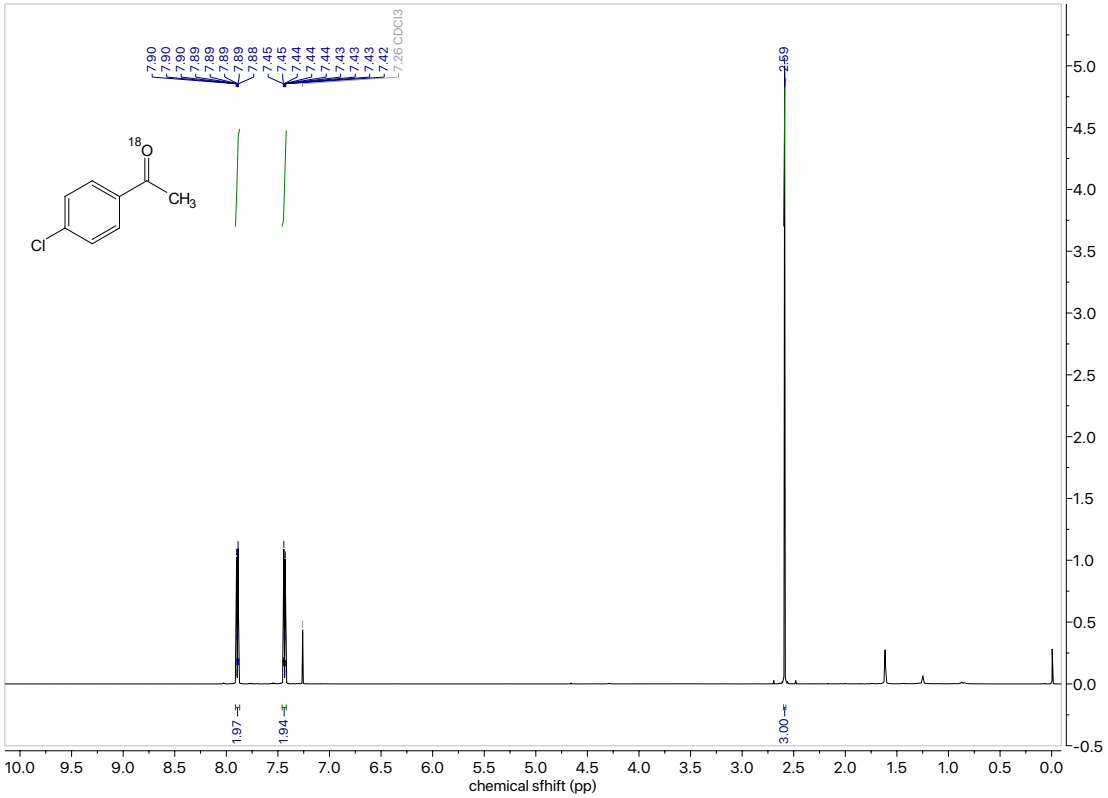
7.90
7.90
7.90
7.89
7.89
7.89
7.88
7.45
7.45
7.44
7.44
7.44
7.43
7.43
7.43
7.42
7.26 CDCl3
2.69
18O
CH3
Cl
1.97
1.94
3.00
10.0 9.5 9.0 8.5 8.0 7.5 7.0 6.5 6.0 5.5 5.0 4.5 4.0 3.5 3.0 2.5 2.0 1.5 1.0 0.5 0.0
chemical sfhift (pp)
5.0 4.5 4.0 3.5 3.0 2.5 2.0 1.5 1.0 0.5 0.0 -0.5

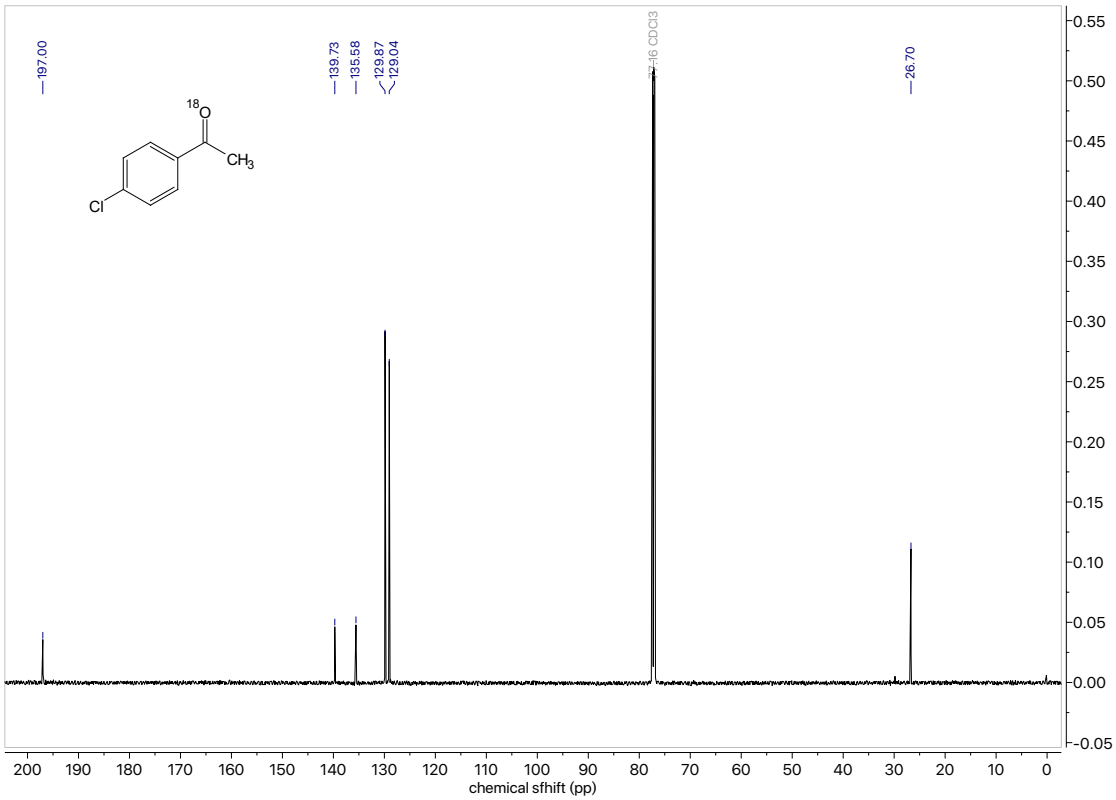
197.00
139.73
135.58
129.87
129.04
77.16 CDCl3
26.70
18O
CH3
Cl
chemical sfhift (pp)

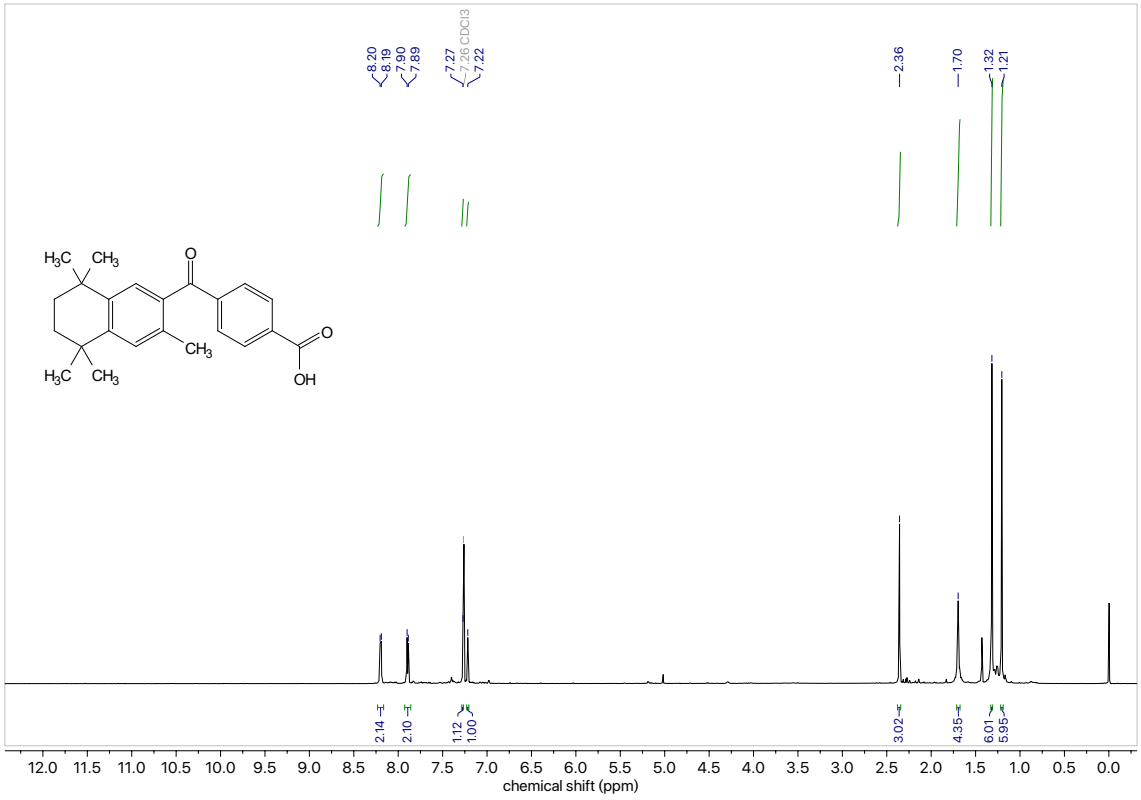
8.20
8.19
7.90
7.89
7.27
7.26 CDCl3
7.22
2.36
1.70
1.32
1.21
H3C
CH3
O
CH3
H3C
CH3
O
OH
2.14
2.10
1.12
1.00
3.02
4.35
6.01
5.95
chemical shift (ppm)

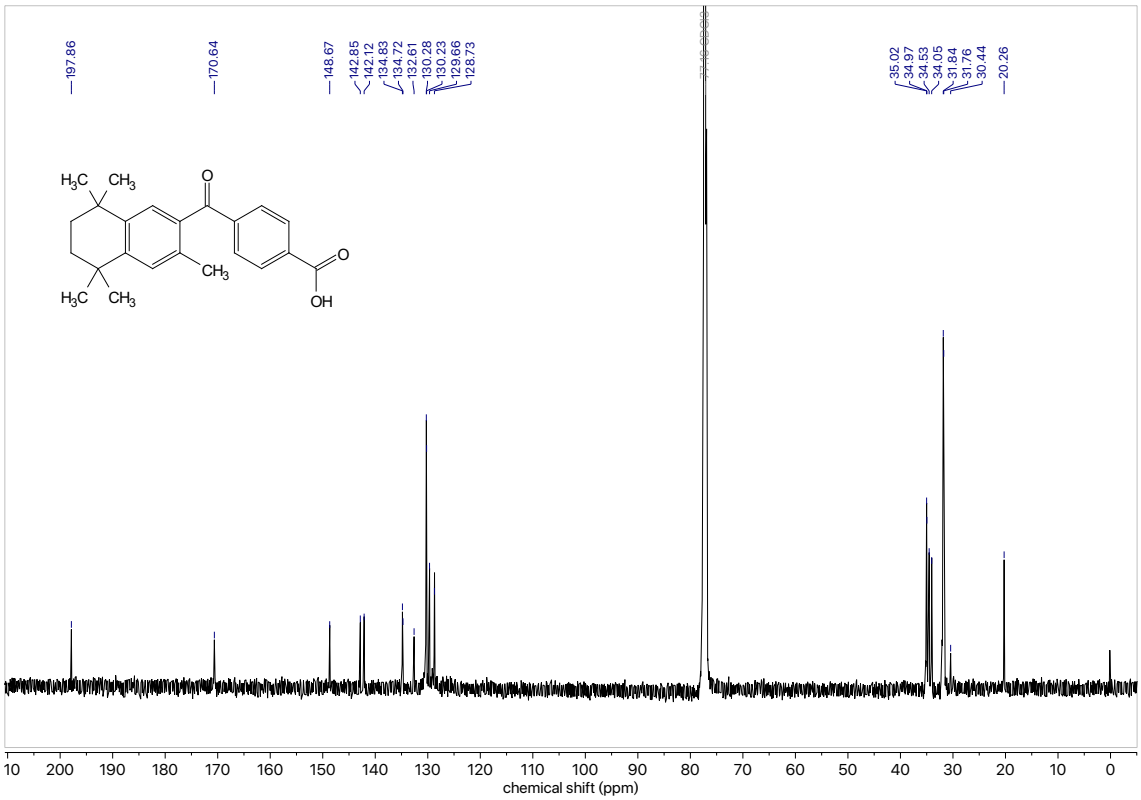
197.86
170.64
148.67
142.85
142.12
134.83
134.72
132.61
130.28
130.23
129.66
128.73
35.02
34.97
34.53
34.05
31.84
31.76
30.44
20.26
H3C
CH3
O
CH3
O
OH
H3C
CH3
10 200 190 180 170 160 150 140 130 120 110 100 90 80 70 60 50 40 30 20 10 0
chemical shift (ppm)

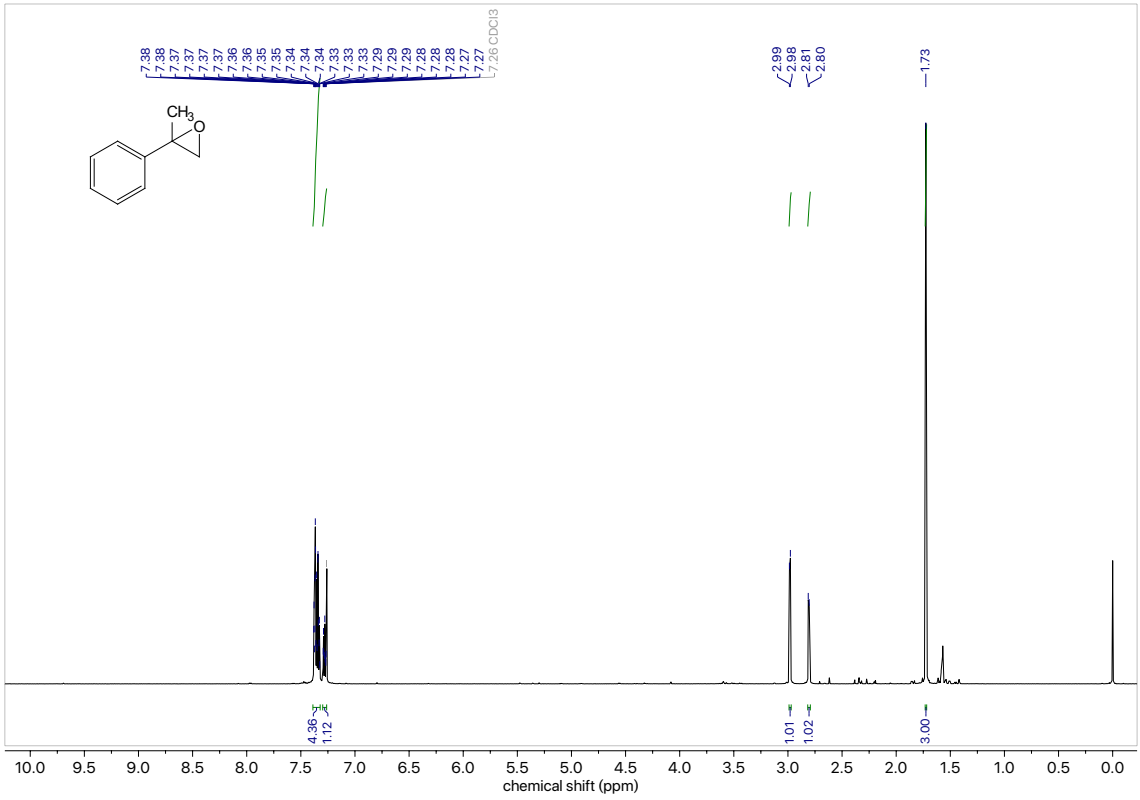
7.38
7.38
7.37
7.37
7.37
7.37
7.36
7.36
7.35
7.35
7.34
7.34
7.34
7.33
7.33
7.33
7.29
7.29
7.29
7.28
7.28
7.28
7.27
7.27
7.26 CDCl3
2.99
2.98
2.81
2.80
1.73
CH3
O
4.36
1.12
1.01
1.02
3.00
10.0 9.5 9.0 8.5 8.0 7.5 7.0 6.5 6.0 5.5 5.0 4.5 4.0 3.5 3.0 2.5 2.0 1.5 1.0 0.5 0.0
chemical shift (ppm)

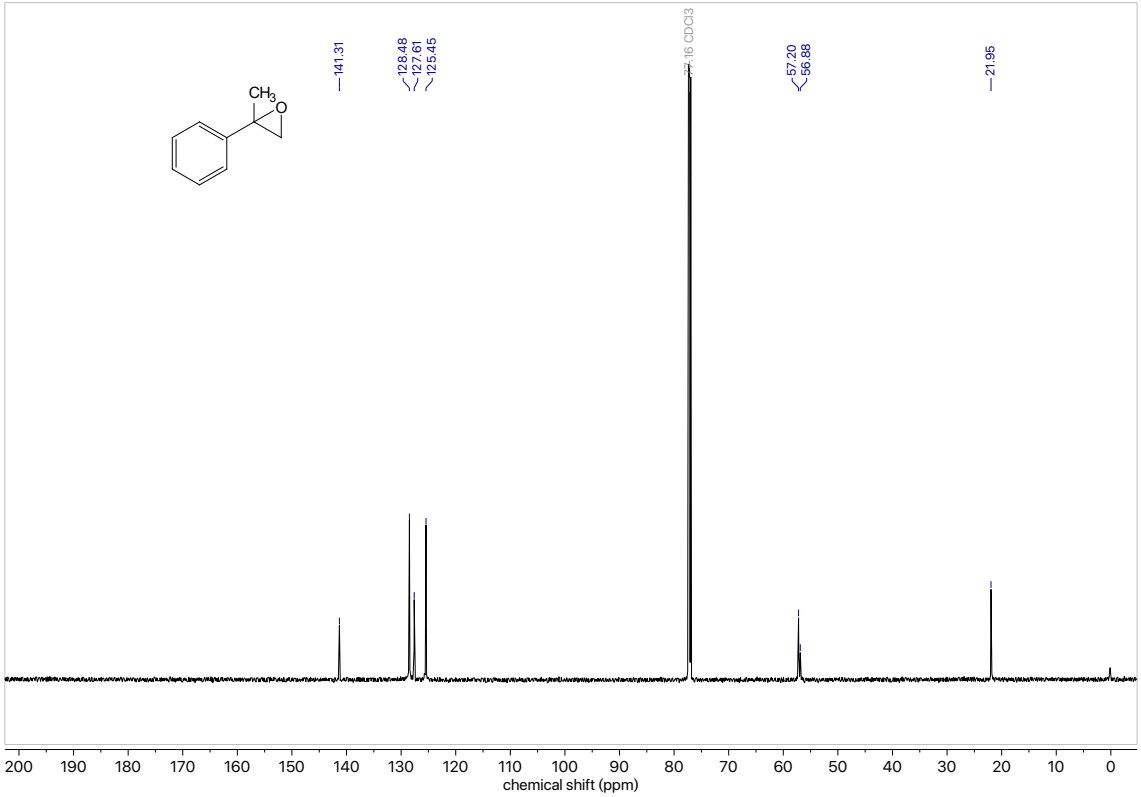
141.31
128.48
127.61
125.45
77.16 CDCl3
57.20
56.88
21.95
CH3
O
200 190 180 170 160 150 140 130 120 110 100 90 80 70 60 50 40 30 20 10 0
chemical shift (ppm)

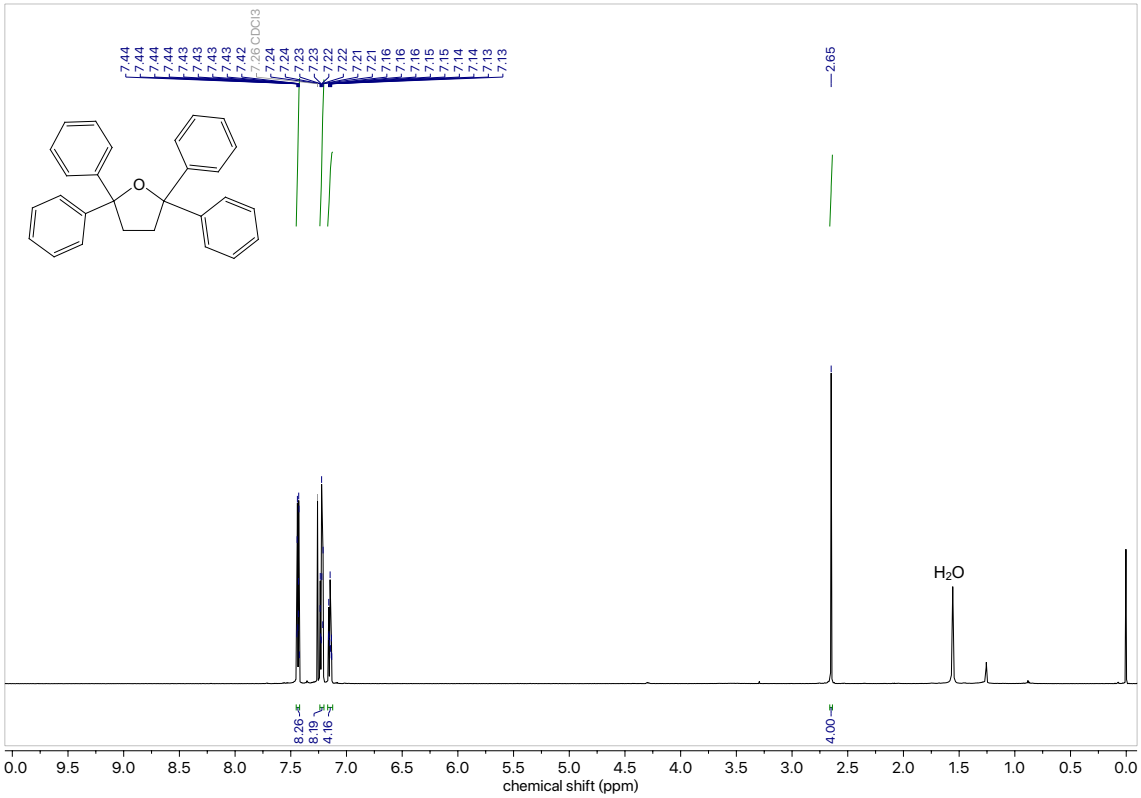
7.44
7.44
7.44
7.44
7.43
7.43
7.43
7.43
7.42
7.26 CDCl3
7.24
7.24
7.23
7.23
7.22
7.22
7.21
7.21
7.16
7.16
7.16
7.15
7.15
7.14
7.14
7.13
7.13
2.65
O
H2O
8.26
8.19
4.16
4.00
0.0 9.5 9.0 8.5 8.0 7.5 7.0 6.5 6.0 5.5 5.0 4.5 4.0 3.5 3.0 2.5 2.0 1.5 1.0 0.5 0.0
chemical shift (ppm)

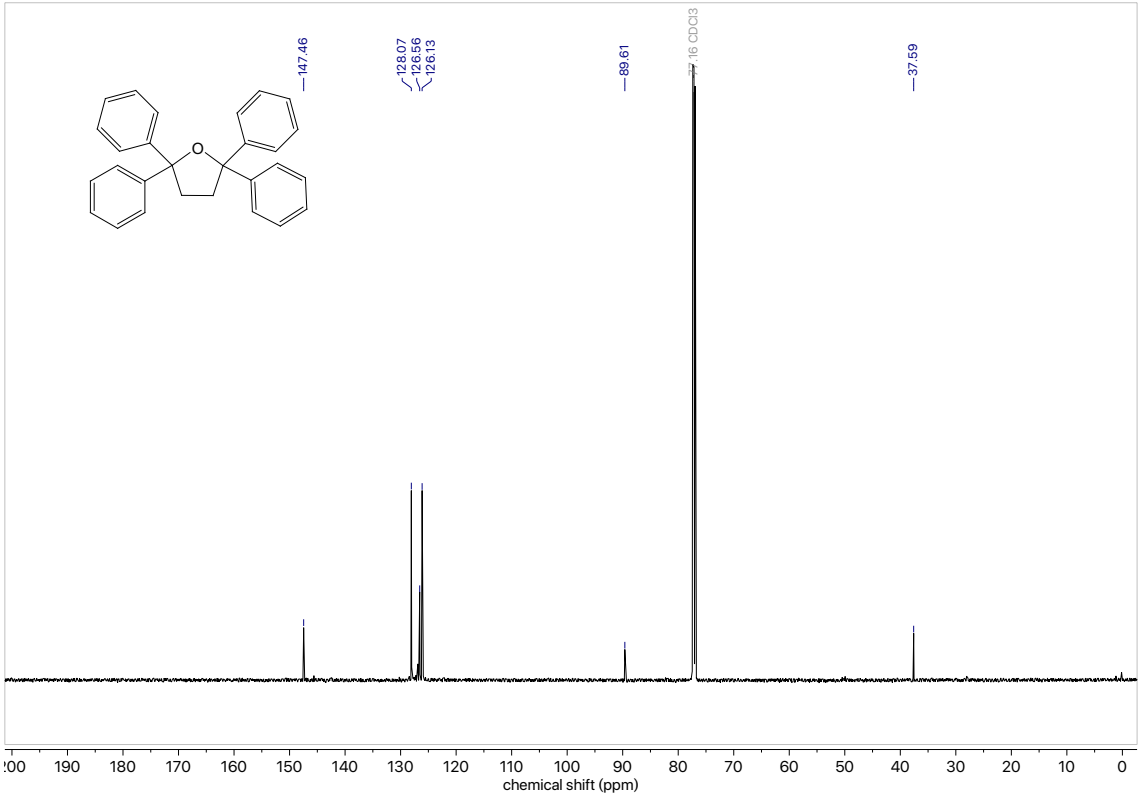
147.46
128.07
126.56
126.13
89.61
77.16 CDCl3
37.59
chemical shift (ppm)

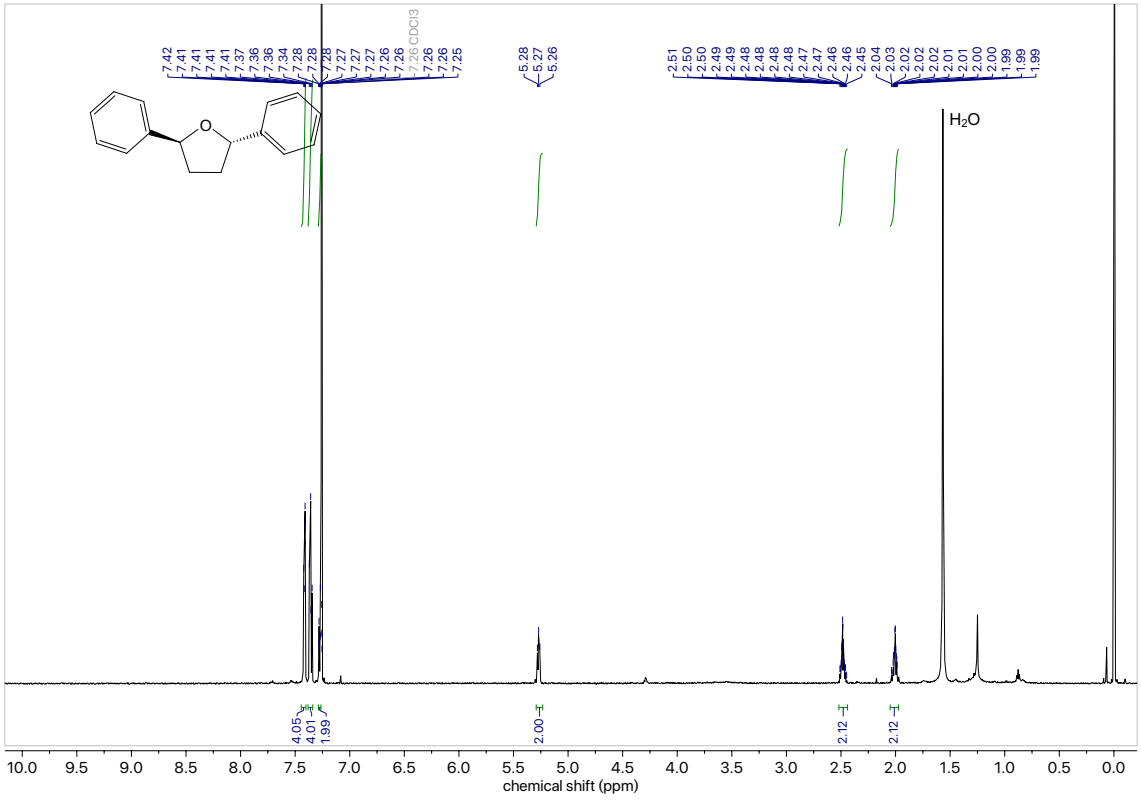
7.42
7.41
7.41
7.41
7.37
7.36
7.36
7.34
7.28
7.28
7.28
7.27
7.27
7.27
7.26
7.26
7.26
7.26
7.26 CDCl3
7.25
5.28
5.27
5.26
2.51
2.50
2.50
2.49
2.49
2.48
2.48
2.48
2.48
2.47
2.47
2.46
2.46
2.45
2.04
2.03
2.02
2.02
2.02
2.01
2.01
2.00
2.00
1.99
1.99
1.99
H2O
4.05
4.01
1.99
2.00
2.12
2.12
chemical shift (ppm)

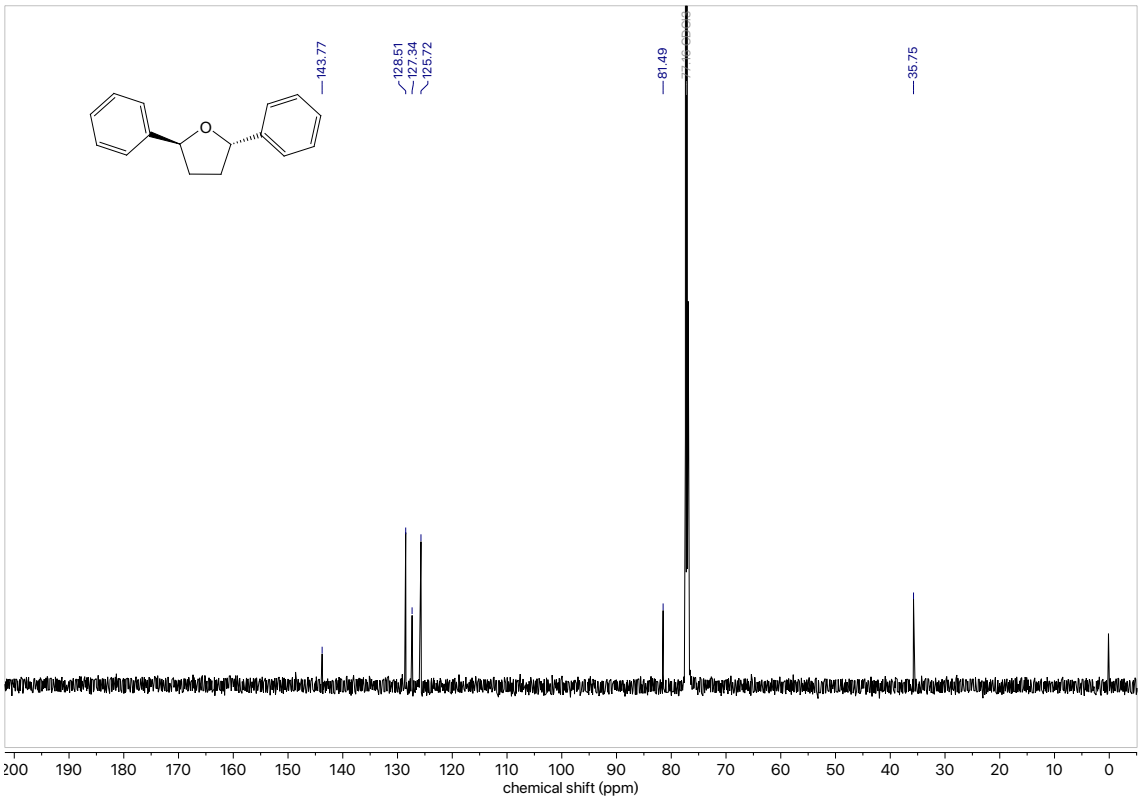
143.77
128.51
127.34
125.72
81.49
35.75
chemical shift (ppm)

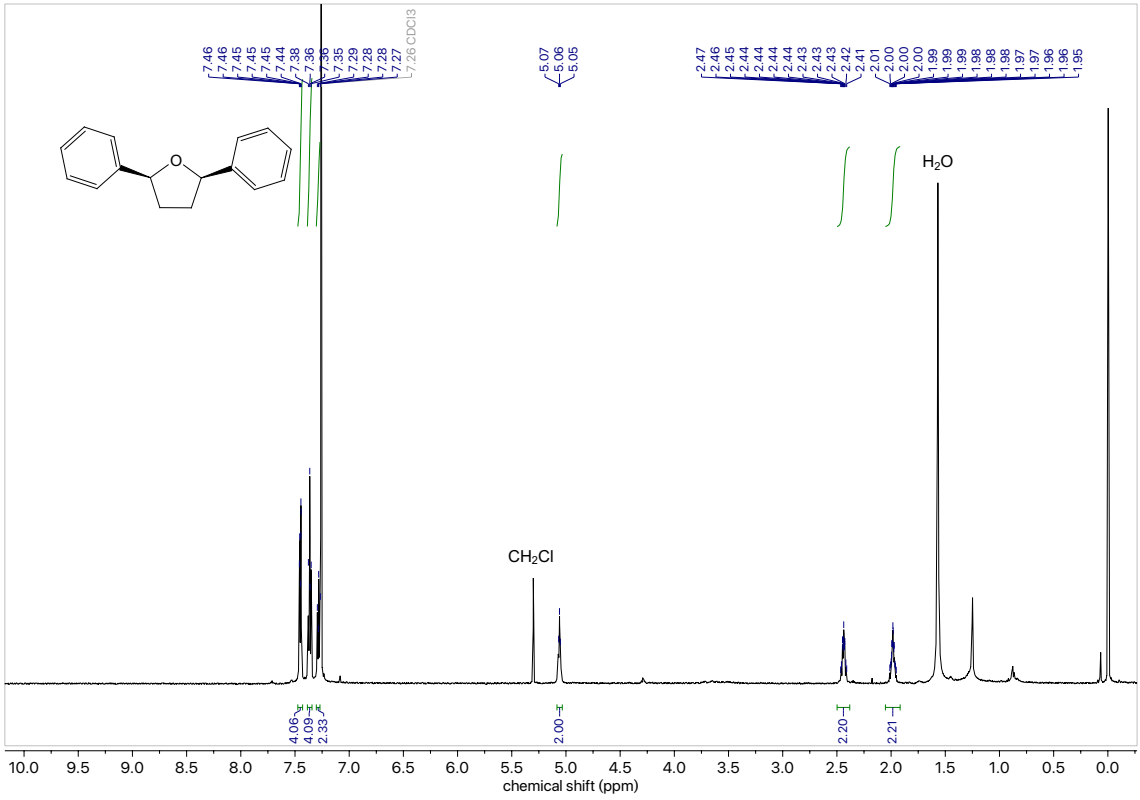
7.26 CDCl3
5.07
5.06
5.05
2.47
2.46
2.45
2.44
2.43
2.42
2.41
2.01
2.00
1.99
1.98
1.97
1.96
1.95
H2O
CH2Cl
4.06
4.09
2.33
2.00
2.20
2.21
chemical shift (ppm)

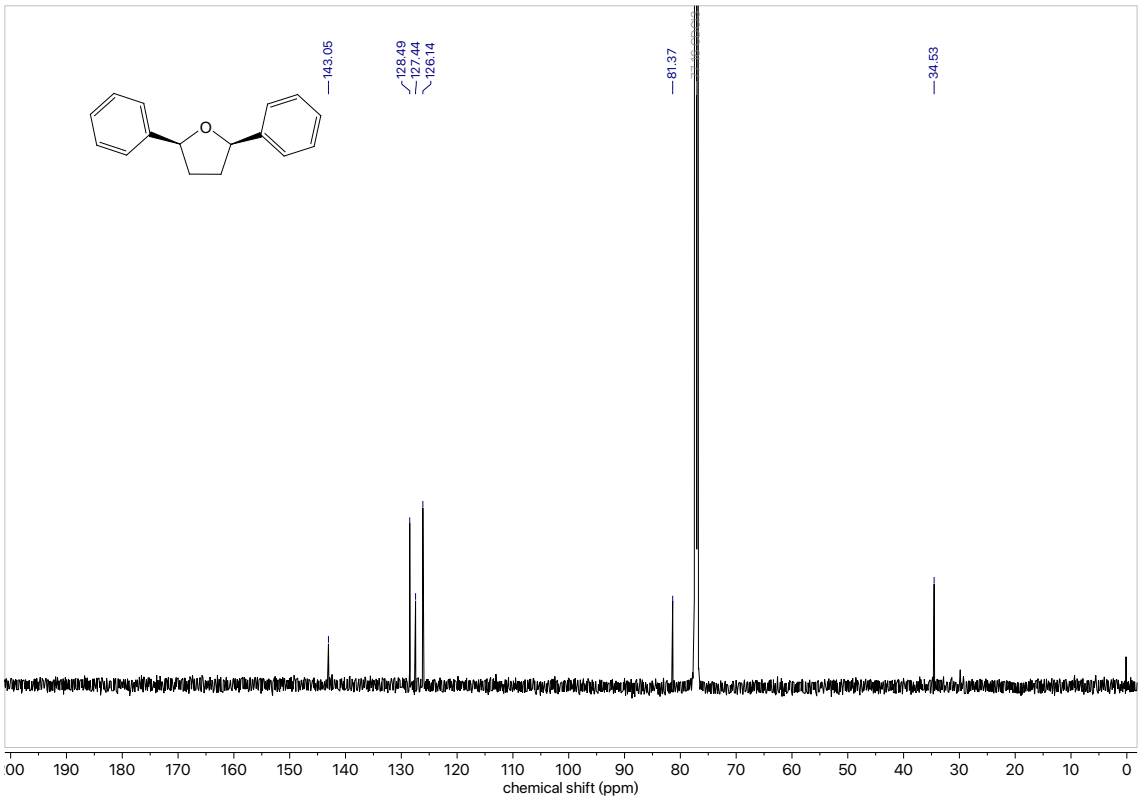
143.05
128.49
127.44
126.14
81.37
34.53
O
chemical shift (ppm)

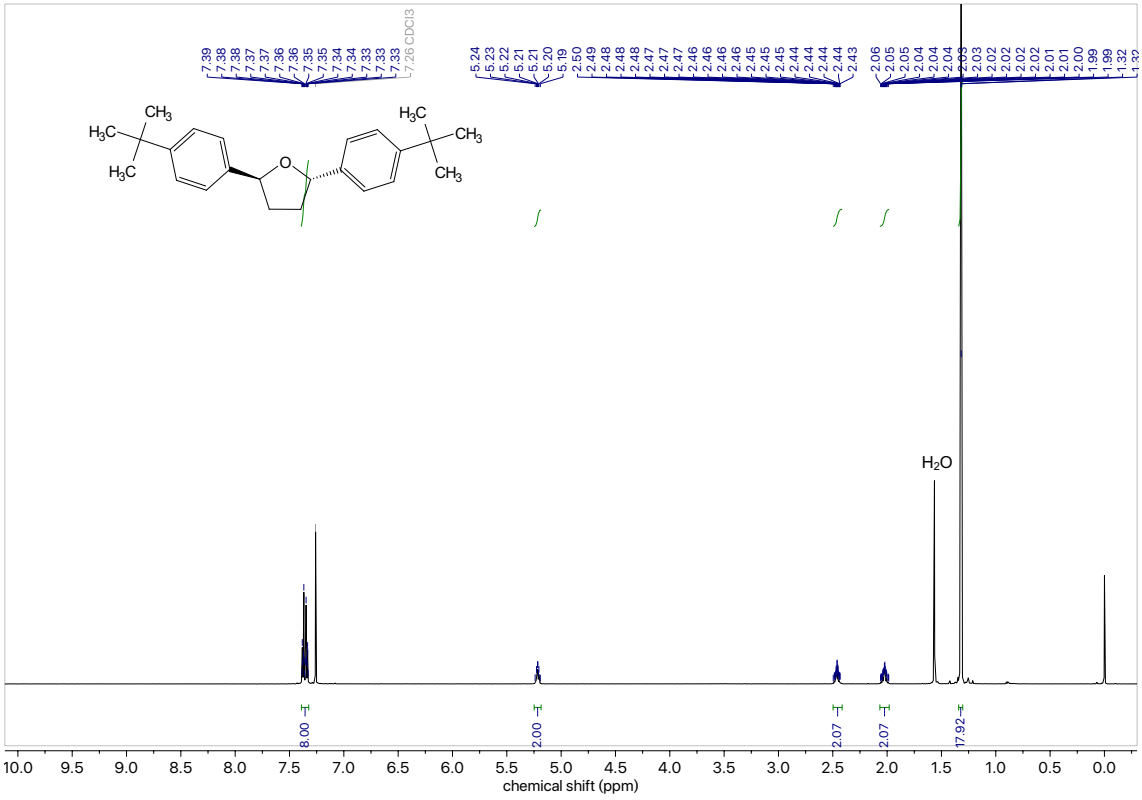
7.39
7.38
7.38
7.37
7.37
7.36
7.36
7.35
7.35
7.34
7.34
7.33
7.33
7.33
7.26 CDCl3
5.24
5.23
5.22
5.21
5.21
5.20
5.19
2.50
2.49
2.48
2.48
2.48
2.47
2.47
2.47
2.46
2.46
2.46
2.46
2.45
2.45
2.45
2.44
2.44
2.44
2.44
2.43
2.06
2.05
2.05
2.04
2.04
2.04
2.03
2.03
2.02
2.02
2.02
2.02
2.02
2.01
2.01
2.00
1.99
1.99
1.32
1.30
CH3
H3C
H3C
H3C
CH3
CH3
O
H2O
8.00
2.00
2.07
2.07
17.92
chemical shift (ppm)

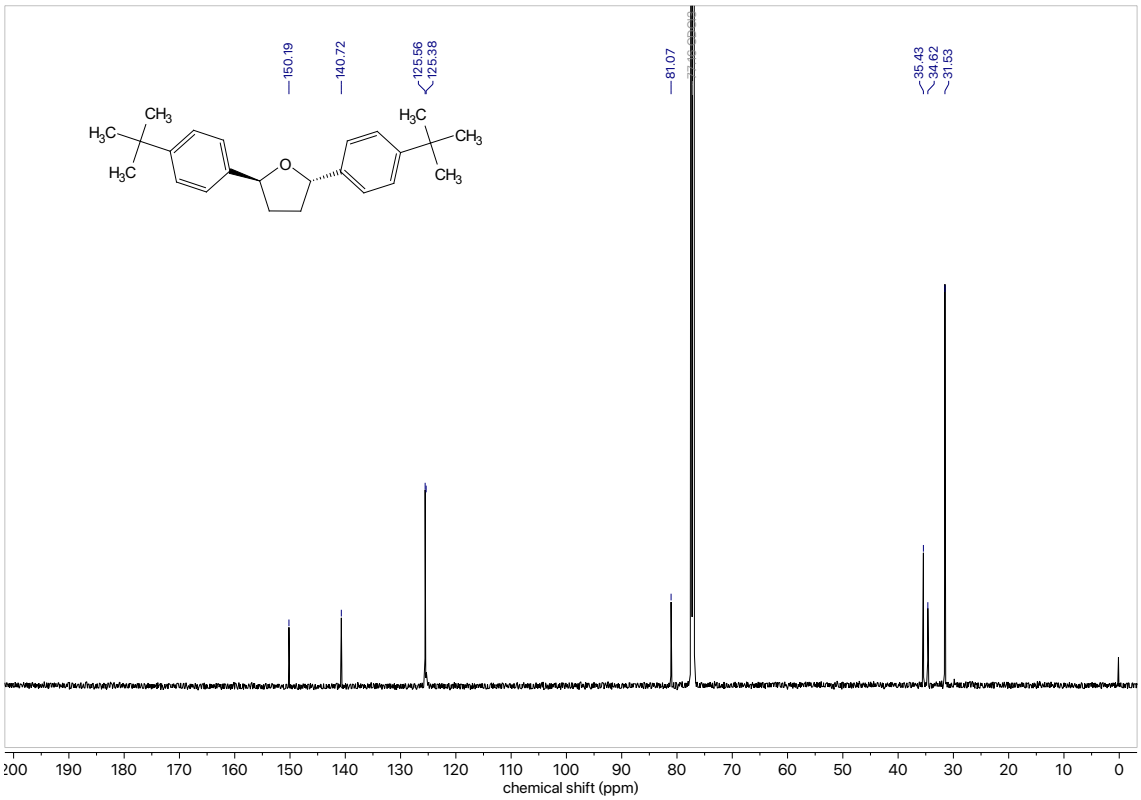
150.19
140.72
125.56
125.38
81.07
35.43
34.62
31.53
chemical shift (ppm)

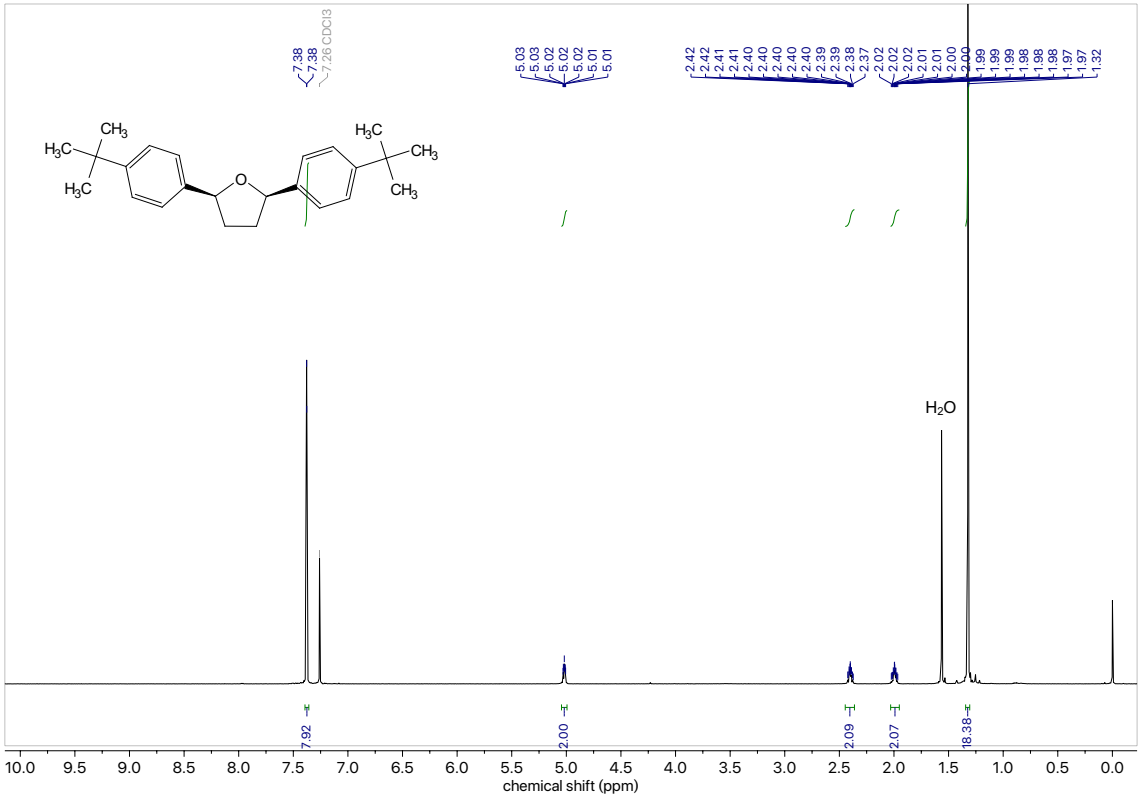
7.38
7.26 CDCl3
5.03
5.02
5.01
2.42
2.41
2.40
2.39
2.38
2.37
2.02
2.01
2.00
1.99
1.98
1.97
1.32
H2O
7.92
2.00
2.09
2.07
18.38
chemical shift (ppm)

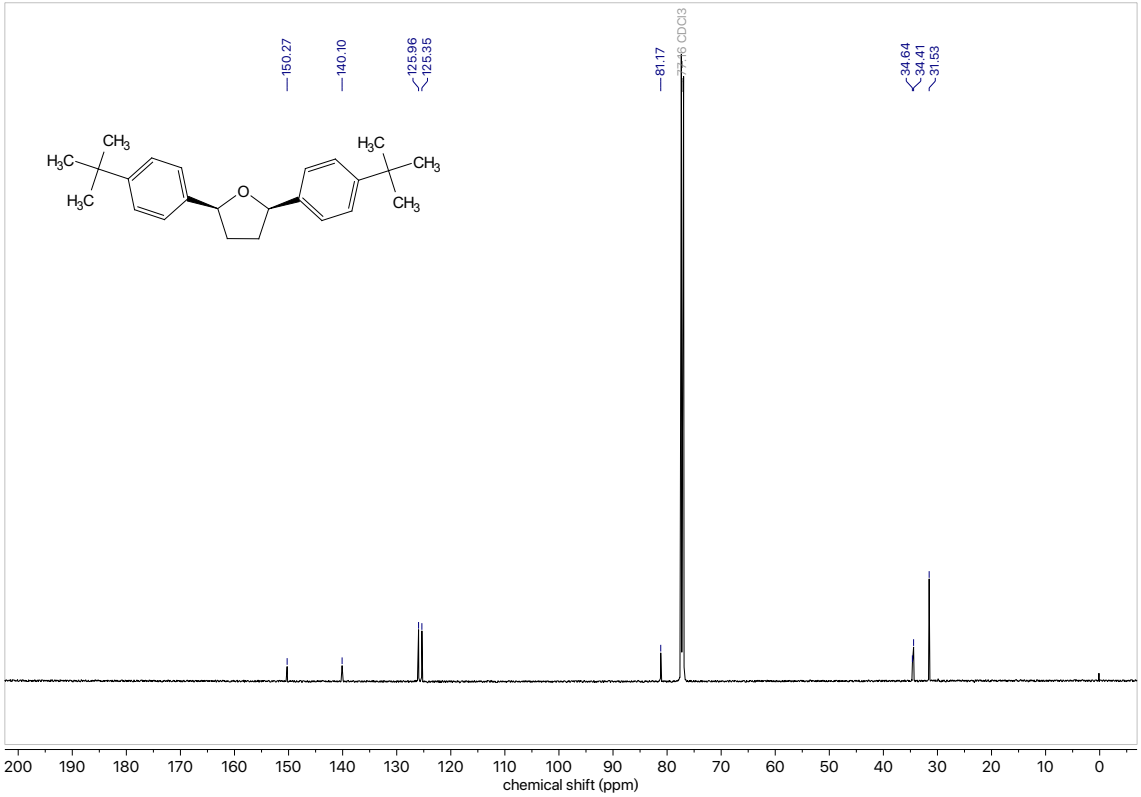
150.27
140.10
125.96
125.35
81.17
77.16 CDCl3
34.64
34.41
31.53
CH3
H3C
H3C
H3C
CH3
CH3
O
200 190 180 170 160 150 140 130 120 110 100 90 80 70 60 50 40 30 20 10 0
chemical shift (ppm)

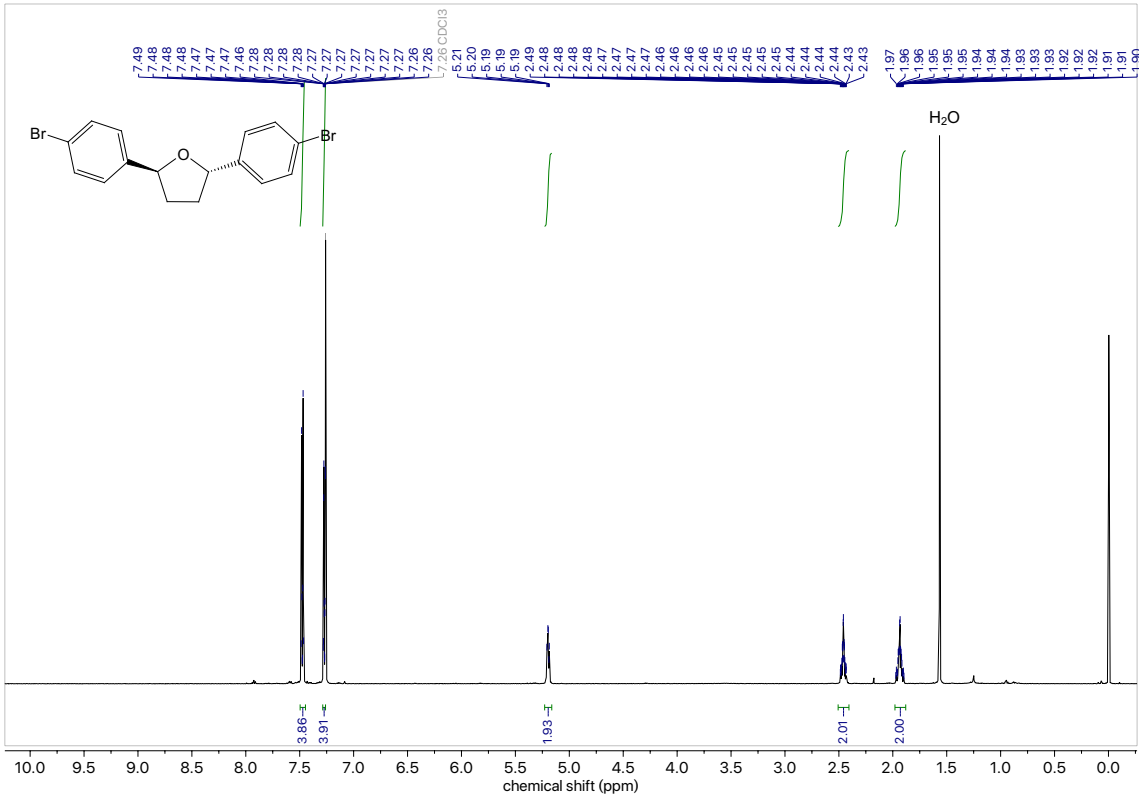
7.26 CDCl3
H2O
Br
Br
O
3.86
3.91
1.93
2.01
2.00
10.0 9.5 9.0 8.5 8.0 7.5 7.0 6.5 6.0 5.5 5.0 4.5 4.0 3.5 3.0 2.5 2.0 1.5 1.0 0.5 0.0
chemical shift (ppm)

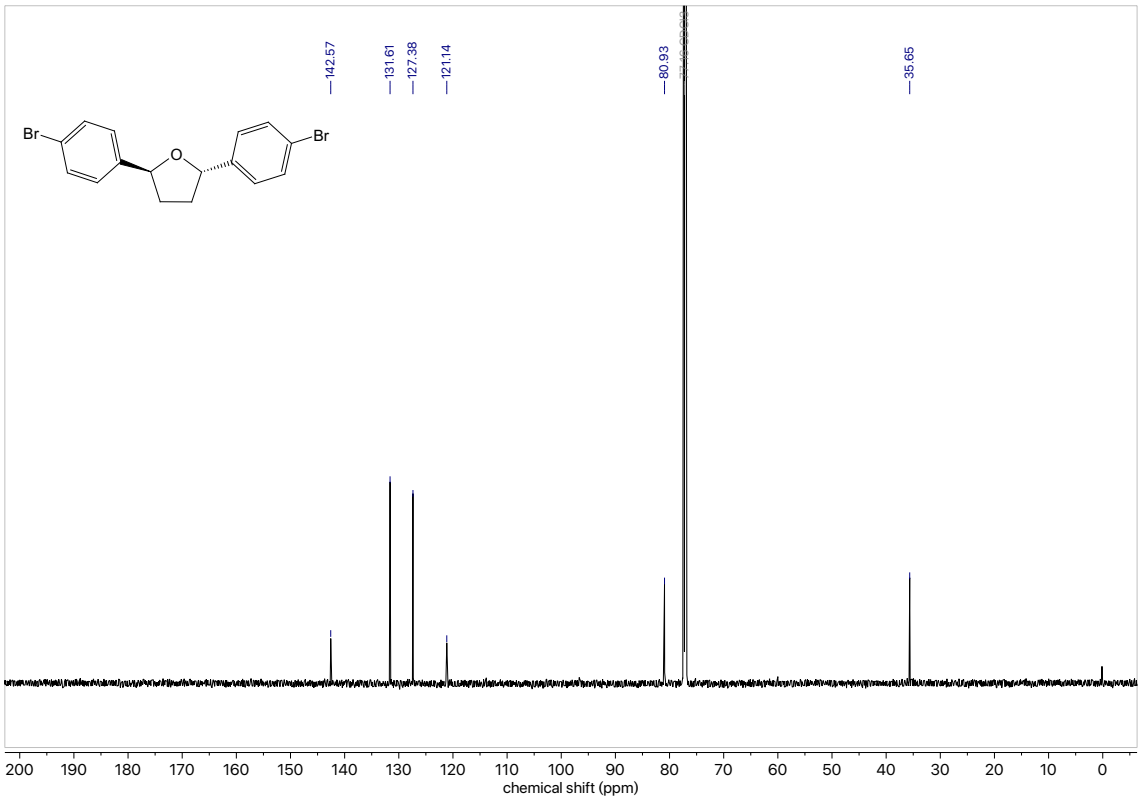
142.57
131.61
127.38
121.14
80.93
35.65
Br
O
Br
200 190 180 170 160 150 140 130 120 110 100 90 80 70 60 50 40 30 20 10 0
chemical shift (ppm)

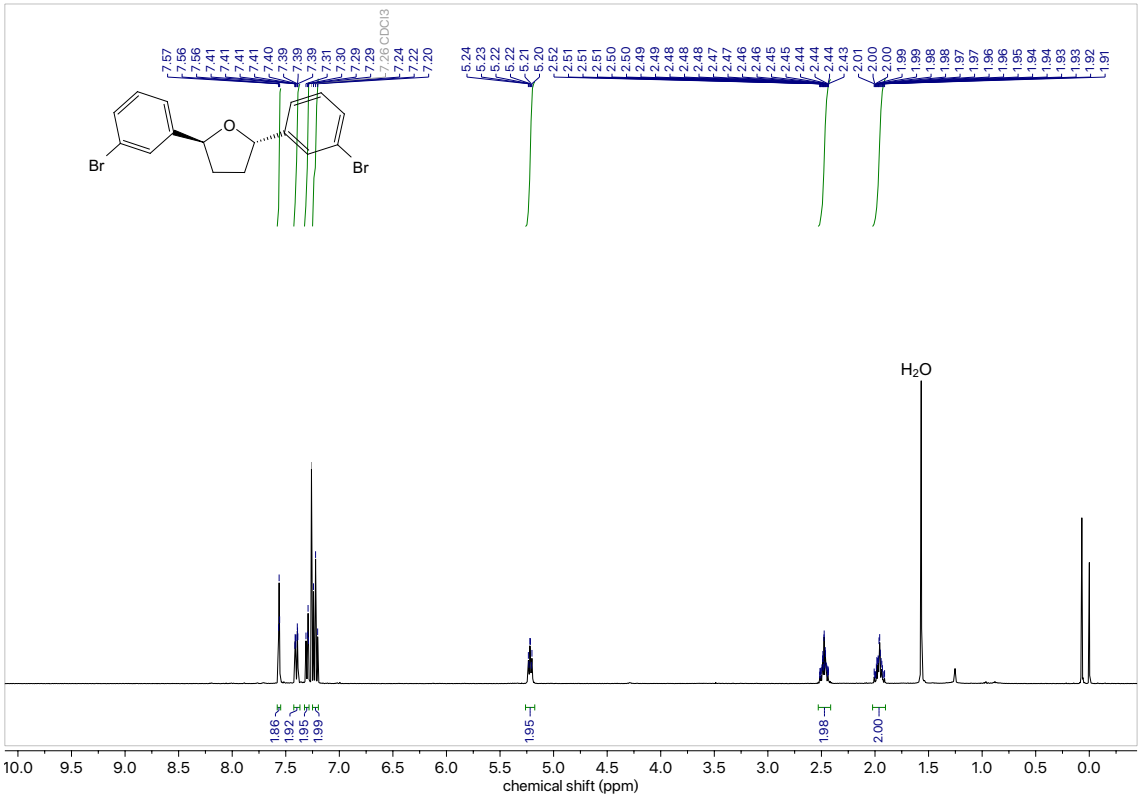
7.57 7.56 7.56 7.41 7.41 7.41 7.41 7.40 7.39 7.39 7.39 7.39 7.31 7.30 7.29 7.29 7.26 CDCl3 7.24 7.22 7.20
5.24 5.23 5.22 5.22 5.21 5.20 2.52 2.51 2.51 2.51 2.50 2.50 2.49 2.49 2.48 2.48 2.48 2.47 2.47 2.46 2.46 2.45 2.45 2.44 2.44 2.44 2.43 2.01 2.00 2.00 1.99 1.99 1.98 1.98 1.97 1.97 1.96 1.96 1.95 1.94 1.94 1.93 1.93 1.92 1.91
Br
O
Br
H2O
1.86 1.92 1.95 1.99
1.95
1.98
2.00
10.0 9.5 9.0 8.5 8.0 7.5 7.0 6.5 6.0 5.5 5.0 4.5 4.0 3.5 3.0 2.5 2.0 1.5 1.0 0.5 0.0
chemical shift (ppm)

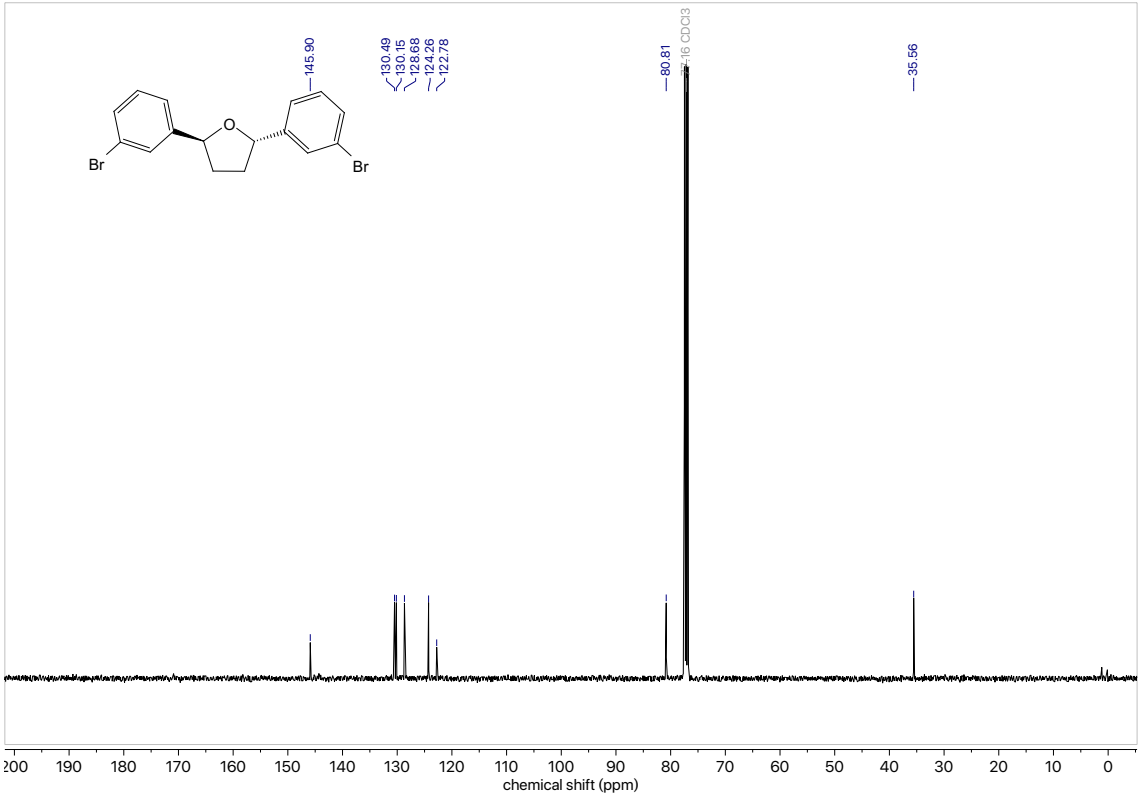
145.90
130.49
130.15
128.68
124.26
122.78
80.81
77.16 CDCl3
35.56
Br
Br
O
chemical shift (ppm)

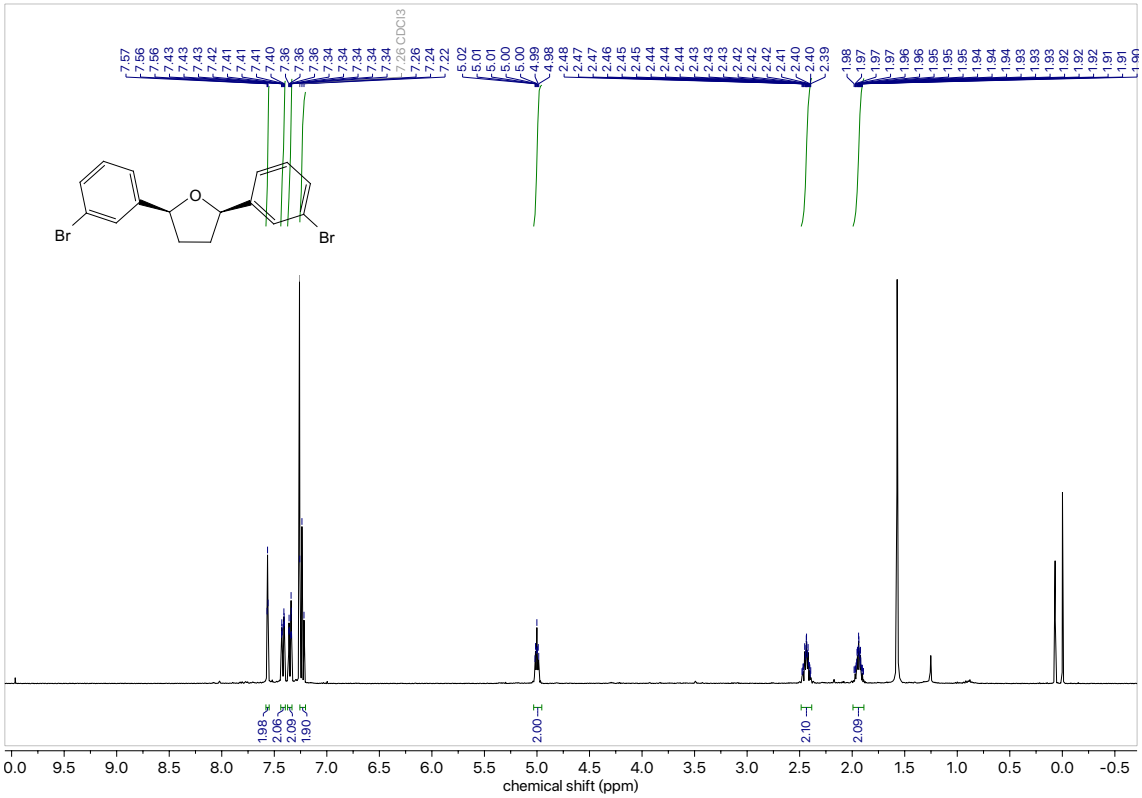
7.26 CDCl3
Br
Br
O
1.98
2.06
2.09
1.90
2.00
2.10
2.09
chemical shift (ppm)

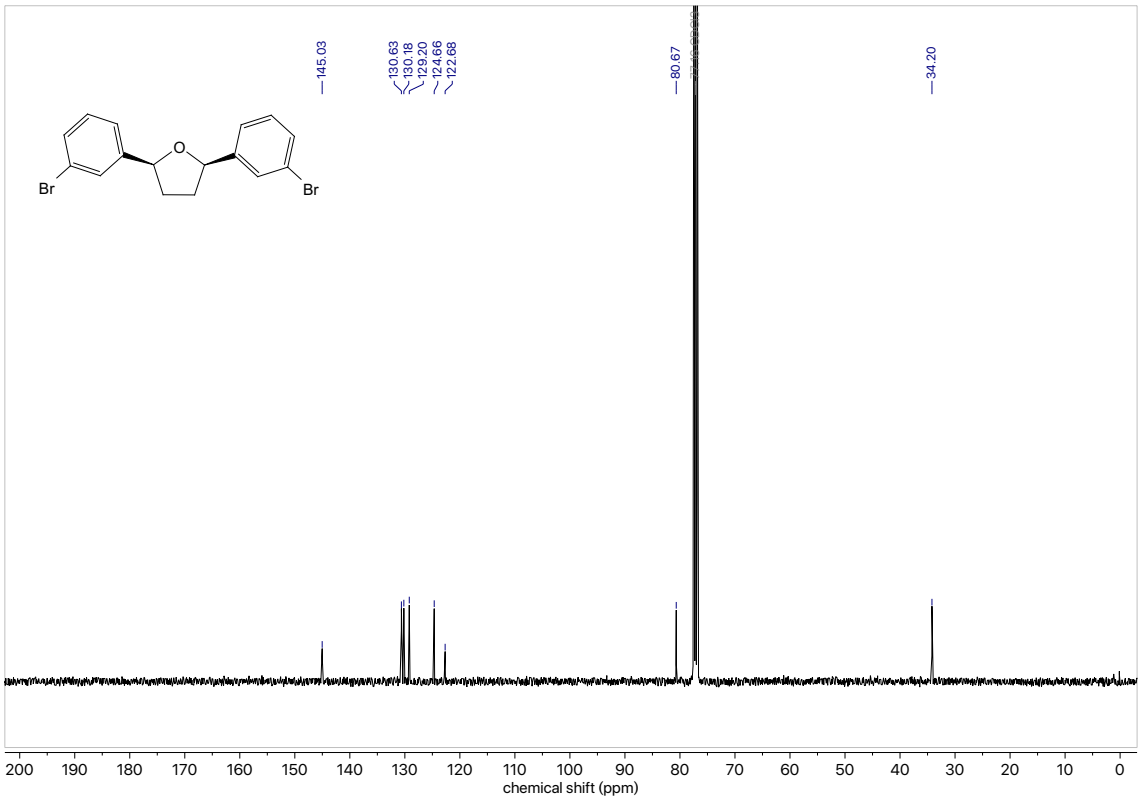
145.03
130.63
130.18
129.20
124.66
122.68
80.67
34.20
Br
Br
O
200 190 180 170 160 150 140 130 120 110 100 90 80 70 60 50 40 30 20 10 0
chemical shift (ppm)

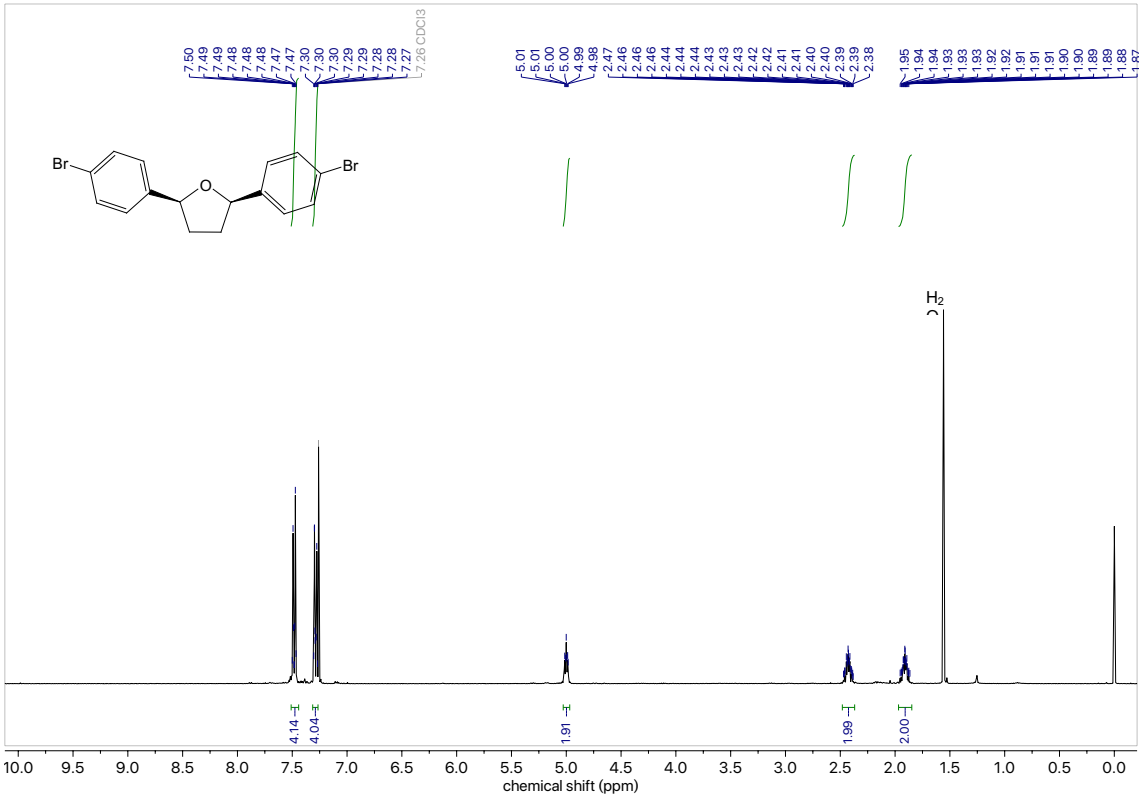
7.50 7.49 7.49 7.48 7.48 7.48 7.47 7.47 7.30 7.30 7.30 7.29 7.29 7.28 7.28 7.27 7.26 CDCl3
5.01 5.01 5.00 5.00 4.99 4.98 2.47 2.46 2.46 2.46 2.44 2.44 2.44 2.43 2.43 2.43 2.42 2.42 2.41 2.41 2.40 2.40 2.39 2.39 2.38
1.95 1.94 1.94 1.93 1.93 1.93 1.92 1.92 1.91 1.91 1.91 1.90 1.90 1.89 1.89 1.88 1.87
Br
Br
O
H2O
4.14
4.04
1.91
1.99
2.00
10.0 9.5 9.0 8.5 8.0 7.5 7.0 6.5 6.0 5.5 5.0 4.5 4.0 3.5 3.0 2.5 2.0 1.5 1.0 0.5 0.0
chemical shift (ppm)

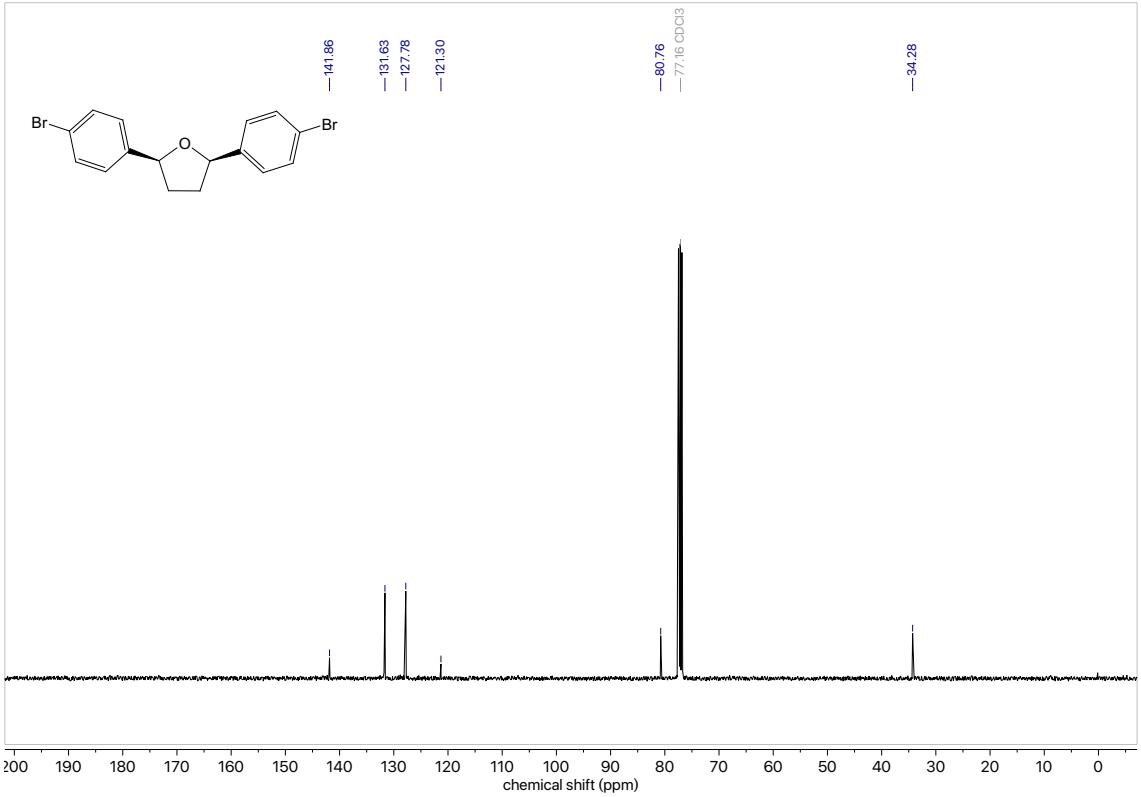
141.86
131.63
127.78
121.30
80.76
77.16 CDCl3
34.28
Br
Br
O
chemical shift (ppm)

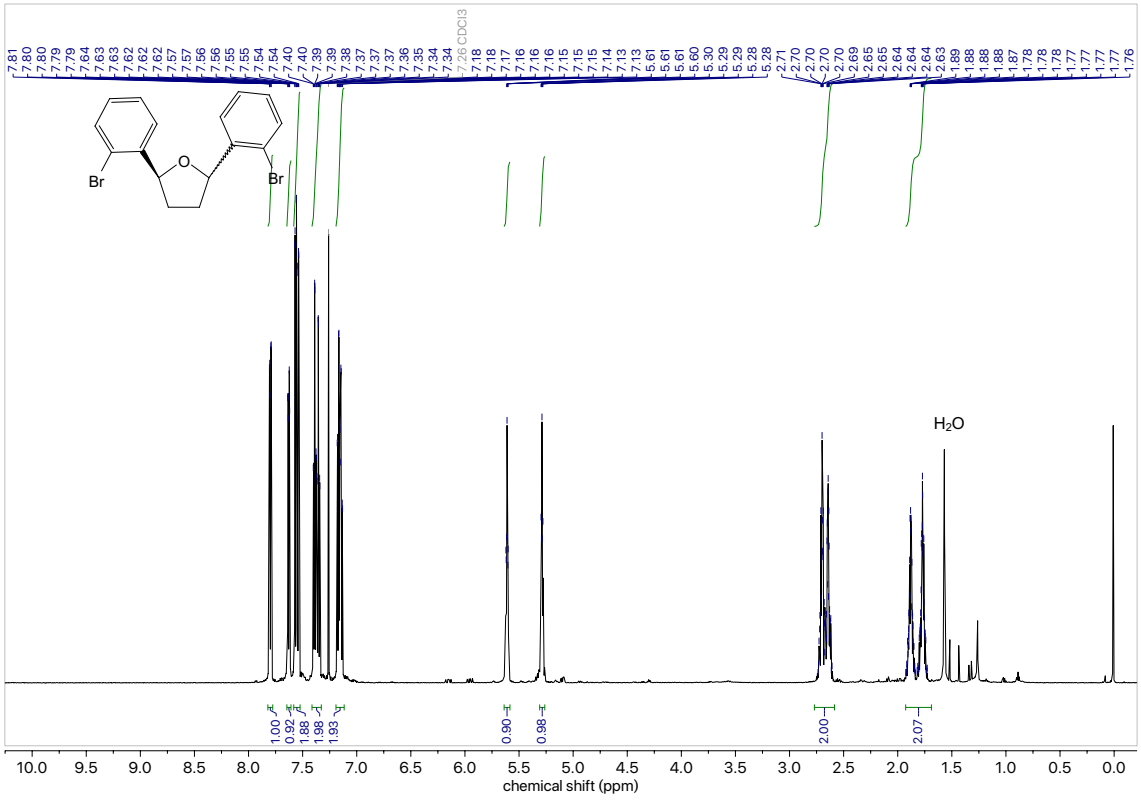
7.26 CDCl3
H2O
Br
Br
O
chemical shift (ppm)

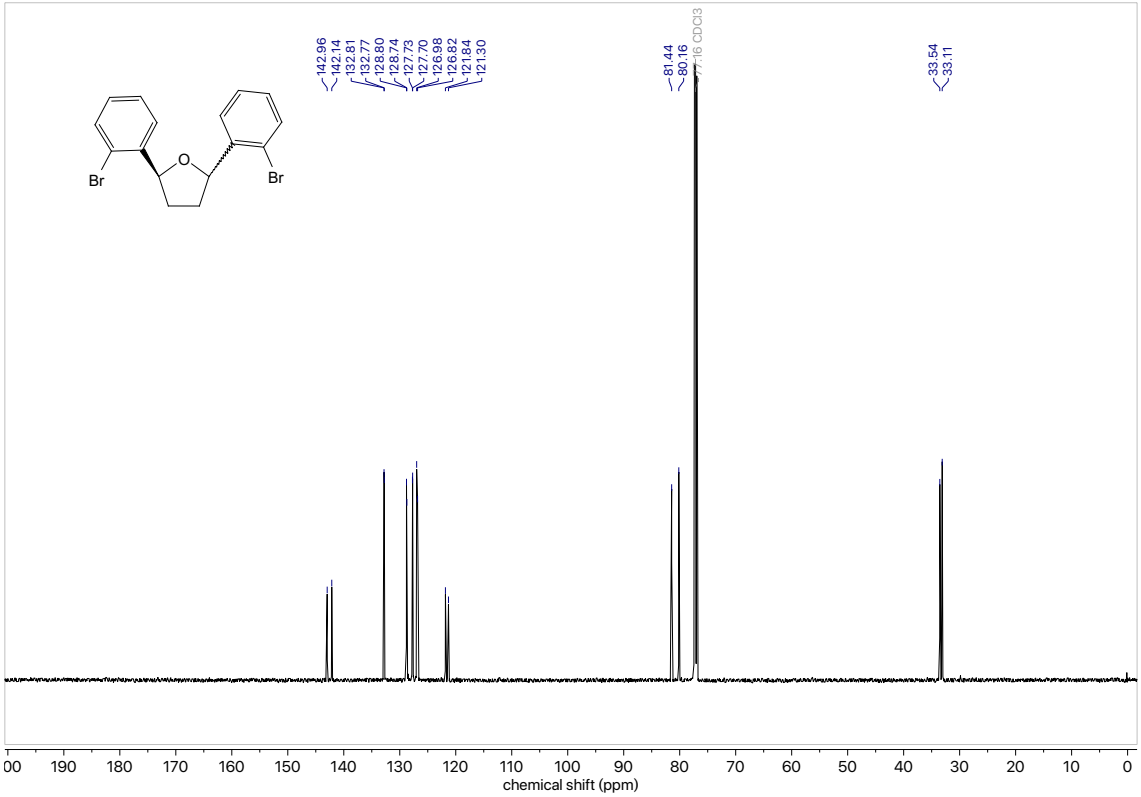
142.96
142.14
132.81
132.77
128.80
128.74
127.73
127.70
126.98
126.82
121.84
121.30
81.44
80.16
77.16 CDCl3
33.54
33.11
Br
Br
O
chemical shift (ppm)

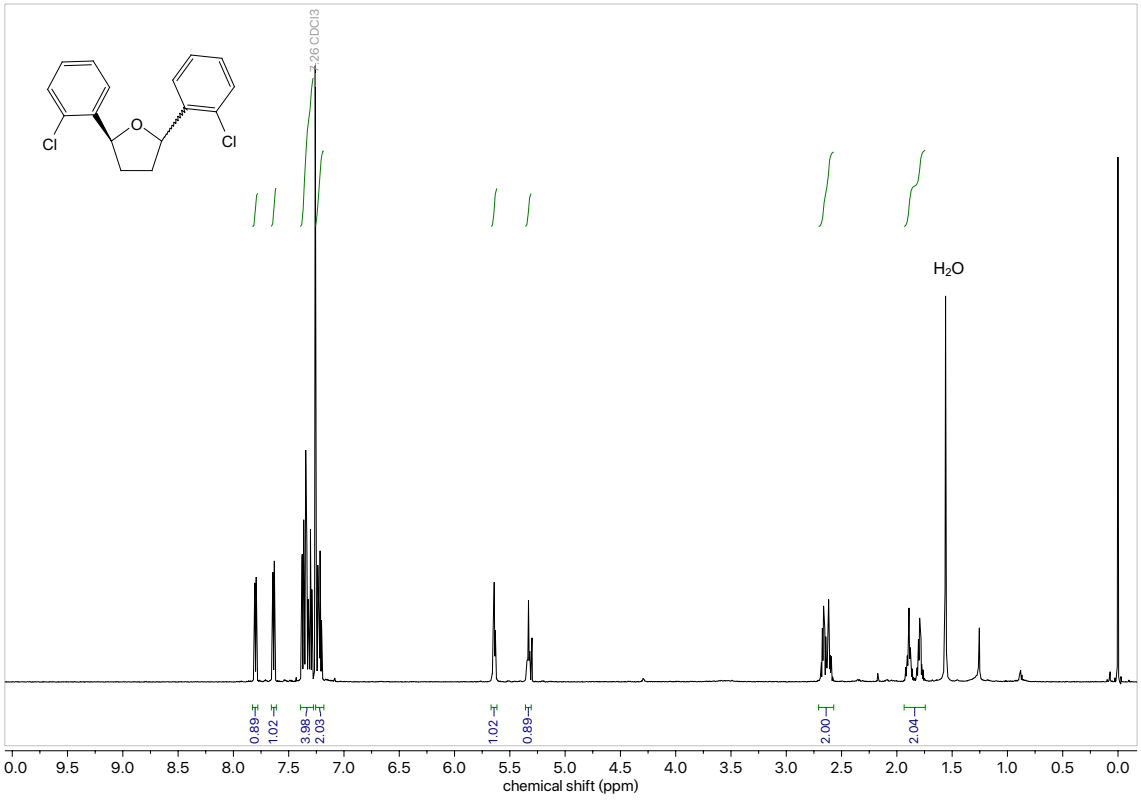
7.26 CDCl3
Cl
Cl
O
H2O
0.89
1.02
3.98
2.03
1.02
0.89
2.00
2.04
chemical shift (ppm)

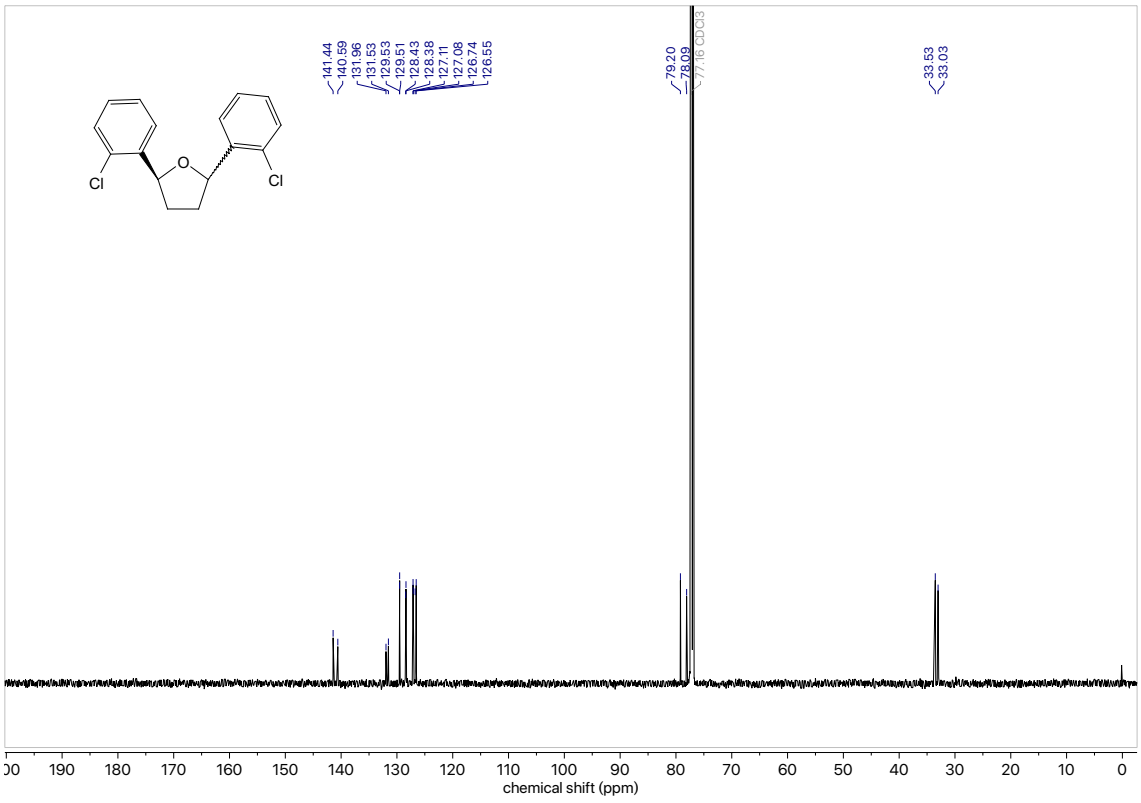
141.44
140.59
131.96
131.53
129.53
129.51
128.43
128.38
127.11
127.08
126.74
126.55
79.20
78.09
77.16 CDCl3
33.53
33.03
Cl
Cl
O
chemical shift (ppm)

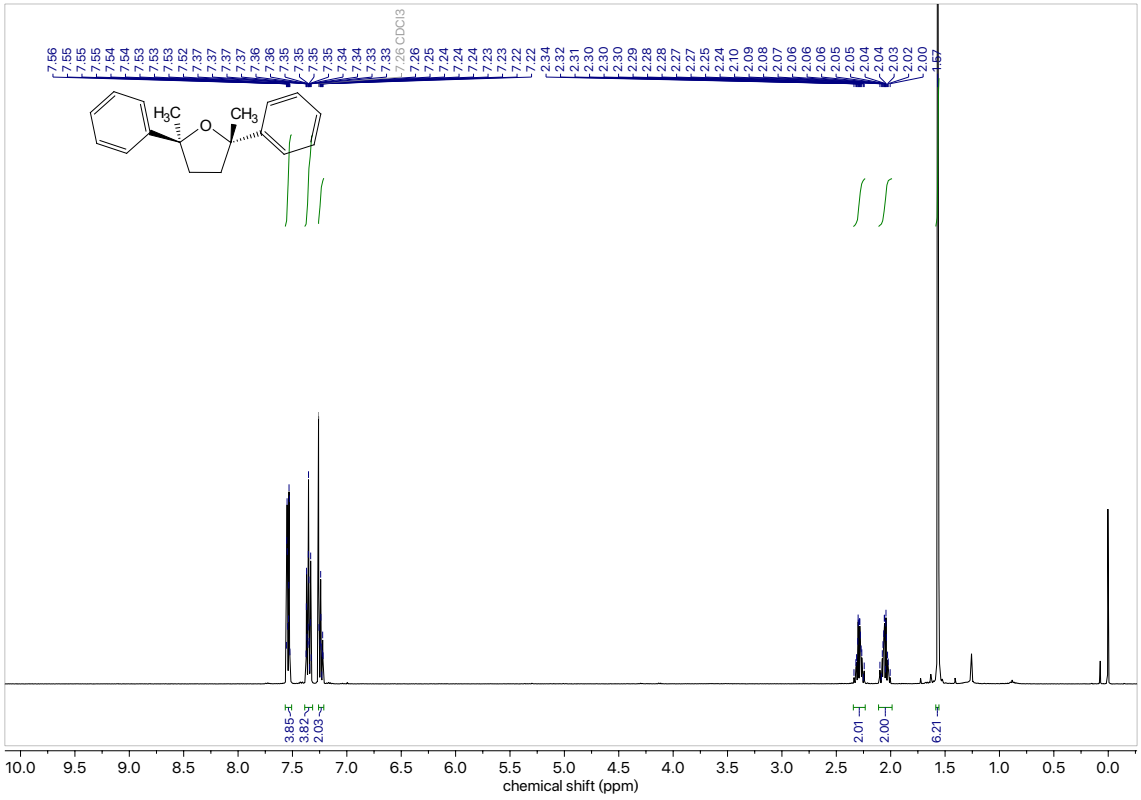
7.26 CDCl3
H3C
CH3
O
3.85
3.82
2.03
2.01
2.00
6.21
chemical shift (ppm)

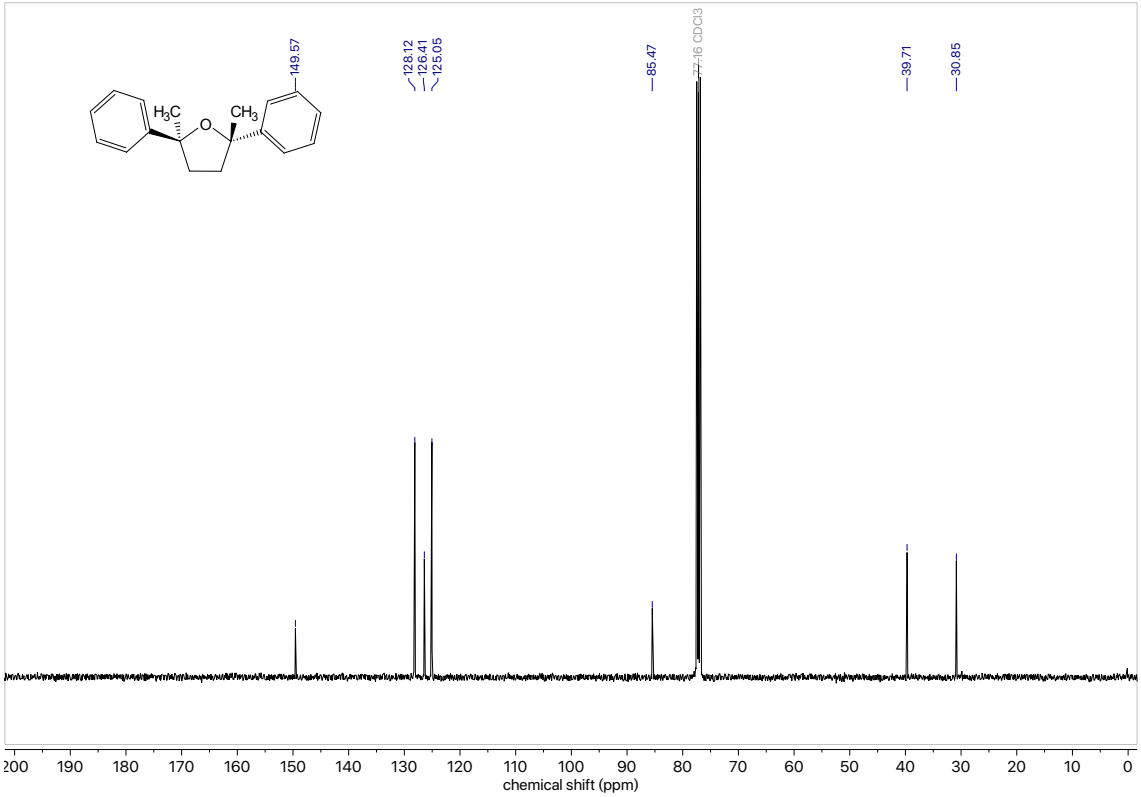
149.57
128.12
126.41
125.05
85.47
77.16 CDCl3
39.71
30.85
H3C
CH3
O
chemical shift (ppm)

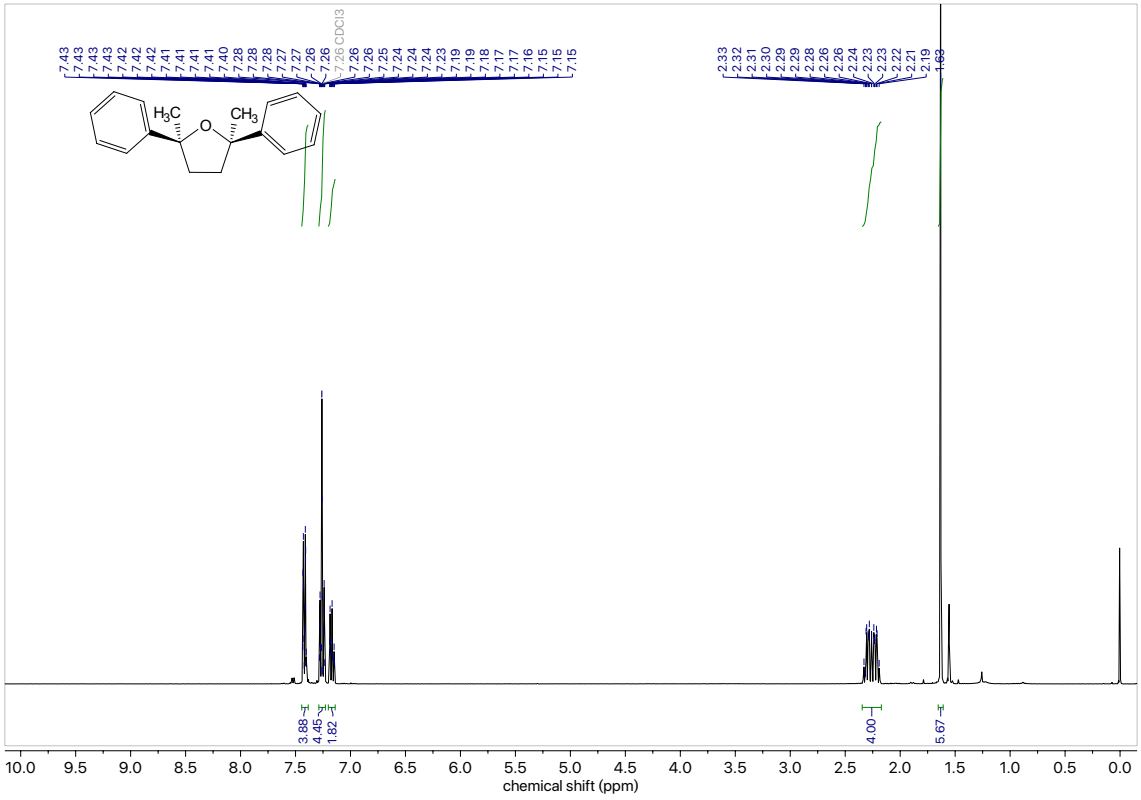
7.43
7.42
7.41
7.40
7.28
7.27
7.26
7.25
7.24
7.23
7.19
7.18
7.17
7.16
7.15
2.33
2.32
2.31
2.30
2.29
2.28
2.26
2.24
2.23
2.22
2.21
2.19
1.83
3.88
4.45
1.82
4.00
5.67
H3C
CH3
O
chemical shift (ppm)

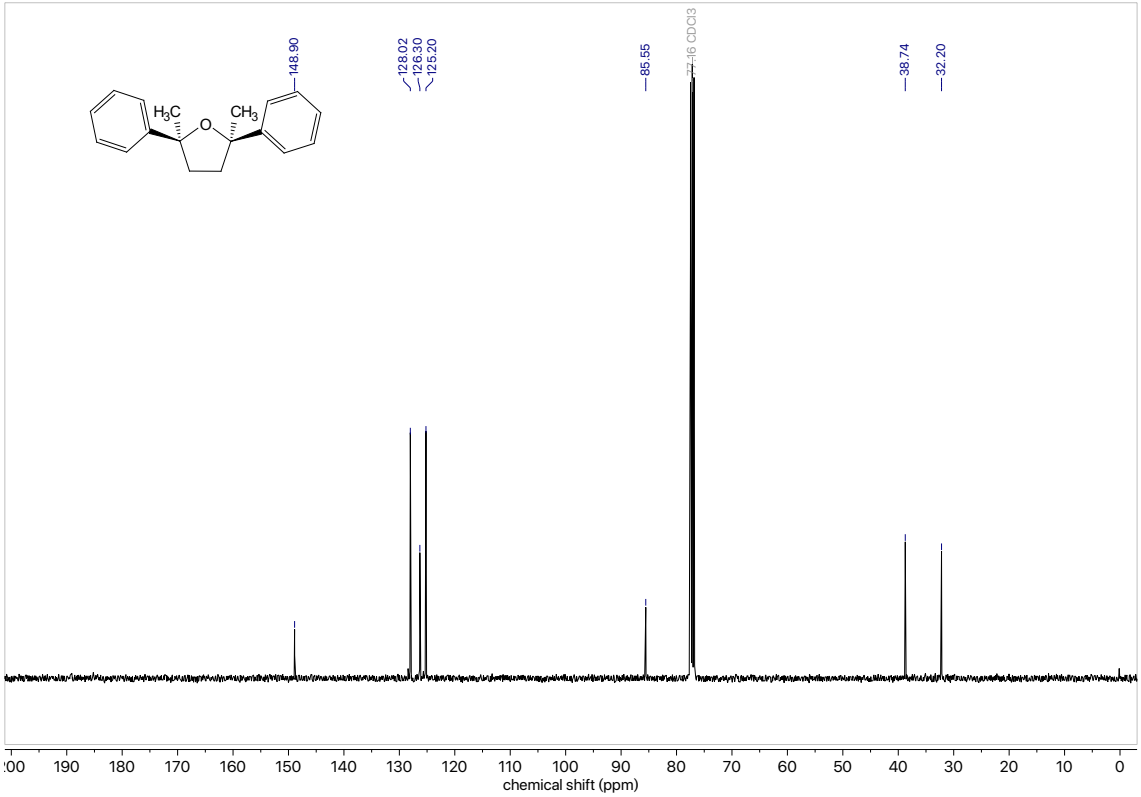
148.90
128.02
126.30
125.20
85.55
77.16 CDCl3
38.74
32.20
H3C
O
CH3
chemical shift (ppm)

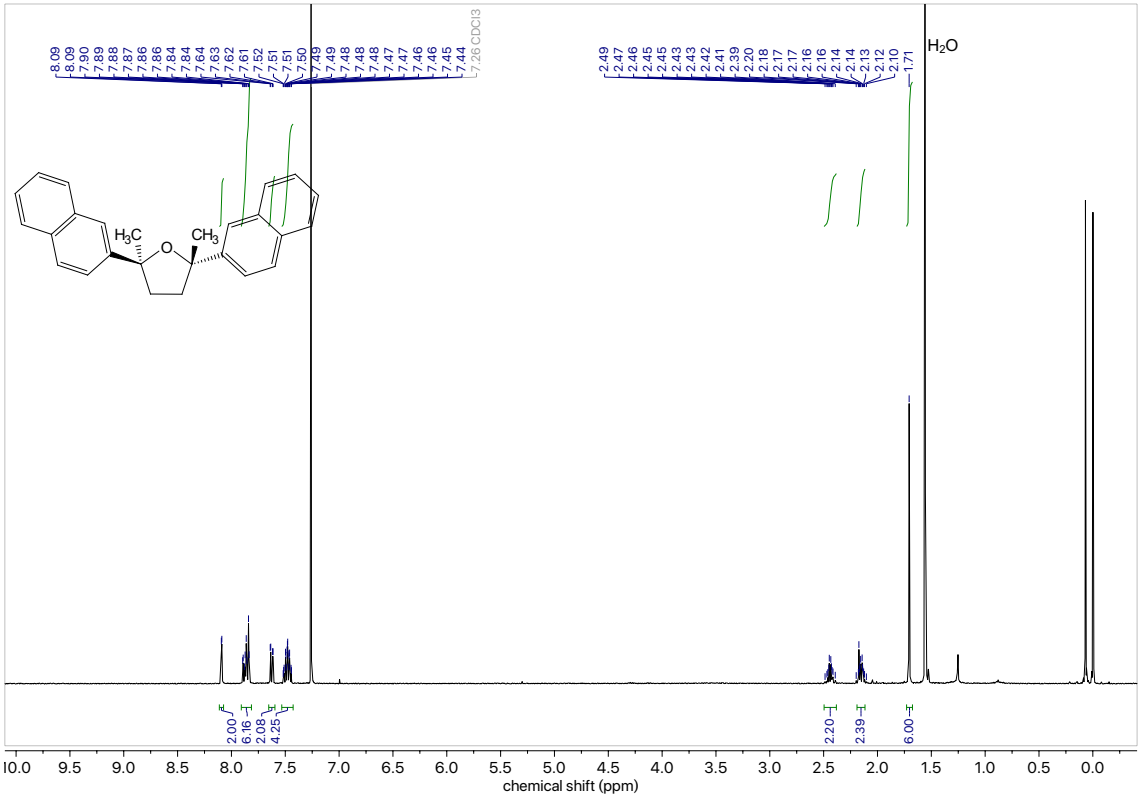
8.09
7.90
7.89
7.88
7.87
7.86
7.84
7.64
7.63
7.62
7.61
7.52
7.51
7.50
7.49
7.48
7.47
7.46
7.45
7.44
7.26 CDCl3
2.49
2.47
2.46
2.45
2.43
2.42
2.41
2.39
2.20
2.18
2.17
2.16
2.14
2.13
2.12
2.10
1.71
H2O
H3C
O
CH3
2.00
6.16
2.08
4.25
2.20
2.39
6.00
chemical shift (ppm)

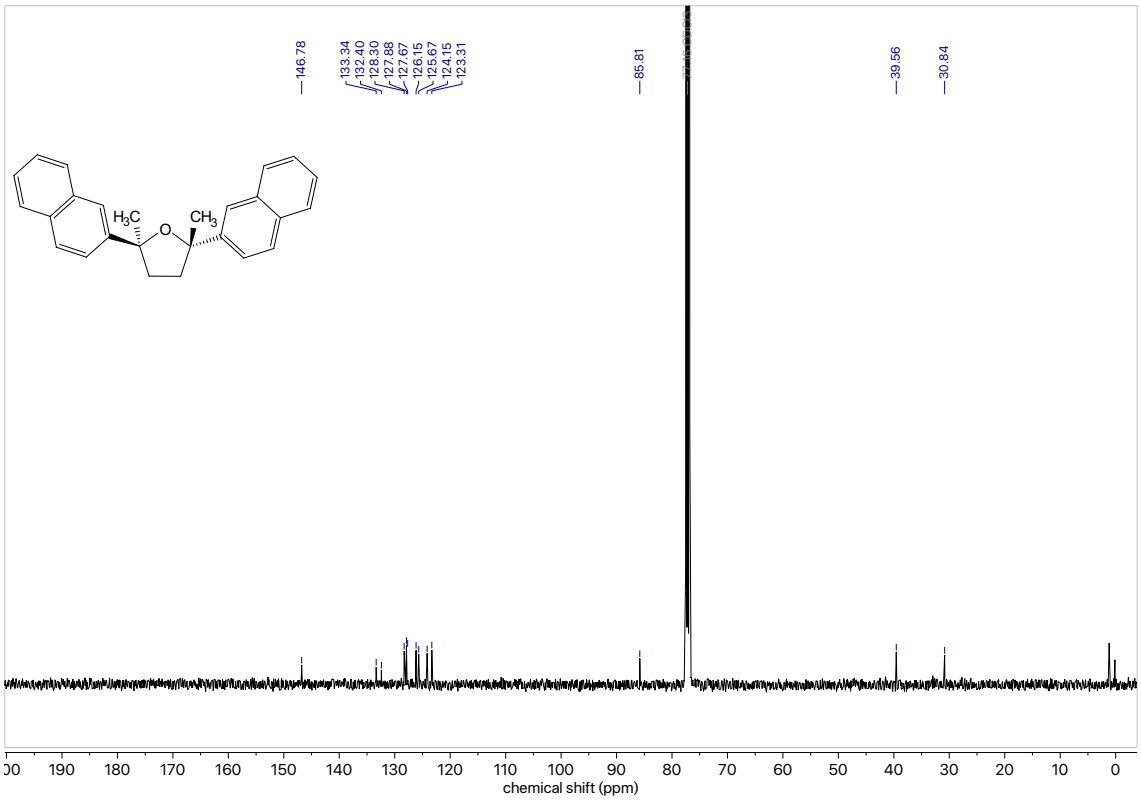
146.78
133.34
132.40
128.30
127.88
127.67
126.15
125.67
124.15
123.31
85.81
39.56
30.84
H3C
O
CH3
chemical shift (ppm)

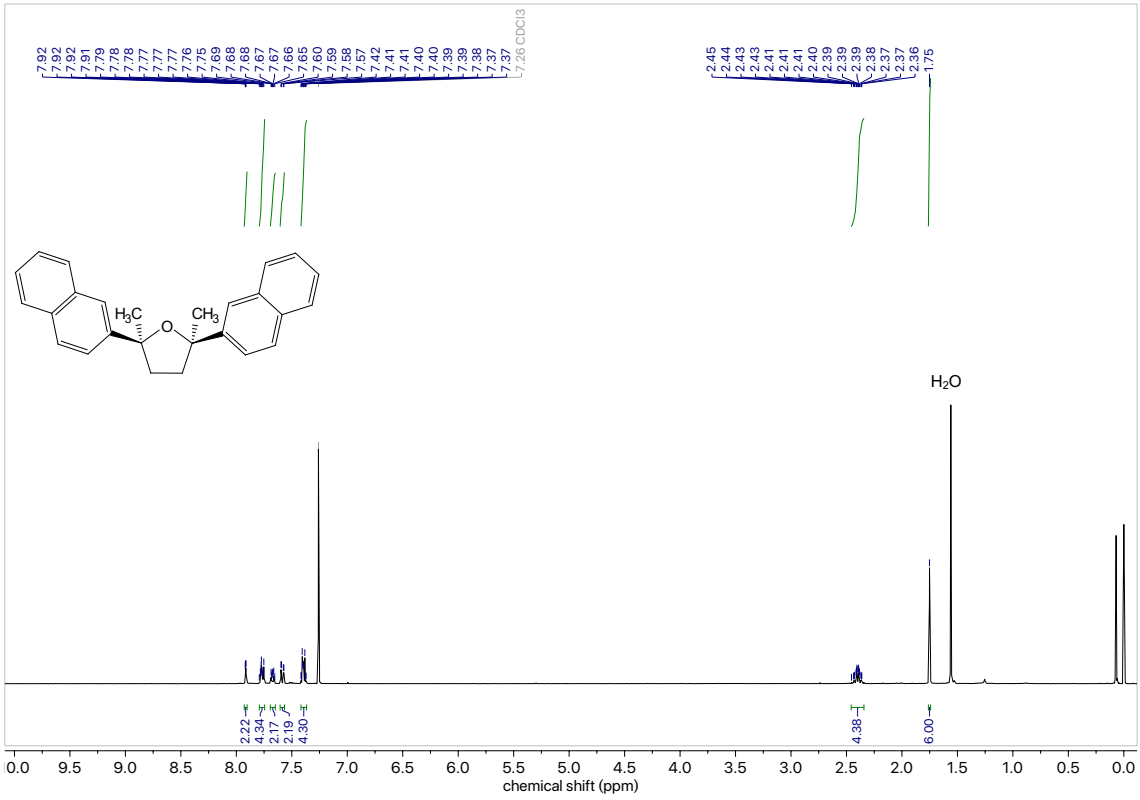
7.92
7.92
7.92
7.91
7.79
7.78
7.78
7.77
7.77
7.77
7.76
7.75
7.69
7.68
7.68
7.67
7.67
7.66
7.65
7.60
7.59
7.58
7.57
7.42
7.41
7.41
7.40
7.40
7.39
7.39
7.38
7.37
7.37
7.26 CDCl3
2.45
2.44
2.43
2.43
2.41
2.41
2.41
2.40
2.39
2.39
2.39
2.38
2.37
2.37
2.36
1.75
H3C
O
CH3
H2O
2.22
4.34
2.17
2.19
4.30
4.38
6.00
chemical shift (ppm)

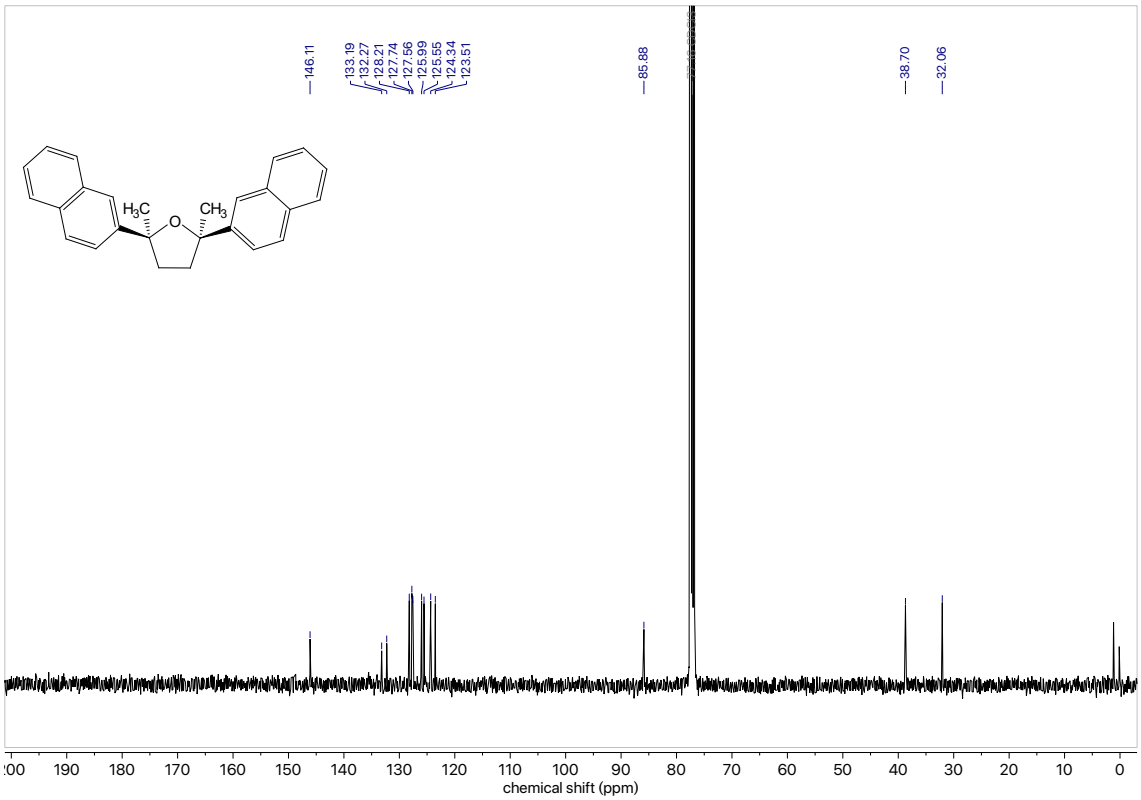
146.11
133.19
132.27
128.21
127.74
127.66
125.99
125.55
124.34
123.51
85.88
38.70
32.06
H3C
CH3
O
chemical shift (ppm)

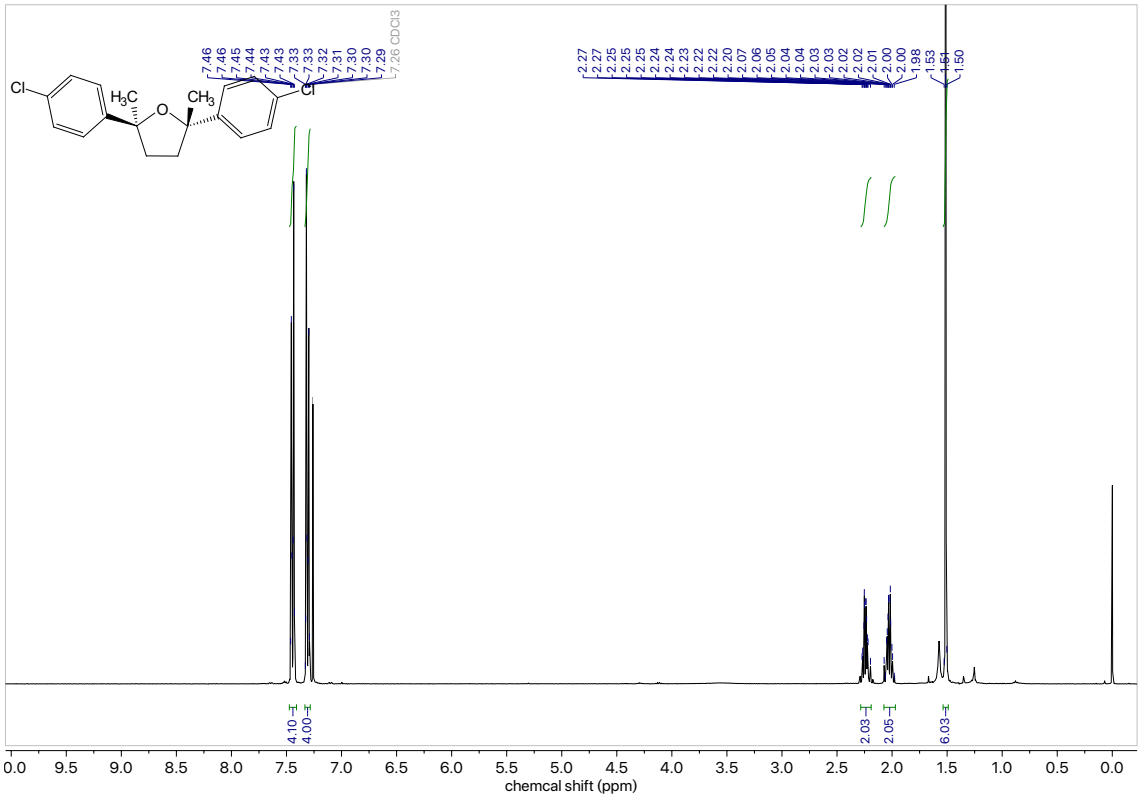
7.46
7.46
7.45
7.44
7.43
7.43
7.33
7.33
7.32
7.31
7.30
7.30
7.29
7.26 CDCl3
2.27
2.27
2.25
2.25
2.25
2.24
2.24
2.23
2.22
2.22
2.20
2.07
2.06
2.05
2.04
2.04
2.03
2.03
2.02
2.02
2.01
2.00
2.00
1.98
1.53
1.51
1.50
Cl
H3C
CH3
O
Cl
4.10
4.00
2.03
2.05
6.03
chemcal shift (ppm)

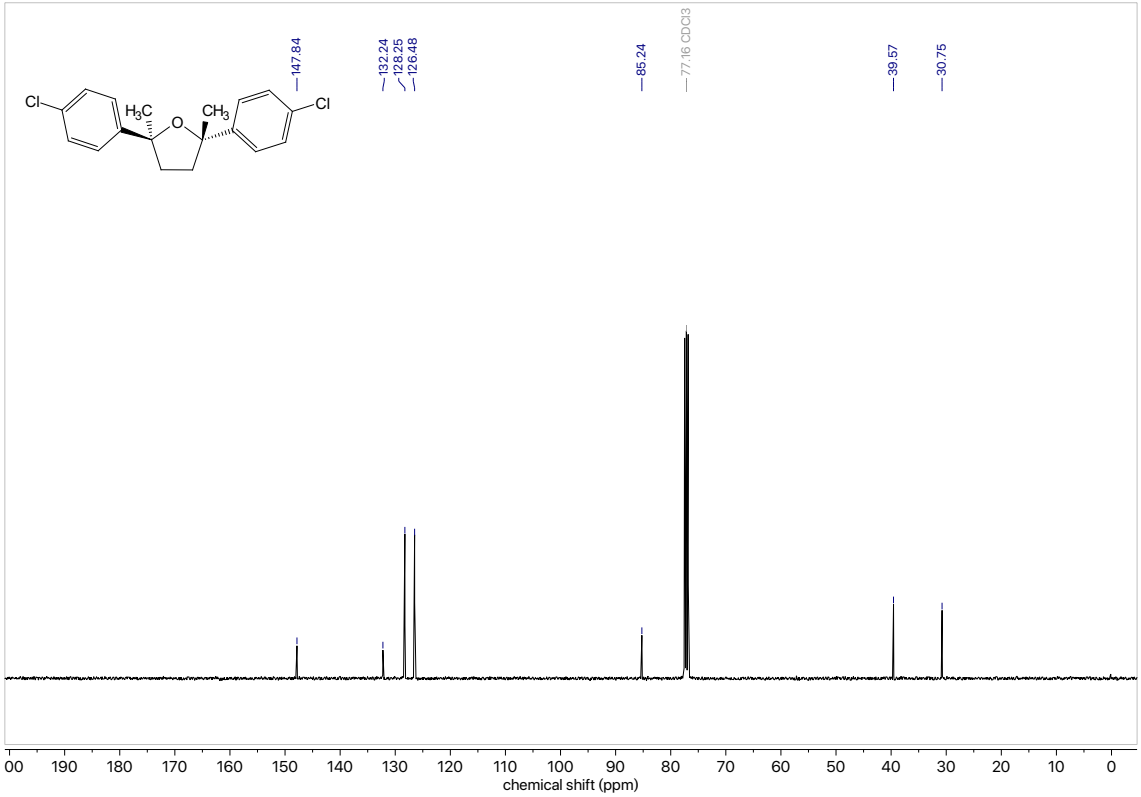
147.84
132.24
128.25
126.48
85.24
77.16 CDCl3
39.57
30.75
Cl
H3C
O
CH3
Cl
chemical shift (ppm)

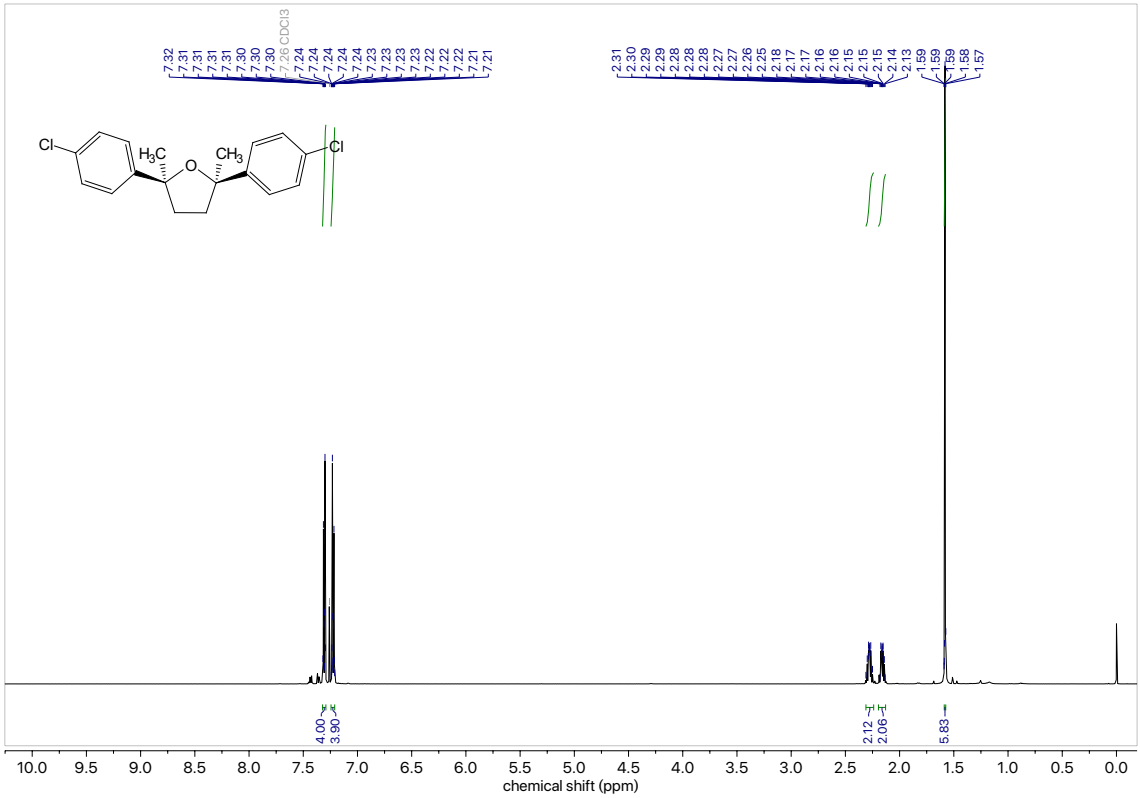
7.26 CDCl3
Cl
H3C
O
CH3
Cl
4.00
3.90
2.12
2.06
5.83
chemical shift (ppm)

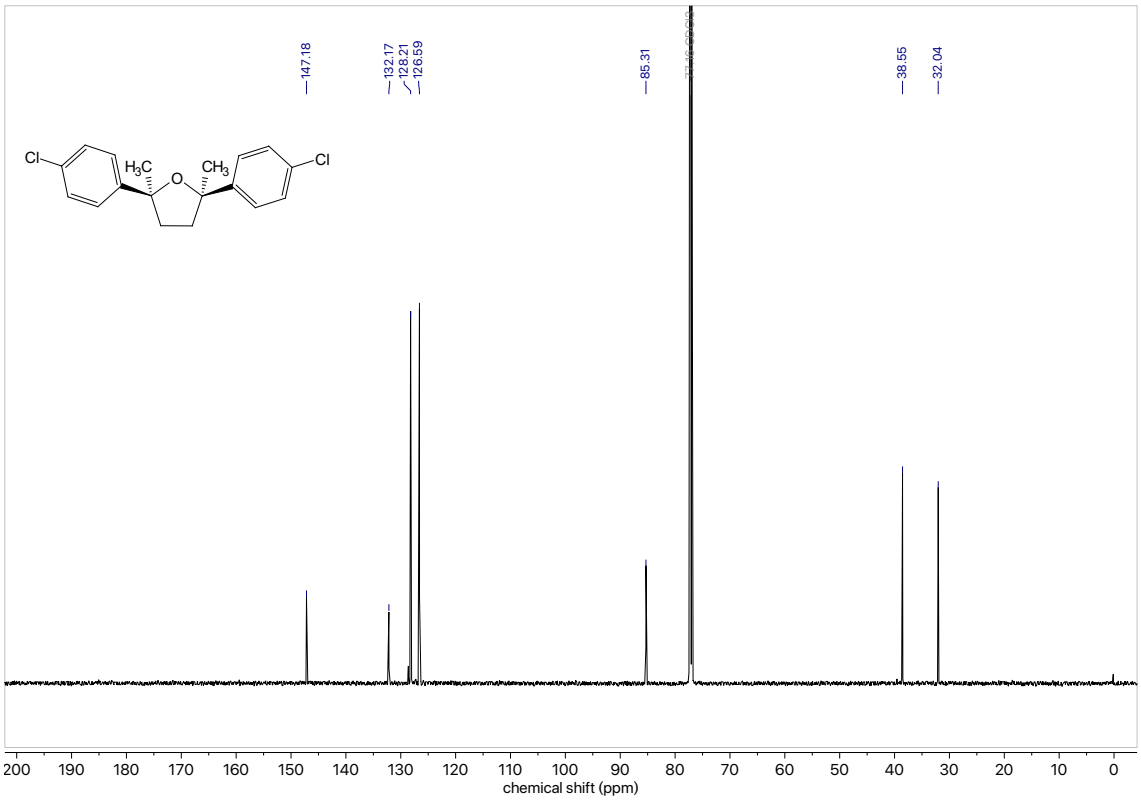
147.18
132.17
128.21
126.59
85.31
38.55
32.04
Cl
H3C
O
CH3
Cl
200 190 180 170 160 150 140 130 120 110 100 90 80 70 60 50 40 30 20 10 0
chemical shift (ppm)

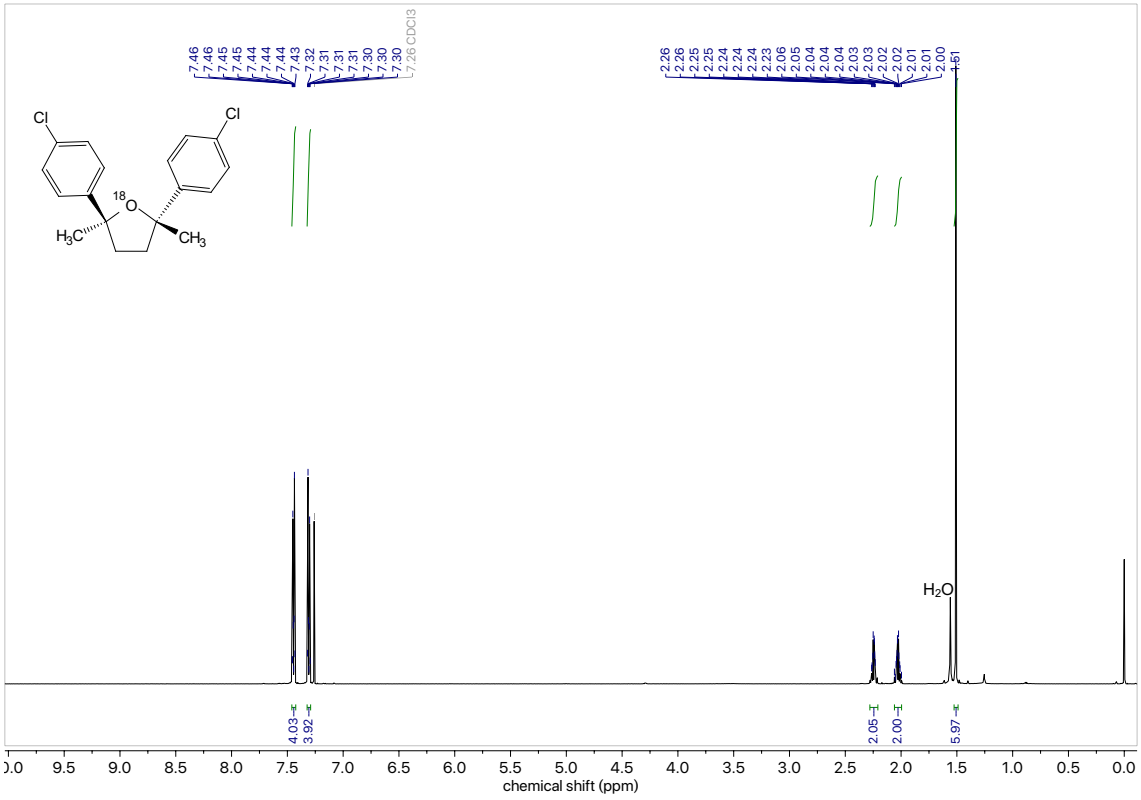
7.46
7.46
7.45
7.45
7.44
7.44
7.44
7.43
7.32
7.31
7.31
7.31
7.30
7.30
7.30
7.26 CDCl3
2.26
2.26
2.25
2.25
2.24
2.24
2.24
2.23
2.06
2.05
2.04
2.04
2.04
2.03
2.03
2.02
2.02
2.01
2.01
2.00
1.61
Cl
Cl
18
O
H3C
CH3
H2O
4.03
3.92
2.05
2.00
5.97
9.5 9.0 8.5 8.0 7.5 7.0 6.5 6.0 5.5 5.0 4.5 4.0 3.5 3.0 2.5 2.0 1.5 1.0 0.5 0.0
chemical shift (ppm)

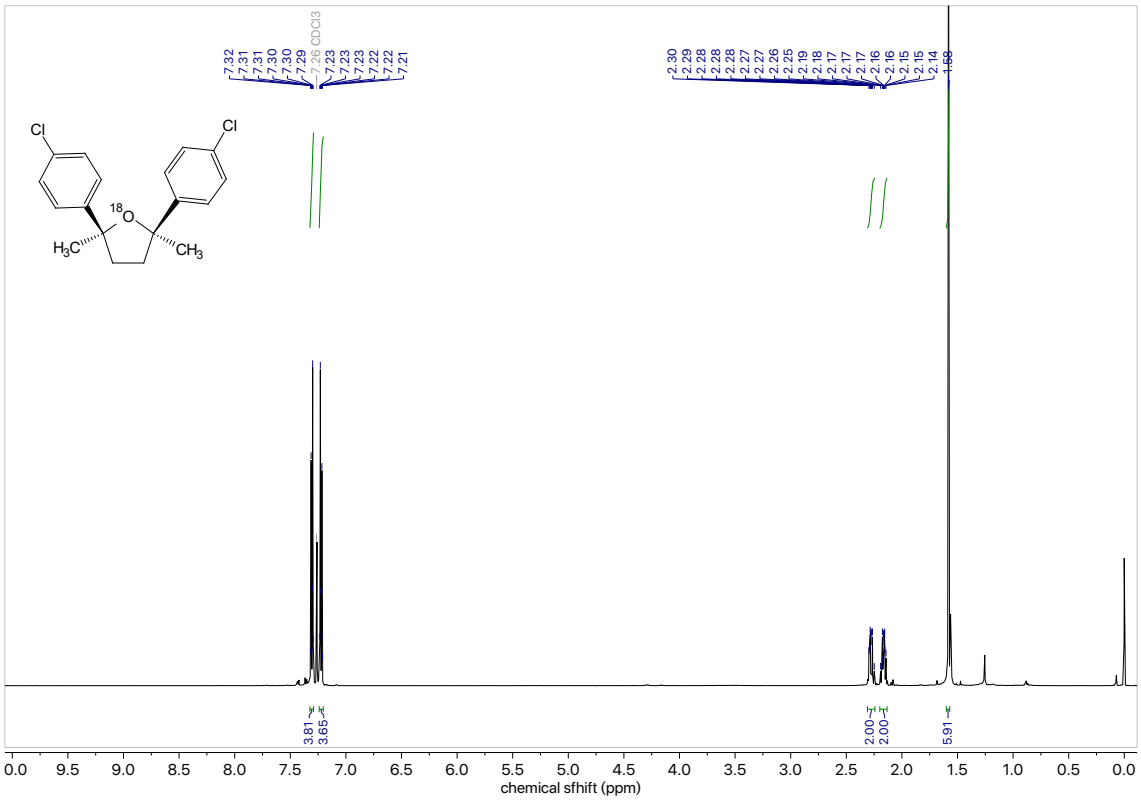
7.32
7.31
7.31
7.30
7.30
7.29
7.26 CDCl3
7.23
7.23
7.23
7.22
7.22
7.21
2.30
2.29
2.28
2.28
2.28
2.27
2.27
2.26
2.25
2.19
2.18
2.17
2.17
2.16
2.16
2.15
2.15
2.14
1.58
Cl
Cl
18O
H3C
CH3
3.81
3.65
2.00
2.00
5.91
chemical sfhift (ppm)

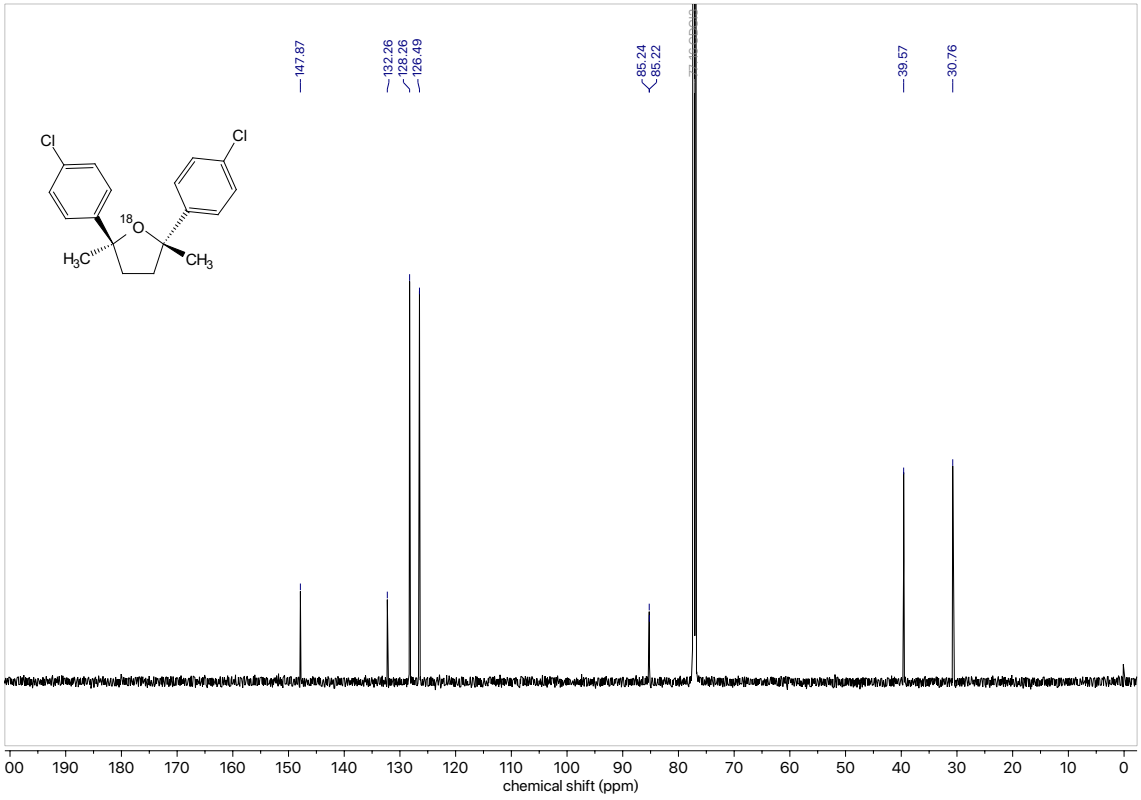
147.87
132.26
128.26
126.49
85.24
85.22
39.57
30.76
Cl
Cl
18O
H3C
CH3
chemical shift (ppm)

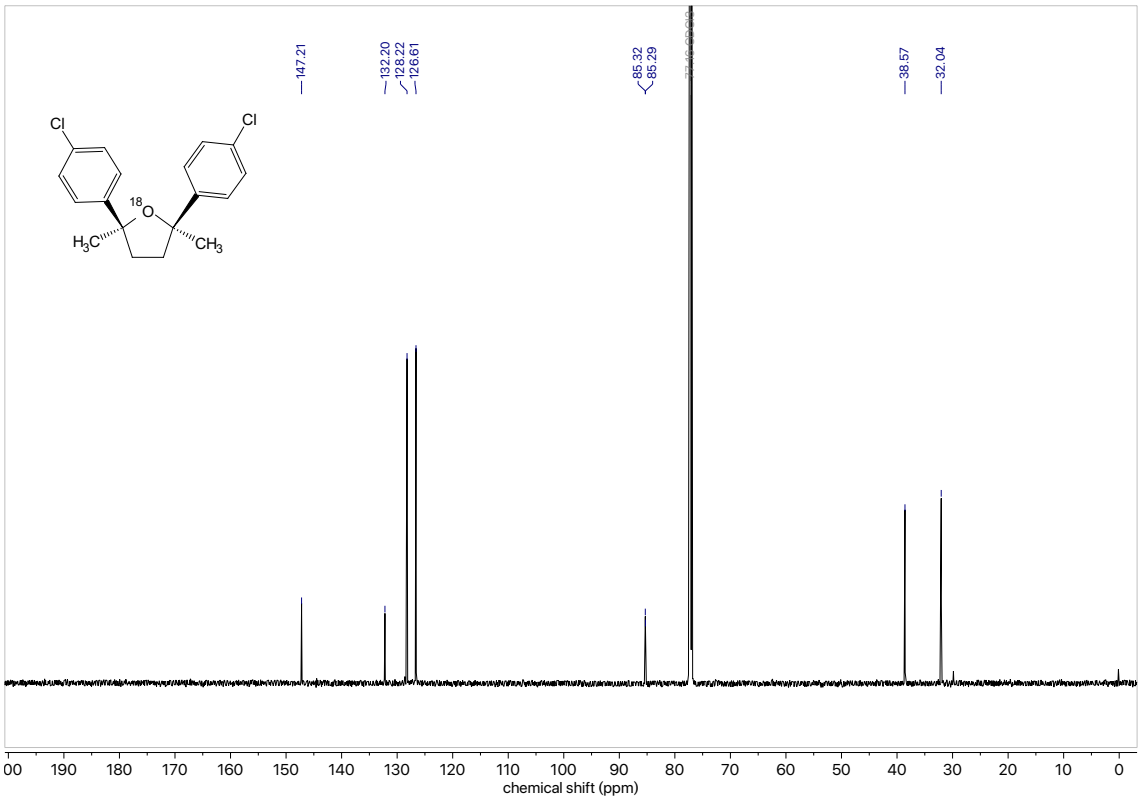
147.21
132.20
128.22
126.61
85.32
85.29
38.57
32.04
Cl
Cl
18
O
H3C
CH3
chemical shift (ppm)

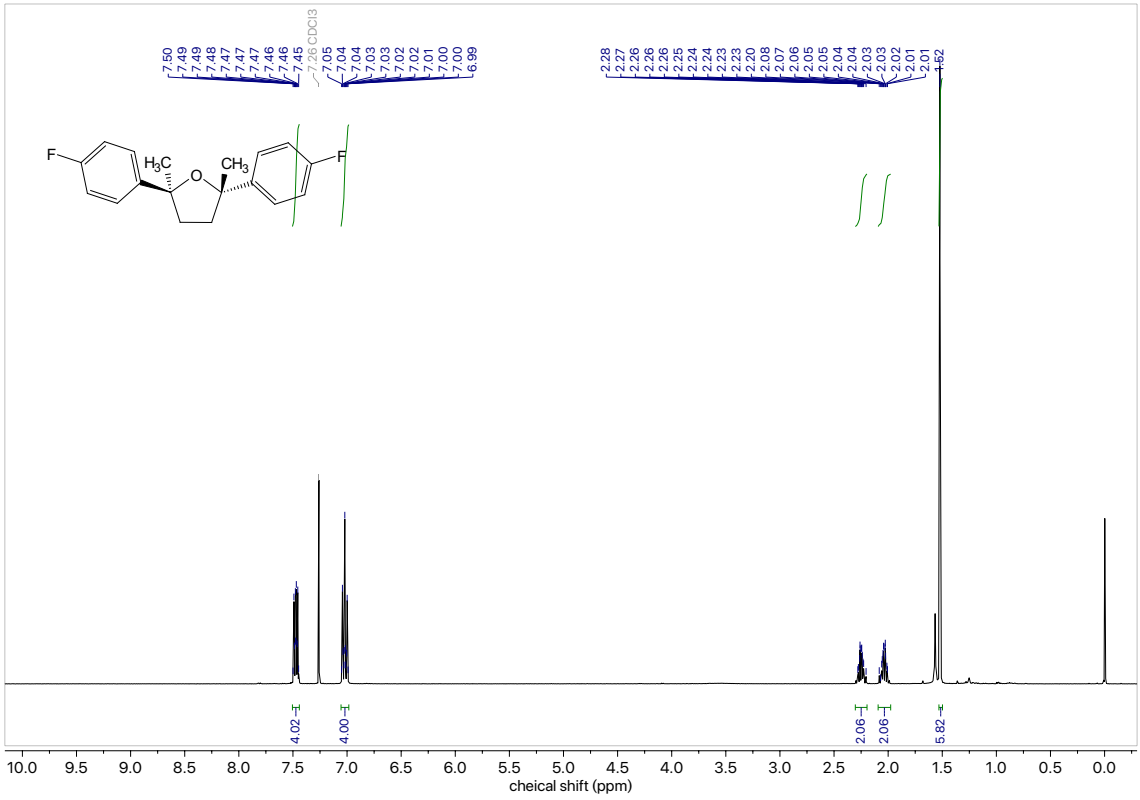
7.50
7.49
7.49
7.48
7.47
7.47
7.47
7.46
7.46
7.45
7.26 CDCl3
7.05
7.04
7.04
7.03
7.03
7.02
7.02
7.01
7.00
7.00
6.99
2.28
2.27
2.26
2.26
2.26
2.25
2.24
2.24
2.23
2.23
2.20
2.08
2.07
2.06
2.05
2.05
2.04
2.04
2.03
2.03
2.02
2.01
2.01
1.52
F
H3C
O
CH3
F
4.02
4.00
2.06
2.06
5.82
cheical shift (ppm)

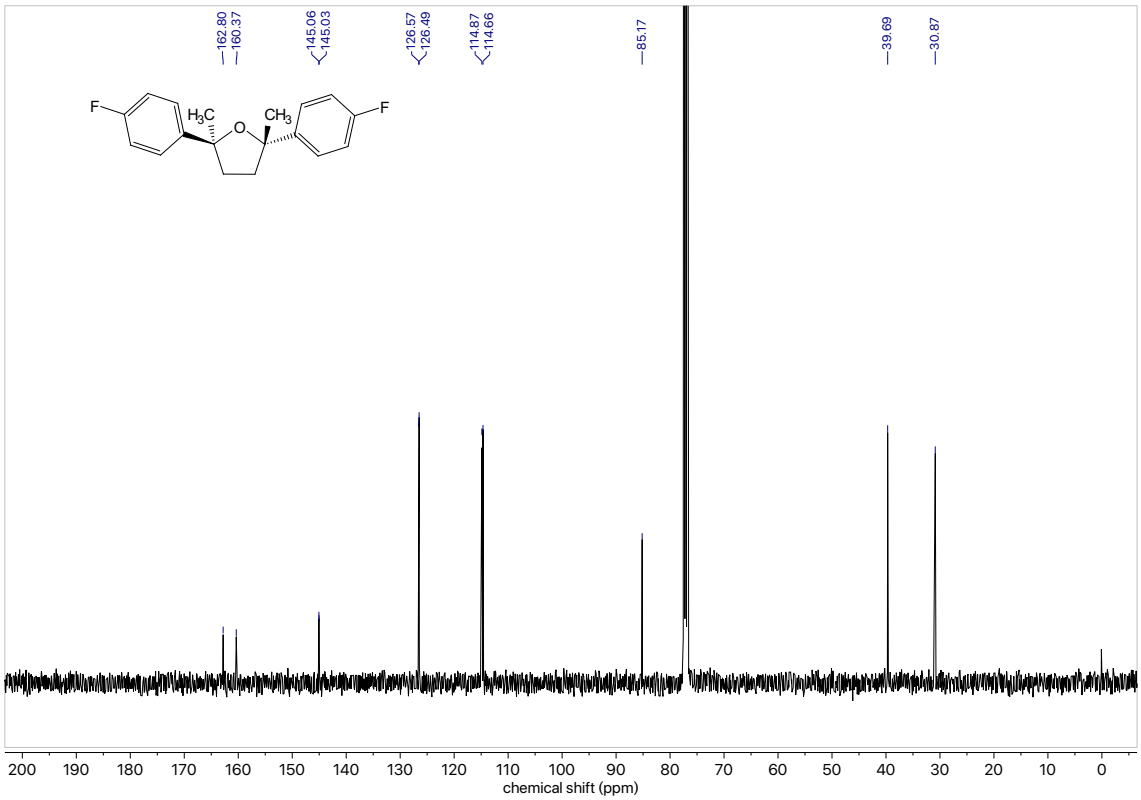
162.80
160.37
145.06
145.03
126.57
126.49
114.87
114.66
85.17
39.69
30.87
F
H3C
O
CH3
F
200 190 180 170 160 150 140 130 120 110 100 90 80 70 60 50 40 30 20 10 0
chemical shift (ppm)

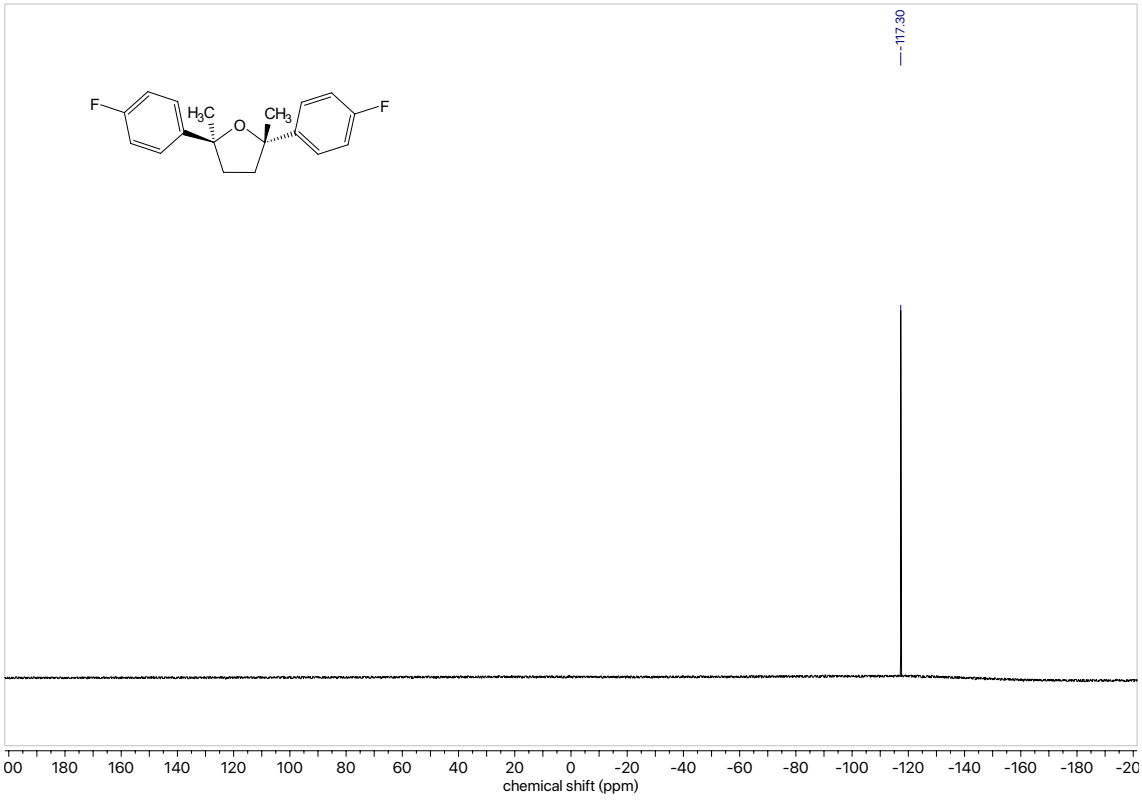
-117.30
F
H3C
O
CH3
F
00 180 160 140 120 100 80 60 40 20 0 -20 -40 -60 -80 -100 -120 -140 -160 -180 -20
chemical shift (ppm)

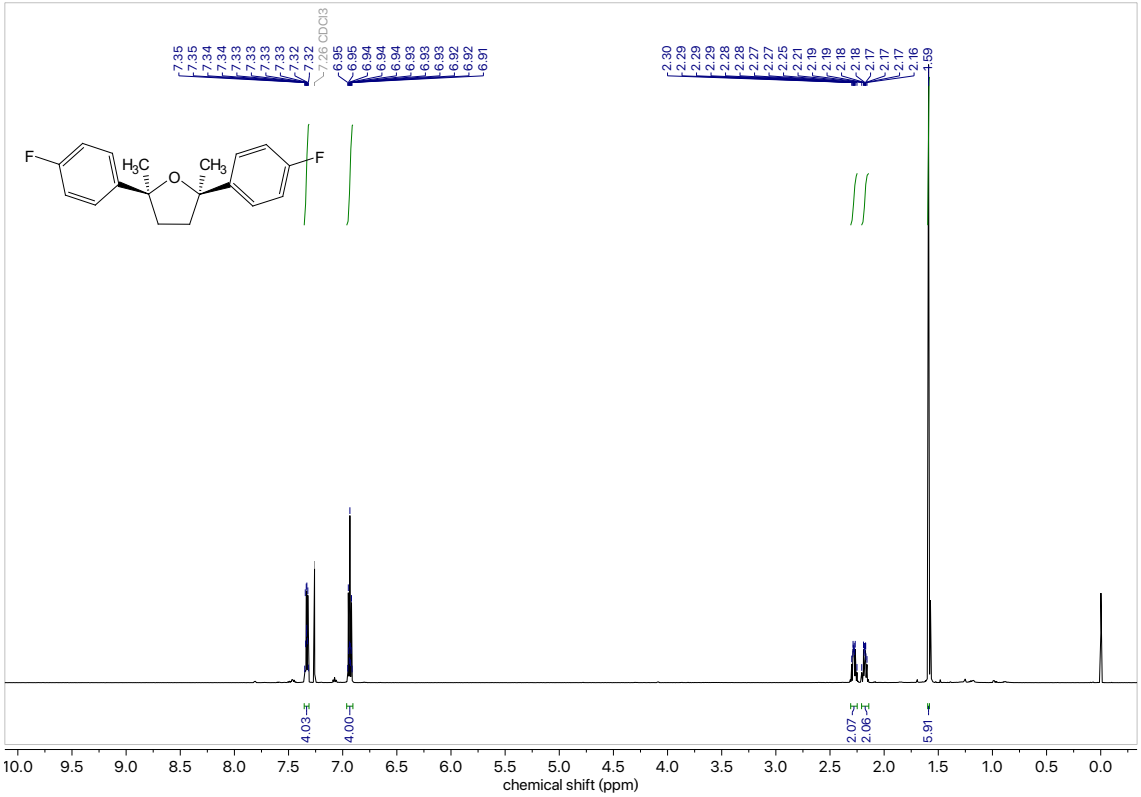
7.35
7.35
7.34
7.34
7.33
7.33
7.33
7.33
7.32
7.32
7.26 CDCl3
6.95
6.95
6.94
6.94
6.94
6.93
6.93
6.92
6.92
6.91
2.30
2.29
2.29
2.29
2.28
2.28
2.27
2.27
2.25
2.21
2.19
2.19
2.18
2.18
2.17
2.17
2.17
2.16
1.59
F
H3C
O
CH3
F
4.03
4.00
2.07
2.06
5.91
10.0 9.5 9.0 8.5 8.0 7.5 7.0 6.5 6.0 5.5 5.0 4.5 4.0 3.5 3.0 2.5 2.0 1.5 1.0 0.5 0.0
chemical shift (ppm)

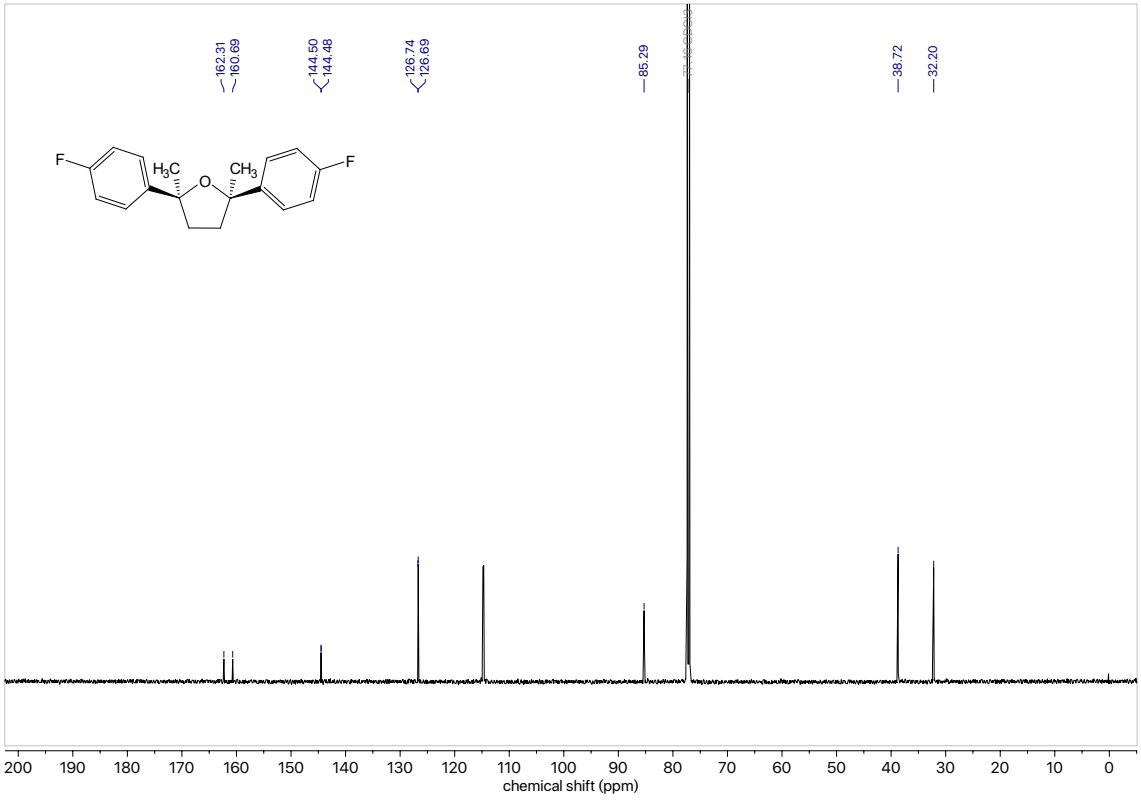
162.31
160.69
144.50
144.48
126.74
126.69
85.29
77.16 CDCl3
38.72
32.20
F
H3C
O
CH3
F
200 190 180 170 160 150 140 130 120 110 100 90 80 70 60 50 40 30 20 10 0
chemical shift (ppm)

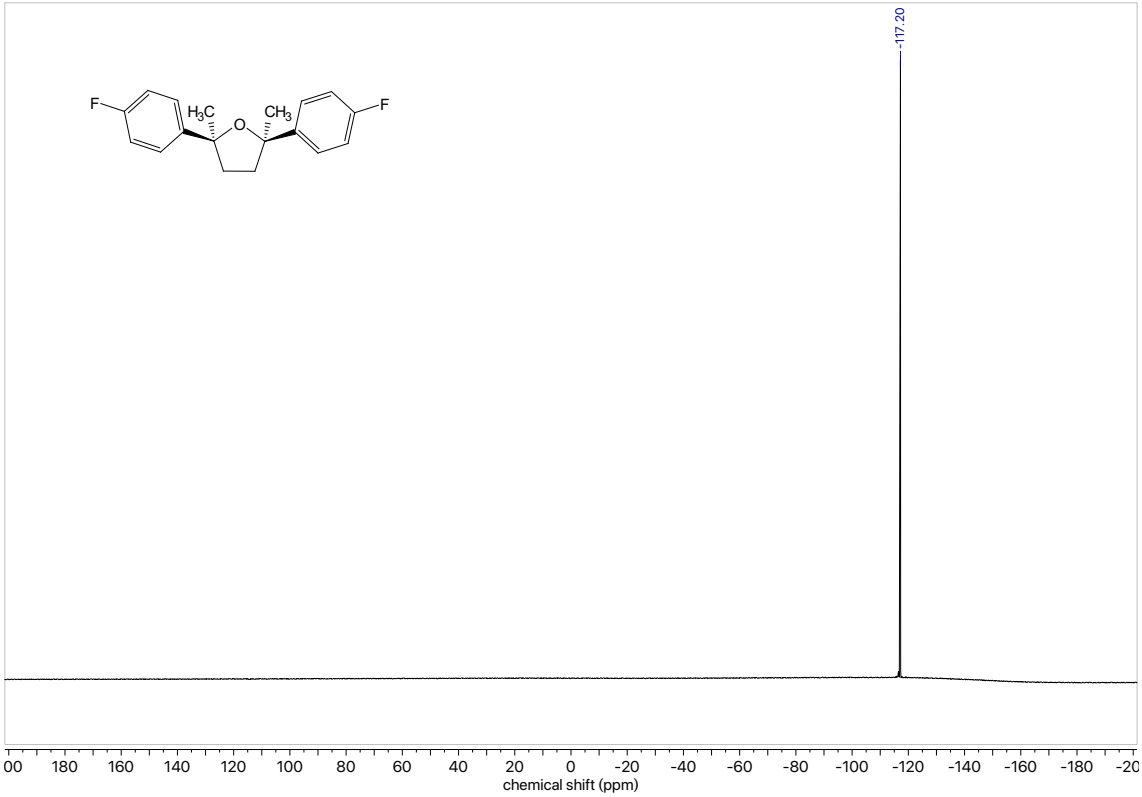

8. Publications

1) N. Shida,* Y. Imada,* Y. Okada, K. Chiba, “Mechanistic Insights on Concentrated Lithium Salt/Nitroalkane Electrolyte Based on Analogy with Fluorinated Alcohols”, *European Journal of Organic Chemistry,* **2019**, *accepted.*
2) Y. Imada, Y. Okada, K. Noguchi, K. Chiba, “Selective Functionalization of Styrenes with Oxygen Using Different Electrode Materials: Olefin Cleavage and Synthesis of Tetrahydrofuran Derivatives”, *Angewandte Chemie International Edition*, **2019**, *58*, 125-129.
3) Y. Imada, Y. Okada, K. Chiba, “Investigating radical cation chain processes in the electrocatalytic Diels–Alder reaction”, *Beilstein Journal of Organic Chemistry*, **2018**, *14*, 642-647.
4) Y. Imada, Y. Yamaguchi, Y. Okada, N. Shida, K. Chiba, “Entropic Electrolytes for Anodic Cycloadditions of Unactivated Alkene Nucleophiles”, *Chemical Communications*, **2017**, *53*, 3960-3963.

9. Reference

9-1-1. Electro-organic chemistry

[1] (a) M. Yan, Y. Kawamata, P. S. Baran, *Chem. Rev*. **2017**, *117*, 13230-13319.; (b) A. Wiebe, T. Gieshoff, S. Möhle, E. Rodrigo, M. Zirbes, S. R. Waldvogel, *Angew. Chem. Int. Ed*. **2018**, *57*, 5594-5619.; (c) Yoshida, J.; Shimizu, A.; Hayashi, R. Chem. Rev. 2018, 118, 4702-4730.; (d) Jiang, Y.; Xu, K.; Zeng, C. Chem. Rev. 2018, 118, 4485-4540.

[2] J. Yoshida, S. Suga, S. Suzuki, N. Kinomura, A. Yamamoto, K. Fujiwara, *J. Am. Chem. Soc.* **1999**, *121*, 9546-9549..

[3] (a) Y. Kawamata, M. Yan, Z. Liu, D. Bao, J. Chen, J. T. Starr, P. S. Baran, *J. Am. Chem. Soc.* **2017**, *139*, 7448-

7451.; (b) E. J. Horn, B. R. Rosen, Y. Chen, J. Tang, K. Chen, M. D. Eastgate, P. S. Baran, *Nature*, **2016**, *533*, 77-81.; (c) Y. Imada, J. L. Röckl, A. Wiebe, T. Gieshoff, D. Schollmeyer, K. Chiba, R. Franke, S. R. Waldvogel, *Angew. Chem. Int. Ed.* **2018**, *57*, 12136-12140.

9-1-2. Electro-catalytic cycloadditions with unique electrolyte $LiClO_4/CH_3NO_2$

[1] (a) Y. Okada, Y. Yamaguchi, A. Ozaki, K. Chiba, *Chem. Sci*. **2016**, *7*, 6387-6393.; (b) M. Arata, T. Miura, K. Chiba, *Org. Lett*. **2007**, *9*, 4347–4350; (b) Y. Okada, R. Akaba, K. Chiba, *Org. Lett.* **2009**, *11*, 1033-1035.; (c) Y. Okada, A. Nishimoto, R. Akaba, K. Chiba, *J. Org. Chem*. **2011**, *76*, 3470–3476; (d) T. Miura, S. Kim, Y. Kitano, M. Tada, K. Chiba, *Angew. Chem. Int. Ed*. **2006**, *45*, 1461-1463.; (e) Y. Okada, K. Chiba, Chem. Rev. 2018, 118, 4592-4630.

9-1-3. Styrene derivatives and their utility

[1] (a) H. Seo, A. Liu, T. F. Jamison, *J. Am. Chem. Soc*. **2017**, *139*, 13969-13972; (b) H. Huang, C. Yu, Y. Zhang, Y. Zhang, P. S. Mariano, W. Wang, *J. Am. Chem. Soc*. **2017**, *139*, 9799-9802; (c) F. Wu, L. Wang, J. Chen, D. A. Nicewicz, Y. Huang, *Angew. Chem. Int. Ed*. **2018**, *57*, 2174-2178.; (d) M. Utsunomiya, J. F. Hartwig, *J. Am. Chem. Soc*. **2003**, *125*, 14286-14287.; (e) K. MuÇiz, L. Barreiro, R. M. Romero, C. Martínez, *J. Am. Chem. Soc.* **2017**, *139*, 4354-4357.; (f) L. J. Xiao, L. Cheng, W. M. Feng, M. L. Li, J. H. Xie, Q. L. Zhou, *Angew. Chem. Int. Ed.* **2018**, *57*, 461-464.; g) N. J. W. Straathof, S. E. Cramer, V. Hessel, T. Noel, *Angew. Chem. Int. Ed*. **2016**, *55*, 15549-15553.; (h) D. J. Wilger, J.-M. M. Grandjean, T. R. Lammert, D. A. Nicewicz, *Nat. Chem.* **2014**, *6*, 720; (i) V. R. Yatham, Y. Shen, R. Martin, *Angew. Chem. Int. Ed*. **2017**, *56*, 10915-10919.; (j) J. P. Wan, Y. Gao, L. Wei, *Chem. Asian J*. **2016**, *11*, 2092-2102.; (h) L. Wang, F. Wu, J. Chen, D. A. Nicewicz, Y. Huang, *Angew. Chem. Int. Ed*. **2017**, *56*, 6896-6900.

[2] (a) M. Zamfir, J. Lutz, *Nat. Commun.* **2012**, *3*, 1-8.; (b) X. Chen, L. Liu, M. Huo, M. Zeng, L. Peng, A. Feng, X. Wang, J. Yuan, *Angew. Chem. Int. Ed.* **2017**, *56*, 16541-16545.

[3] (a) W. Oppolzer, K. Keller, *J. Am. Chem. Soc.* **1971**, *93*, 3836-3837.; (b) K. A. Parker, D. Fokas, *J. Am. Chem. Soc.* **1992**, *114*, 9688-9689.; (c) G. Dujardin, M. Maudet, E. Brown, *Tetrahedron Lett.* **1997**, *38*, 1555-1558.

9-2-1. Understanding the effect of $LiClO_4$ / NM on radical cation chemistry: Leading to the exploration of alternative electrolytes

[1] C. K. Prier, D. A. Rankic, D. W. C. MacMillan, *Chem. Rev*. **2013**, *113*, 5322–5363.

[2] N. A. Romero, D. A. Nicewicz, *Chem. Rev*. **2016**, *116*, 10075-10166.

[3] J. Kou, C. Lu, J. Wang, Y. Chen, Z. Xu, R. S. Varma, *Chem. Rev*. **2017**, *117*, 1445-1514.

[4] J. I. Yoshida, A. Shimizu, R. Hayashi, *Chem. Rev*. **2018**, *118*, 4702-4730.

[5] M. Yan, Y. Kawamata, P. S. Baran, *Chem. Rev*. **2017**, *117*, 13230-13319.

[6] A. Wiebe, T. Gieshoff, S. Möhle, E. Rodrigo, M. Zirbes, S. R. Waldvogel, *Angew. Chem. Int. Ed*. **2018**, *57*, 5594-5619.

[7] N. Shida, Y. Imada, S. Nagahara, Y. Okada, K. Chiba, *Commun. Chem*. **2019**, *2*, 3-5.

[8] E. P. Farney, S. J. Chapman, W. B. Swords, M. D. Torelli, R. J. Hamers, T. P. Yoon, *J. Am. Chem. Soc.* **2019**, *141*, 6385-6391.

[9] Y. Okada, K. Chiba, *Chem. Rev.* **2018**, *118*, 4592-4630.

[10] Y. Okada, Y. Yamaguchi, A. Ozaki, K. Chiba, *Chem. Sci.* **2016**, *7*, 6387-6393.

[11] A. Ozaki, Y. Yamaguchi, Y. Okada, K. Chiba, *Chinese J. Chem*. **2019**, 561-564.

[12] K. Nakayama, N. Maeta, G. Horiguchi, H. Kamiya, Y. Okada, *Org. Lett*. **2019**, *21*, 2246-2250.

[13] Y. Okada, N. Maeta, K. Nakayama, H. Kamiya, *J. Org. Chem*. **2018**, *83*, 4948-4962.

[14] K. Chiba, T. Miura, S. Kim, Y. Kitano, M. Tada, *J. Am. Chem. Soc*. **2001**, *123*, 11314-11315.

[15] M. Arata, T. Miura, K. Chiba, *Org. Lett*. **2007**, *9*, 4347-4350.

[16] Y. Okada, R. Akaba, K. Chiba, *Org. Lett*. **2009**, *11*, 1033-1035.
[17] Y. Okada, A. Nishimoto, R. Akaba, K. Chiba, *J. Org. Chem*. **2011**, *76*, 3470-3476.
[18] T. Miura, S. Kim, Y. Kitano, M. Tada, K. Chiba, *Angew. Chem. Int. Ed*. **2006**, *45*, 1461-1463.
[19] S. Sankararaman, R. Sudha, *J. Org. Chem*. **1999**, *64*, 2155-2157.
[20] M. Ayerbe, F. P. Cossío, *Tetrahedron Lett*. **1995**, *36*, 4447-4450.
[21] L. Eberson, M. P. Hartshorn, O. Persson, F. Radner, *Chem. Commun*. **1996**, *0*, 2105-2112.
[22] I. Colomer, A. E. R. Chamberlain, M. B. Haughey, T. J. Donohoe, *Nat. Rev. Chem.* **2017**, *1*, 0088.
[23] Y. Imada, Y. Yamaguchi, N. Shida, Y. Okada, K. Chiba, *Chem. Commun.* **2017**, *53*, 3960-3963.
[24] Y. Imada, N. Shida, Y. Okada, K. Chiba, *Chinese J. Chem*. **2019**, 557-560.
[25] Y. Yamada, J. Wang, S. Ko, E. Watanabe, A. Yamada, *Nat. Energy* **2019**, *4*, 269-280.
[26] J. Wang, Y. Yamada, K. Sodeyama, C. H. Chiang, Y. Tateyama, A. Yamada, *Nat. Commun.* **2016**, *7*, 1-9.
[27] K. Kimura, J. Motomatsu, Y. Tominaga, *J. Phys. Chem. C* **2016**, *120*, 12385-12391.
[28] Y. Yamada, M. Yaegashi, T. Abe, A. Yamada, *Chem. Commun*. **2013**, *49*, 11194-11196.
[29] R. Tatara, D. G. Kwabi, T. P. Batcho, M. Tulodziecki, K. Watanabe, H.-M. Kwon, M. L. Thomas, K. Ueno, C. V. Thompson, K. Dokko, Y. Shao-Horn, M. Watanabe, *J. Phys. Chem. C*, **2017**, *121*, 9162-9172.
[30] S. Maeda, Y. Kameda, Y. Amo, T. Usuki, K. Ikeda, T. Otomo, M. Yanagisawa, S. Seki, N. Arai, H. Watanabe, Y. Umebayashi, *J. Phys. Chem. B* **2017**, *121*, 10979-10987.
[31] R. Tatara, K. Ueno, K. Dokko, M. Watanabe, *ChemElectroChem*, **2019**, *6*, 4444-4449.
[32] B. Klassen, R. Aroca, M. Nazri, G. A. Nazri, *J. Phys. Chem. B* **1998**, *102*, 4795-4801.
[33] J. Grondin, D. Talaga, J.-C. Lasségues, W. A. Henderson, *Phys. Chem. Chem. Phys*. **2004**, *6*, 938-944.
[34] J. Grondin, J.-C. Lasségues, M. Chami, L. Servant, D. Talagaa, W. A. Henderson, *Phys. Chem. Chem. Phys.* **2004**, *6*, 4260-4267.
[35] M. Chabanel, D. Legoff, K. Touaj, *J. Chem. Soc., Faraday Trans*. **1996**, *92*, 4199–4205.
[36] Y. Yamada, K. Furukawa, K. Sodeyama, K. Kikuchi, M. Yaegashi, Y. Tateyama, A. Yamada, *J. Am. Chem. Soc.* **2014**, *136*, 5039-5046.
[37] I. Colomer, C. Batchelor-Mcauley, B. Odell, T. J. Donohoe, R. G. Compton, *J. Am. Chem. Soc.* **2016**, *138*, 8855-8861.
[38] A. D'Aprano, B. Sesta, A. Princi, *J. Electroanal. Chem*. **1993**, *361*, 135-141.

9-2-2. Application of LiTFSI / NM electrolyte for electrochemical radical cation Diels-Alder reaction with lipophilic compounds.

[1] For recent reviews, see: (a) Kärkäs, M. D. *Chem. Soc. Rev.* **2018**, *47*, 5786-5865. (b) Möhle, S.; Zirbes, M.; Rodrigo, E.; Gieshoff, T.; Wiebe, A.; Waldvogel, S. R. *Angew. Chem., Int. Ed.* **2018**, *57*, 6018-6041. (c) Wiebe, A.; Gieshoff, T.; Möhle, S.; Rodrigo, E.; Zirbes, M.; Waldvogel, S. R. *Angew. Chem., Int. Ed.* **2018**, *57*, 5594-5619. (d) Waldvogel, S. R.; Lips, S.; Selt, M.; Riehl, B.; Kampf, C. J. *Chem. Rev.* **2018**, *118*, 6706-6765. (e) Nutting, J. E.; Rafiee, M.; Stahl, S. S. *Chem. Rev.* **2018**, *118*, 4834-4885. (f) Yoshida, J.; Shimizu, A.; Hayashi, R. *Chem. Rev.* **2018**, *118*, 4702-4730. (g) Jiang, Y.; Xu, K.; Zeng, C. *Chem. Rev.* **2018**, *118*, 4485-4540. (h) Yan, M.; Kawamata, Y.; Baran, P. S. *Chem. Rev.* **2017**, *117*, 13230-13319.
[2] For selected reviews, see: (a) Ischay, M. A.; Yoon, T. P. *Eur. J. Org. Chem.* **2012**, 3359-3372. (b) Studer, A.; Curran, D. P. *Nat. Chem.* **2014**, *6*, 765-773. (c) Fukuzumi, S.; Ohkubo, K. *Org. Biomol. Chem.* **2014**, *12*, 6059-6071. (d) Luca, O. R.; Gustafson, J. L.; Maddox, S. M.; Fenwicka, A. Q.; Smith, D. C. *Org. Chem. Front.* **2015**, *2*, 823-848. (e) Qiu, G.; Li, Y.; Wu, J. *Org. Chem. Front.* **2016**, *3*, 1011-1027.
[3] Francke, R.; Little, R. D. *Chem. Soc. Rev.* **2014**, *43*, 2492-2521.
[4] For selected examples, see: (a) Beil, S. B.; Müller, T.; Sillart, S. B.; Franzmann, P.; Bomm, A.; Holtkamp, M.; Karst, U.; Schade, W.; Waldvogel, S. R. *Angew. Chem., Int. Ed.* **2018**, *57*, 2450-2454. (b) Gütz, C.; Selt, M.; Bänziger, M.; Bucher, C.; Römelt, C.; Hecken, N.; Gallou, F.; Galvão, T. R.; Waldvogel, S. R. *Chem. Eur. J.* **2015**, *21*, 13878-13882. (c) Kulisch, J.; Nieger, M.; Stecker, F.; Fischer, A.; Waldvogel, S. R. *Angew. Chem., Int. Ed.* **2011**, *50*, 5564-5567. (d) Malkowsky, I. M.; Griesbach, U.; Pütter, H.; Waldvogel, S. R. *Eur. J. Org. Chem.* **2006**, 4569-4572. (e) Zhao, H.-B.; Xu, P.; Song, J.; Xu, H.-C. *Angew. Chem., Int. Ed.* **2018**, *57*, 15153-15156. (f) Imada, Y.; Okada, Y.; Noguchi, K.; Chiba, K. *Angew. Chem., Int. Ed.* **2019**, *58*, 125-129.
[5] For selected examples, see: (a) Horcajada, R.; Okajima, M.; Suga, S.; Yoshida, J. *Chem. Commun.* **2005**, 1303-

1305. (b) Tajima, T.; Nakajima, A.; Doi, Y.; Fuchigami, T. *Angew. Chem., Int. Ed.* **2007**, *46*, 3550-3552. (c) Tajima, T.; Nakajima, A. *J. Am. Chem. Soc.* **2008**, *130*, 10496-10497. (d) Sawamura, T.; Kuribayashi, S.; Inagi, S.; Fuchigami, T. *Org. Lett.* **2010**, *12*, 644-646.

[6] (a) Chiba, K.; Kono, Y.; Kim, S.; Nishimoto, K.; Kitano, Y.; Tada, M. *Chem. Commun.* **2002**, 1766-1767. (b) Hayashi, K.; Kim, S.; Kono, Y.; Tamura, M.; Chiba, K. *Tetrahedron Lett.* **2006**, *47*, 171-174. (c) Kim, S.; Tsuruyama, A.; Ohmori, A.; Chiba, K. *Chem. Commun.* **2008**, 1816-1818. (d) Kim, S.; Yamamoto, K.; Hayashi, K.; Chiba, K. *Tetrahedron* **2008**, *64*, 2855-2863. (e) Kim, S.; Ikuhisa, N.; Chiba, K. *Chem. Lett.* **2011**, *40*, 1077-1078.

[7] (a) Tanaka, F.; Arata, M.; Hayashi, K.; Kim, S.; Chiba, K. *Electrochemistry* **2006**, *74*, 625-627 (b) Nagano, T.; Mikami, Y.; Kim, S.; Chiba, K. *Electrochemistry* **2008**, *76*, 874-879. (c) Okada, Y.; Kamimura, K.; Chiba, K. *Tetrahedron* **2012**, *68*, 5857-5862.

[8] (a) Okada, Y.; Chiba, K. *Chem. Rev.* **2018**, *118*, 4592-4630. (b) Okada, Y.; Yamaguchi, Y.; Ozaki, A.; Chiba, K. *Chem. Sci.* **2016**, *7*, 6387-6393. (c) Yamaguchi, Y.; Okada, Y.; Chiba, K. *J. Org. Chem.* **2013**, *78*, 2626-2638. (d) Okada, Y.; Nishimoto, A.; Akaba, R.; Chiba, K. *J. Org. Chem.* **2011**, *76*, 3470-3476.

[9] Imada, Y.; Yamaguchi, Y.; Shida, N.; Okada, Y.; Chiba, K. *Chem. Commun.* **2017**, *53*, 3960-3963.

[10] (a) Kim, S.; Noda, S.; Hayashi, K.; Chiba, K. *Org. Lett.* **2008**, *10*, 1827-1830. (b) Okada, Y.; Chiba, K. *Electrochim. Acta* **2010**, *55*, 4112-4119. (c) Okada, Y.; Yoshioka, T.; Koike, M.; Chiba, K. *Tetrahedron Lett.* **2011**, *52*, 4690-4693. (d) Okada, Y.; Yamaguchi, Y.; Chiba, K. *Eur. J. Org. Chem.* **2012**, 243-246.

[11] (a) Shoji, T.; Kim, S.; Chiba, K. *Angew. Chem., Int. Ed.* **2017**, *56*, 4011-4014. (b) Okamoto, K.; Shoji, T.; Tsutsui, M.; Shida, N.; Chiba, K. *Chem. Eur. J.* **2018**, *24*, ,17902-17905.

9.3 Electrode material selective functionalization of styrenes with oxygen: olefin cleavage and tetrahydrofurans formation

[1] a) M. Yan, Y. Kawamata, P. S. Baran, *Chem. Rev.* **2017**, *117*, 13230-13319; b) J.I. Yoshida, A. Shimizu, R. Hayashi, *Chem. Rev*. **2018**, *118*, 4702-4730 ; c) N. Fu, G. S. Sauer, A. Saha, A. Loo, S. Lin, *Science*, **2017**, *357*, 575-579.; d) S. Tang, S. Wang, Y. Liu, H. Cong, A. Lei, *Angew. Chem. Int. Ed*. **2018**, *57*, 4737-4741; *Angew. Chem.* **2018**, *130*, 4827-4831; e) Z. W. Hou, Z. Y. Mao, H. B. Zhao, Y. Y. Melcamu, X. Lu, J. Song, H. C. Xu, *Angew. Chem. Int. Ed.* **2016**, *55*, 9168–9172; *Angew. Chem*. **2016**, *128*, 9314-9318.; f) Y. F. Liang, R. Steinbock, A. Münch, D. Stalke, L. Ackermann, *Angew. Chem. Int. Ed*. **2018**, *57*, 5384-5388; *Angew. Chem*. **2018**, *130*, 5482-5486.

[2] J. Kulisch, M. Nieger, F. Stecker, A. Fischer, S. R. Waldvogel, *Angew. Chem. Int. Ed*. **2011**, *50*, 5564-5567; *Angew. Chem.* **2011**, *123*, 5678-5682.

[3] a) Y. Okada, K. Chiba, *Chem. Rev*. **2018**, *118*, 4592-4630; b) Y. Imada, Y. Yamaguchi, N. Shida, Y. Okada, K. Chiba, *Chem. Commun*. **2017**, *53*, 3960-3963.

[4] T. Gieshoff, D. Schollmeyer, S. R. Waldvogel, *Angew. Chem. Int. Ed*. **2016**, *55*, 9437-9440; *Angew. Chem.* **2016**, *128*, 9587-9590.

[5] T. Shoji, S. Kim, K. Chiba, *Angew. Chem. Int. Ed.* **2017**, *56*, 4011-4014 ; *Angew. Chem.* **2017**, *129*, 4069-4072.

[6] a) A. Medici, P. Pedrini, A. DeBattisti, G. Fantin, M. Fogagnolo, A. Guerrini, *Steroids*, **2001**, *66*, 63–69; b) I.M. Malkowsky, U. Griesbach, H. Pütter, S. R. Waldvogel, *Eur. J. Org. Chem.* **2006**, 4569-4572. ; c) S. B. Beil, T. Müller, S. B. Sillart, P. Franzmann, A. Bomm, M. Holtkamp, U. Karst, W. Schade, S. R. Waldvogel, *Angew. Chem. Int. Ed.* **2018**, *57*, 2450–2454; *Angew. Chem.* **2018**, *130*, 2475-2479.

[7] C. Gütz, M. Selt, M. Bänziger, C. Bucher, C. Rçmelt, N. Hecken, F. Gallou, T. R. Galvo, S. R. Waldvogel, *Chem. Eur. J*. **2015**, *21*, 13878-13882.

[8] I. M. Malkowsky, C. E. Rommel, K. Wedeking, R. Frçhlich, K. Bergander, M. Nieger, C. Quaiser, U. Griesbach, H. Pütter, S. R. Waldvogel, *Eur. J. Org. Chem*. **2006**, 241-245.

[9] H. Zhao, P. Xu, J. Song, H. Xu, *Angew. Chem. Int. Ed*. **2018**, *57*, 15153-15156; *Angew. Chem.* **2018**, *130*, 15373-15376.

[10] M. C. Figueiredo, V. Trieu, S. Eiden, M. T. M. Koper, *J. Am. Chem. Soc.* **2017**, *139*, 14693-14698.

[11] H. Seo, A. Liu, T. F. Jamison, *J. Am. Chem. Soc*. **2017**, *139*, 13969-13972.

[12] a) H. Huang, C. Yu, Y. Zhang, Y. Zhang, P. S. Mariano, W. Wang, *J. Am. Chem. Soc*. **2017**, *139*, 9799-9802; b) F. Wu, L. Wang, J. Chen, D. A. Nicewicz, Y. Huang, *Angew. Chem. Int. Ed*. **2018**, *57*, 2174-2178; *Angew. Chem.* **2018**, *130*, 2196-2200.

[13] a) M. Utsunomiya, J. F. Hartwig, *J. Am. Chem. Soc*. **2003**, *125*, 14286-14287.; b) K. MuÇiz, L. Barreiro, R. M. Romero, C. Martínez, *J. Am. Chem. Soc.* **2017**, *139*, 4354-4357.

[14] a) L. J. Xiao, L. Cheng, W. M. Feng, M. L. Li, J. H. Xie, Q. L. Zhou, *Angew. Chem. Int. Ed.* **2018**, *57*, 461-464; *Angew. Chem.* **2018**, *130*, 470-473.; b) N. J. W. Straathof, S. E. Cramer, V. Hessel, T. Noel, *Angew. Chem. Int. Ed.* **2016**, *55*, 15549-15553; *Angew. Chem*. **2016**, *128*, 15778-15782.; c) D. J. Wilger, J.-M. M. Grandjean, T. R. Lammert, D. A. Nicewicz, *Nat. Chem.* **2014**, *6*, 720; d) V. R. Yatham, Y. Shen, R. Martin, *Angew. Chem. Int. Ed*. **2017**, *56*, 10915-10919; *Angew. Chem.* **2017**, *129*, 11055-11059.

[15] a) J. P. Wan, Y. Gao, L. Wei, *Chem. Asian J*. **2016**, *11*, 2092–2102.; b) A. Rubinstein, P. J. Lozanao, J. J. Carbó, J. M. Poblet, R. Neumann, *J. Am. Chem. Soc*. **2014**, *136*, 10941-10948.; c) M. M. Hossain, S. G. Shyu, *Tetrahedron* **2014**, *70*, 251-255.; d) R. Lin, F. Chen, N. Jiao, *Org. Lett.* **2012**, *14*, 4158-4161.; e) G. Z. Wang, X. L. Li, J. J. Dai, H. J. Xu, *J. Org. Chem*. **2014**, *79*, 7220-7225.; f) A. K. Singh, R. Chawla, L. D. S. Yadav, *Tetrahedron Lett*. **2015**, *56*, 653-656.; g) E. L. Clennan, G. I. Pan, *Org. Lett*. **2003**, *5*, 4979-4982.; h) K. Suga, K. Ohkubo, S. Fukuzumi, J. *Phys. Chem. A* **2003**, *107*, 4339-4346.; i) Y. Deng, X. J. Wei, H. Wang, Y. Sun, T. No□l, X. Wang, *Angew. Chem. Int. Ed.* **2017**, *56*, 832–836; *Angew. Chem.* **2017**, *129*, 850-854.; j) T. Wang, N. Jiao, *J. Am. Chem. Soc.* **2013**, *135*, 11692-11695.; k) X. Wu, A. P. Davis, A. J. Fry, *Org. Lett.* **2007**, *9*, 5633-5636.

[16] S. G. Van Ornum, R. M. Champeau, R. Pariza, *Chem. Rev.* **2006**, *106*, 2990-3001.

[17] a) N. L. Bauld, R. Pabon, *J. Am. Chem. Soc*. **1983**, *105*, 633–634; b) L. Wang, F. Wu, J. Chen, D. A. Nicewicz, Y. Huang, *Angew. Chem. Int. Ed*. **2017**, *56*, 6896-6900; *Angew. Chem*. **2017**, *129*, 7000-7004.; c) S. Lin, M. A. Ischay, C. G. Fry, T. P. Yoon, *J. Am. Chem. Soc.* **2011**, *133*, 19350-19353.; d) J. Zhao, J. L. Brosmer, Q. Tang, Z. Yang, K. N. Houk, P. L. Diaconescu, O. Kwon, *J. Am. Chem. Soc*. **2017**, *139*, 9807-9810.; e) Y. Okada, Y. Yamaguchi, A. Ozaki, K. Chiba, *Chem. Sci*. **2016**, *7*, 6387-6393.

[18] a) R. J. Perkins, H. C. Xu, J. M. Campbell, K. D. Moeller, Beilstein *J. Org. Chem.* **2013**, *9*, 1630-1636,; b) C. Cai, H. Xu, *Nat. Commun.* **2018**, *9*, 3551.

[19] R. B. Teponno, S. Kusari, M. Spiteller, *Nat. Prod. Rep*. **2016**, *33*, 1044-1092.

[20] CCDC 1861076 and 1861075 (*trans*-3 c, *cis*-9 c) contain the supplementary crystallographic data for this paper. These data can be obtained free of charge from The Cambridge Crystallographic Data Centre.

[21] Q. Li, C. Batchelor-Mcauley, N. S. Lawrence, R. S. Hartshorne, R. G. Compton, *J. Electroanal. Chem*. **2013**, *688*, 328-335.

[22] M. Katz, P. Riemenschneider, H. Wendt, *Electrochim. Acta* **1972**, *17*, 1595-1607.

[23] C. M. Cardona, W. Li, A. E. Kaifer, D. Stockdale, G. C. Bazan, *Adv. Mater*. **2011**, *23*, 2367-2371.

[24] M. Swart, T. V. D. Wijst, C. F. Guerra, F. M. Bickelhaupt, *J. Mol. Model.* **2007**, *13*, 1245-1257.

[25] a) U. Akbulut, J. E. Fernandez, R. L. Birke, *J. Polym. Sci. Polym. Chem. Ed.* **1975**, *13*, 133-149.; b) U. Akbulut, S. Eren, L. K. Toppare, *Polymer* **1984**, *25*, 1028-1030.

[26] Y. Zhang, G. Jin, Z. Yang, H. Zhao, *Microchim. Acta*, **2004**, *147*, 225-230.

[27] a) M. Shao, P. Liu, R. R. Adzic, *J. Am. Chem. Soc.* **2006**, *128*, 7408-7409.; b) S. L. McLellan, *Diss. Abstr. B* **1975**, *36*, 744.

[28] T. Ozawa, A. Hanaki, H. Yamamoto, *FEBS Lett.* **1977**, *74*, 99–102.

[29] a) J. M. McCord, I. Fridovich, *J. Biol. Chem.* **1969**, *244*, 6049–6055; b) D. Vasudevan, H. Wendt, *J. Electroanal. Chem.* **1995**, *392*, 69-74.; c) D. W. Sawyer, J. L. Roberts, *J. Electroanal. Chem.* **1966**, *12*, 90-101.

[30] A. A. Frimer, *Chem. Rev*. **1979**, *79*, 359-387.